"WELDED STEEL BEAM-TO-COLUMN CONNECTIONS"

BY

ALIYU AYIKO ABUBAKAR

A thesis submitted to the Faculty of Engineering
in fulfillment of the requirements for the
Degree of Doctor of Philosophy

The University of Aston in Birmingham
August 1984

To my wife Rabi and our two children Abdul Kareem and Ajuma Hariretu for their perseverance

The University of Aston in Birmingham

WELDED STEEL BEAM-TO-COLUMN CONNECTIONS

By

Aliyu Ayiko Abubakar

Thesis submitted for the degree of Doctor of Philosophy
August 1984

SUMMARY

This thesis contains experimental and theoretical work associated with welded steel main and secondary beam-to-column connections subject to static loading.

A review of the previous work indicates that information on welding the main beam directly to the column is limited. Frictional forces, reduction in strength of welds due to the flexibility of the beam and column flanges and reduction in column strength due to a combination of axial load, bending moment and web buckling, have often been ignored. Information on secondary beam-to-column connections is also limited.

The thesis describes tests carried out by the author to determine the failure load of the flange weld connecting beams to columns with various ratios of bending moment and shear force applied to the beam. These experiments demonstrate the importance of friction resistance and indicate that when $\mu M/VD > 1$ failure of the weld occurs by rotation about the compression flange of the beam and when $\mu M/VD < 1$ failure of the weld occurs by slipping and rotation about the beam compression flange. Three distinct modes of failure of the fillet weld in beam-to-column connections are identified. The strength of the tension flange weld is shown to be affected by the flexibility of the beam and column flanges. A simple practical theory is developed which incorporates these effects with a reasonable degree of accuracy.

Tests on short columns subject to various combinations of axial load and web bucking load show that the axial load reduces the buckling strength of the web. An interaction formula is developed for this loading condition.

Thirteen tests are carried out on eccentric loads only. The proportions of the bending load resisted by each of the weld groups forming the connection are determined. Theories are developed for calculating the weld size based on the proportion of the load taken by the welds and incorporating the geometrical properties of the sections.

Key Words:

Beam-to-column connection, failure criterion, web buckling.

CONTENTS

ACKNOWLEDGEMENTS

This work was carried out at the Department of Civil Engineering of the University of Aston in Birmingham under the supervision of Dr L H Martin whom the author would like to thank for his guidance, continued help, useful suggestions and encouragement given throughout the course of his investigations.

The author would also like to thank Mr J Hollins of the Department of Civil Engineering for services rendered, Mr V Williams of the Department of Civil Engineering workshop for carrying out all the welding, Mr S Wigstaff of the Structural Engineering Laboratory of the Department of Civil Engineering for his assistance in carrying out the tests, and the Federal Government of Nigeria for providing the funds.

Finally I wish to thank Carol for doing all the typing.

LIST OF TABLES

LIST OF FIGURES

PLATES

NOTATION

A	Area of cross section of the column.
A_f	Area under the stress distribution graph for a rigid flange.
a	Throat thickness of fillet weld.
a_f	Area under the stress distribution graph for a flexible flange.
B	Width of column flange.
B_e	Effective length of flange weld.
b_{bf}	Breadth of beam flange.
d_c	Depth of column web between flanges.
d_t	Depth of the tee section.
d_w	Depth of web section.
E	Youngs modulus of elasticity.
e	Eccentricity of the applied force - column web buckling test.
F	Applied force (friction test).
F'	Strength of the connection based on the straight line theory for weld failure criterion.
F_x	Force on the weld in the x-direction transverse to the length of the weld-failure criterion tests.
F_y	Force on the weld in the y-direction transverse to the length of the weld-failure criterion tests.
F_{wy}	Ultimate shear strength of flange weld.

F_{wx} Ultimate tensile strength of flange weld.

f_{By} Yield stress of Box-section steel.

f_b Maximum bearing stress - column tests.

f_{wx} Force per unit legth of weld in the x-direction transverse to the length of the weld.

f_{wy} Force per unit length of weld in the y-direction transverse to the length of the weld.

f_{fy} Yield stress of column section steel.

f_{cwy} Yield stress of column section web steel.

f_{cfy} Yield stress of column section flange steel.

f'_w Force per unit length of weld at the end of the flange for elastic theory for I-section (trapezoidal stress distribution).

F_{WR} Resultant force on the weld - Beam-to-column connection.

H Horizontal force in the beam flange - Beam-to-column connection.

H_R Resultant force on the weld.

h Depth of box-section.

I_{WA} Second moment of area of a weld group about the axis AA.

I_{WG} Second moment of area of a weld group about the centroidal axis of the weld group.

I_{WO} Second moment of area of a weld group about the axis OO.

I_{wx} Second moment of area of a weld group about the axis XX.

I_{wy} Second moment of area of a weld group about the axis YY.

K Factor associated with weld failure criterion.

k Effective length of weld for a Box-section connection.

L Length (used in the theoretical analysis).

ℓ Effective length (used in the theoretical analysis).

l_e Effective weld length for a fully welded Beam-to-column connection.

L_{wt} Total effective weld length for a fully welded Beam-to-column connection.

M Bending moment.

M_{bp} Plastic moment of resistance of the beam section.

M_{cp} Plastic moment of resistance of column section.

M_{cwv} Moment of resistance of column web in punching shear.

M_p Plastic moment of resistance of a section.

M'_p Enhanced plastic moment of resistance of a section.

N Normal reaction (friction test).

P Axial load applied to the column.

R_w Resultant force on a weld group.

r Root radius for a section.

r_b Root radius for the beam section.

r_{c} Root radius for the column section.

S Plastic modulus of a steel section.

S_b Width of stiff bearing.

T Thickness of the column flange.

t_{bf} Thickness of the beam flange.

t_{bw} Thickness of the beam web.

t_{cw} Thickness of the column web.

t_{Bf} Thickness of Box-section flange.

U Deflection.

V Vertical reaction.

W Transverse load applied to the column.

x Distance.

z Elastic section modulus.

α Failure plane angle.

θ Angle of rotation.

Δ Displacement.

μ Coefficient of friction between steel and steel.

σ Standard deviation.

δ Small displacement (vertical slip).

CHAPTER 1

INTRODUCTION

The steel skeleton frame is in common use throughout the world. The members of the skeleton are standard rolled sections which are connected at the ends or at points along their length. The members may act as beams, columns, ties or bracing.

The requirements for ideal connections[58] are:

1. it should be simple to manufacture and assemble,

2. it should be standardised for situations where the dimensions and loads are similar thus avoiding a multiplicity of dimensions, plate thicknesses, weld sizes and bolts,

3. it should be manufacturd from materials and components that are readily available,

4. it should be designed and detailed so that work is from the top of the joint not from below where the workman's arms will be above his head. There should also be sufficient room to locate a spanner, or space to weld if required,

5. it should be designed so that welding is generally confined to the workshops to ensure a good quality and reduce costs,

6. it should be detailed to allow sufficient clearance and adjustment to accommodate the lack of accuracy in site dimensions,

7. it should be designed to withstand not only the normal working loads but also the erection forces,

8. it should be designed to avoid the use of temporary supports to the structure during erection,

9. it should be designed to develop the required load-deformation characteristics at the service load and ultimate load,

10. it should be detailed to resist corrosion and to be of reasonable appearance,

11. it should be low in cost and cheap to maintain.

Welding, bolting and a combination of welding and bolting have been used to make beam-to-column connections. The most commonly used connections are shown in Figure 1.1. The end plate welded to the beam and bolted to the column is a popular connection and has the advantage of relative simplicity and ease of erection. However, the structural behaviour and design of such a connection are relatively complex.

Considerable research has been carried out on the behaviour of bolted and welded beam-to-column connections. Connections utilizing a combination of welding and bolting fail to utilize the many advantages of a fully welded connection.

The economy of a connection depends on, among other things, the material cost and labour cost. In most cases, designing beam-to-column connections for full moment capacity leads to a fully stiffened and therefore expensive connection. There is therefore a need to reduce the amount of material used and the amount of welding. Considerable savings can be made if the beam is welded directly to the column and column stiffeners are not used. In America, to avoid site welding, a length of the beam is welded directly to the column in the welding shop and to obtain the desired beam span, the remaining length of beam is bolted to the two welded beam-to-column connections. In this country, to avoid site welding, an end plate is welded to both ends of the beam in the welding shop which is then bolted to the column on site. Site welding is expensive.

This thesis is concerned with the behaviour of unstiffened welded beam-to-column connection in which the beam is welded directly to the column flange (hereafter referred to as a main beam-to-column connection) and a connection in which the beam is welded to the column web via a tee which has its flanges butt welded to the column flanges and its web fillet welded to the column web at right angles to the column web (hereafter referred to as a secondary beam-to-column connection); both subject to static loads producing vertical shear and bending moment as

shown in Figures 3.2 and 3.6 respectively. Research literature on these types of connections is limited.

It is known that when the column is not provided with stiffeners, the design of the connection has to be based on a reduced effective weld length. The reduction in strength has often been attributed to the non-uniform stress distribution resulting from the distortion of the geometry of the sections. This non-uniform stress distribution is due to the flexibility of the flanges of the sections (beam and column). However, none of the previous researchers considered the influence of the flange width on the flexibility of the flange in their derivation of the effective weld length formulae. Rolloos infact, stated in his conclusion that he could not find any influence of the flange width on the effective weld length. This thesis presents a series of tests designed to ascertain the influence of the flange width and flange thickness on the flexibility of the flange and thereby develop the effective weld length formula which incorporates the influence of both the flange width and the flange thickness.

A steel frame is subject to various forces and combinations of forces including wind forces. The steel frame has to be designed to withstand bending moments or any combination of forces which may be imposed on it, i.e. to be rigid and moment resisting. Such a frame usually consists of various forms of beam-to-column connections joined together to form the required skeleton. The requirement of strength, rigidity and moment resistance calls for adequate bracing. The column in beam-to-column connections is subject to various combinations of forces. Columns

subject to axial load and bending moment has been studied extensively (12, 22, 38, 39, 41) but not when also subject to a web buckling load. In the beam compression region, the column is subject to the concentrated action of the beam flange force. As the column often carries an axial load, the buckling strength of the column web could be reduced Tests by Graham et al.[23] have shown that in most cases, the deciding factor in beam-to-column connections is a crippling of the column web. It is therefore necessary that the effect of a column axial load on the column web buckling strength be determined. Results are included in this thesis of tests carried out to determine the effect of an axial load on a column on the web buckling strength.

The existing failure criteria for fillet welds are based on methods which are probably more suited to the prediction of the faiure mechanism of solid materials. Moreover these methods assume the throat to be the critical plane. Tests carried out in this thesis have shown that the actual failure plane varies. A failure criterion based on the actual failure plane and on the ultimate strength of the weld, a desirable thing for a proper design of beam-to-column connections, has been developed in this thesis based on theoretical and experimental analysis.

When a secondary beam-to-column connection is subject to loads producing vertical shear and bending moment, the applied bending moment is resisted in differing proportions by the three weld groups forming the connections. The determination of the proportion of the applied bending moment transmitted to the tee web/column web weld is complicated by the resistance offered by the tee flange/column flanges butt welds.

Graham et al[23] determined this proportion by treating the column flange as a two span beam on three supports with a uniformly distributed load. The flanges of the tee were treated as supports for the column flanges and they found the proportion of the beam flange force transmitted to the column web through the tee web to be dependent on the width of the beam flange to the tee flange ratio. A determination of this proportion has been carried out in this thesis by considering the yield line pattern on the column web at ultimate load.

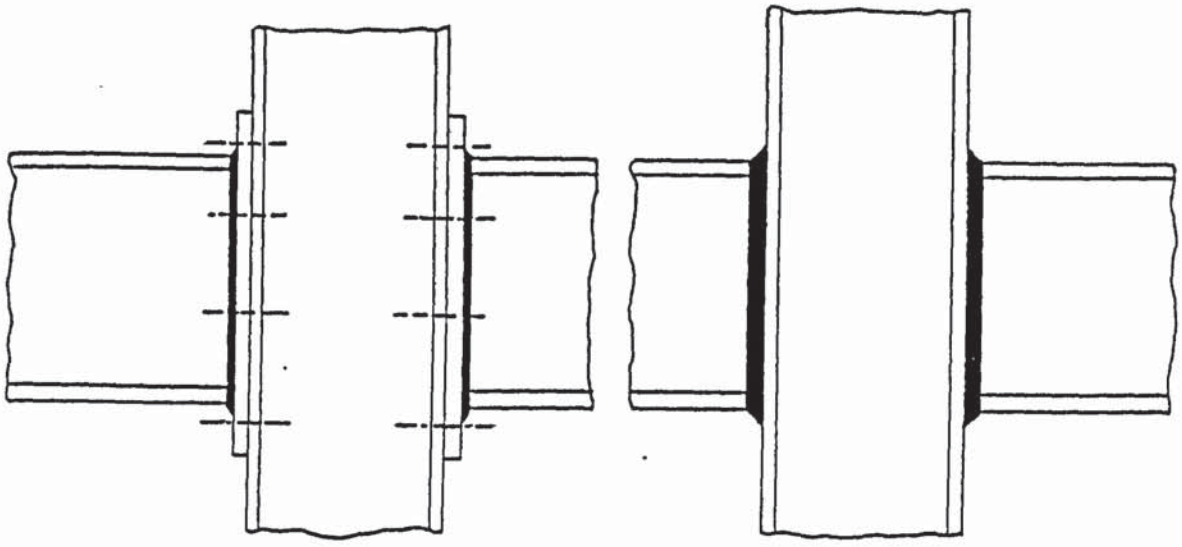

(a) Connection with an end plate (b) All round welded

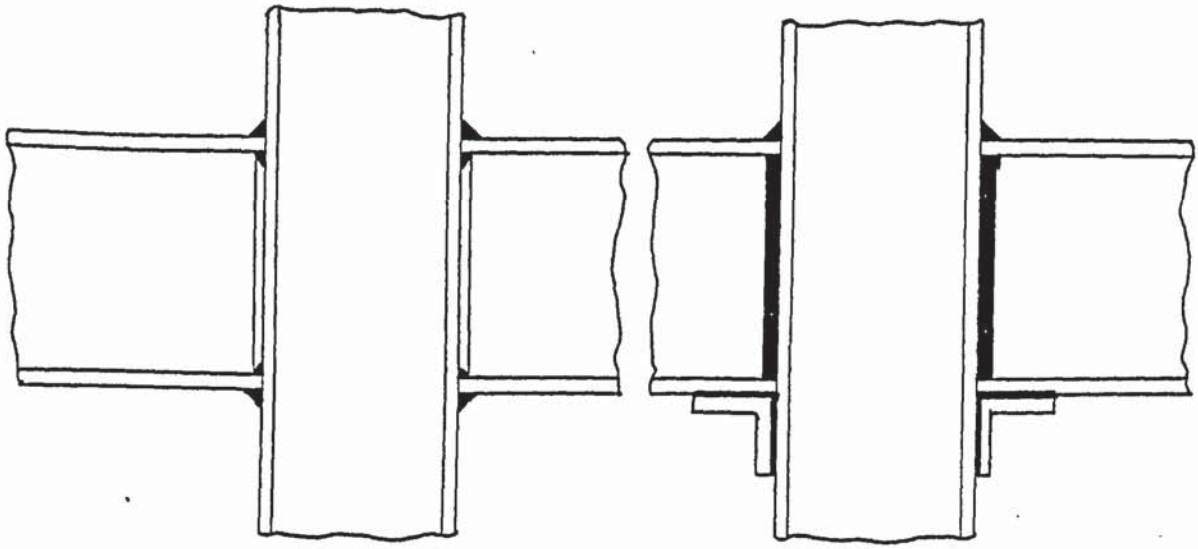

(c) Flange welds only (d) All round welded with beam seat

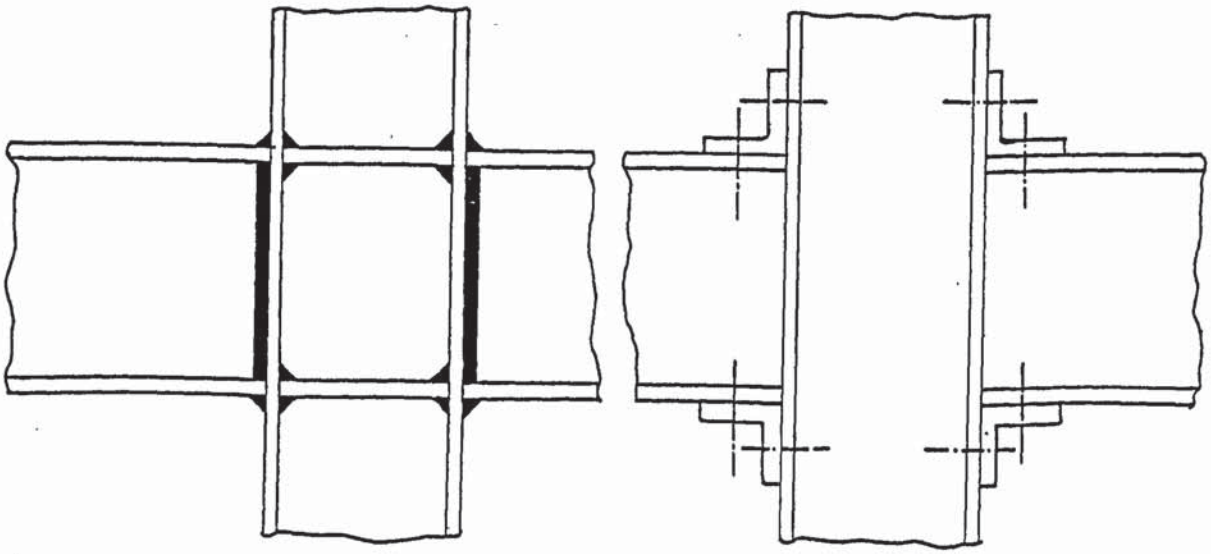

(e) All round welded with column stiffeners (f) Completely bolted connection

Figure 1.1 Some common Beam-to-Column connections

CHAPTER 2

LITERATURE REVIEW

This literature review is historical and includes works on beam-to-column connections, fillet welds and columns subject to combinations of axial load and lateral loads, relevant to this author's research.

Early experimental work on beam-to-column connections was carried out by Uhler and Jensen[1] in 1930 who showed the essential differences between riveted and welded connections. The types and number of connections tested are shown in figure 2.1.

The objective of the investigation was to determine the strength, stiffness and flexibility of web welded and flange welded beam-to-column connections. Uhler and Jensen concluded that under working load, high stresses are developed in the weld between the web of the beam and the flange of the column and the factor of safety ranges from 0.3 to 3.2. For short beams, web welds may be satisfactory. They observed that bearing increased joint rigidity but reduced maximum weld stress and flange welded connections gave nearly full joint rigidity. They recommended the use of full negative moment for the design of flange welded connections.

The study of the behaviour of fillet welded beam-to-column connections cannot be complete without adequate knowledge of the strength and failure mode of fillet welds. A theoretical study of the strength of

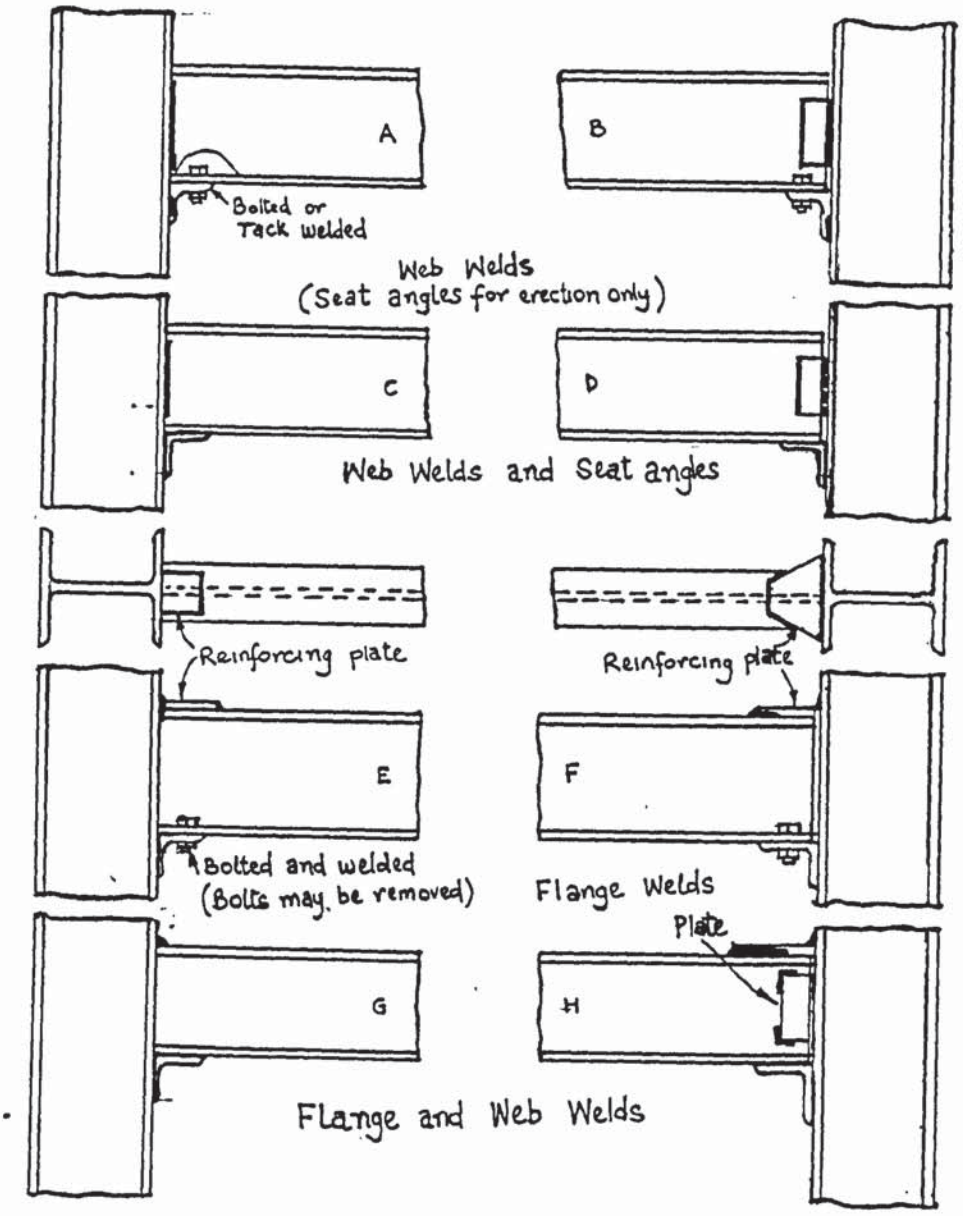

Figure 2.1 Uhler and Jonsen's Beam-to-column connection

fillet welds was carried out in 1930 by Biber[2]. Biber looked at possible critical sections such as the bond between the weld and the base metal, weld leg and weld throat. End or transverse fillet welds of a simple lap joint (shown in figure 2.2) were also considered.

In the stress analysis, Biber ignored the couple due to the load eccentricity and assumed a uniform stress distribution. The stress at the throat was also assumed to be purely tensile. He assumed that welds in tension have the same strength as welds in compression. This assumption was later proved to be correct[51].

Biber concluded that the critical section was the throat which failed in tension on a 45^0 plane. The failure plane angle has since been shown to vary[16, 51].

Biber extended the annalysis to fillet welds of unequal leg lengths. This analysis showed that the critical section could change from the throat to either the parallel or transverse leg of the fillet depending on the ratio of the leg lengths. The weld profile was also considered in this analysis and it was concluded that a concave profile would naturally reduce the strength of the weld and ensure that the throat was generally the critical section while the convex profile increased weld strength to a point at which the leg became the critical section and further reinforcement gave no extra strength.

Figure 2.2 Biber's Transverse Lap Joint

A theoretical analysis similar to that of Biber[2] was made in the same year by Schuster[3]. Schuster, however, pointed out the significance of the fillet weld root in relation to penetration and stress concentration. Although he did not offer an alternative method of solution, Schuster concluded that an elastic study of behaviour would not serve any useful purpose. Instead, he suggested a solution similar to that of Biber[2].

A uniform load along a critical plane (not necessarily the throat) was assumed. This assumption of uniformity was justified by the suggestion that the stress distribution would become more or less uniform when the weld became plactic just prior to failure.

Again like Biber, Schuster neglected the load couple produced in a simple lap joint due to load eccentricity and the fillet weld was assumed to be subjected to both tensile and shear stresses. The resultant of these stresses was found to be a maximum on a critical plane at an angle of 48.5^{0} from the vertical leg. Since the difference was small, the throat was considered as the critical section. The ultimate strength of the base metal was used as the limiting strength instead of that of the weld. Schuster probably assumed the weld to have a higher ultimate strength than the base metal.

In 1932, Freeman[4] discribed a series of tests on full size welded specimens to investigate the strength of all types of joints which were likely to be used in practice. The investigation also included the effect of varying the fillet length, thickness and width of plate in relation to

the weld strength. Longitudinal, side, and transverse fillet welds were tested under both tensile and compressive shearing loads. Freeman did not obtain sufficient results from which any firm conclusion could be drawn. However, he noticed a reduction in the strength of the weld as the fillet increased. This observation is of significance in the work on effective weld length.

An important contribution to the study of weld strength was made in 1934 by Jensen [5]. Twenty tests were conducted on fillet welds of 2 inches (5o mm) length and 0.375 inch (9.4 mm) leg. Jensen used run-on run- off plates for his test welds which led to good consistency in results. This was an improvement on previous experimental techniques and was adopted as a means of ensuring the reliability of the strength of end of fillet welds. Jensen's specimen made it possible to vary the forces applied to the legs of the weld. Only lap welds had been investigated previously. A study of the possible position of the critical plane was made and he also compared his work with the contemporary theories of Biber [2] and Schuster [3].

Jensen criticized the adoption of the throat as the critical section when using the Vector addition method. He pointed out that although this method is simple, the angle of the resultant to the throat or any other section should be considered. He discovered that the method of applying the resultant force to the throat underestimated the weld strength by approximately 37% when the ultimate shear strength of the weld is used instead of the safe working stress.

The idea of Schuster[3] that the critical plane was subjected to both tensile and shear stresses was extended by Jensen. He combined the two stresses using the principal stress theory and assumed the critical plane to be at or near the throat as suggested by Schuster[39]. Infact, the stresses used in the principal stress theory were computed on the throat. He suggested that the weld in type A specimen would be predominantly in shear and that of bype B predominantly in tension (see figure 2.3).

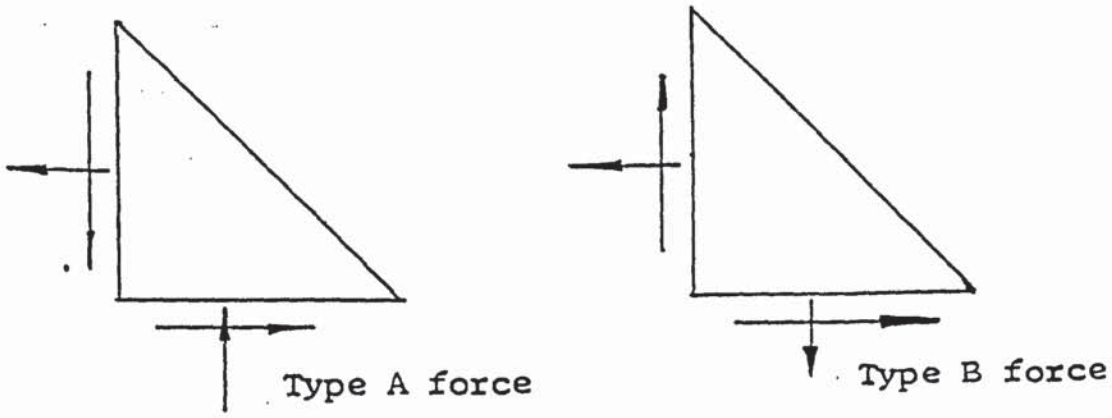

Figure 2.3 Weld forces in Jensen's analysis

The Couples produced by the external forces were assumed to either cancel each other in type B or, to be insignificant in type A.

Jensen was able to predict the ultimate strength of the welds with varying ratios of the forces applied to the weld legs using the maximum shear stress criterion in conjunction with the value of ultimate shear strength obtained from the control tests. The maximum shear stress criterion was used for both types of welds even though Jensen himself

suggested that weld B was predominantly in tension.

Jensen compared the actual failure planes with the planes of maximum shear stress and maximum principal stress. This comparison was presented with diagrams and actual plane angles were not quoted.

Jensen discovered that type A welds showed good correlation between the actual and predicted weld strength and that in all the six tests, the actual critical plane was reasonably coincident with the plane of maximum shear stress. These planes were shown to be approximately at the throat. He noticed that type B welds did not show good correlation at low values of F_x/F_y and that the plane of maximum principal stress bore little relationship to the actual fracture planes which were generally well away from the throat.

For the welds loaded on both legs, Jensen found that the method proposed by Biber[2] for the lap joints could not be adapted. Although he showed that the actual critical plane was not at the throat, he ignored this fact when presenting his theory. He has clearly shown that welds of type A and B do not behave in the same way, especially with regard to the ultimate strength. He noticed that welds of type B were as much as 40% stronger than welds of type A.

The work of Schreiner[6] in 1935 on longitudinal fillet welds of lapped specimens subject to pure bending and shear showed that when there is no plate bearing the neutral axis passes through the centroid of the weld and the stress distribution at failure is triangular. His

observation that failure occured first in the compression weld was contrary to the common belief that the compression yield point was at least equal to the tension yield point. The work of this author and that of other researchers [2, 51] has shown that failure occured first in the tension weld.

A paper on welding design was published in 1936 by Jennings [7]. This paper highlighted the subject of residual stresses and stress concentrations in welds and pointed out that in designs, rigid joints should be avoided as much as possible in order to prevent the development of excessive residual stresses which might cause failure either during fabrication or in service. Jennings assumed that the critical section was at the throat. He pointed out the significance of the bending moment in lap joints due to load eccentricity. This bending moment was taken to be Pt/4 (see figure 2.4) and was thought to give rise to a stress on the throat of a rectangular distribution at failure. The stress distribution along the longitudinal welds was thought to be uniform.

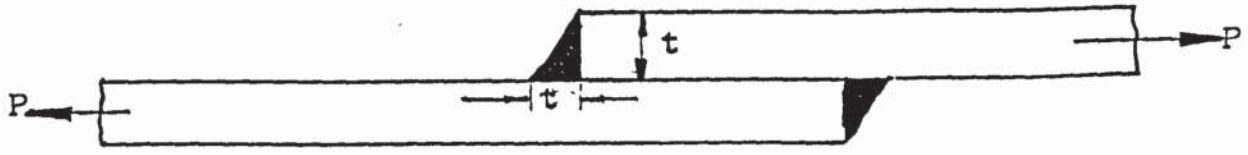

Figure 2.4 Dimensions in Jensen's double lapped specimen

Solakian[8] in his work on the stress distribution in fillet welds presented data for the stress distribution across the throat of the fillet weld, as shown in Figure 2.5. This graph is of particular interest because designers and stress analysts usually assume that failure will occur in the throat, in determining the strength of a weld.

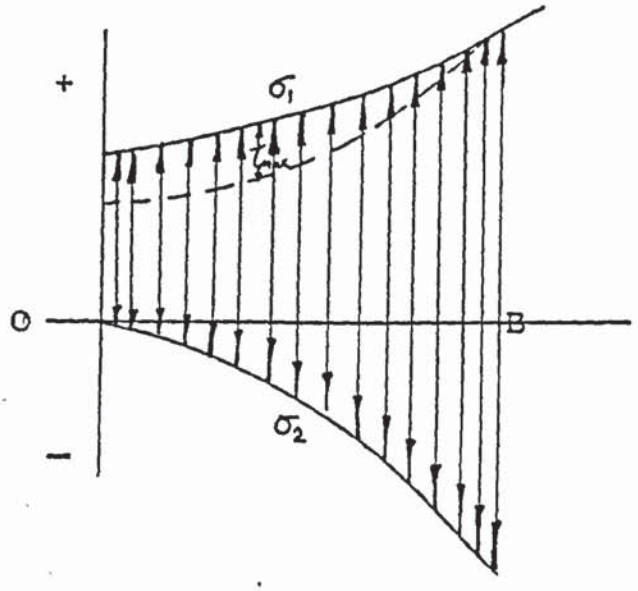

Figure 2.5 Principal stress and maximum shear stress distribution as reported by Salakian

In 1938, Jensen and Crispen[9] carried out investigations to clarify the lack of agreement between the contemporary theories of Shedd[53] and Schreiner[6]. They looked at simple longitudinal welded connections with plate bearing subject to combined bending and shear (see figure 2.6). The aim was to determine the stress distribution along the weld. Three tests were conducted and the stress analysis was based upon strain measurements. One of the three test specimens was thermally stress relieved.

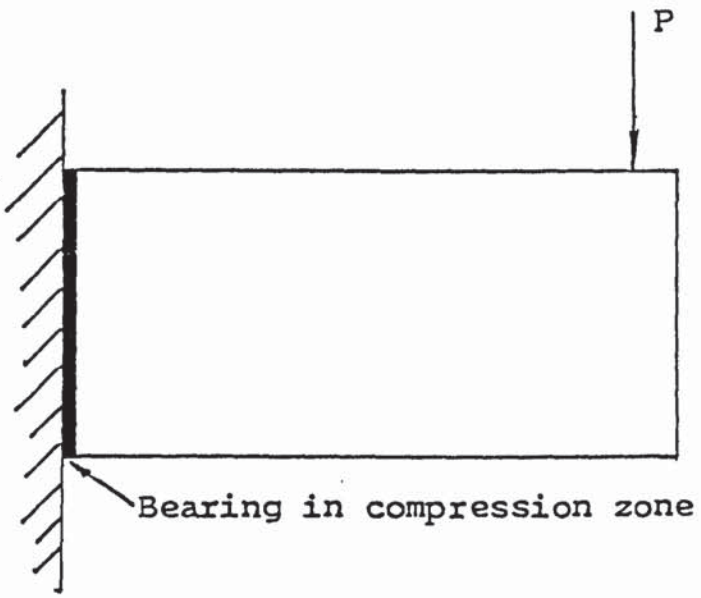

Figure 2.6 Jensen and Crispen's connection

Schreiner[6] who delt mainly with ultimate loads assumed a straight line distribution of stresses for loads below the yield point and non-linear distribution for loads slightly above the yield point. Shedd, however, suggested a general equation for the stress distribution of the form $Y^n = aSy$, and a specific one for the stresses on the extreme fibres for static loads and repeated loads of the form $S = 2(n+2)m/h^2$.

The experimental results of Jensen and Crispen were presented as in figure 2.7 and were found to be similar for all three specimens above and below the yield point. It is evident from the figure that the neutral axis passes through the weld centroid. Jensen and Crispen concluded that Shedd was correct below the yield point and Schreiner was correct at the limit state. It is difficult to see how Jensen and Crispen could arrive at this conclusion from their three tests, and moreover, Schreiner's theory is for connections without bearing.

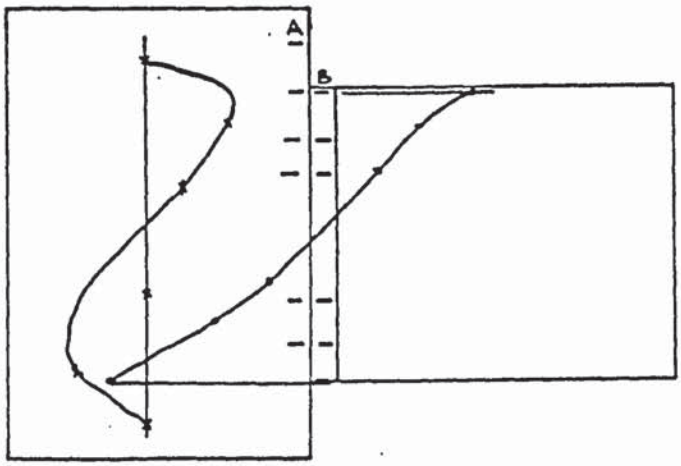

Figure 2.7 Experimental results of Jensen and Crispen

The moment-rotation characteristics and the ability to carry vertical loads of beam-to-column connections was studied in 1942 by Johnston and Deits[10]. Altogether, twenty-one specimens were tested, all being welded with gaps inbetween the end of the beam and the column. Only six of these twenty-one specimens however, produced useful results.

In all the six specimens the beam web adjacent to the welds yielded before the fracture of the welds. As a result of this and the uncertainty as regards the size of the weld, their test results can only be taken as a guide to the ultimate strength of the welds.

In 1945, Norris[11] investigated the stress distribution in fillet welds by photoelastic procedures, but attempts to solve the problem by the methods of the theory of elasticity were not very successful. Norris constructed such a model and reported the stress distribution along the

sides AB and BC (see figure 2.8 a and b) of the weld. An approximate graph of the results he obtained is shown in figure 2.8b.

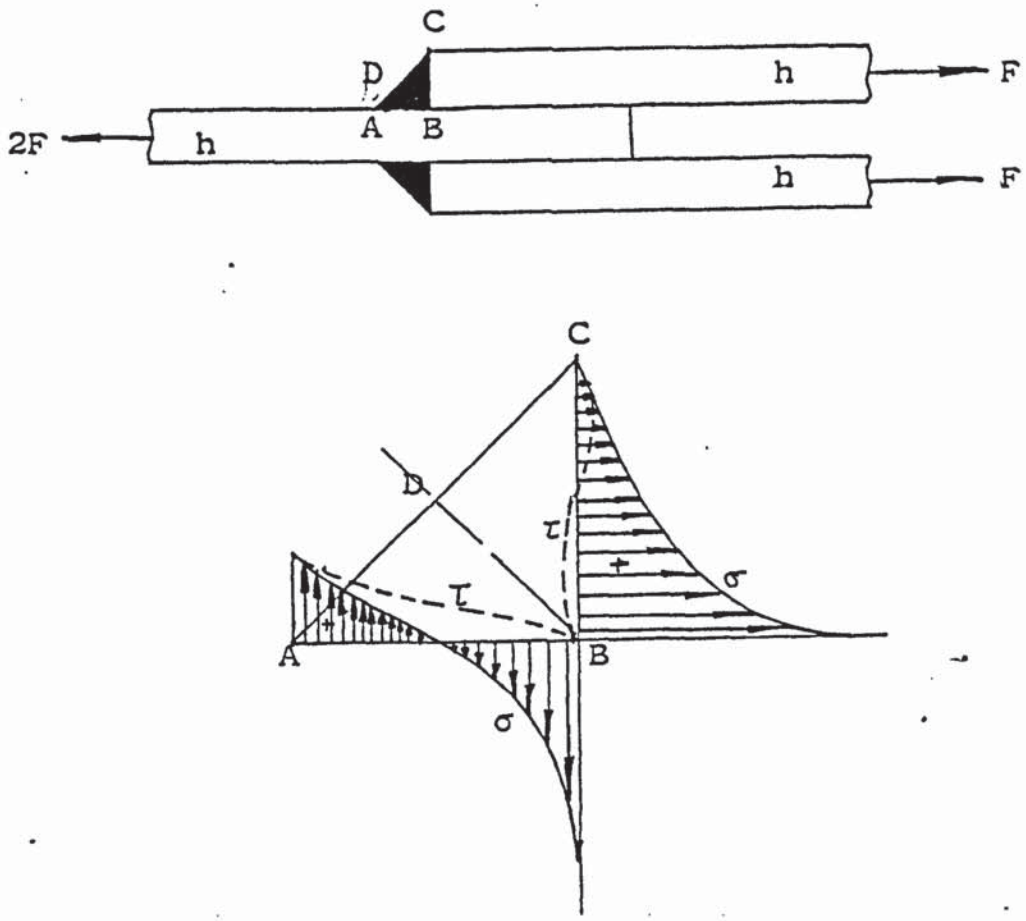

Figure 2.8 (a) Transverse fillet weld specimen tested by Norris

(b) Stress distribution on the legs as reported by Norris

The column in beam-to-column connections is frequently subjected to various combinations of forces. An investigation of the crushing strength of thin steel webs under various loading conditions was reported by Winter and Pian [12] in 1946. This work which was sponsored by the American iron and steel institute and Cornell University, recommended empirical formulae for the determination of crushing strength and factors of safety to be applied to these formulae in design.

One hundred and thirty-six tests involving eighteen different kinds of beams of thicknesses which ranged from 0.046 inch (1.15 mm) to 0.1473 in (3.69 mm) and depth 4 inches (100 mm) to 8 inches (200 mm) were carried out. The tests were designed to simulate loading conditions which a beam may be subjected to in practice.

They noticed that web distortion was confined to the immediate neighbourhood of the load. The web of lighter beams bulged out laterally but distortion of the heavier beams was confined to the regions directly adjacent to the load. Failure was observed to be due mainly to lateral distortion of the areas immediately adjacent to the load. They suggested that the phenomenon in that region was not simple yielding but a lateral displacement which they attributed to either plastic or elastic instability of these regions. They observed that bulging of the entire web occured subsequent to local distortion adjacent to the load and consequently attributed the primary cause of failure to local distortion. They concluded that the failure load is independent of flange thickness for the same web thickness and condition of loading. For the range of $\sqrt{b/t}$ from 2.5 to 8, they observed that the crushing strength for span failure was about twice that for reaction failure (b is the width of bearing and t is the web thickness). They however, concluded that the large degree of manufacturing imperfection associated with their specimens rendered their results not fully representative of rolled sections.

An important contribution to the subject of limit state design was made in 1951 by Koenigsberger [13]. He presented a method of determining the working loads of eccentrically loaded joints. The method presents a

means of determining the working loads of welded joints by evaluating stresses in the welds in the plastic state prevailing immediately prior to failure, and then applying a load factor. Analysis, previously, had been confined to the elastic state but this has resulted in high and unknown safety factors. The assumption by Koenigsberger that all welds in the joint were at a plastic state immediately prior to failure was in accordance with Schreiner's[6] suggestion.

Koenigsberger extended the analysis to brackets subjected to torsion and shear. This work is however not relevant to this thesis.

Koenigsberger used elemental analysis to determine the ultimate strength of the weld and was the first to treat the position of the centre of rotation as variable. He however, found the calculation required too complex and consequently he presented the solution in the form of graphs drawn for unit stress, unit weld size and unit spacing between welds.

Certain general assumptions made by Koenigsberger are considered to be important.

1. Failure occurred after the weld metal had reached a plastic state throughout, with a limiting ultimate shear stress.

2. Deformations in the plastic state occurred with an approximately uniform state of stress.

3. Conditions 1 and 2 above prevailed throughout the weld throat before fracture.

4. The centre of rotation lay on an axis passing through the weld centroid.

In 1952, an analytical and experimental study of the strength of rolled steel columns subjected to various combinations of axial load and end bending moment was undertaken by Ketter et al.[14]. This work which was the sixth in the series considered various conditions of end restraint and sixteen columns of slendeness ratio varying from 27 to 111. The main aim was to study the influence of relative magnitude of axial load on column strength, and consequently, more emphasis was placed on yielding and the criterion of strength. A solution based on simple elastic theory was also included together with an approximate buckling solution based on the work by Jezek.

They presented the initial yield interaction curves for the various loading conditions (see figure 2.9). Further work was expected to be carried out on this subject, consequently, no firm conclusions had been drawn. They however, noticed that residual stress in columns reduced their strength. None of the loading conditions studied was similar to that of this author.

In 1954, Vreedenburgh[15] analysed the contemporary limiting stress theories and compared them with his own test results. Having found none of them compatible, he suggested an empirical solution involving a pearoid

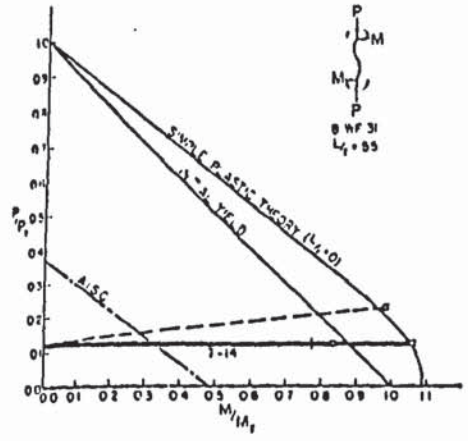
P
M
M
P
8 WF 31
$L_1 = 55$
SIMPLE PLASTIC THEORY ($L_1 = 0$)
$\frac{1}{2}$ - $\frac{1}{2}$ YIELD
AISC
T-14
P/P_y
M/M_y

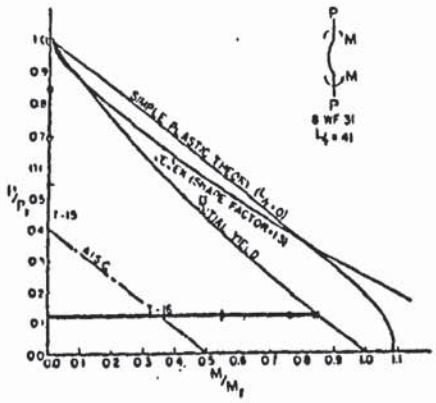
P
M
M
P
8 WF 31
$L_1 = 41$
SIMPLE PLASTIC THEORY ($L_1 = 0$)
T-15
AISC
T-16
P/P_y
M/M_y

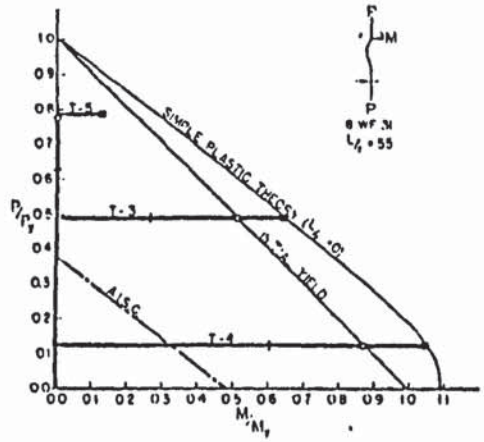
P
M
P
8 WF 31
$L_1 = 55$
T-5
SIMPLE PLASTIC THEORY ($L_1 = 0$)
T-3
AISC
T-4
P/P_y
M/M_y

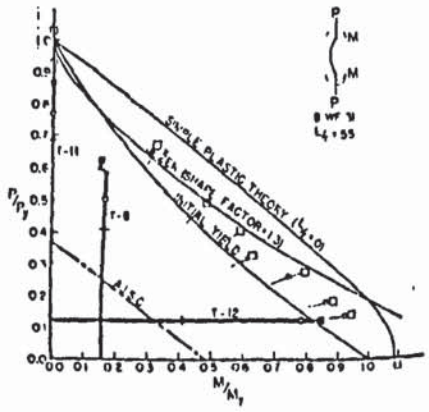
P
M
M
P
8 WF 31
$L_1 = 55$
SIMPLE PLASTIC THEORY ($L_1 = 0$)
T-11
T-8
AISC
T-12
P/P_y
M/M_y

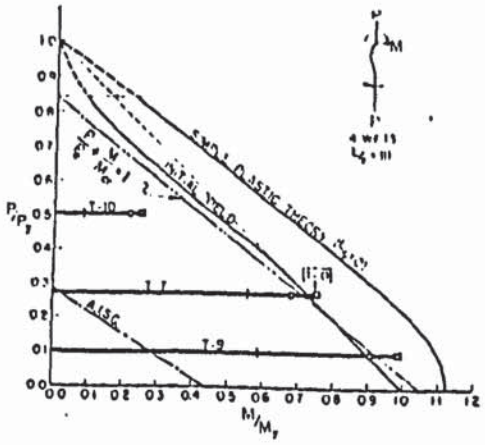
P
M
P
4 WF 13
$L_1 = 111$
SIMPLE PLASTIC THEORY ($L_1 = 0$)
T-10
T-7
AISC
T-9
P/P_y
M/M_y

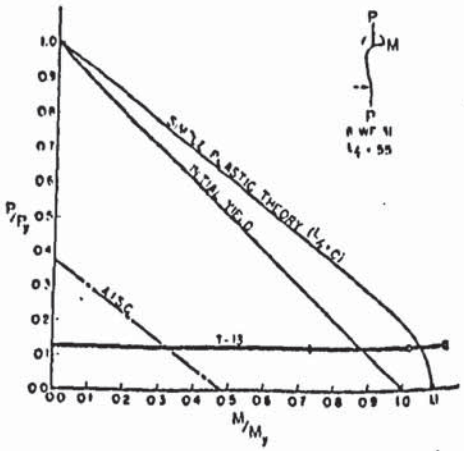
P
M
P
8 WF 31
$L_1 = 55$
SIMPLE PLASTIC THEORY ($L_1 = 0$)
AISC
T-13
P/P_y
M/M_y

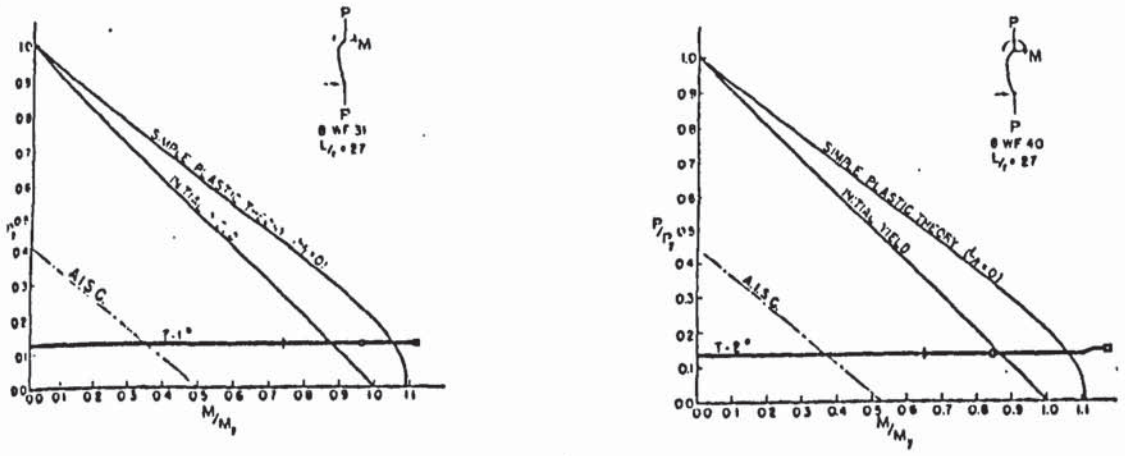

Figure 2.9 Interaction curves for the various loading conditions considered by Ketter et al

shaped limit state curve.

In 1959, Archer et al[16] carried out tests to determine the combined effects of shear force and bending moment on fillet welds. Their main aim was to derive an expression for the ultimate carrying capacity of welds subjected to bending moment about an axis perpendicular to their longitudinal axis. The work by Schreiner[6], according to Archer et al did not consider small ratios of eccentricity of load to weld length, and consequently could not be applied to short column brackets with small load eccentricities. They observed that the fracture angle varied with load eccentricity. They also found that the existing vector method gave safety factors of between 3.6 and 7.6.

An empirical expression for the maximum stress was proposed as follows:

$$\text{Maximum shear stress} = 1/2\sqrt{0.7\sigma_b^2 + 4\tau^2}$$

where σ_b = normal stress due to bending at extreme fibre

τ = shear stress due to vertical shear load.

The empirical constant of 0.7 in the above equation was based on the belief that the stress distribution due to bending lies inbetween the triangular and rectangular blocks when the weld is in a plastic state prior to failure.

They suggested that the above expression could be applied to joints with load eccentricities that their experiments covered i.e. eccentricities of between 0 and 1.3.

In the same year, Lightenberg[17] investigated the ultimate strength of beam-to-column connections. He tested connections in which web welds and flange welds were working in collaboration (see figure 2.10). The criterion $\sigma_c = \sigma_1^2 + 1.8(\tau_1^2 + \tau_{11}^2)$ which was proposed by Van der Eb and adopted by commission xv of the I.I.W in 1961 was referred to by Lightenberg. In that expression, σ_c was a critical stress of magnitude of the order of 4000 to 5000 kg/cm^2 and σ_1, τ_1 and τ_{11} were normal and shear stresses acting on the fillet throat.

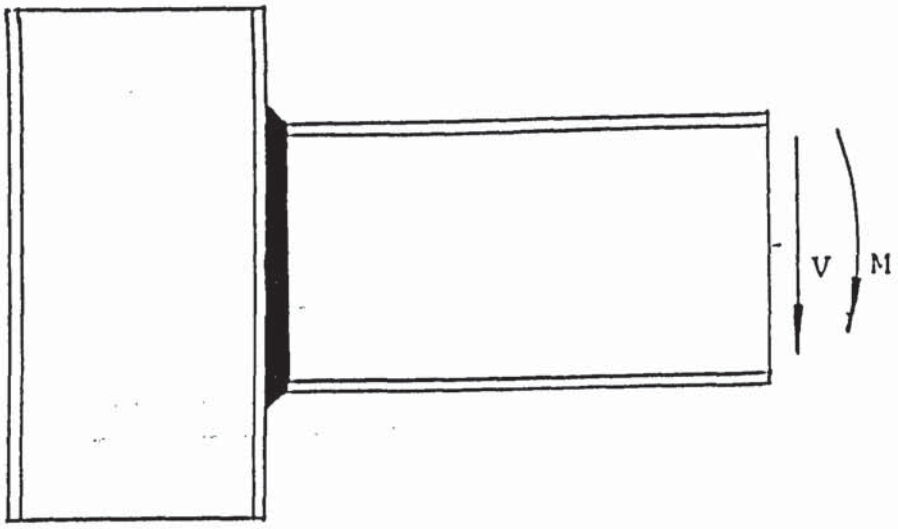

Figure 2.10 Lightenberg's Beam-to-column connection

Lightenberg suggested that for a group of welds working together, deformation is an important criterion since individual welds will be

subjected to differing deformation and that welds with a predominantly tensile stress at the critical plane were brittle compared with welds which were predominantly in shear at the critical plane. He pointed out that the determination of load-deformation characteristics would be difficult because of large deformations in the base material near the weld. He however estimated load-deformation characteristics (see figure 2.11).

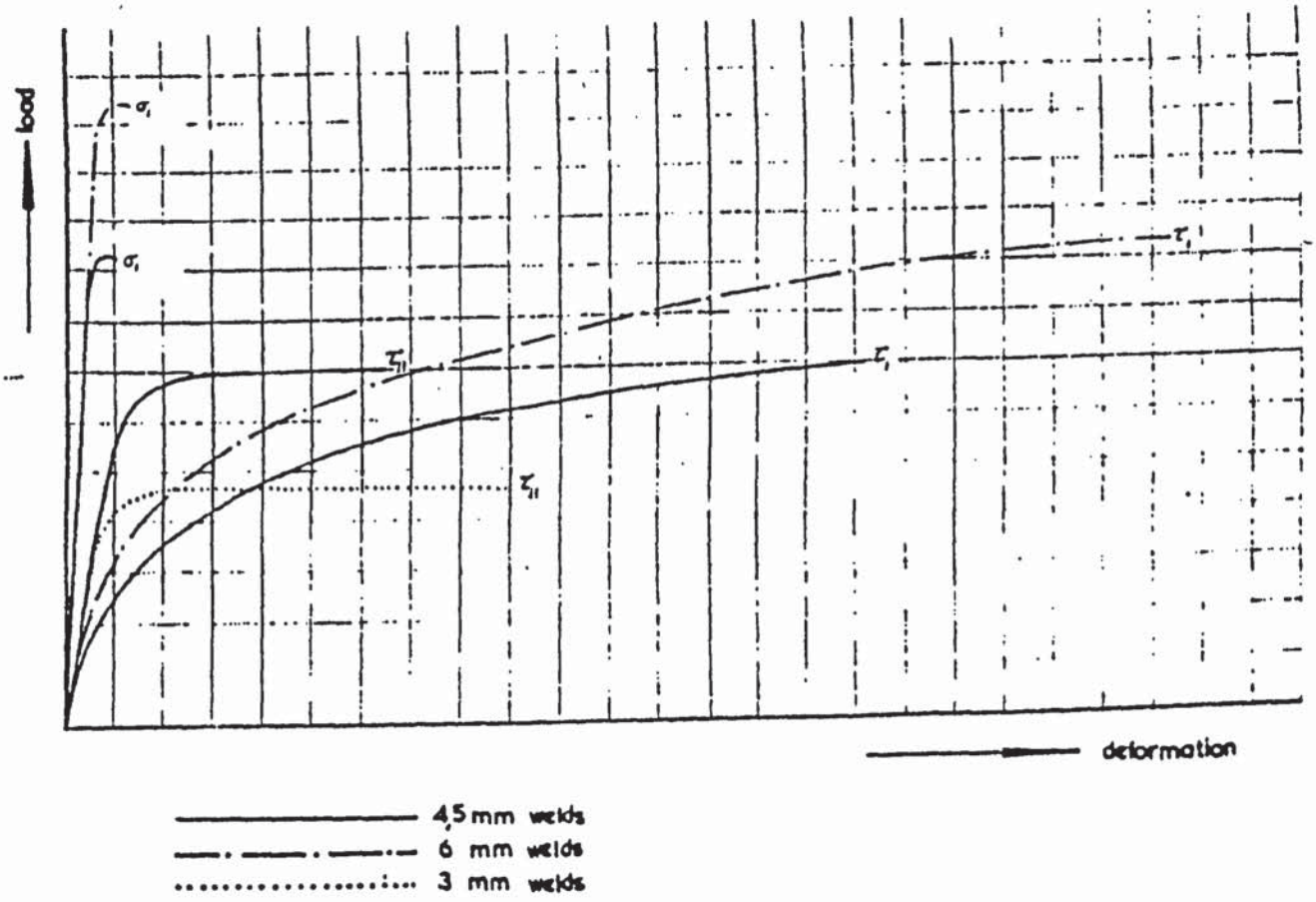

Figure 2.11 Load-deformation characteristics obtained by Lightenberg

With regard to the stress distribution in the weld group, the following variables were thought by Lightenberg to be the most important.

1. The flange width - flange deformation could control the shear force distribution along the flange; Lightenberg tested two flange widths - 119 mm and 200 mm.

2. Weld size - ideally weld thickness should be compatible with profile thickness everywhere. Two series were tested:

   (i) Flange welds 6 mm web 3 mm.

   (ii) Flange and web welds 4.5 mm.

3. Column rigidity - this would influence the stress distribution. Lightenburg tested a "rigid" column and a "ductile" column.

4. Load eccentricity. This ranged from $^{e}/_{d} = \infty$ to $^{e}/_{d} = 0.54$.

Before loading the web and flange welds in isolation, Lightenberg carried out twenty four tests on all round welded specimens using these four variables. He then proposed a theory based on the comparative stress criterion - $\sigma_c = \sqrt{\sigma_1^2 + 1.8(\tau_1^2 + \tau_{11}^2)}$ but pointed out the following:

a. it was not certain that any of the welds would be loaded uniformly over their whole length,

b. there was the possibility of forces being transmitted by plate bearing,

c. the flange weld under tension would be the first to break.

For the theory, the following assumptions were made:

(i) full plasticity for all the welds at the time of failure,

(ii) the neutral axis is at half beam height,

(iii) uniform shear loading between all of the welds,

(iv) equal strengths for corresponding welds above and below the neutral axis,

(v) equal strengths for welds on either sides of the flange,

(vi) the critical plane is always at the throat for all welds.

(vii) the bending stress distribution for all welds is rectangular,

(viii) the combined strength is equal to the sum of all the individual weld strengths.

Lightenberg then conducted twelve tests with welds at the outside flange only; four of which were under pure bending and for which a critical stress of value 4150 kg/cm^2 was established, the rest were subjected to bending and shear. For these, the shear load was assumed to be shared equally between the two welds.

The actual ultimate capacity of the welds in the 119 mm flange tests, was found to be well in excess of Lightenberg's prediction. This increased strength was attributed to the greater strength of welds under compression as indicated by the limit curve of Vreedenburgh[15].

Contrary to his expectation, Lightenberg found the actual strength of the welds in the 200 mm flange specimens to be half the computed value. He then concluded that for wide flanges, only half the flange width was effective in shear. This probably corroborates Freeman's[4] findings that the strength of fillet welds decreases as the length increases.

Lightenberg discovered that in pure bending, the observed strength was greater than the computed value in his tests on combinations of inner flange welds and web welds. He attributed this to plate bearing. Again, the observed shear strength was well below his expectation. In this case, he sugested that only the web welds were effective in resisting shear whereas all the welds resisted bending.

Lightenberg then turned to the results of his tests on all round welded specimen. He subtracted the actual strength of the flange outer welds from the total strength to give the actual strength of the weld group, the flange inner welds and the web welds. The strength he obtained was incompatible with his theoretical predictions except for pure bending condition. Actual strengths were well below predicted strengths for other conditions. This led him to suggest that the criterion broke down readily if the web welds carried a shear load corresponding to only half to one-third of their theoretical shear capacity.

The summary of Lightenberg's theory is as follows:

Weld group (a), flange outer welds only.

(i) both welds load uniformly by bending moment

(ii) shear load was uniform for the narrow flange

(iii) only 1/2 x flange width is effective in resisting shear for the wide flange

Weld group (b), flange inner welds + web welds.

(i) all welds were fully plastic under pure bending

(ii) shear forces were taken only by web welds, but only 1/2 x theoretical strength if the weld thickness were adapted to the profile thickness, and 1/3 if this was not the case.

Weld group (c), all round welded

(i) $\frac{M_a}{P_{sa}} = \frac{M_b}{P_{sb}} = \frac{M}{P_s}$

where M_a = Moment resistance of group (a) welds

M_b = Moment resistance of group (b) welds

M = Applied bending moment

P_{sa} = Shear resistance of group (a) welds

P_{sb} = Shear resistance of group (b) welds

where P_s = Applied shear load.

Lightenberg claimed that his theory was in good agreement with his results. His range of results is however limited ie only three values of the ratio of e/d were used viz 0.54, 1.7 and ∞ . The ultimate capacity of a connection for e/d = ∞ is relatively easy to predict. This then leaves two values of e/d to verify his theory. The limits of his theory were not stated and it would therefore be erroneous to apply his theory outside the range of the tests. Lightenberg concluded that the elastic theory of beams was quite insufficient and that load-deformation patterns should be relied upon more for the working of welds in combination.

In the same year, an experimental and theortical investigation into the behaviour of certain types of beam-to-column connections was carried out by Huang et al[18] with the purpose of developing improved design methods for safe, efficient and economical beam-to-column connections. They developed a theory based on mathematical models and physical models to predict the overall load-deflection behaviour of connections. In their analysis, they assumed that due to strain hardening, the flange carries a bending moment which exceeds the yield moment and that shear force is resisted by the web. They also carried out plastic analysis and finite element analysis of the connection.

They tested unstiffened, fully groove welded beam-to-column connection, flange welded, web bolted connection with round holes and flange welded web bolted connections with slotted holes.

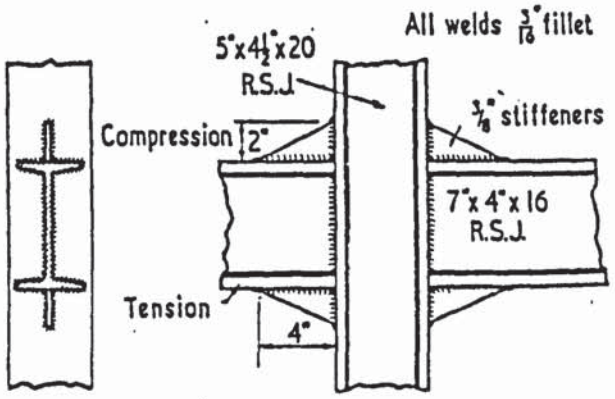

1—*Specimen 1*

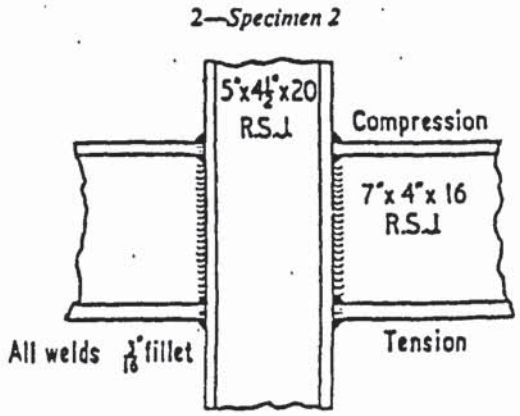

2—*Specimen 2*

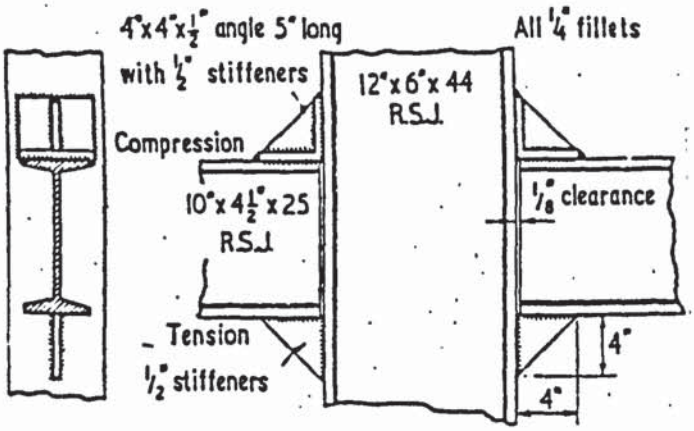

3—*Specimen 3*

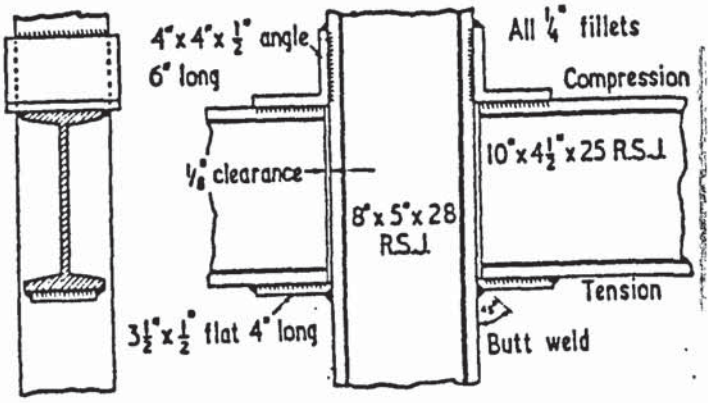

4—*Specimen 4*

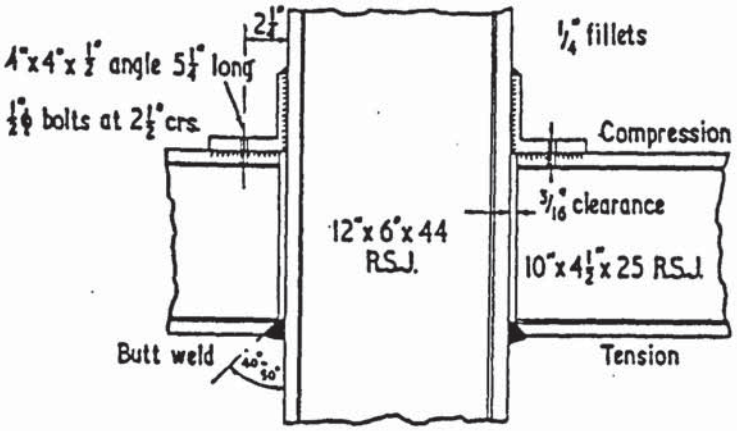

5—*Specimen 5*

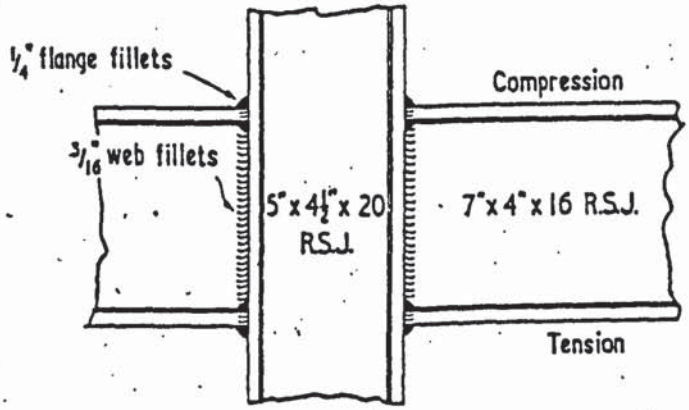

6—*Specimen 6*

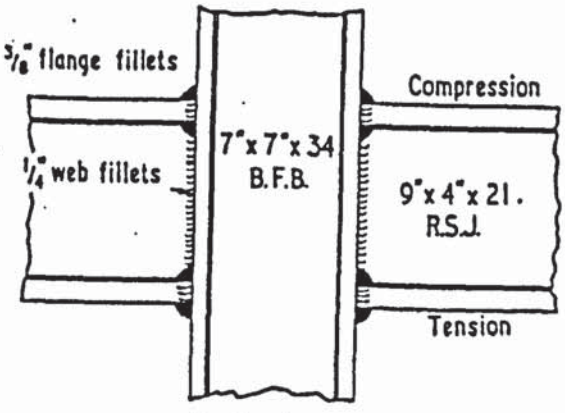

7—*Specimen 7*

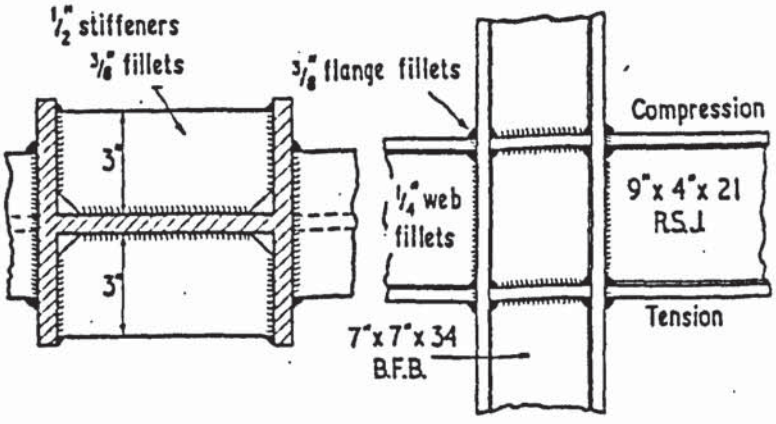

8—*Specimen 8*

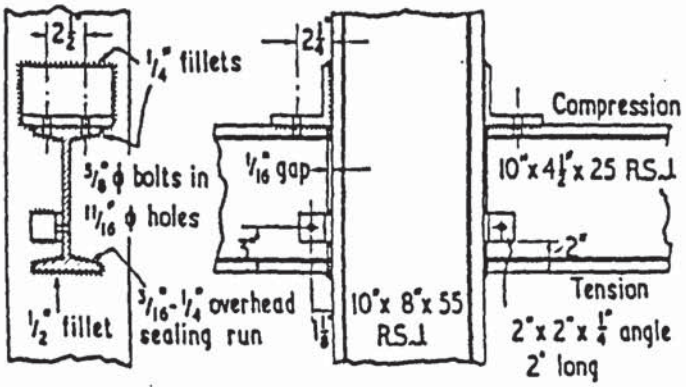

9—*Specimen 9*

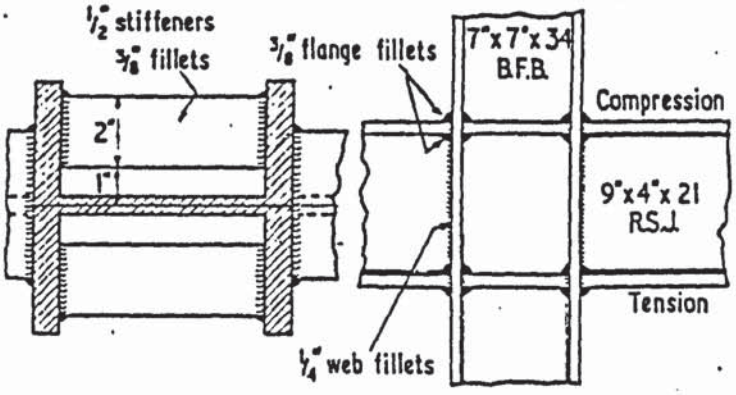

10—*Specimen 10*

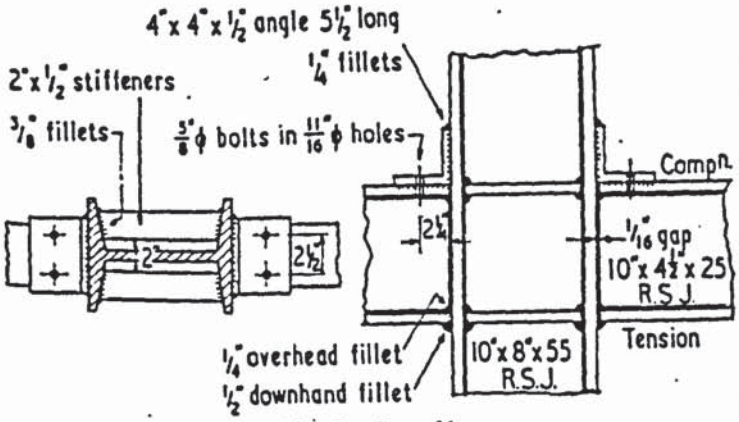

11—*Specimen 11*

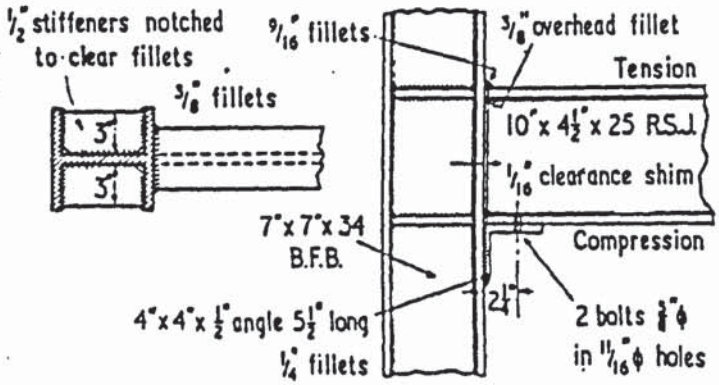

12a—*Specimen 12*

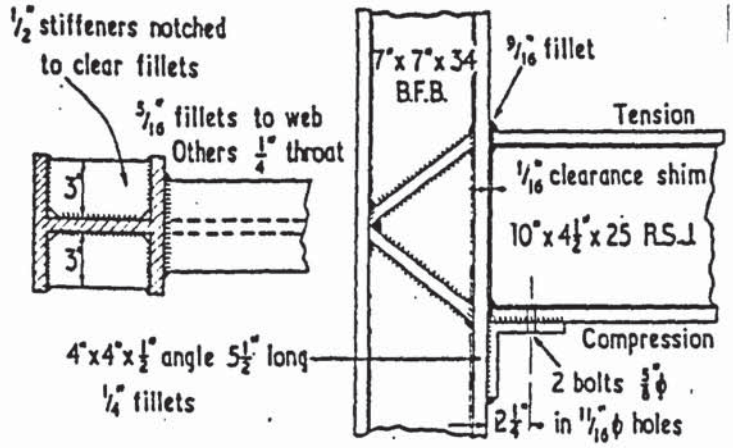

13a—*Specimen 13*

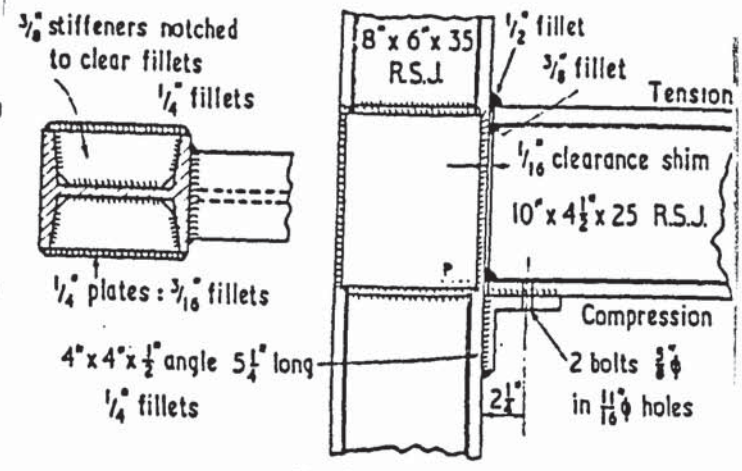

14—*Specimen 14*

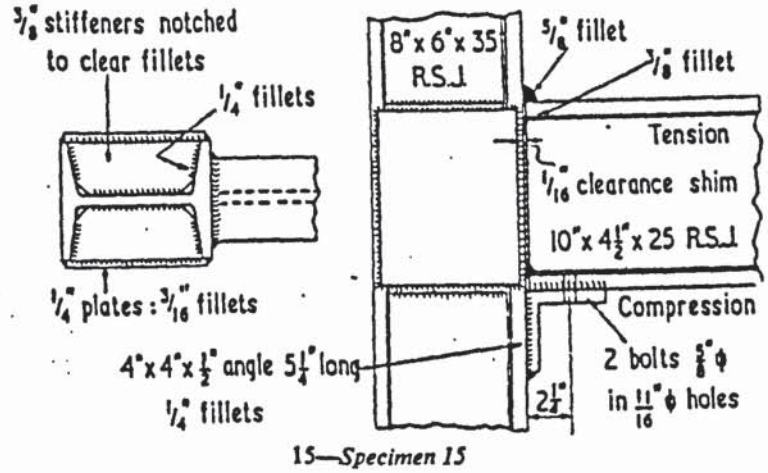

15—*Specimen 15*

Figure 2.12 Johnson's
Beam-to-column connections

They oberserved a good correlation between the theoretical predictions and their test results. They concluded that flange welded web-bolted connections may be used under the assumption that full plastic moment of the beam section is developed as well as full shear strength.

Also in the same year, Regec et al.[19] carried out a series of tests to investigate the load-rotation charactreristics of symmetrically loaded beam-to-column connections in which the beam flanges and webs were groove welded to the column flanges. The tests were designed to simulate seismic conditions and consequently the connections were subjected to three cyclic loads, at a span of 41 inches (1025 mm). Apart from the cyclic loading and the use of bearing stiffeners, the test arrangement was similar to that of this author.

The connection was found to have developed the plastic limit load, sufficient rotation capacity and adequate elastic stiffness and was therefore recommended for use in plastic design.

In the same year, an experimental investigation into the moment-rotation characteristics of various types of beam-to-column connections was carried out by Johnson[20]. Fifteen connections employing various types of stiffeners were tested (see figure 2.12). Weld sizes were also varied in order to determine the effect of weld size on the rigidity of such connections. The test arrangement and procedure was similar to that of this author. The moment-rotation characteristics of all the connections tested were presented in graphical form (see figure 2.13).

The tests showed that in the unstiffened connection, an increase of weld size by 1/16 of an inch from 3/16 inch to 1/4 inch (4.6875 mm to 6.25 mm) led to an increase in rigidity of the connection and the joint transmitting the full plastic moment of the beam. He pointed out that in unstiffened connections, the flexibility of the flanges results in stress concentrations in beam-to-column flange connections and that weld failure itself started in the corner near the root fillet of the tension flange of the beam. He noticed that even with stiffeners, this tendency still existed but to a lesser extent and at much higher loads. He recommended a continuous fillet weld round the entire beam profile if this was to be obviated.

The tests showed that horizontal stiffeners were unsatisfactory with one-sided connections. Only vertical stiffeners were satisfactory for this type of connection. Horizontal stiffeners were however discovered to be sufficient for double sided connections. He realised the problem stiffeners posed in the case of a beam framing into the column web and suggested the use of side plates providing a surface for such connections.

He recommended that stiffeners should be used and should not be larger than the beam flanges. He further recommended that for connections with equal sized beams on both sides and invariable identical end moments, horizontal stiffeners need not be welded to the web of the column. He concluded that if the throat area of the weld is made equal to the corresponding cross-sectional area of the beam, the beam-to-column connection should be able to transmit the full plastic moment of the beam. He observed that every weld failure occured in a plane inclined at about

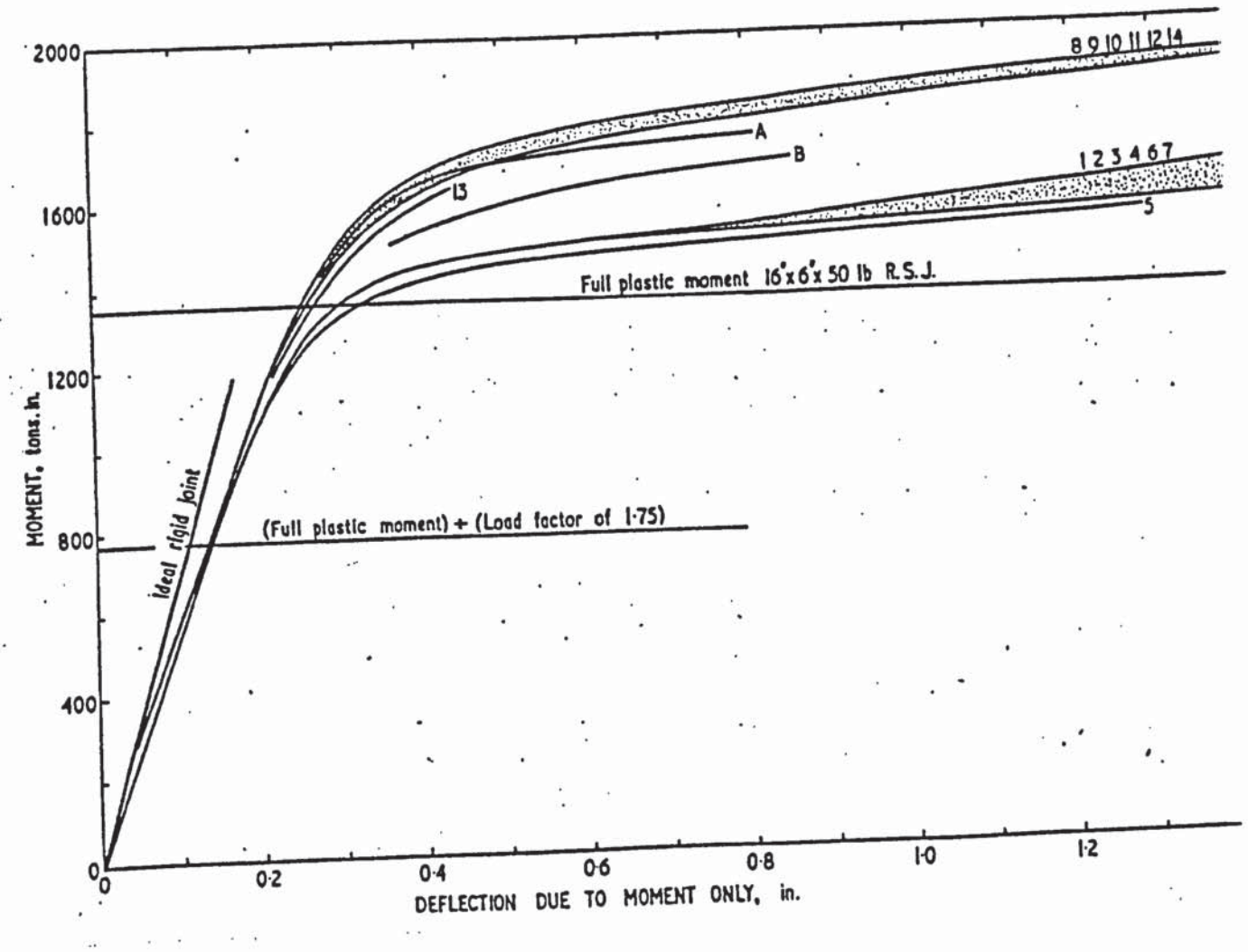

Figure 2.13 (a) Moment-Deflection characteristics for all the specimens tested by Johnson

20^0 to the direction of the applied forces.

Two months later, Johnson[21], in continuation of his earlier investigation carried out similar tests using full size beam and column sections. He felt scale effect might be of signifcance.

Sixteen variously stiffened fillet welded beam-to-column connections were tested, some with gaps between the beam and the column flange. All the specimens were basically similar except for the size of the gap between the beam and the column, the weld size and stiffener thickness. The gaps varied from 0 to 1/16 inch. Figure 2.13b shows a typical specimen and the method of loading.

Johnson concluded that if beam-to-column connection is designed in such a way that the column stiffeners are thicker than the beam flange thickness and the throat areas of the fillet welds are made equal to or greater than the corresponding sectional areas of the joist, the connections will safely transmit the theoretical full plastic moment of the beam. End clearance of up to 1/8 inch (3.125 mm) did not seem to have any effect on the sizes of the fillet weld required. He recommended that each web stiffener should be half the width of the flange of the beam and approximately the same mean thickness. He stated that exact fitting of stiffeners to the column for profile is not necessary but stiffeners must be in contact with the column web. A clearance of 1/32 inch (0.78 mm) between flange and stiffener was thought to be acceptable.

He further recommended that stiffeners in compression may be positioned by continuous 3/16 inch (4.7 mm) fillet welds and stiffeners in tension must have flange welds equal to those which connect the beam to the column. In such connections the web welds require to be only 3/16 inch (4.7 mm) fillets.

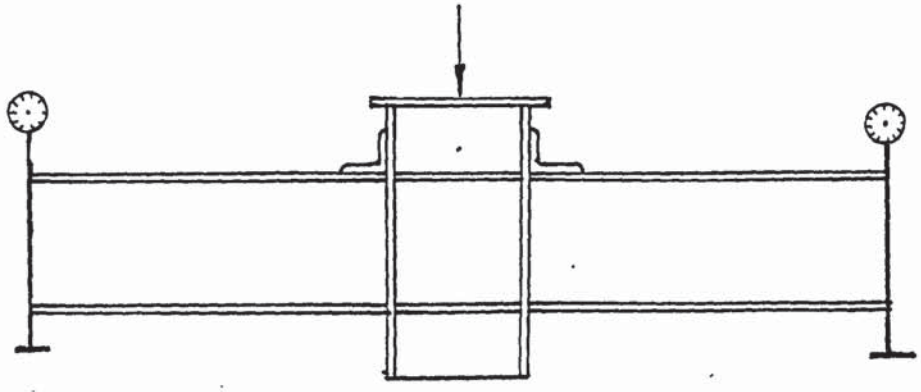

Figure 2.13(b) Johnson's experimental arrangement

Interaction curves relating axial thrust, applied end bending moment and slenderness ratio for the ultimate capacity of pin ended wide flange beam-columns were developed and presented in 1959 by Galambos and Ketter[22] using numerical integration method. Two conditions were considered viz: equal end moment applied such that the resulting deformation was one of single curvature and an end moment applied only at one extremity of the member. The influence of residual stress was considered in the analysis.

In 1960, Graham et al [23] having discovered that certain information on beam-to-column connections was lacking, conducted a series of tests on beam-to-column connections to provide information on column stiffening, moment rotation capacity and the effect on the flange connection of beam framing into the column web.

The investigations were both experimental and analytical and considered both stiffened and unstiffened connections. Tests simulating these practical conditions were carried out on both two-way and four-way connections. In the two-way connection tests, the attention was concentrated on whether column stiffeners were required and if so, how they were to be designed. Figure 2.14 shows the various types of two-way connections tested. Five different types of connections employing various types of stiffeners were tested. Figure 2.15 gives the summary of the test results. Tests were also carried out to simulate the tension and compression region criterion (see figure 2.16).

They noticed that failure in thin webbed unstiffened connections was due to web buckling. A detailed account of the behaviour of each of the connections was presented. They showed how the secondary beam may be connected to the column web via the stiffeners. The tests also showed that in many beam-to-column connections stiffening may not be necessary. The three types of secondary beam-to-column connections they tested are shown below (figure 2.17).

A report presenting views and ideas of member countries regarding the design methods for welded connections was published in 1964 by

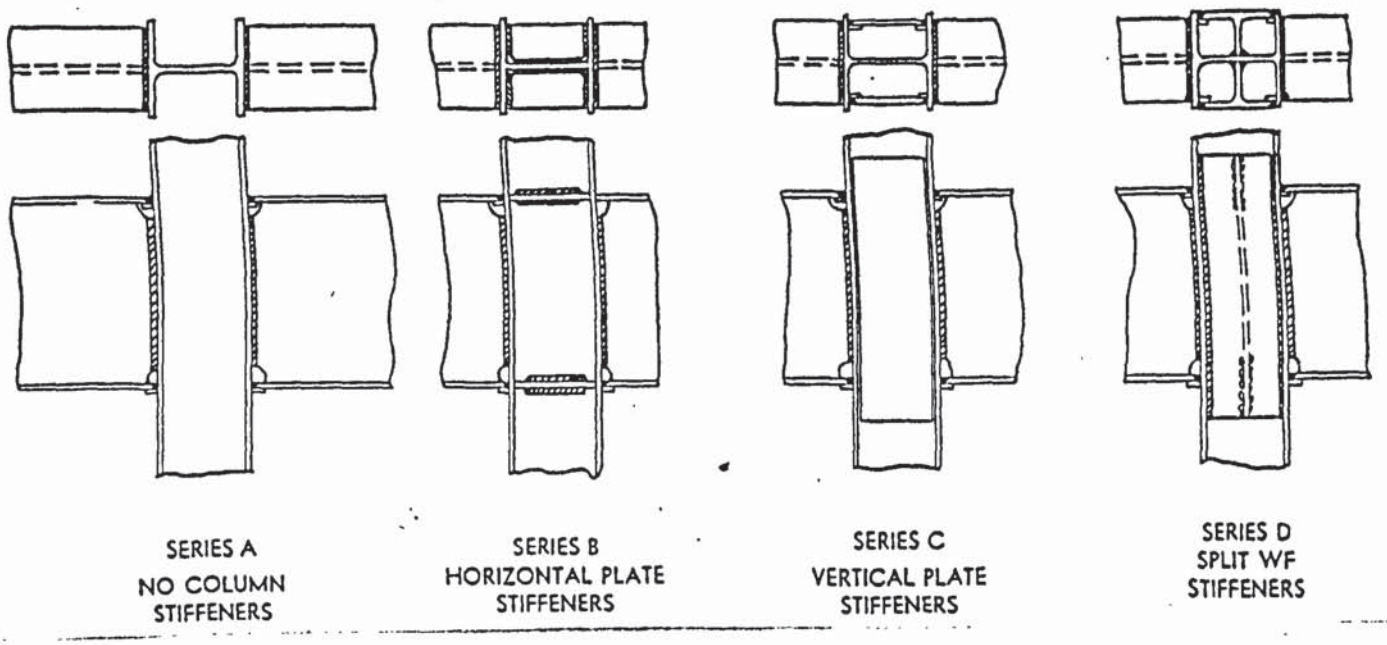

Figure 2.14 Two-way connections tested by Graham et al.

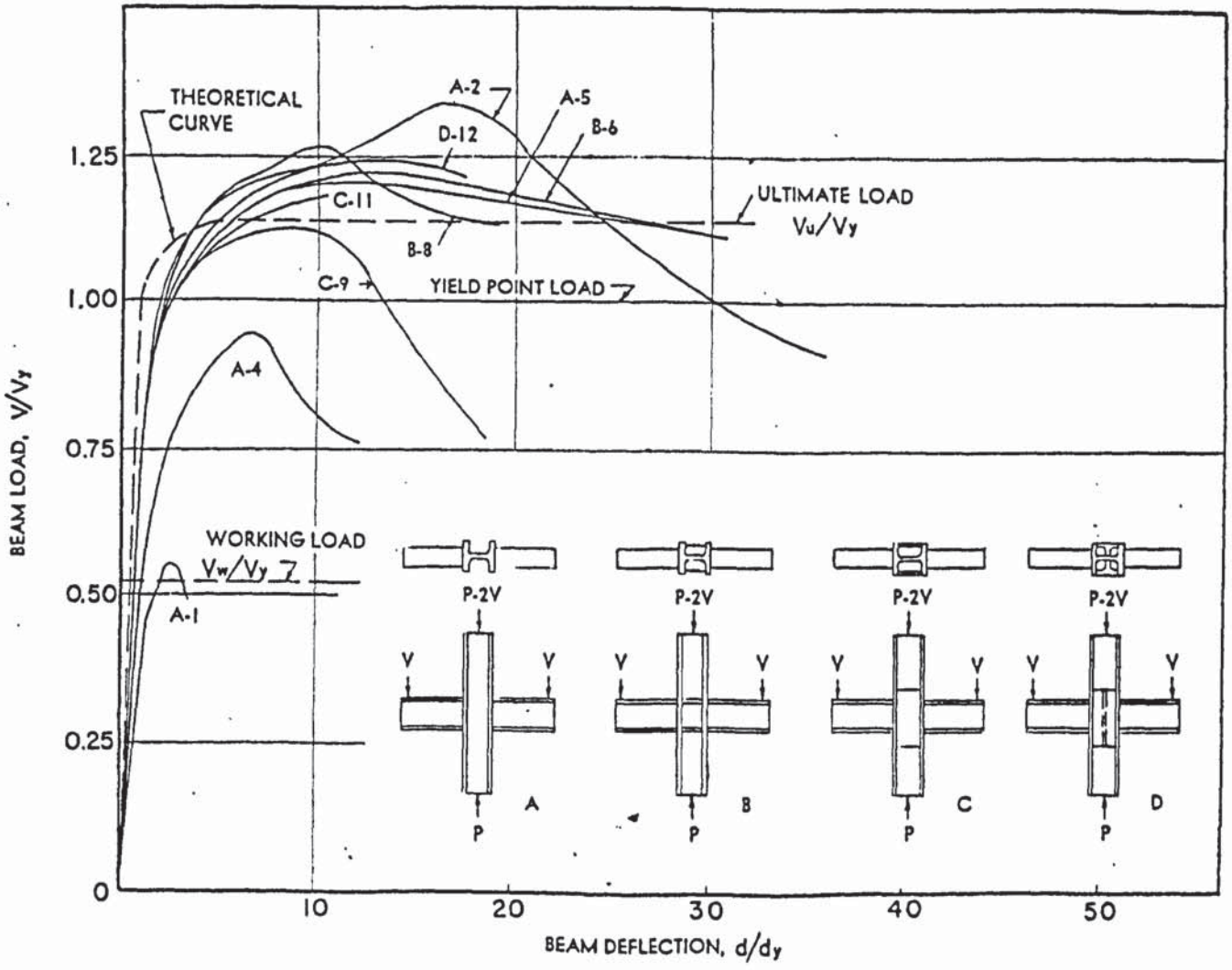

Figure 2.15 Summary of test results obtained by Graham et al.

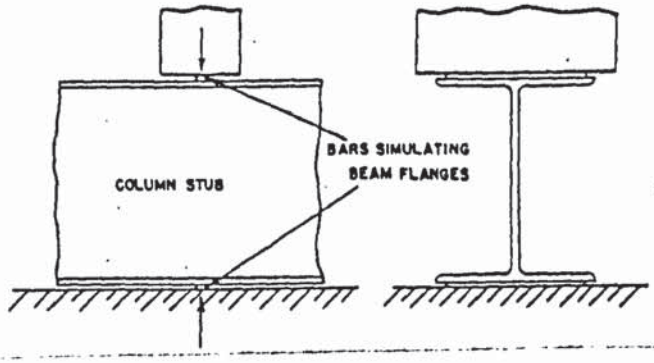

(a)

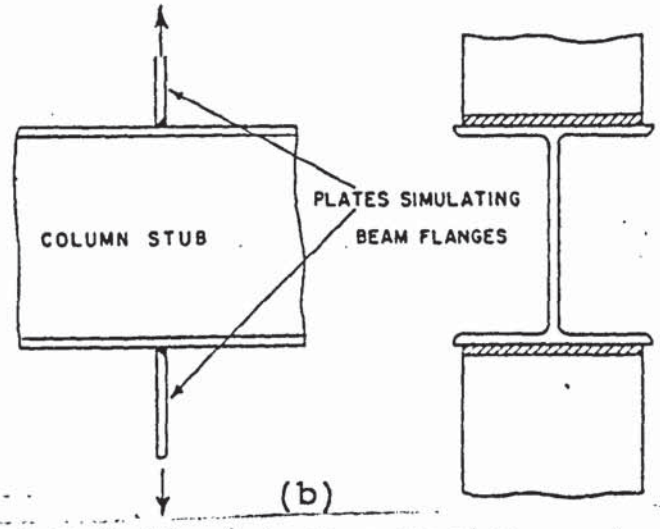

(b)

Figure 2.16 (a) Compression region criterion
(b) Tension region criterion

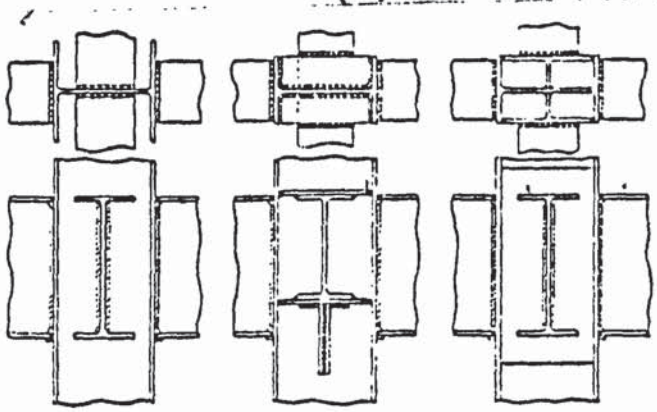

Figure 2.17 Four-way connections tested by Graham et al.

Commission XV of the International Institute of Welding (IIW)[25]. The calculation required for the analysis of connections subject to static loads was presented. The approved formulae were all based on the failure criterion proposed by Van der Eb which was approved at the ISO/TC44 meeting in Helsinki in 1961 i.e. $\sigma c = \sigma_1^2 + 1.8 (\tau_1^2 + \tau_{11}^2)$.

This criterion ignored residual stresses, assumed uniform stress distribution and assumed the weld throat was the critical plane. The safe working load σ_c was related to σ_p, the strength of the parent metal.

Reference was made to beam-to-column connections under combined bending and shear. For web welded connections with plate bearing (see figure 2.18), it was suggested that rotation took place about the bottom end of the weld and that stresses due to bending would be only tensile and of a triangular distribution, being a maximum at the top of the weld. Rotation had previously been assumed to take place at the neutral axis and the shear stress distribution was assumed to be uniform along the full length of the weld.

For flange welded connections (see figure 2.19) only the tension weld was assumed to resist the applied moment, rotation being assumed to take place about the compression weld.

It was recommended that this type of connection should not be subjected to high shear stresses presumably because of the limited deformation of these transverse welds.

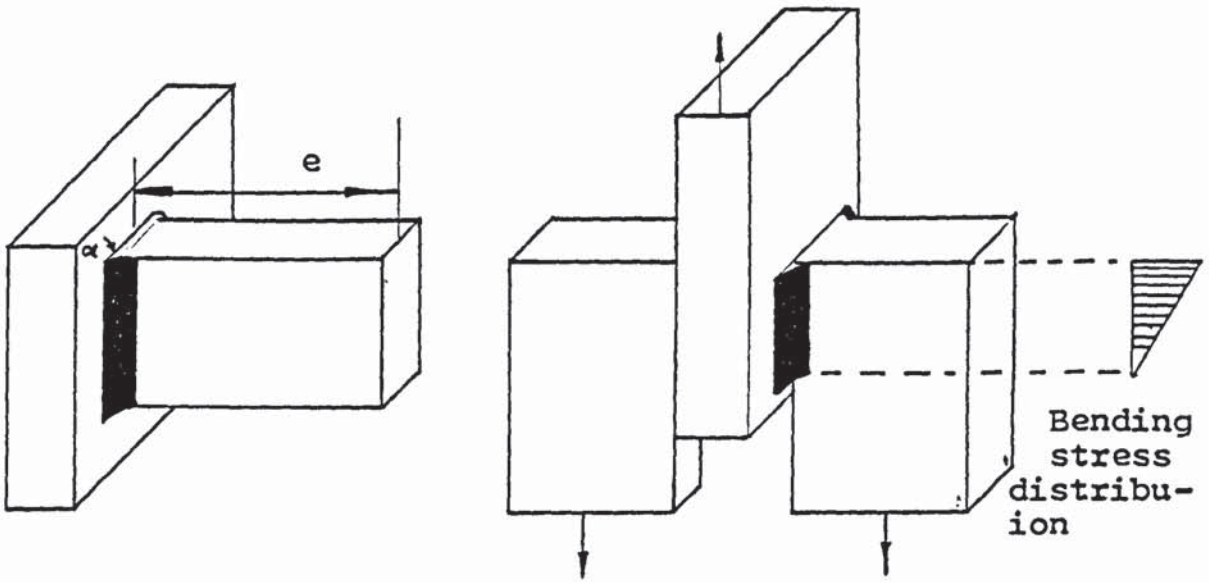

Figure 2.18 Welded connection with plate bearing considered by Commission XV

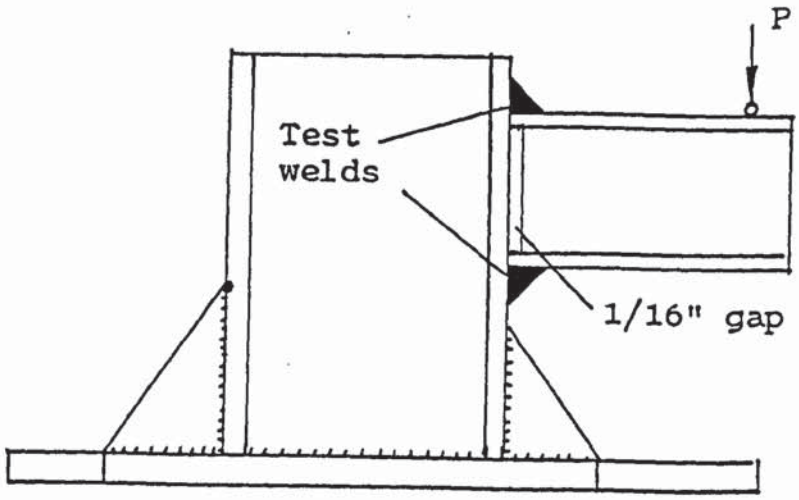

Figure 2.19 Flange welded connection considered by Commission XV

A suggestion of web welds resisting shear and all the welds resisting bending moment was made in the case of the combination of web and flange

welds. This might have been based on Lightenberg's [17] findings.

Criticism of the method of calculation proposed by the IIW are:

1. The throat is assumed to be the critical plane, whereas the angle of the actual plane varies. The use of a fixed plane of minimum area introduces variable safety factors.

2. The distribution of bending stress is triangular throughout, whereas full or partial plasticity pertains at failure.

3. Welds in compression are assumed to have the same strength as those in tension. Tests [51] have shown that compression welds are weaker.

In 1964, Archer et al [26] made an extensive study of the theoretical limiting stress criteria based on the principal stresses. A detailed analytical study of the strength of fillet welds subject to a load applied perpendicularly to the longitudinal axis of the weld was made. Seven different strength theories were considered and were compared with the experimental results of Jensen [5]. The failure criterion selected was used to estimate the ultimate capacity of flange and web welded connections.

The methods of strength prediction proposed by Biber, Jensen and Jennings and the cutrent Vector addition method were reviewed by Archer er al. A rigorous analysis of the welds of the test specimen

investigated by Jensen was presented. The iterative calculations which had to be applied to their proposed theory was found to be too tedious.

They also studied beam-to-column connections under combined bending and shear. The high scatter in the experimental results is not surprising. The welds were relatively short and for such welds, run on and run off tags should have been provided to ensure satisfactory weld quality. Some pairs of welds were also not of equal length. A graph showing the relationship between ultimate load and e/d was produced (see figure 2.20). The high scatter in their results makes it difficult for any useful conclusion to be drawn from this graph.

Based on the ultimate capacity of the tension weld, Archer et al produced design graphs for beam-to-column connections as shown in figure 2.21.

In welded beam-to-column connections, flange deformation has an effect on the distribution of load along the length of the flange weld. A study of this effect was first made by Elzen [27] in 1966, who carried out tests to determine the effective weld length when the applied force is directly perpendicular to the column flange face. Elzen was mainly interested in the effect of the shape of the column on the effective weld length and consequently studied stiffened and non-stiffened H - and box-sections (see Figure 2.22 for Elzen's H-section specimen).

The tests simulate a beam-to-column connection under pure bending conditions. The strip represented the bottom flange in beam-to-column

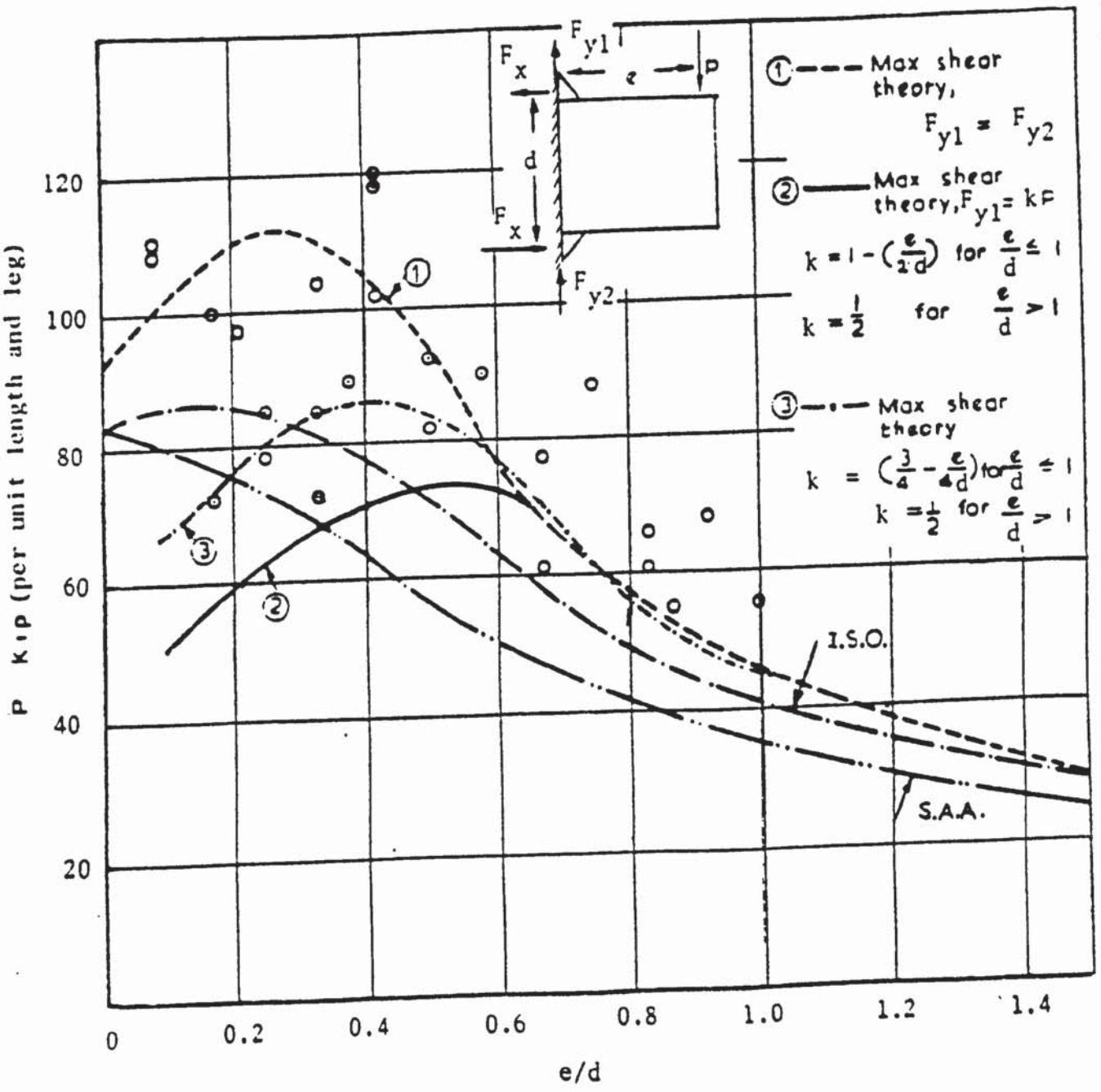

Figure 2.20 Relationship between Ultimate load and e/d obtained by Archer et al.

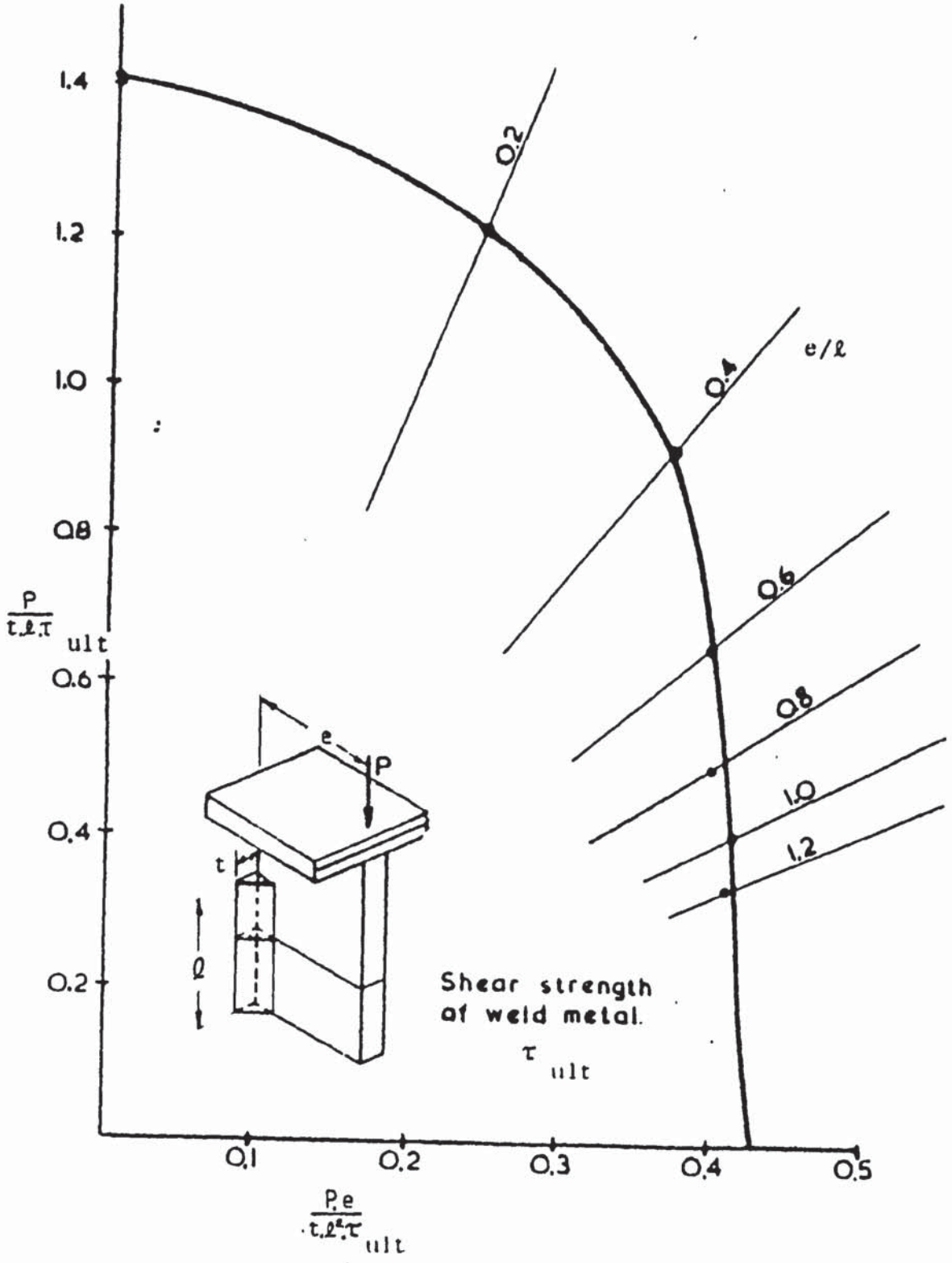

Figure 2.21(a) Design graph for Beam-to-column connection produced by Archer et al.

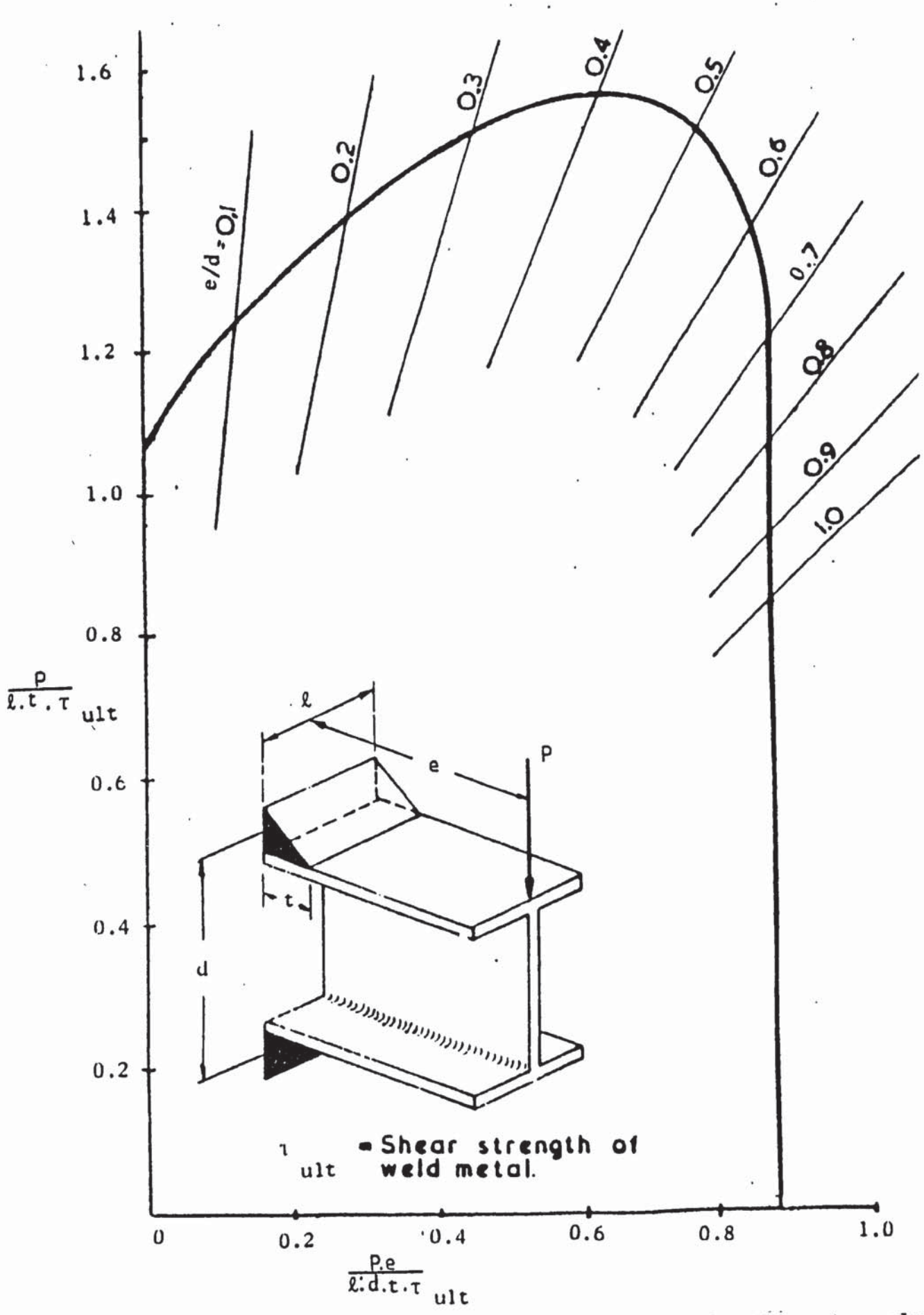

Figure 2.21(b) The second Design graph for Beam-to-column connection produced by Archer et al.

connections (tensile flange). Measurements were taken of the deformation of the column flanges and the stress distribution in the "beam flange" just above the welds by means of strain gauges. The strips which represented the beam flanges were 12 mm thick and 180 mm wide. There was no variation of the column flange width. For each test, Elzen noted the breaking load, flange thickness and sheet thickness. He defined the effective weld length as:

$$le = \frac{P \text{ breaking} \times \text{total weld length}}{P \text{ breaking of stiff section}}$$

In defining his effective weld length this way, Elzen assumed that for a stiffened section, the weld length is 100% effective. This assumption of 100% effective weld length for stiffened test pieces was thought by Elzen to be justified by the considerably smoother elongation of these test pieces shown by the strain gauges. The H-section gave considerably lower peak stresses than the box section (see figure 2.23). It can be seen that the stress distribution for the stiffened specimen is not quite uniform. It is however probable that for a rigid column, the weld length could be fully effective with a non-uniform stress distribution.

Elzen used the above equation and his test results to obtain the effective weld lengths for the H - and box-sections and using these values derived expressions for the effective weld length involving the side plate thickness σ and flange and top plate thickness β :

H-section $le = 2\sigma + x\beta$

Box-section $le = 2\sigma + y\beta$

where x and y have average values of 7.5 and 4.86 respectively.

Elzen observed that H-sections produced smaller deflections than box-sections.

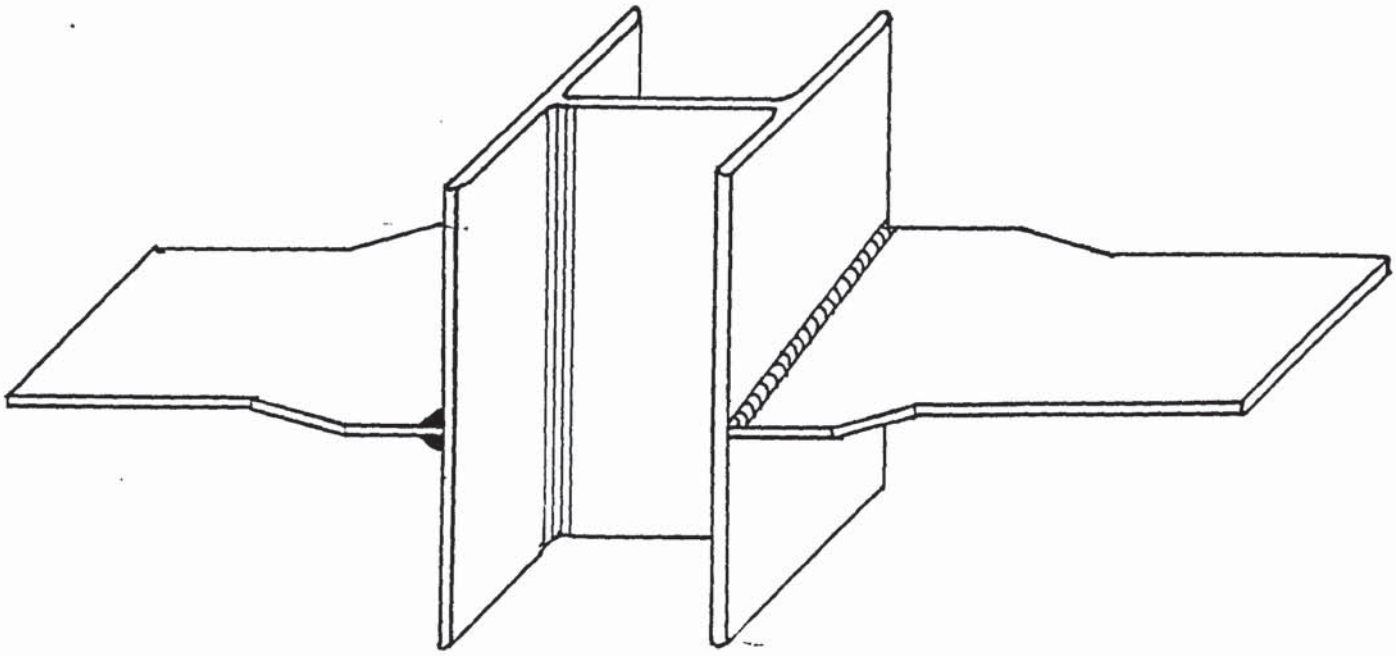

Figure 2.22 Elzen's H-specimen

Elzen's work is important for this author's work on the main beam-to-column connection, because it demonstrates the effect of the column flange flexibility on the strength of the weld. For the test to fully simulate beam-to-column connections under the usual loading conditions however, the effect of the compression weld on the tension weld should also be

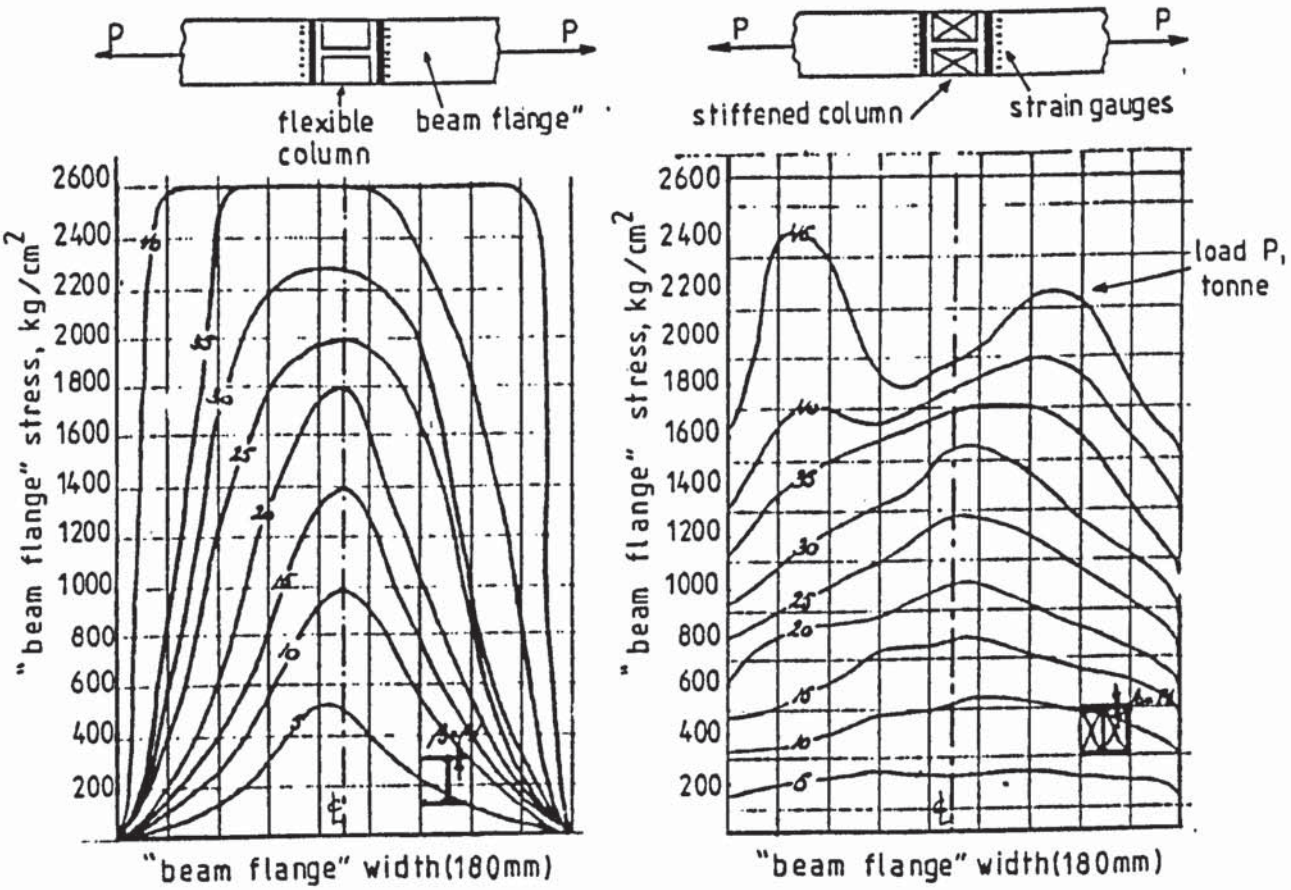

Figure 2.23 Stress distribution along the flange showing the effect of flange flexibility obtained by Elzen.

considered.

A year later, Batterman and Johnston[28] carried out an extensive study on the strength of columns. They sought to interrelate systematically, the residual stress and initial curvature effects but the study neglected the contribution of the web. Their results showed that separate effects of residual stress and initial curvature cannot be added to give a good approximation of the combined effect on maximum column strength. Residual stress has little effect on the maximum strength of very slender columns, either straight or initially crooked which have strengths approaching the Euler load.

In 1969, tests similar to that of Elzen[27] were reported by Rolloos[29]. Rolloos' tests were to determine the effective weld length of simulated beam-to-column connections as shown in figure (2.24). Like Elzen, Roloos used both stiffened and unstiffened H- and box-sections. Roloos, however, was more concerned about the effect of the non-uniform stress distribution in the weld due to the flexibility of both the column and beam flanges. Elzen used two different grades of steel for his tests (Fe 37 and Fe 52) and four different types of electrodes for the welds. The tests in Fe 52 were designed to determine whether the results obtained in the test series II in 1968 by the IIW doc XV-213 differed significantly from similar tests in Fe 37. Rolloos tested four identical test specimens in all the cases in order to obtain information on the scatter of test results. The use of different types of electrodes for the tests was aimed at confirming the earlier results of IIW doc XV-213-66 and XV-244-68 that the fracture of the test specimens without stiffeners depended on the

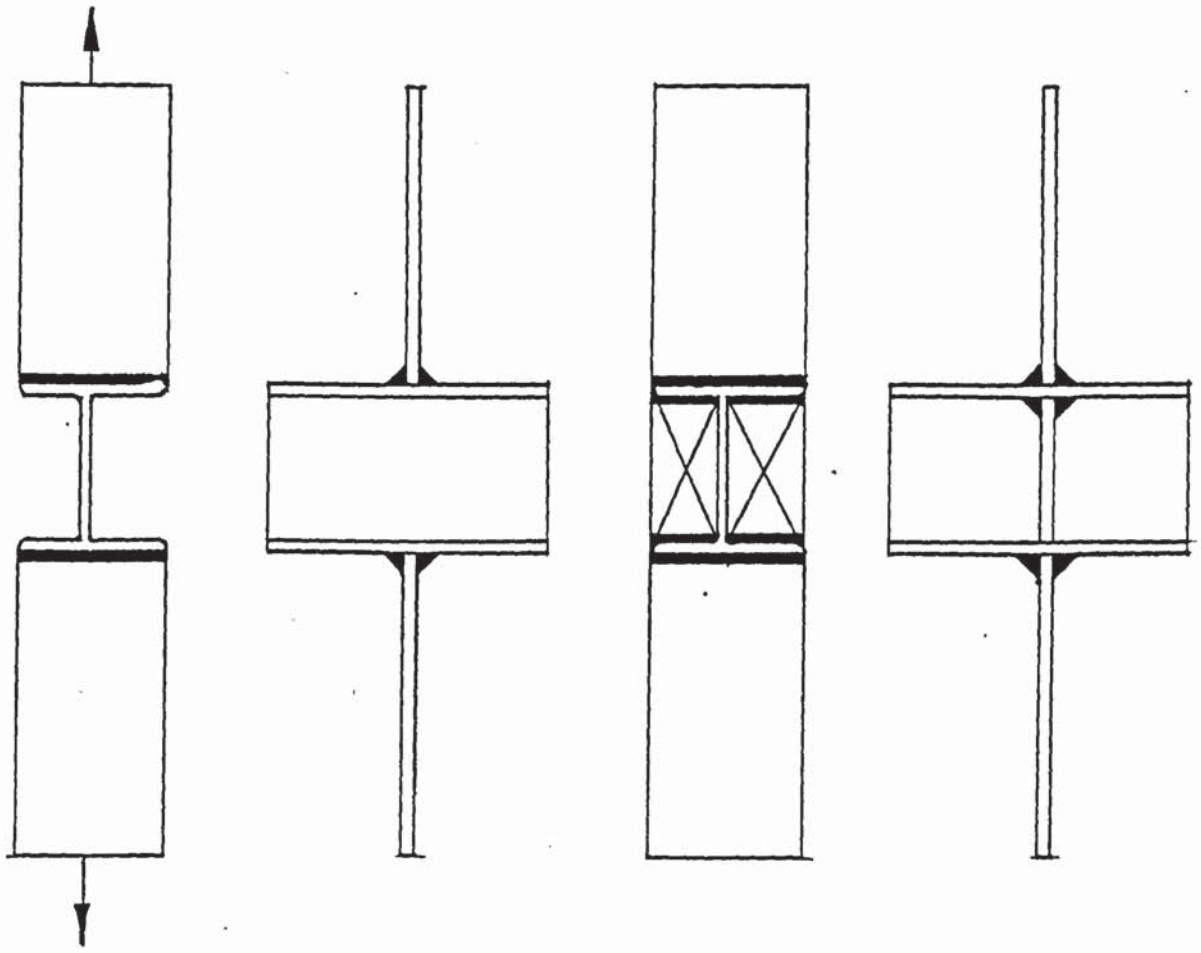

(a)

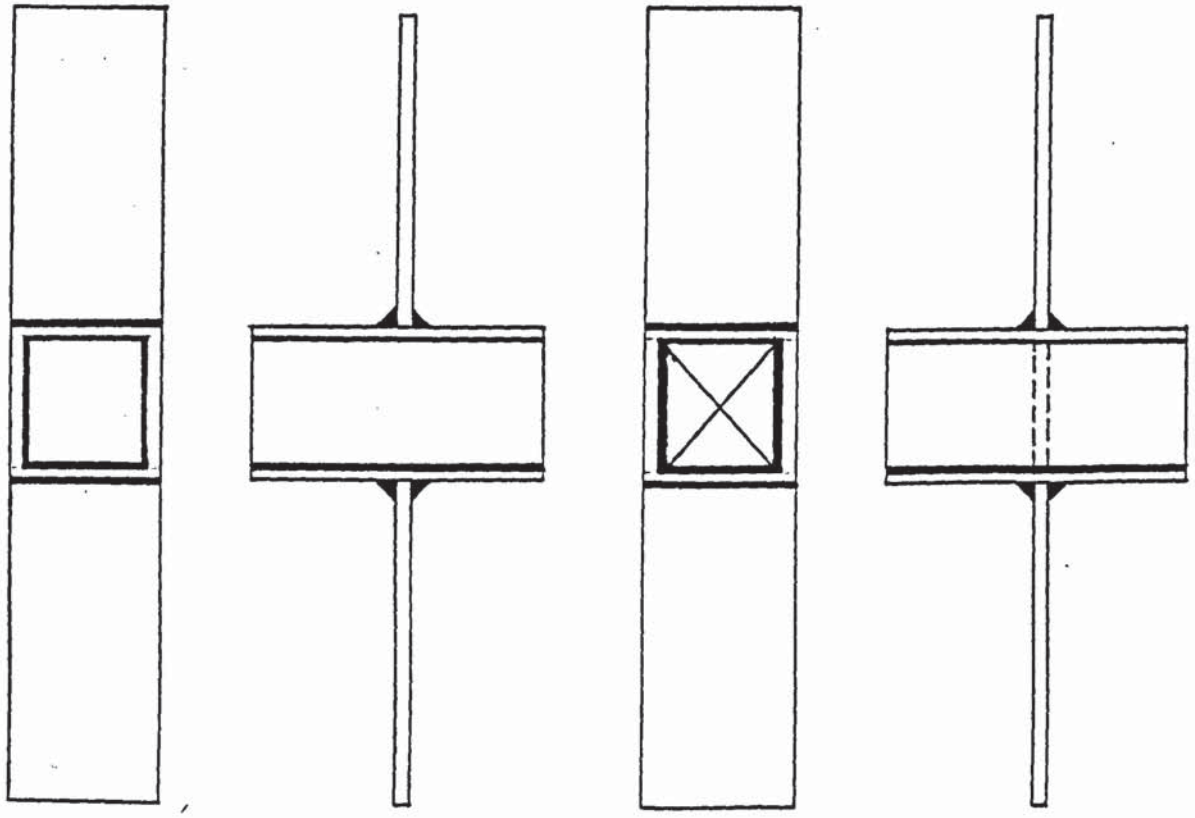

(b)

Figure 2.24 Simulation of beam-to-column connection

(a) H-section connection
(b) Box-section connection

electrode type used as the test specimens without stiffeners. To eliminate the dependence of the type of electrode used, Rolloos defined the effective weld length as:

$$le = \frac{\hat{P}'_{(o)}}{\hat{P}'_{(s)}} \; b$$

where le = the effective weld length

$\hat{P}_{(o)}$ = the reduced fracture load in tons for column without stiffeners

$\hat{P}_{(s)}$ = the reduced fracture load in tons for column with stiffeners

b = width of strip in milimetres

This expression is similar to that of Elzen [27].

Rolloos made the welds in Fe 52 specimens in two runs, the first with one electrode (Conarc 54) and the second with another electrode (Phoenix Union). Rolloos varied the flange thickness but not the flange width. This was maintained at 180 mm. He also carried out tests in Fe 37 with a flange width of 240 mm.

Rolloos determined the stress distributions from the strain gauge readings. Like Elzen, Rolloos assumed the weld lengths of stiffened specimens to be fully effective. Because, the effective weld length was

thought to depend mainly on the stiffness of the column flange and web plate (box-type column), the flange thickness β and the web thickness σ were taken to be the only variables. Rolloos arrived at the following conclusions:

1. The strength of the test specimens without stiffening plates is independent of the electrode type used, but depends mainly on the stiffness relations in the column.

2. The effective length found for a H-type column is about 1.3 times larger than the effective weld length found for a box-type column.

3. The effective weld length of a beam-to-column connection in Fe 37 is about 1.3 times larger than the effective weld length of a connection in Fe 52.

4. No influence could be found of the flange width on the effective weld length.

5. The effective weld length of H-type columns can be represented by:

   Fe 37: $l_e = 2\sigma + 8.0\beta$

   Fe 52: $l_e = 2\sigma + 6.4\beta$

6. The effective weld length of box-type columns can be represented by:

$$\text{Fe 37: } l_e = 2\sigma + 6.4\beta$$

$$\text{Fe 52: } l_e = 2\sigma + 4.8\beta$$

A criticism of the work by Rolloos is that he only investigated two close widths of columns but concluded that the effective length was independent of the width. The work did not take into account the effect of the column axial load and the effect of the compression weld on the tension weld.

Rolloos work is however important for this author's work on the main beam-to-column connection because it has shown the effect of the flexibility of the column flanges on the stress distribution in the weld in beam-to-column connections.

Extensive work on the effective weld lengths and joint efficiency in beam-to-column connections was carried out by various researchers in Japan. A compilation of the work in Japan was carried out by Kato et al [30] in 1971. This compilation included the work of Naka at al. [65], Miki et al. [66] and Okumura et al [67]. The work in Japan was similar to IIW's [41] work on the effective weld length in welded beam-to-column connections, but the strips which simulated the flange of the beam were groove welded to the H-section.

Naka et al. concentrated their work on the relationship between the stress concentration factor in the elastic range and joint efficiency and the influence of the dimensions of the test specimens on the maximum strength of the joints based on the results of their experiments.

Miki et al. investigated the stress concentration factor in the beam flange in the elastic range and also simplified the theoretical analysis of the stress distribution in the elastic range at the beam-to-column connection which had been put forward by Igarachi et al (56).
Miki et al. backed up their theoretical analysis by model tests. They also investigated the factor of relaxation C using steel models (steel grade Sm 41 - similar to Fe 37).

Miki et al defined the effective width of the column web ($_{c}b_{e}$) as:

$$_{c}b_{e} = {}_{b}t_{f} + \alpha k$$

Where $_{b}t_{f}$ = plate thickness of the beam flange

α = has a mean value of 6.77

k = distance from the outer face of the flange to the web toe of fillet of member to be stiffened.

The expression for joint efficiency was thought to be of the form:

$\eta = b\beta$

Where $b\beta$ is the stress concentration factor in the elastic range in beam flange and is a function of $F = 2ct_{f}^{3}/(3_{b}t_{f} * {}_{b}B^{2})$

C is considered as the function of the yield ratio of the material, the deformation capacity of the joint etc.

They also found that the joint efficiency of the beam flange (η) for high tensile steel is rather larger than that for mild steel in the case of groove welding, but the former smaller than the latter in the case of fillet welding.

In 1971, Fielding and Huang[33] carried out experimental and theoretical investigations into the condition of high shear stress and the effect of high axial shear force on simulated stiffened beam-to-column connections.

In their derivation of the theory for such connections, they adopted Von Mises yield criterion which was verified by tests. Their work showed the existing AISC design formula for such connection to be conservative.

Using the method of curve fitting, two interaction equations with four constants that are dependent on the size of the section were derived by Chen and Atsuta[36] for doubly symmetric wide flange sections subjected to combined axial force and biaxial bending.

A year later, Chen and Atsuta[37] extended their work to three dimensional analysis for biaxially loaded columns. This later analysis assumed the moment- curvature-thrust relationship to be elastic-perfectly plastic.

AISC specification, 1973 stipulated two formulae giving the requirements for stiffening the compression region of a column web at an interior beam-to-column moment connection. The formulae specified the strength a column will develop in resisting the compression forces delivered by the beam flange as:

$$P_{max} = (t_b + 5k)\, t\sigma_y$$

This equation was developed from the concept that the column flange acts as a bearing plate as shown in figure 2.25 below. The AISC specified that the application of the above formula be limited to cases in which the column web depth to thickness ratio (d_c/t) is small enough to preclude instability. The limiting ratio was defined as :

$$d_c/t = \frac{180}{\sqrt{\sigma_y}}$$

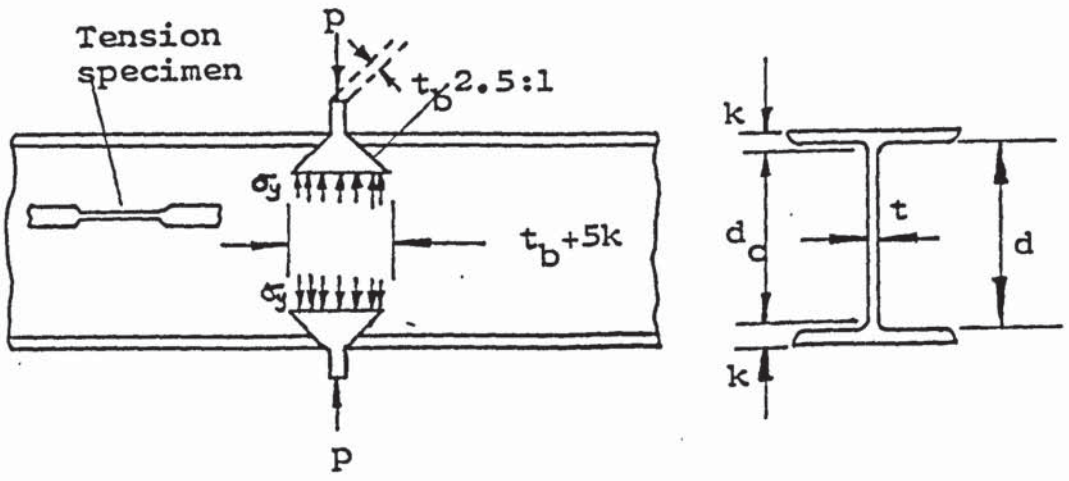

Figure 2.25 Simulation of compression region, Chen and Newlin

Tests were carried out by Chen and Newlin[38] to verify the validity of these formulae. Their tests showed the first equation above to be conservative for grades of steel up to 100 ksi (690 MN/M^2) yield stress for all the sections. They also discovered that the existing AISC specifications do not permit consideration of any load carrying capacity in compression region of sections with d_c/t ratios greater than $180/\sqrt{\sigma_y}$. They therefore carried out tests to develop a method of determing ultimate loads for such a condition.

They observed early yielding near the junction of the web and flange but noticed that this local yielding did not spread throughout the connection panel until just prior to ultimate load when the panels started to buckle.

They based their assumption that the concentrated beam flange load acted as a square panel of dimensions $d_c \times d_c$ (see figure 2.25) on the observations of the test results and results of their previous tests. Consequently they arrived at the following formula for the critical elastic buckling stress for simply supported edges:

$$\sigma_{cr} = \frac{P_{cr}}{d_c\, t} = \frac{\pi E}{3(1-\nu^2)} \left(\frac{t}{\frac{d_c}{2}}\right)^2$$

They observed that the elastic buckling load of a fixed edge long plate compressed by two equal and opposite forces is twice the buckling load of the same plate when it is simply supported. Their previous tests also showed that sections made of 100 ksi (690 MN/M^2) yield stress steel, having d_c/t ratio greater than that given by $180/\sqrt{\sigma_y}$, attained stress that approached twice the critical stress predicted by the simply

supported theory. Their test arrangement is similar to that of Graham et al.[23]

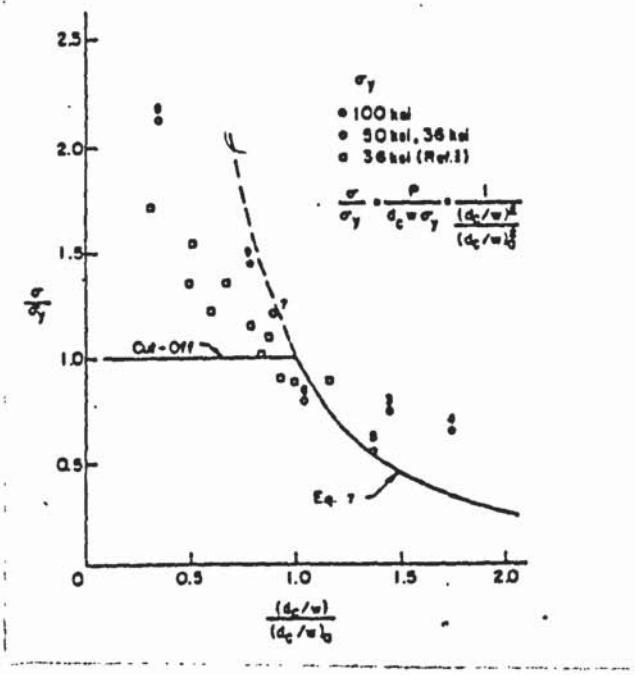

Figure 2.26 Curve for accurate strength prediction by Chen and Newlin

They concluded that the existing AISC formula 1.15-1 and 1.15-2 are conservative for grades of steel up to 100 ksi (690 MN/M^2) yield stress. When $d_c/t > 180/\sigma y$ stiffeners are not required but definetly required when $t < C_1 A_f/Ct_b + Sk)$ or $d_c > 4{,}100\ t^3/(A_f C_1 \sqrt{\sigma y})$ or both. In the above expressions A_f is the area of one beam flange, C is the ratio of beam yield stress to column yield stress.

In January the following year, Chen et al.[39] carried out further study on the AISC formula governing column compression region stiffening requirement - $W = \frac{C_1 A_f}{t_b + 5k}$ and the instability effect. They extended their investigation to include columns of high strength steel.

The tests they carried out are similar to those of Graham et al.[23] and Chen and Newlin[38]. Their analysis was based on the assumption that the flanges act as bearing plates to spread the concentrated beam flange force over the length (t_b + 5k) and that the flanges provided simply supported edge conditions for the web panel.

Just like Chen and Newlin, they concluded that as far as strength and stability are concerned, the AISC specifications are conservative. Consequently they produced a graph which they felt could be used to predict the strength and stability of columns more accurately. See Figure 2.26.

In beam-to-column connections, rotation is usually assumed to occur in the middle of the beam. This situation could however be altered if the compression region is stiffened or the column flange is rigid enough to prevent deformation. Rotation could therefore take place at the beam compression flange, restricting the deformation of the weld in that region. Dawe and Kulak[40] carried out theoretical and experimental investigation into such cases in 1974. They developed methods of predicting the ultimate capacity for connections in which the deformation of the weld is restricted in the compression zone. Their method was based on the recognition of a load-deformation response of individual weld elements and the assumption that a continuous line of weld can be broken down into a series of these individual elements.

They based the prediction of capacities of full size eccentrically loaded welded connections on the load-deformation response of individual

weld elements expressed by the relationship:

$$R = Rult\ (1 - e^{-\mu\Delta})^{\lambda}$$

Where R = weld element load at any deformation

Rult = ultimate load attainable by the weld element at any given angle of loading.

Δ = deformation of the weld element due to the combined effect of shearing, bending and bearing stresses as well as local bearing deformations in the connecting plates;

μ, λ = experimentally determined regression coeficients.

e = base of natural logarithm

The analysis was based on the load-deformation response of a simple lap joint. They pointed out the existence of frictional forces between the plates in bearing in the compression zone.

They concluded that the existing factors of safety for these types of connections are unjustifiably high and vary with the ratio of eccentricity to weld length.

In 1974, Tebedge and Chen[41] developed interaction curves for simply supported columns based on their experimental and theoretical work

on short and long columns subjected to compression combined with biaxial bending under symmetric and unsymmetric loading conditions. These interaction relations which were presented in tabular form, were intended to be used for design and direct analysis. The interaction equation for short columns was thought to be of the form:

$$\left(\frac{M_x}{M_{Pcx}}\right)^{\alpha} + \left(\frac{M_y}{M_{Pcy}}\right)^{\alpha} = 1$$

$$\text{or} \quad \left(\frac{M_x}{M_{ux}}\right)^{\beta} + \left(\frac{M_y}{M_{uy}}\right)^{\beta} = 1.0$$

$$\alpha = 1.60 - \frac{P}{2\ln P} \quad \text{for short columns}$$

$$\text{and } Mm = 1.07 - \frac{\frac{\ell}{ry}\sqrt{\sigma y}}{3,160} \qquad M_{Px} \leq M_{Px}$$

$$\beta = 1.40 + P$$

where M_x, M_y = maximum applied moment about x and y axes respectively

MP_{cx}, MP_{cy} = plastic moments modified to include effect of axial compression

M_{ux}, M_{uy} = maximum end moment that can be resisted by member in plane of bending including axial load but in absence of other moment

M_m = maximum moment that can be resisted by member in strong axis bending in absence of axial load

γ_y = radius of gyration

σ_y = yield stress

P = applied axial load.

Comparison of the Column Research Council (CRC) interaction formulae with their calculated theoretical values showed the formula to be over-conservative for short columns, conservative for intermediate colums and less conservative for long columns.

The interaction curves for different grades of steel are shown in figure 2.27 below.

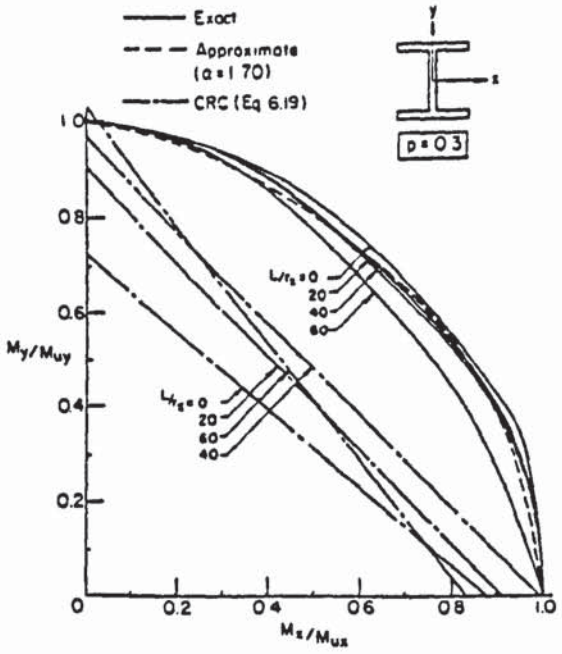

Figure 2.27 Interaction curves for different grades of steel by Tebedge and Chen

A paper presenting the results of experimental and theoretical study of unsymmetrical secondary beam-to-column connections in which an axial load was applied to the column was published in 1975 by Chen and Rentschler (42) Figure 2.28 shows the experimental arrangement. The theoretical analysis ignored the effect of column axial load and beam shear on the connection. Their attention was mainly on how this type of connection can be designed. They first of all carried out preliminary tests to provide the necessary information on member sizes, connection geometry and stiffener requirements.

Eight different specimens involving two different column sizes were tested under the preliminary scheme. These tests involved cases where the beam flange is narrow enough to be welded directly to the column web and

cases where a plate had to be welded to the column flanges to provide a surface for the beam to be welded on. In the case where the beam was welded directly to the column, the test was supposed to provide experimental evidence which could be used to check the existing yield line theory and to provide information on stiffening requirements.

The tests involved the variation of the beam flange width up to the point where the beam flange is wider than the distance between the column flanges. No conclusion could be drawn from this investigation since only preliminary test results were presented.

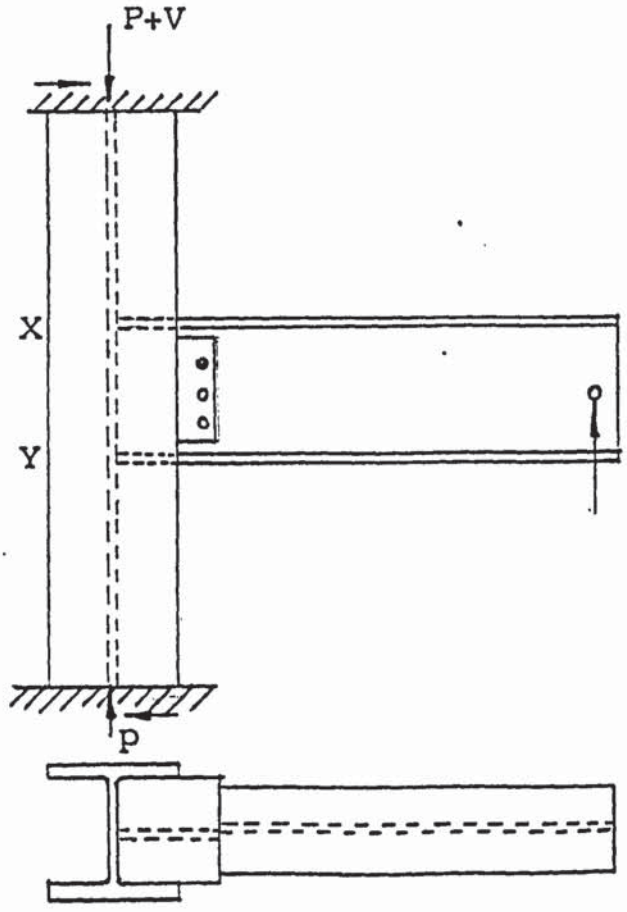

Figure 2.28 Secondary beam-to-column connection tested by Chen and Rentschler

In 1976, Parfitt et al.[43] carried out tests on three types of connections involving beams and columns to study the behaviour and then develop a theory for the design method of moment resisting beam-to-column connections. Twelve full size beam-to-column connections consisting of three interrelated welded connections were tested. See figure 2.29.

Parfitt et al. found that buckling of the beam seat web could occur in the case of stiffened seated beam connections. To stop this happening, they suggested the use of beam web stiffeners. Such a connection, they intimated, could be used in plastic design because of its observed rotation capacity and adequate elastic stiffness. The flange welded only connection was found to have attained 51% of its predicted plastic limit load based on the whole section.

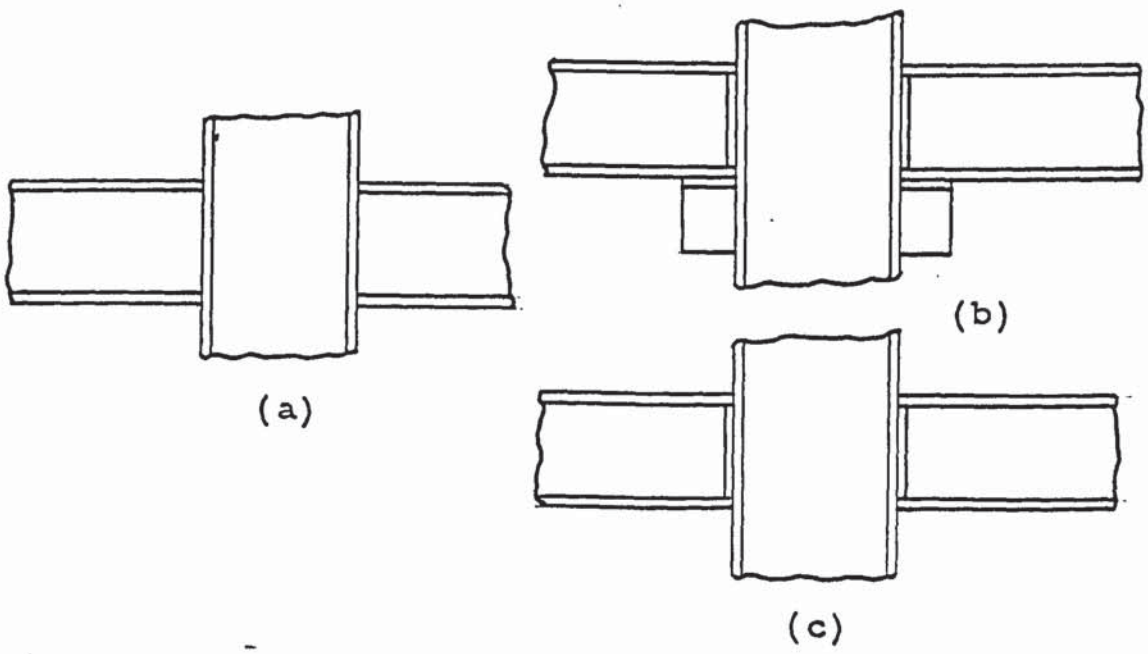

Figure 2.29 Parfitt and Chen's connection geometries

(a) fully welded

(b) flange welded web unconnected with beam seat

(c) flange welded only

They found the basic patterns of stress distribution in the panel zone of the column to be essentially the same for all the connections they tested. They however, found the stress distribution in the beam flanges and web to be significantly affected by the amount of shear force transferred to the beam flange.

A document was published by Commision XV of the IIW[44] in 1976 setting out general design rules for welded connections submitted to static loads. These recommendations were based on a decade of international cooperation and were meant to be guidelines rather than definite rules. The ISO stress criterion of $\sigma c = \sqrt{\sigma_1^2 + 1.8\,(\tau_1^2 + \tau_{11}^2)}$ was changed to $\sigma c = \beta\sqrt{\sigma_1^2 + 3\,(\tau_1^2 + \tau_{11}^2)}$ where σc was to be taken as the permissible stress in the base material and $\beta = 0.7$ for base metal Fe 360

$= 0.82$ for base metal Fe 510

For other grades of steel, the values of were to be determined by linear interpolation proportional to the guaranteed yield strength of the steel.

In the case of load distribution among the individual welds of a joint, the commission suggested two approaches:

1. the load in the weld should be assumed to depend directly on the stress in the adjacent parent metal or

2. the joint is to be considered to constitute a separate unit in the structure and the loading of the individual welds was to be derived from the load of the entire joint.

The recommendation for beam-to-column connections was that, the moment should be allocated to the flange welds as a couple of forces and the shear force to the web welds. Where the columns are not provided with stiffeners an effective width factor was to be applied to the beam flange width. Assuming both the beam and column have equal flange widths, the commission proposed the following formula:

$$\text{Effective flange width} = C_1 \; t_1 + 2t_2$$

where t_1 = the column flange thickness

t_2 = the column web thickness

and the table below gives the value of C_1

C_1		
7	5	Tensile flange Fe 360
10	7	Compression flange Fe 360
5	4	Tensile flange Fe 510
7	6	Compression flange Fe 510
I- Section Column	Box-Section Column	

Table 2.1

The flange widths for stiffened columns were assumed to be 100% effective.

No account was taken of effects of plate bearing and the neutral axis was assumed to be at half beam height. Consequently this method is bound to be conservative and could give variable safety factors.

In the same year, Higgs[45] conducted a series of tests to assess the specific contribution of plate bearing. His specimens were web welded, one in which the plates were in direct shear and the other with grooved back plates which were meant to get rid of direct bearing, e/d ranged from 0.13 to ∞ . Higgs found that plate bearing increased shear resistance by about 31%. Friction was thought to be responsible for this increase in ultimate capacity.

In continuation of the work which was started in 1975 by Chen and Rentschler[42], Rentschler et al[47] carried out similar tests to the preliminary tests of Chen and Rentschler using full scale beam and column sections. The tests were designed to provide all the necessary information for the design of welded-secondary beam-to-column connections, consequently, they investigated the strength, stiffness, ductility and stiffening requirements for such connections.

Four different specimens using different combinations of welding and bolting were tested. Rentschler et al designed their connections in such a way that the beam section at the beam-to-column junction could resist the beam plastic moment Mp and 81% of the beam shear, Vp, required to

cause shear yielding of the beam. Just as in the preliminary tests an axial load was applied to the column.

A detailed report on the performance of each of the four specimens was given. They concluded that the axial load has an effect on yielding and deformation of the connections and that further theoretical work would be carried out to provide a thorough understanding and recommendations and guidelines for the design of such connections.

A paper reviewing the appropriate design rules for unstiffened welded and bolted connections was presented by Witteveen et al [48] in 1980. They explained the design philosophy and derived the requirements for adequate rotational capacity and stiffness. They also presented design rules governing the calculation of the moment capacity of unstiffened welded and bolted connections. They presented a method for balancing the material cost of the beams against the labour cost of the connections. They suggested that in the case of relatively stiff connections the first plastic hinges are likely to be formed in the connections at the supports and in the midspan after some rotation.

Expressions for the minimum rotational capacity were derived using the Dutch design rules regarding the amount of midspan deflection allowed under service load at failure, considering the beam to be uniformly loaded and assuming that plastic hinges will first form at the beam supports.

The expression for the minimum stiffness at failure was also derived by assuming that a plastic hinge will first form at the midspan section of

the beam. Using the load factor, these expressions were adjusted for seismic loading conditions.

Witteveen et al., like Elzen and Rolloos attributed the non-uniform stress distribution in the tension flange to the flexibility of the flange of the column. They suggested that due to the fact that the middle region of the beam is connected to a relatively rigid web and the edges of the beam are connected to the relatively flexible part of the flange of the column, the yield stress will be reached first in the middle region of the flange of the beam. They noticed that due to the flexibility of the flanges only a part of the weld will be effective. They therefore derived a formula for the effective length which like the previous ones involves only the column web thickness and column flange thickness. Their formula is bm = 2 twk + 7tfk with the following limitations:

$a_{weld} = 0.5t_{fl}$ where t_{fl} = beam flange thickness

t_{wk} = column web thickness

$t_{fl} < 1.2\, t_{fk}$ t_{fk} = column flange thickness

If the last condition is not satisfied,

$$b_m = t_{wk} + 2\, r_k + 7\, \frac{t_{fk}^2}{t_{fl}}$$

A further requirement for the effective weld length to ensure sufficient deformation capacity is that the flange of the beam be able to yield prior to failure of the weld. By assuming that $a_{weld} = 0.5t_{fl}$ and that the actual strength of the weld is at least 40% higher than the

actual yield load of the flange of the beam, they arrived at the following expressions:

$$\hat{F}_{\text{tension weld}} \geq 1.4\, b_m t_{fl} \sigma_y$$

$$\hat{F}_{\text{yield beam flange}} = b_1 t_{fl}$$

where b_1 = the beam width

The requirement then becomes:

$$b_m \geq 0.7 b_1$$

They recommended the use of stiffeners between the flanges of the column in the tension zone if this requirement is not satisfied, to ensure sufficient rotation capacity by yielding of the beam flange. The whole analysis was based on the theory of plasticity.

Tests by Voorn[49] have shown that for a given moment capacity, welded connections without stiffeners generally fulfill the requirements for adequate stiffness but not necessarily the requirements for rotation capacity.

A paper presenting an up to date account of the research on beam-to-column connections in Japan was presented by Kato[50] in 1982. He discussed why the structural design in Japan is based mainly on earthquake loading and emphasized the importance of the contribution of shear

deformation capacity of joint panels to the overall ductility of the sections. He suggested some design criteria for beam-to-column moment connections suitable for seismic design.

Tests carried out by Higgs[51] on the strength of mild steel fillet welds subject to static loading and flange welded beam-to-column connections under combined bending and shear have shown that welds under compression are weaker than welds in tension. He observed that failure of the fillet weld is initiated at the weld root, the factor controlling the initiation being the weld ductibility, and that residual stress has no influence on the ultimate strength of fillet welds.

He tested short fillet welds in both the as welded condition and in stress relieved condition using L-shaped and double lapped specimen (see figure 2.31) and full size beam-to-column connection (see figure 2.31).

Higgs discovered that welds under tension and compression are of equal ultimate strength for the range of F_x/F_y from 0 to 2 but welds under compression are weaker for the range of F_x/F_y from 2 to ∞ . The average ratio of weld strengths is 0.916 when $F_x/F_y = \infty$.

In the case of beam-to-column connections he discovered that the flange weld under tension is the critical weld and always fails first irrespective of the ratio of S/D. The distribution of the load between the tension and compression weld is a complex function of the elastic compression of the weld, elastic/plastic deformation of the flange/weld combination, load-deformation characteristics of both tension and

compression welds, and the nature of the load applied to the tension flange. Three distinct modes of failure were observed by Higgs Viz end mode, which occurs when there is poor fit up, bending mode which occurs when Fx is dominant and shear mode which occurs when Fy is dominant.

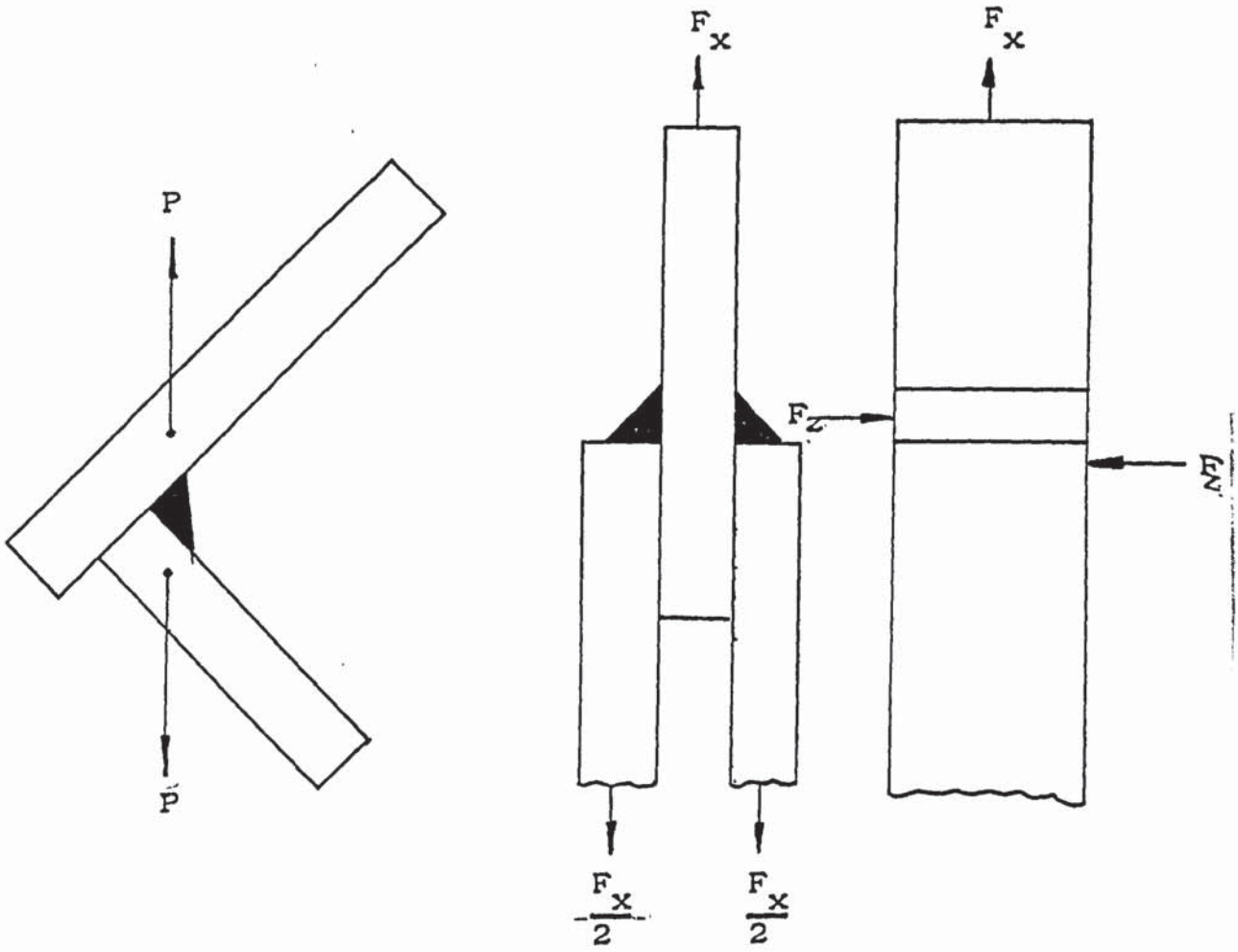

Figure 2.31 Higgs' failure criterion specimens (a) L-style (b) double lapped

He concluded that all the existing methods for ultimate load prediction overestimate the ultimate load capacity to varying degrees.

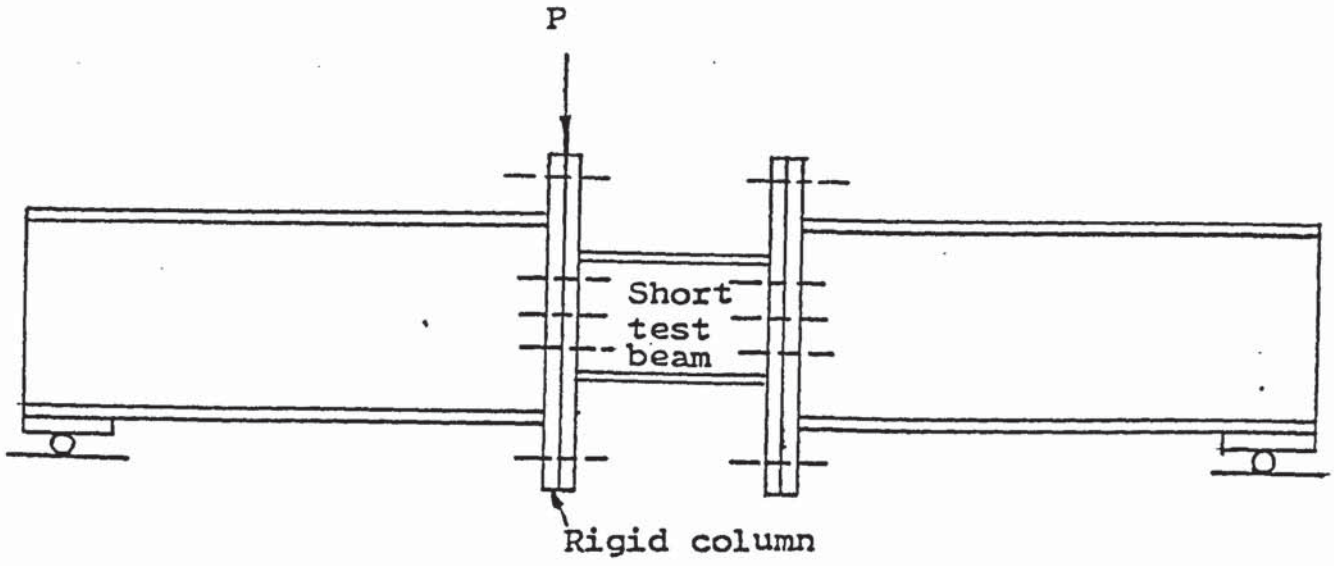

Figure 2.32 Higgs' Beam-to-column connection

A theoretical investigation into the strength of fillet welds subjected to tension, shear and a combination of tension and shear was carried out by Kamtekar [52]. The strength of fillet welds as a function of the weld geometry and the ultimate tensile strength of the weld metal was determined, based on the equivalent forces acting on the welds, and allowing for the effect of longitudinal residual stresses. He compared the various strength formulae with the experimental results of other

workers (Biggs et al). He also investigated the effect of unequal leg lengths on the strength of welds and showed how the method of analysis can be applied to more complex loading conditions.

In the analysis of the tension and shear fillet welds, the principal stresses in the weld were determined by considering the stresses acting on three mutually perpendicular axes (x,y,z).

In the determination of the strength of fillet welds the force system on the weld was assumed to consist of direct forces, shear forces and moments acting on the faces of the weld which are joined to the members that it connects. Longitudinal residual stress was assumed to have a magnitude equal to the yield stress of the weld metal, all other stresses were neglected. It was assumed that the weld metal will obey Von Mises yield criterion. Allowance was also made for cases where the weld metal has an elastic - perfectly plastic uniaxial stress-strain curve and where the weld metal has a strain hardening type stress-strain curve.

He observed that agreement between theory and experimental results seems to be better for tension fillet welds.

One result of Kamtekar which is of most importance to this author's work is that on the failure criterion. His analysis showed that the interaction curve is made up of two straight lines parallel to the x and y axes. This agrees with the experimental results of this author. Kamtekar's theory can be applied to any fillet weld.

CHAPTER 3

EXPERIMENTAL WORK AND RESULTS

3.1 OBJECTIVES

The usual practice in designing welds in beam-to-column connections is to assume the bending moment is resisted by the flange welds and the shear force is resisted by the web welds. For these assumptions to be correct, however, the column has to be provided with stiffeners to transfer the loads from the beam flanges into the column web. Where there are no stiffeners, the design has to be based on a reduced effective weld length.

There is evidence (27,29,48) to show that when the column is not provided with stiffeners, the resulting stress distribution over the length of the weld is non-uniform and this leads to the reduction in the load carrying capacity of the weld. The resulting non-uniform stress distribution is due to the flexibility of both the beam and column flanges.

None of the previous work on effective weld length for beam-to-column connections considered the effect of the flange width on the flexibility of the flanges.

In beam-to-column connections, the column is subjected to an axial load, a bending moment and a tranverse load which may cause web buckling. A column subject to axial load and bending moment has been studied (12,22,38,39,41) but not when also subject to web buckling.

Often, beams have to be connected to the column web in addition to the connection to the column flanges to form a four-way connection. A way of connecting the secondary beam to the column is by means of a T-section. The web of the tee is welded to the web of the column and the flange to the flanges of the column. See Figure 3.6. Tests (23) have shown that even if the secondary beam is welded directly to the column web, the stiffening action provided by the two secondary beams strengthens the connection more than it is weakened by the triaxial stresses imposed on the column by these additional connections. A knowledge of the proportion of the load taken by each of the weld groups making the connection, when the connection is subjected to loads producing vertical shear and bending moment is required for the design of such a connection.

In beam-to-column connections, when $\mu m/vd > 1$, rotation occurs at the bottom flange of the beam in addition to a vertical slip. As a result of this relative movement between the beam and the column, a frictional force μH is introduced. An accurate investigation of beam-to-column connections therefore, calls for the establishment of the value of this slip coefficient.

Consequently the following are judged to be pertinent to the work contained in this research:

1. Developing a formula for the effective weld length incorporating the flange width and flange thickness.

2. Studying the behaviour and developing a theory for a column subject to axial load and web buckling load.

3. Developing a theory for the design of the welds in secondary beam-to-column connections.

4. Determining the coefficient of friction between the end of the beam and the flange face of the column.

3.2 DESCRIPTION OF TESTS

The experimental work has been divided into three main sections as follows:

1. Design and testing of main beam-to-column connections.

2. Design of the loading rig and testing of columns subject to axial and transverse loads producing web buckling.

3. Design and testing of secondary beam-to-column connections.

Subsidiary tests which had to be carried out are:

a. tests to determine the coefficient of friction between steel and steel,

b. tests to determine the failure criterion for fillet welds subject to external forces,

c. tests to determine the effects of flange flexibility,

d. tests to determine the yield strength of the flange and web material of the steel column.

3.2.1 BEAM-TO-COLUMN CONNECTIONS

The effect of flange width and flange thickness on the flexibility of the flange and hence the effective weld length can be studied by carrying out tests in which these two parameters are varied. Figure 3.1 shows the third design of the specimen for such tests. A total of three specimens were tested, and each specimen was loaded to failure using a Denison machine. The first specimen which incorporated an angle plate instead of the T-section, proved unsuccessful because the gap between the angle plate and the protrusion of the web directly below the angle plate was too small. The second specimen replaced the angle section with a T-section with sufficient distance between the connected plates. This test was also unsuccessful because of the flexibility of the top plate which suffered

excessive deformation and the difficulty in detecting the failure of the weld. A third specimen was then made similar to the second specimen but with a much thicker flange. This specimen, again, did not eliminate the difficulty in detecting the failure of the weld. As a result of these difficulties, this type of specimen was abandoned.

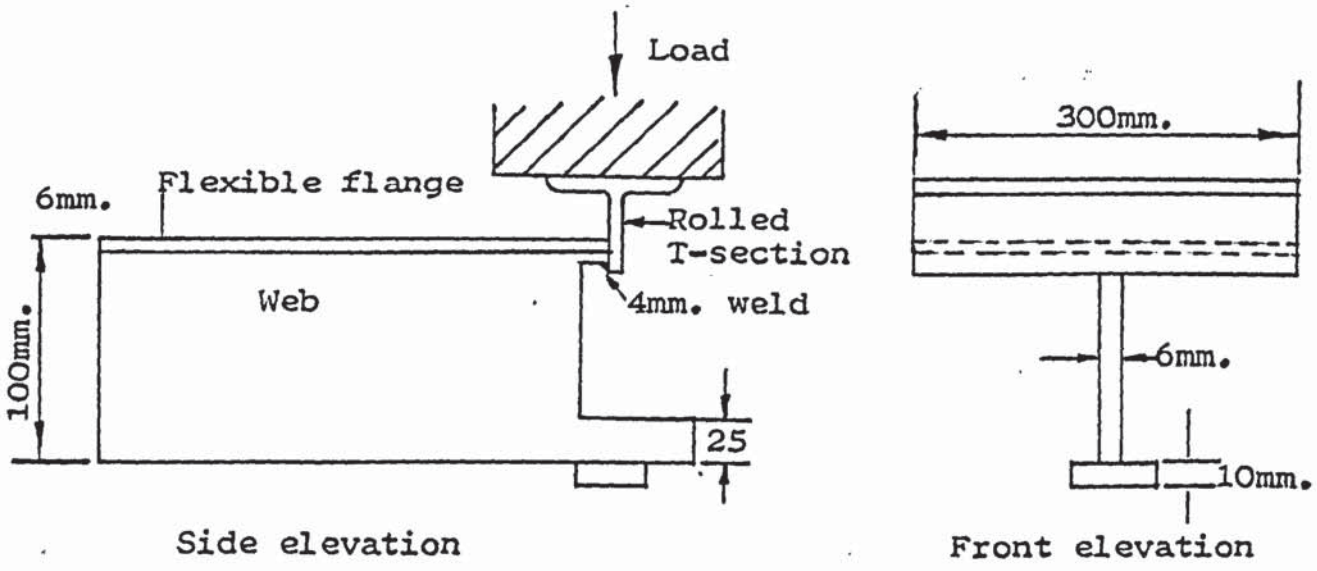

Figure 3.1 Specimen for the variation of flange width and thickness

It was decided that an I-section should be used for the specimens loaded as shown in Figure 3.2. Variation of the flange width and flange thickness would involve either the use of different sections or the fabrication of both the beam and the column sections. Using different sections introduces some unnecessary variables into the analysis of the connection because of the differences in the mechanical properties of the rolled sections. Fabrication of the sections would involve extensive

welding which due to weld shrinkage on cooling, could introduce residual stresses and other weld defects. It has been shown that the magnitude of residual stresses in weldments could be equal to the yield stress of the weld metal [52]. Moreover, because there will be so many welds, any of the other welds could fail before the test weld.

To eliminate the variables associated with the differences in the mechanical properties of beam and column sections, it was decided to use the same structural section for both the beam and the column. The 203 x 203 x 45 kg. universal bearing pile was one of the sections considered and calculations show that tests on fully welded specimens may be successfully carried out with this section (see calculations in the Appendix). However, this section is expensive and not readily available. It was then decided that the 152 x 152 x 23 kg. universal column be used. The theory predicts that web crushing of this section will take place before weld failure if the specimens are fully welded. Even with two welds at the outer flanges, web crushing could also occur before weld failure. It was therefore decided to make the connections with only one weld at the outer bottom flange (see figure 3.2 and plate 1).

Before the connections were welded up, measurements were taken of the flange width, flange thickness, web thickness and depth of the 152 x 152 x 23 kg. universal column. Measurement of the thicknesses were carried out with a micrometer screw gauge and the width and depth with a steel tape. Each of these measurements were taken in four different locations on the section. Consequently the dimensions given in section 3.3 are the mean of these four measurements. The standard deviation for

each measurement is included to give a measure of the dispersion.

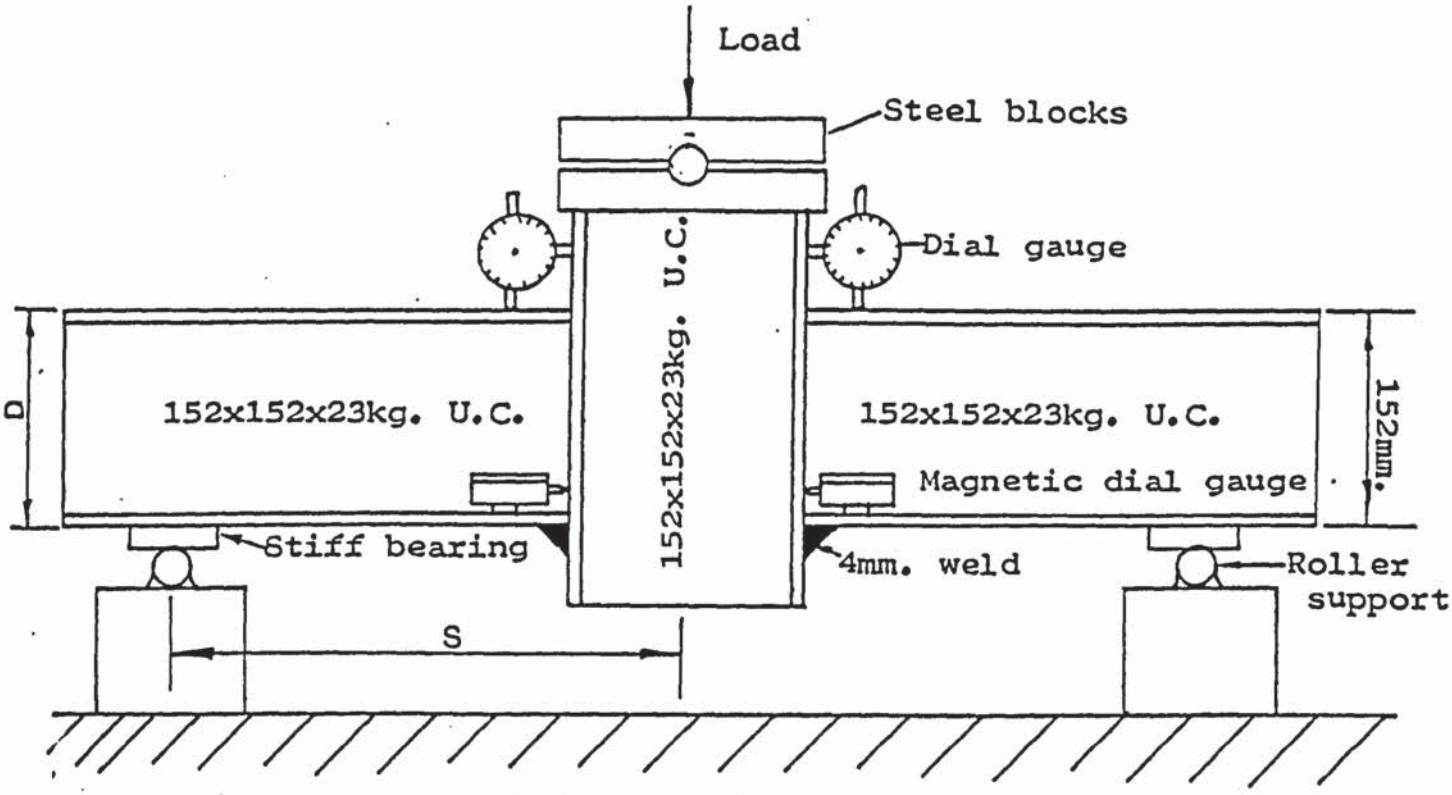

Figure 3.2 Test arrangement-Beam-to-column connection

Each specimen was placed on roller support on the 50 ton Denison machine. An axial compressive load was then applied to the column in increments after a plumb-line had been used to ensure axial alignment of the column with the Denison machine centre-line. Readings were taken of the vertical and horizontal deflections on either side of the connection at each load application and this procedure was continued until failure of the weld was observed. At failure, the deformations of both flanges were observed and the maximum permanent plastic deformation was measured using a steel rule and a flat steel section. The angle of the failure plane was

also measured on a shadow graph at a magnification of 20. All the specimens were tested as welded; only visual inspection of the weld was undertaken prior to carrying out the tests. All the welding was done by a skilled welder.

Altogether, ten connections were tested at values of S/D of 0.5, 1.0, 2.0, 3.0 and 4.0. The weld size was mainta ined at 4 mm leg throughout, and the results of the test are given in section 3.3.1.

3.2.2 COLUMN WEB BUCKLING TESTS

These tests were designed to show the effect of column axial load on the web buckling strength of the column. The first phase of these tests was devoted to the design of the loading rig and the test specimens. Figure 3.4 shows the test specimen and instrumentation and figure 3.5 and plate 2 show the test arrangement. Electrical resistance strain gauges were fixed on the column flanges to check axial alignment and to determine the stress distribution in the flanges. Two strain gauges were applied opposite each other along the web for determining the strain on the web due to the applied horizontal load. A 100 ton hydraulic testing machine supplied the axial load and the horizontal load was supplied by a 50 ton capacity hydraulic ram incorporating a pressure gauge both of which were calibrated against the Denison machine prior to using them for the tests. (See data and graph in the Appendix). A frame was made for the application of the horizontal load. It consisted of four lengths of a universal column (152 x 152 x 37 kg. U.C) connected together as shown in

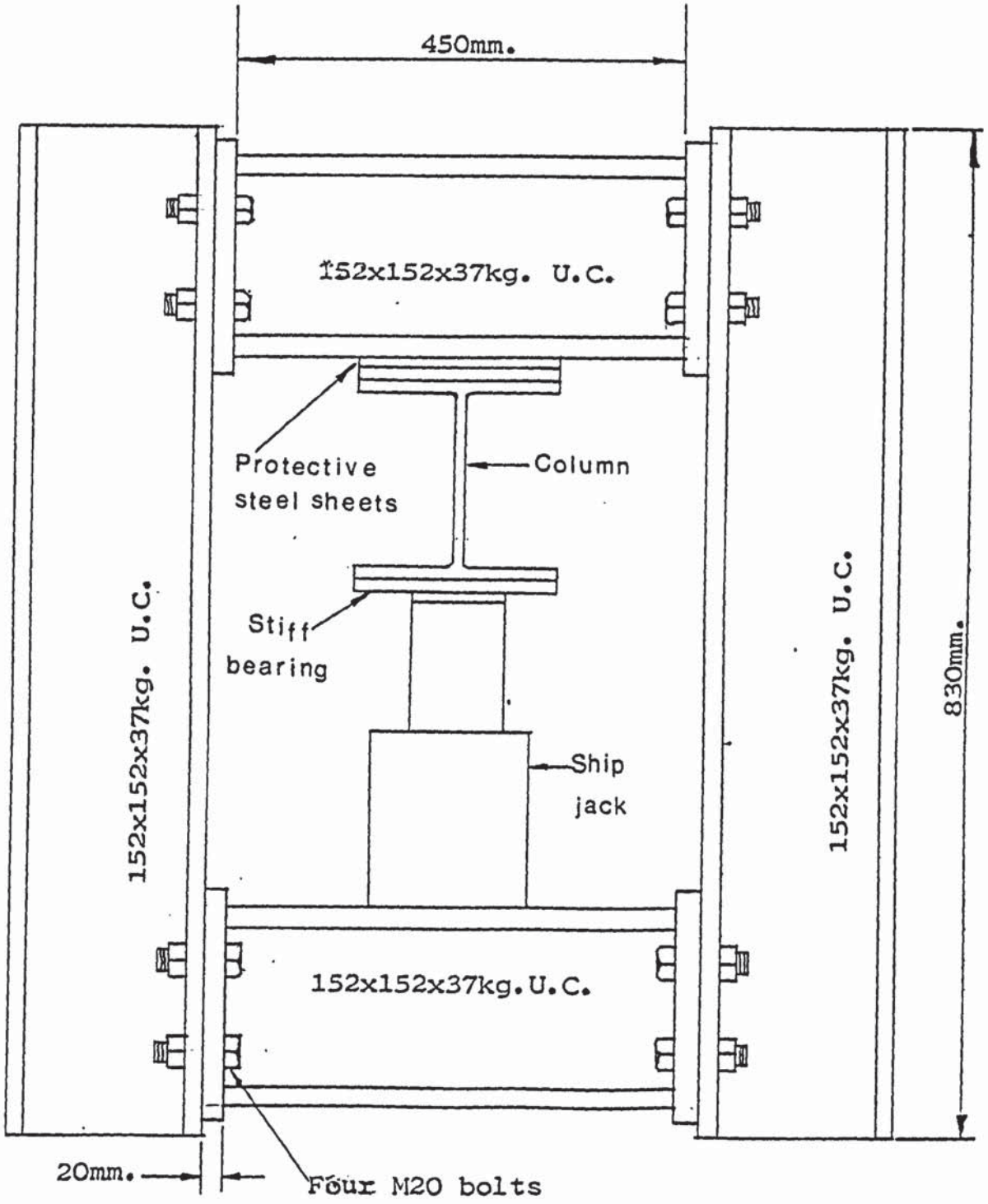

Figure 3.3 Biaxial loading rig for column web buckling test.

Figure 3.3. The shorter members had an end plate welded to both ends and each of the end plates had four holes of about 21 mm diameter for the M20 bolts.

Each specimen was observed for defects and initial crookedness of the web prior to testing. Measurements were also taken of the web thickness, flange thickness, the length and depth of each specimen and the dimensions of the stiff bearing. Apart from the length, and depth of the specimens which were measured with a steel tape, all the other measurements were carried out with a micrometer screw gauge. These dimensions are given in section 3.3.

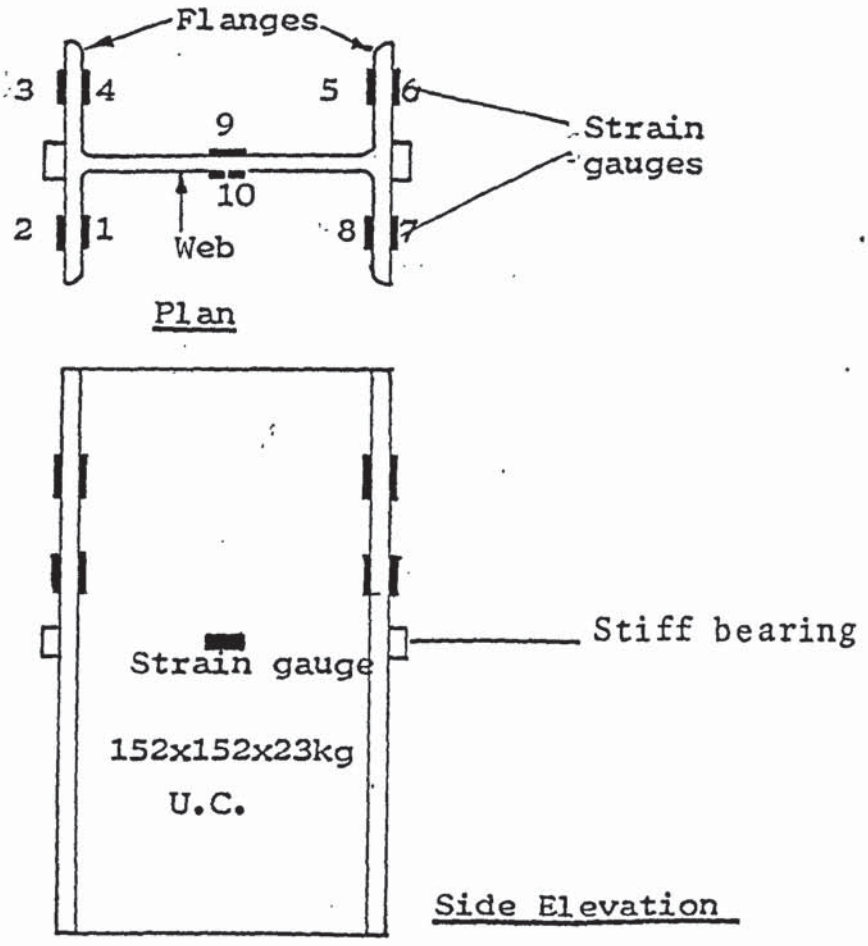

Figure 3.4 Column specimen showing arrangement and position of strain gauges

The axial load was first applied after a plumb line had been used to check that the column specimen was positioned properly. The horizontal load was then applied in increments until web buckling was observed. The data logger (shown in plate 4) recorded all the strain gauge readings. The column axial load ranged from zero to 80 tons (797.36 kn). At each load application the section was observed for any sign of yielding along the web.

Seven specimens were tested altogether. The section used was the 152 x 152 x 23 U.C., the same section used for making the beam-to-column connections. The size of the specimen (450 long) was determined from calculations which precluded column buckling due to the axial load and ensured its suitability for the loading rig.

3.2.3 SECONDARY BEAM-TO-COLUMN CONNECTIONS

The work on this connection consisted of the design of the test rig, design and manufacture of the test specimens and testing of the specimens shown in figure 3.6 and Plate 6, for the purpose of determining the behaviour of the connection and the stress distribution along the web of the tee. Interest was centred mainly on the proportion of the load taken by each of the weld groups making the connection. Tests were therefore carried out on stiffened and unstiffened connections.

One size of beam and column was used throughout the test to eliminate beam and column sizes as variables. The column section was the

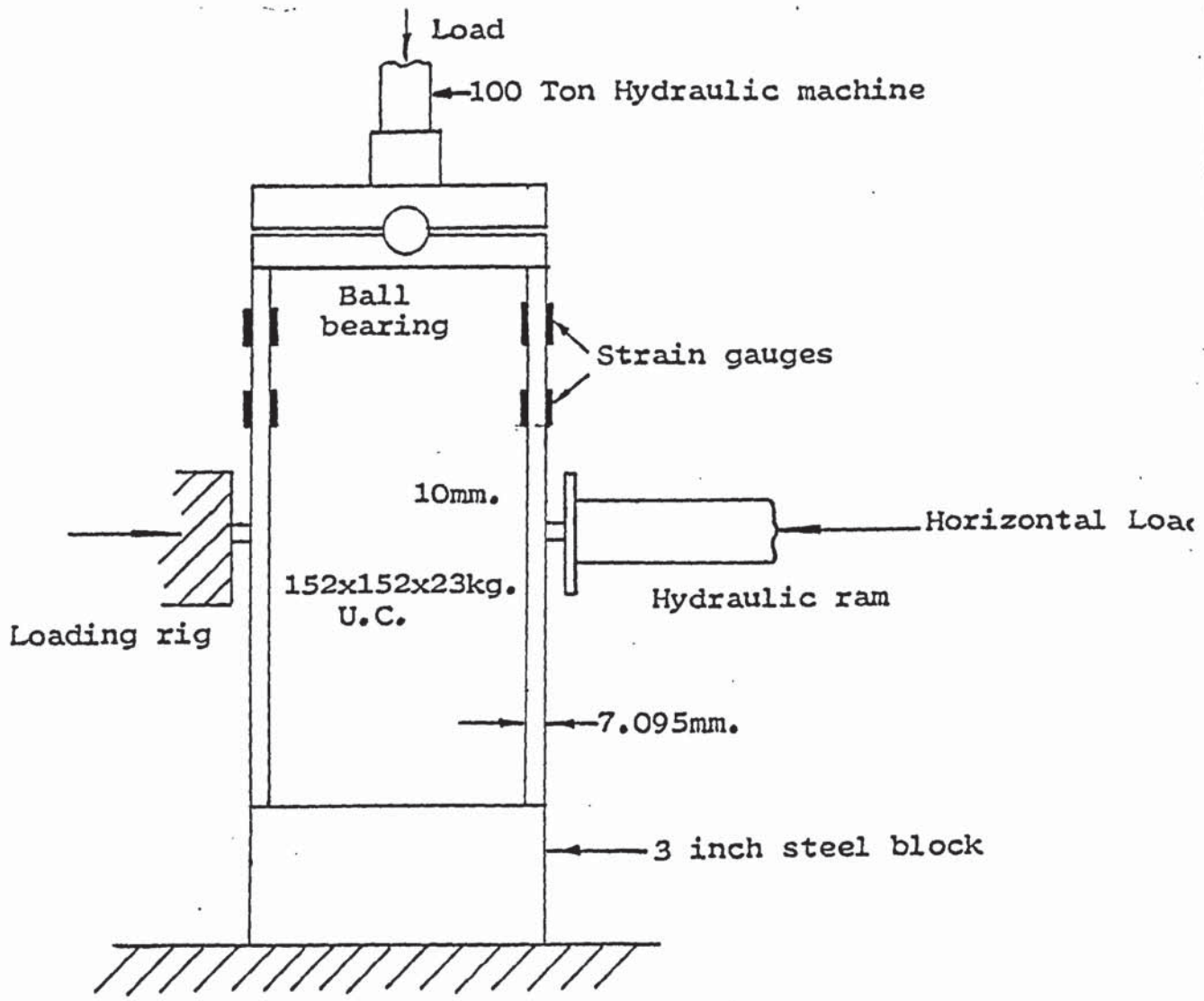

Figure 3.5 Test arrangement for column web buckling test

152 x 152 x 23 kg U.C. and the beam section was the 305 x 127 x 37 kg U.B. The test programme was divided into four groups of tests depending on the stiffening employed (see Figure 3.7).

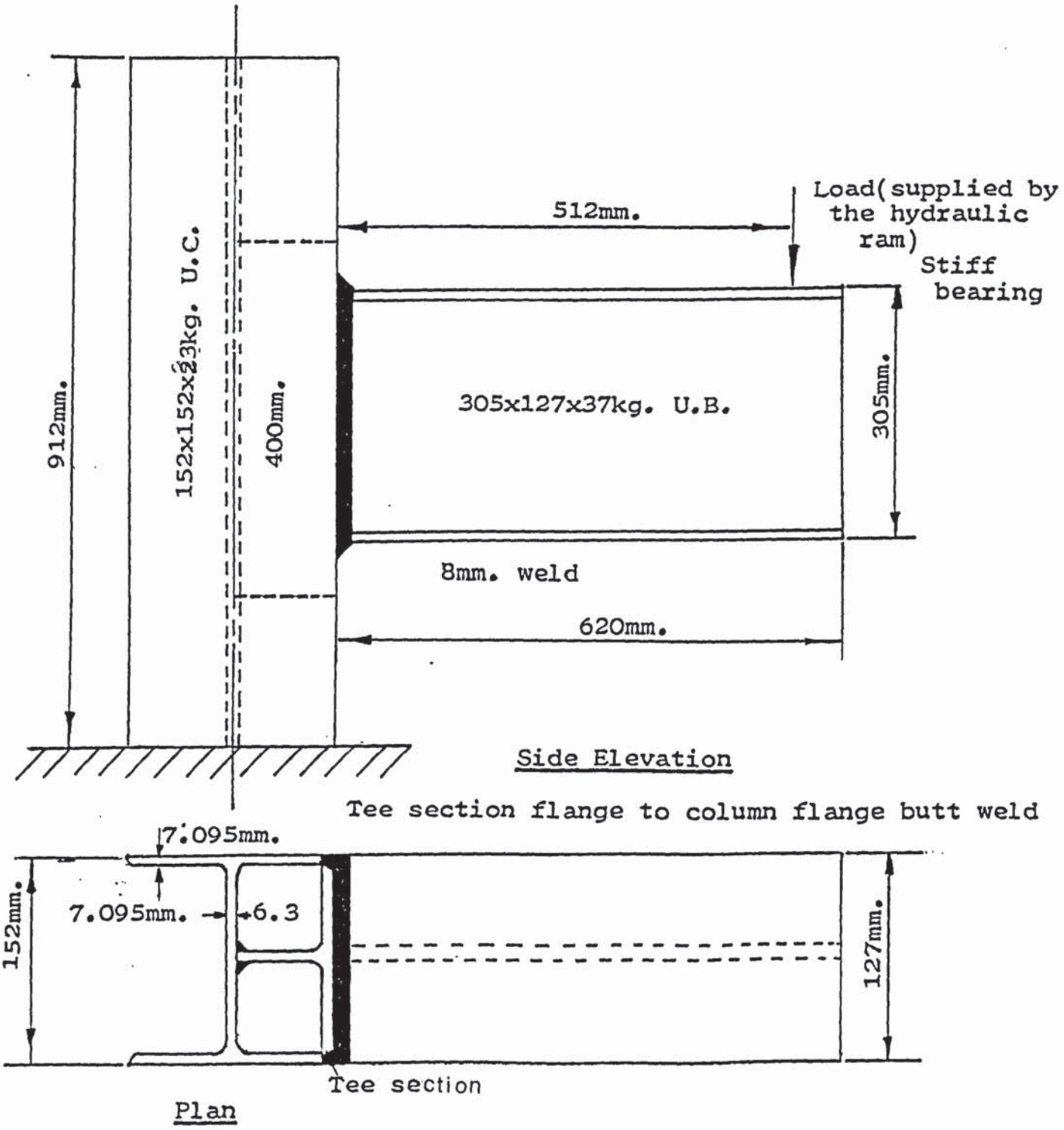

Figure 3.6 Secondary beam-to-column connection

The tests specimens consisted of a 620 mm beam welded directly to a tee with the flanges butt welded to the column flanges. The web was welded to the column web at right angles to the column web by means of fillet welds as shown in figure 3.6.

All the specimens were subjected to the same type of loading and at the same distance from the face of the tee flange (512 mm). The column was fastened to the loading rig to prevent it from buckling. So that the formation of plastic hinges and local yielding could be observed the column was coated with white wash. Dial gauges were used to measure vertical and horizontal deflections of the beam. Electrical resistance strain gauges were placed along the tee on both sides with each gauge directly opposite the one on the other side. The readings of each pair were averaged and the average taken as the strain at that point. This was to eliminate the error in the strains which may be introduced as a result of the initial crookedness of the tee web. Strain measurements were taken using a Pickel box.

A device was made by the author for fixing the strain gauges along the tee web. This device consisted of a board 418 milimeters long and 54 millimetres wide with the position of each strain gauge marked on as shown in figure 3.8. The gauges were first fixed on a sellotape which was placed adhesive side up, on the device. The gauge wires were then soldered onto the strain gauges. This was then carefully transferred to the tee web which had been thoroughly cleaned first with a rotary electric grinder and then a fine emery cloth. The gauges were then fixed to the tee web after further cleaning the web with a cleaning fluid

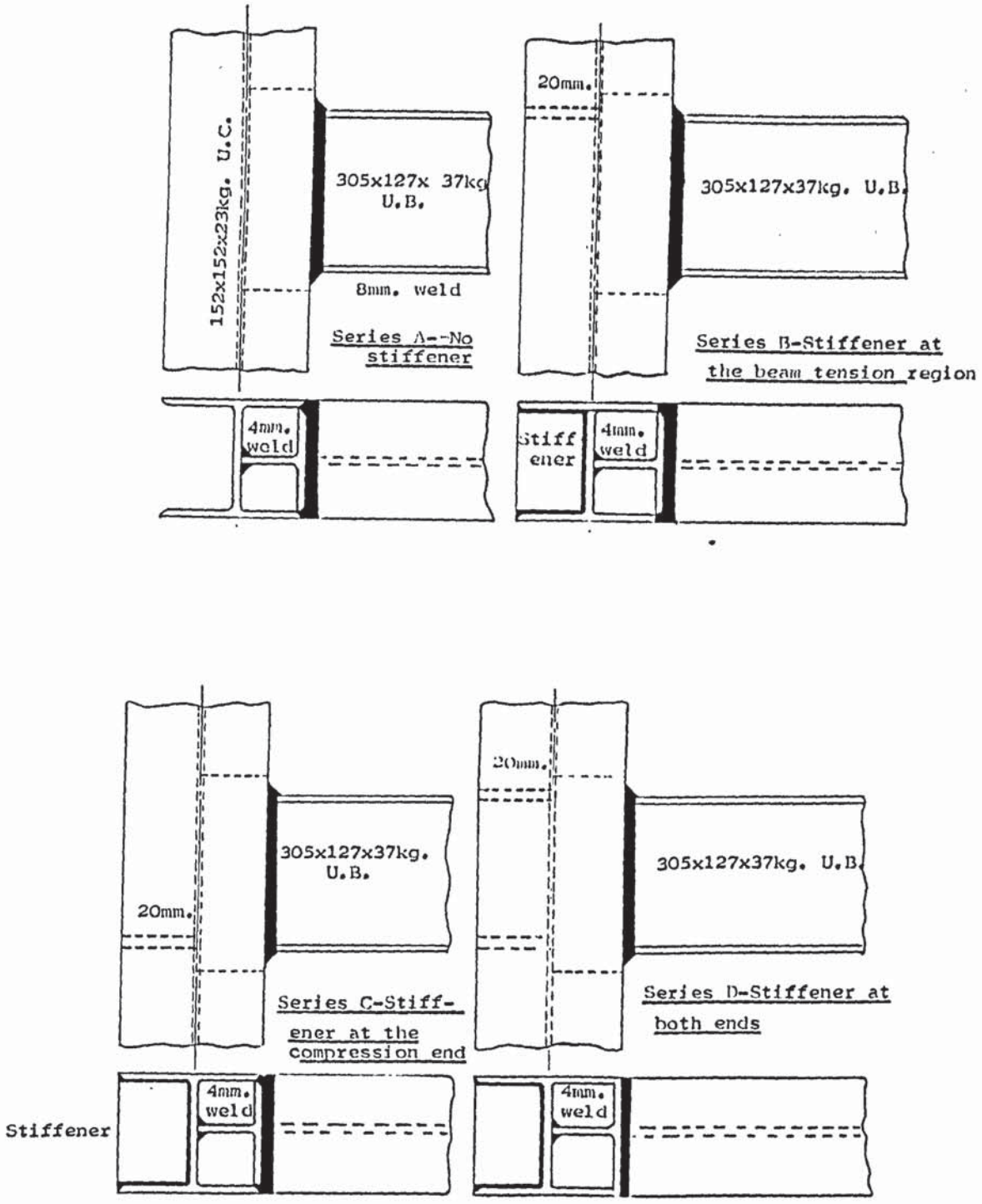

Figure 3.7 The four beam-to-column connections tested

(Trichloroethylene). This procedure was repeated for the other side of the web.

A vertical load was applied to the beam in increments of 1 ton (9.967 kn), at a distance of 512 mm from the face of the tee flange, by a 100 ton hydraulic testing machine incorporating a load cell. At each load application, all the strain gauge readings and the vertical and horizontal deflections of the beam were recorded. The column was observed for evidence of yielding during each load application. This procedure was continued until the weld between the tee flange and the column flange failed. Eleven specimens were tested altogether. All the results of the tests are given in section 3.3.

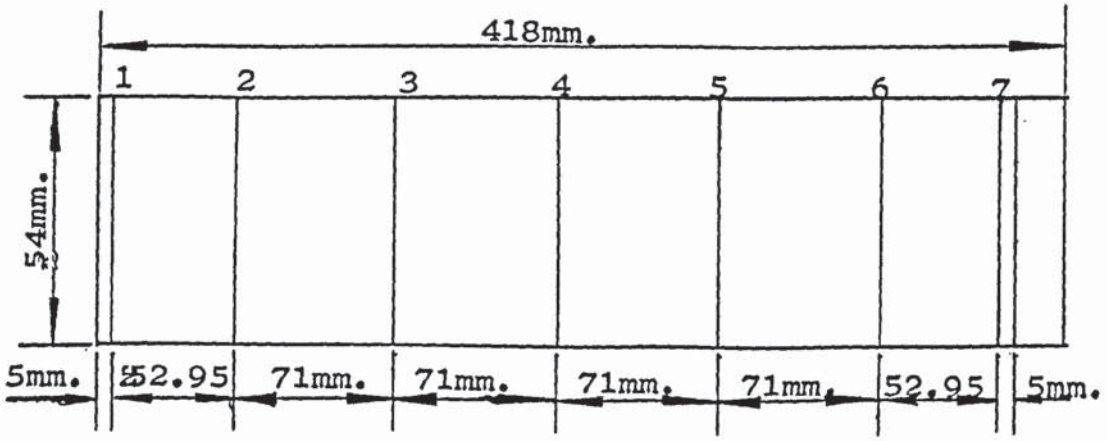

Figure 3.8 Device for fixing strain gauges along the tee web.

Figure 3.8 Device for fixing strain gauges along the tee web

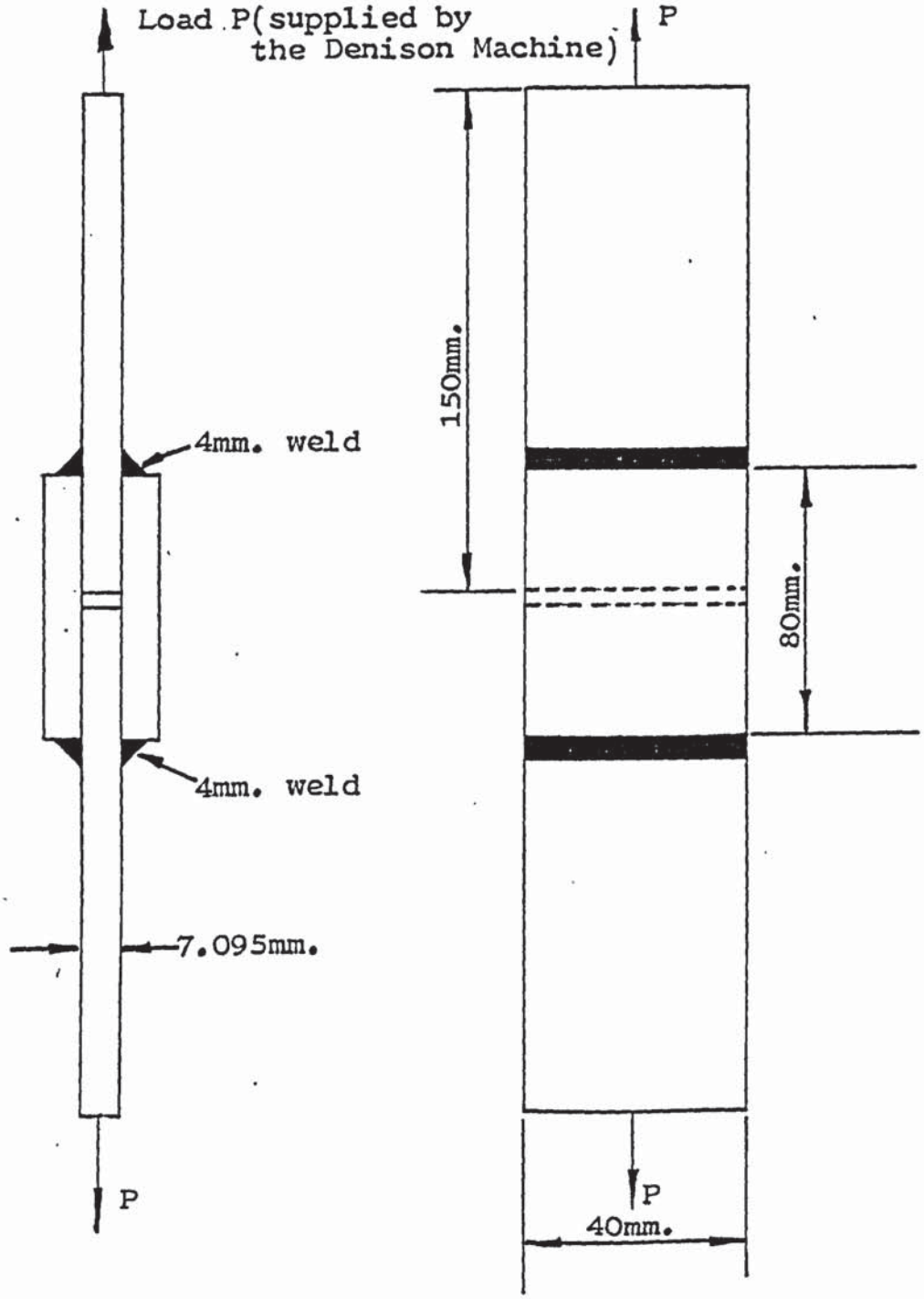

Figure 3.9 Double lapped tension specimen

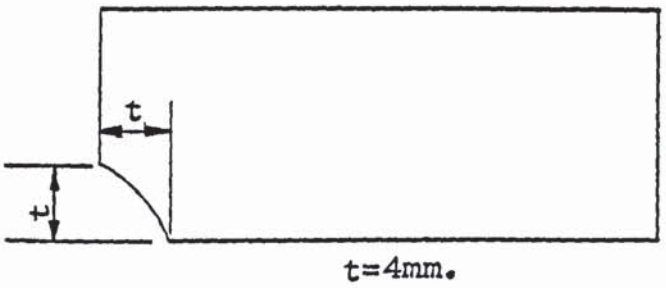

Figure 3.10 Gauge for checking weld leg length.

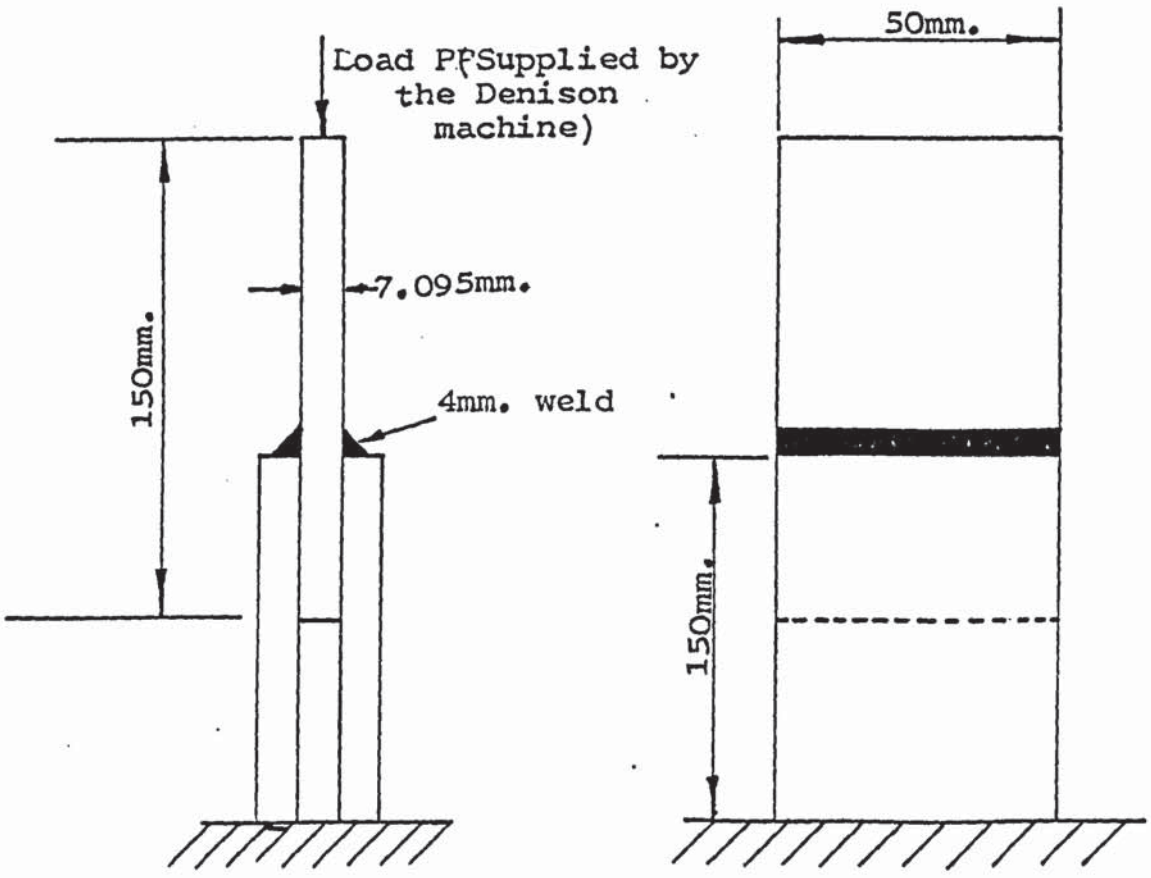

Figure 3.11 Double lapped compression specimen

3.2.4 SUBSIDIARY TESTS ON TRANSVERSE STRENGTH OF FILLET WELD

The strength of a fillet weld is related to the strength of the parent material[51]. Pieces of steel were therefore cut from the flanges of the universal column and welded together and loaded to failure as shown in figure 3.9 on the Denison machine. Two tests provided information on the strength of a fillet weld subject to a transverse force with no flange deformation.

To compare the strength of a fillet weld in compression to its strength in tension, pieces of steel were cut from the flanges of the universal column, welded together and also tested using the Denison machine as shown in figure 3.11.

Prior to carrying out the tests the thickness of the steel plate was measured with a micrometer screw gauge and the size of the weld checked with a specially designed gauge (see Figure 3.10). The results are presented in section 3.3.

3.2.5 SUBSIDARY FAILURE CRITERION TESTS FOR FILLET WELDS

These tests were designed to simulate the rupture mechanism of welds in beam-to-column connections subject to loading conditions producing bending moment and vertical shear. This rupture mechanism has previously been thought to be governed by a critical value of the strain energy of distortion as proposed by Von Mises. This criterion when applied to the

weld states that the weld metal will yield when the principal stresses satisfy the equation:

$$\tfrac{1}{2}\ (F_x - F_y)^2 + (F_y - F_z)^2 + (F_z - F_x)^2 \quad = F_w^2$$

where F_x and F_y are the stresses in the horizontal and vertical directions respectively, F_z is the stress in the direction perpendicular to the x and y directions and F_w is the strength of the weld. Expanding the above equation and taking F_z to be zero gives:

$$F_x^2 + F_y^2 - F_x F_y \quad = F_w^2$$

This equation may be written as $F_x^2 + F_y^2 + K F_x F_y = F_w^2$ where k is a constant, the value of which has always been taken to be -1. None of the previous work on the failure criterion for fillet welds has established explicitly the value of this constant k. It was therefore thought necessary that tests should be carried out on suitably designed specimens to establisgh the failure criterion of the weld under the afore mentioned loading conditions.

The test specimen was designed in such a way as to allow the weld to be subjected to both vertical (longitudinal) and horizontal (transverse) loads simultaneously (see figure 3.12). The test set up envisaged was a biaxial loading rig incorporating a hydraulic jack applying the load in the horizontal direction and the Denison machine providing the vertical

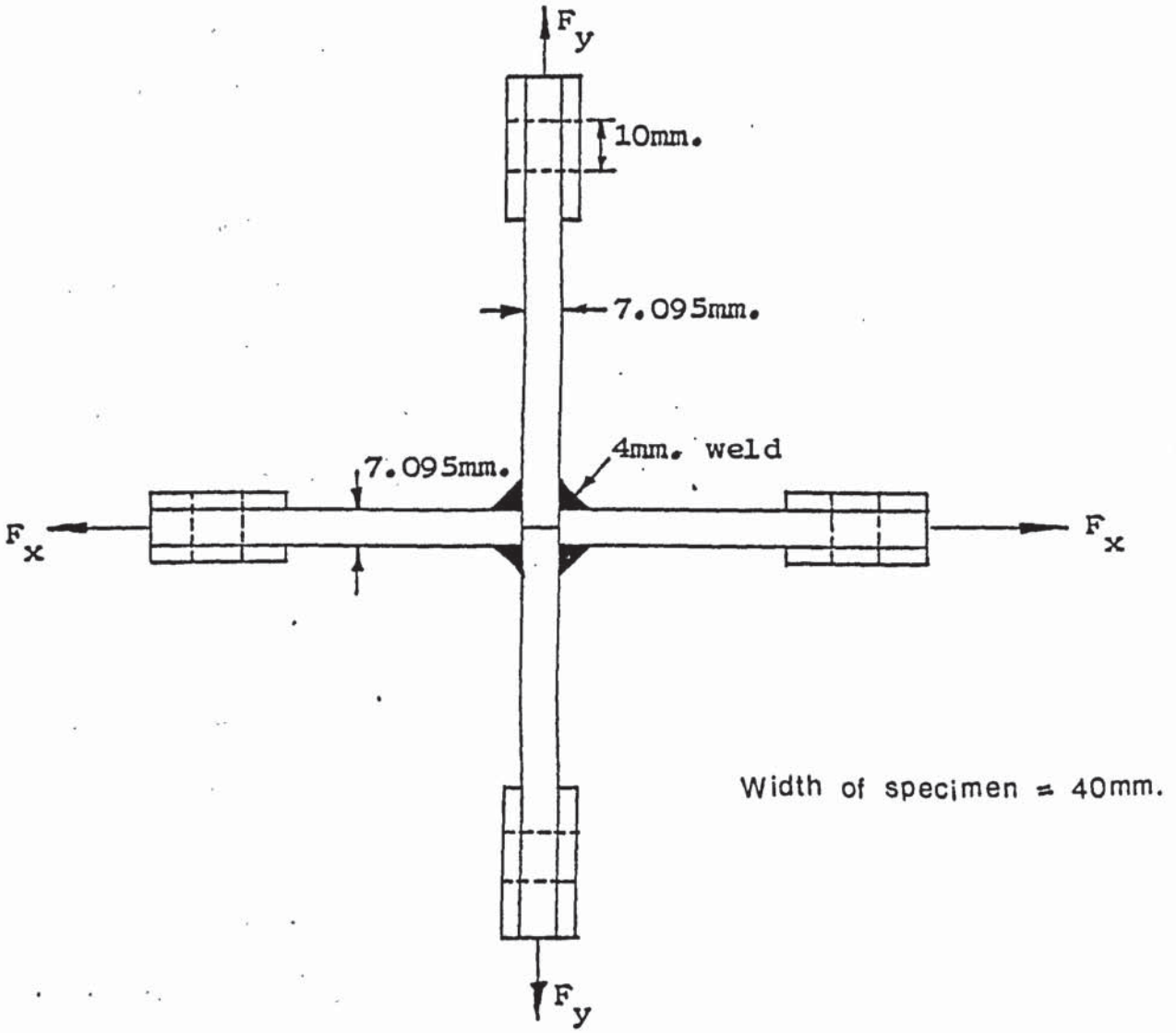

Figure 3.12 Failure criterion test specimen

load. The cruciform shape for the specimen was adopted and the dimensions of the specimen were such that the available biaxial loading rig could be used without any modification to the rig. The testing procedure adopted was to fix the load in the horizontal direction at a known value and then apply the load in the vertical direction until failure of the weld. A different value of the horizontal load was selected for each test. A uniform increment was maintained throughout the tests. Twelve specimens were tested altogether but the first six tests did not produce useful results as the welds were too short. Table 3.8 gives the summary of the test results and Figure 3.54 gives the resulting interaction curve. The hydraulic jack was calibrated against the Denison machine prior to using it for the tests (see data in the Appendix).

3.2.6 SUBSIDIARY TESTS TO DETERMINE THE COEFFICIENT OF FRICTION BETWEEN STEEL AND STEEL

The occurrence of plate bearing in beam-to-column connections under service loading conditions is inevitable. For ultimate load prediction therefore, it is essential that the coefficient of friction between the faying surfaces be determined accurately. The value of this coefficient is generally assumed to be 0.45. This coefficient is not a constant for steel-to-steel but depends on such factors as the type of steel and the type of machining finish given to the surfaces. In the tests in section 3.2.1 the two surfaces are the flange face of the rolled 152 x 152 x 23 kg u.c. and the machined end of the same section welded to this column as a beam.

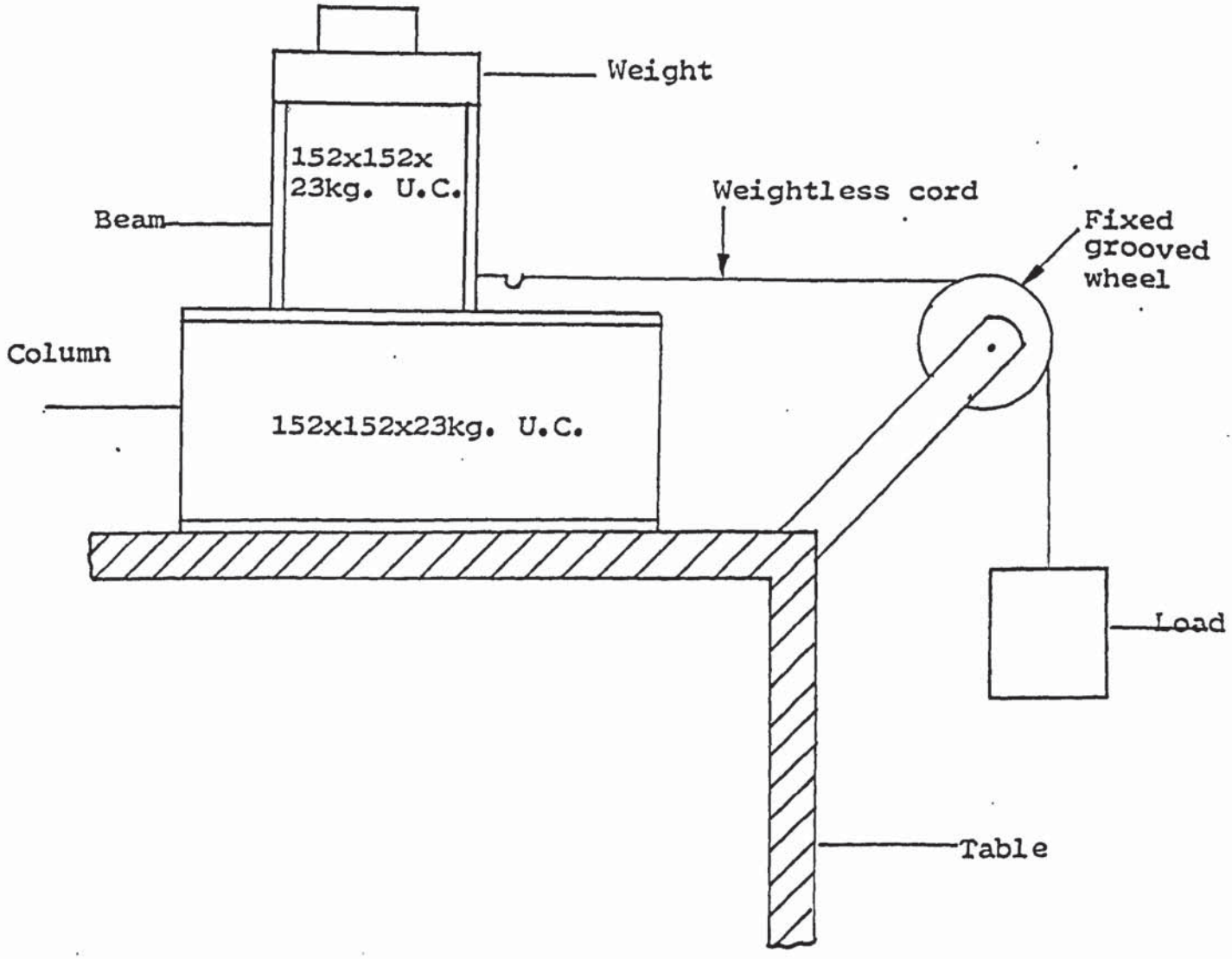

Figure 3.13 Test arrangement for the determination of the coefficient of friction

In the friction tests, the column was laid horizontally on a rigid flat surface. The beam which had a hook welded on in such a position as to prevent tipping of the beam, was then placed on the column with its axis vertical (see figure 3.13). A scale pan was attached to a cord which passed through a fixed grooved wheel to the hook on the beam. The load to cause movement of the light beam was first determined. Different loads were then placed on top of the beam and for each of these loads, the load placed on the scale pan to cause movement of the beam and the load was noted. Both sides of the column were used alternately. A graph of vertical load (F) against the normal reaction (N) was plotted and the coefficient of friction determined from the graph. All the test results are given in Section 3.3 and the Appendix.

This coefficient was also determined using another method in order to confirm the result obtained from the first method. The beam was laid on the column as in the first method. The column was placed on a horizontal board on a table and was prevented from slipping when tilted by a wooden block fixed infront of it. The board was then slowly tilted at the other end until the beam started to move. The angle at which this movement was noticed was recorded. The tangent of this angle is the coefficient of friction. This method gave an average of 0.225 for the value of μ. See analysis in Section 3.3.

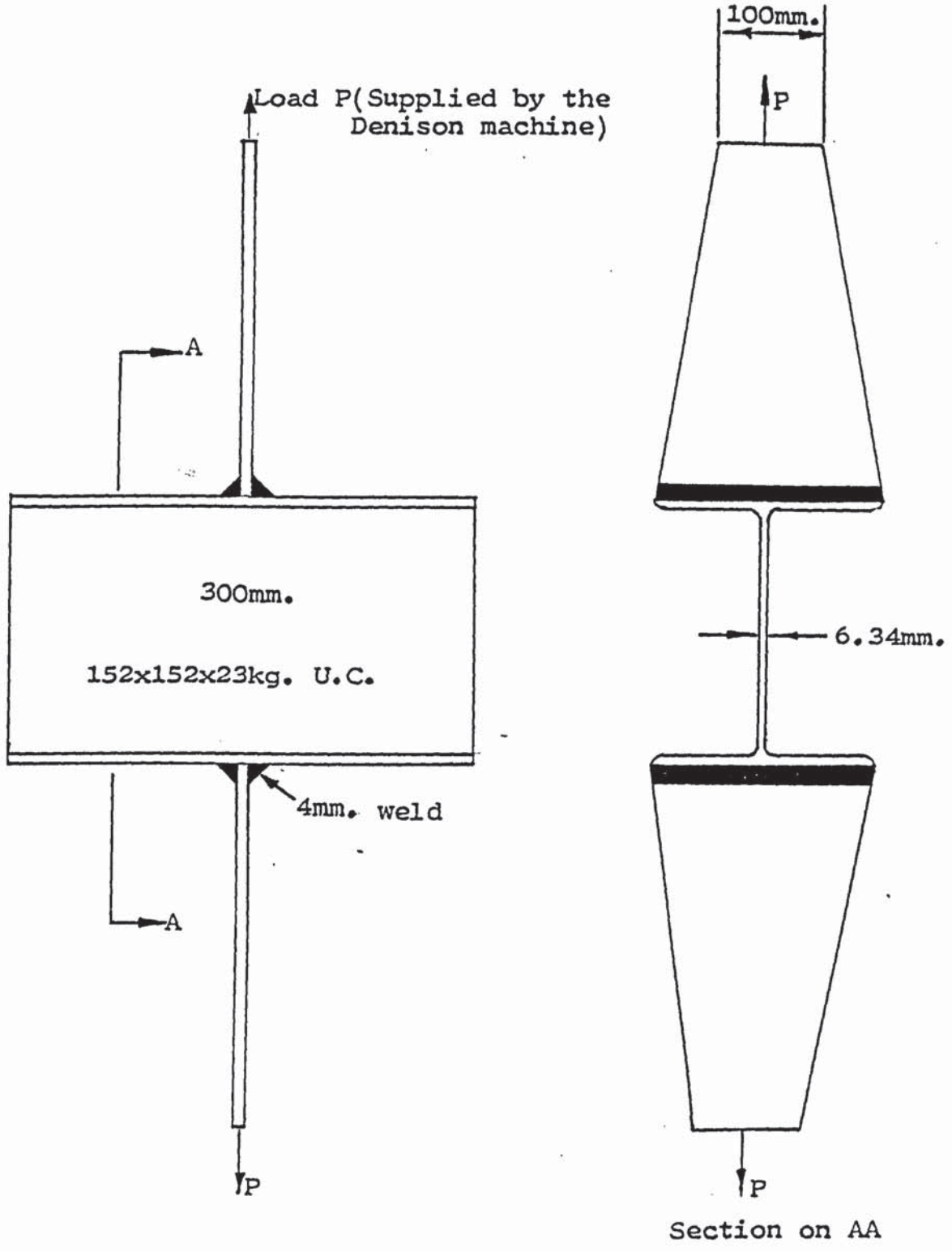

Figure 3.14 Test specimen for the determination of the effect of flange flexibility

3.2.7 SUBSIDIARY TESTS ON THE EFFECT OF FLANGE FLEXIBILITY

To determine the effect of the flexibility of the flanges of the beam and column on the weld strength, two tests were carried out as shown in figure 3.14 and plate 2. This specimen is similar to that tested by Elzen [27], Rolloos [29] and Graham et al [23]. The only difference is that the strips which were cut from the flanges of the universal column were fillet welded to the column just like in the case of Elzen and Rolloos instead of being groove welded as in the case of Graham et al. The first of the specimens failed at 199.5 KN and the second at 190.37 KN giving a mean effective weld length to actual length ratio of 0.38. All the results of the tests are presented in section 3.3.6.

3.2.8 SUBSIDIARY TESTS TO DETERMINE THE YIELD STRENGTH OF THE 152 x 152 x 23 kg. U.C

In tests involving welds it is necessary to determine the yield strength of the parent material. Manufacturers guarantee the value of the yield strength but often, this is lower than the actual value. This test was therefore designed to determine the yield stress of the flange and web material of the universal column.

Three pieces of steel were cut from the flanges and the same number from the web of the universal column and machined to the shape shown in Figure 3.15. Measurements were taken of the width and thickness of each of the specimens using a micrometer screw gauge at four different

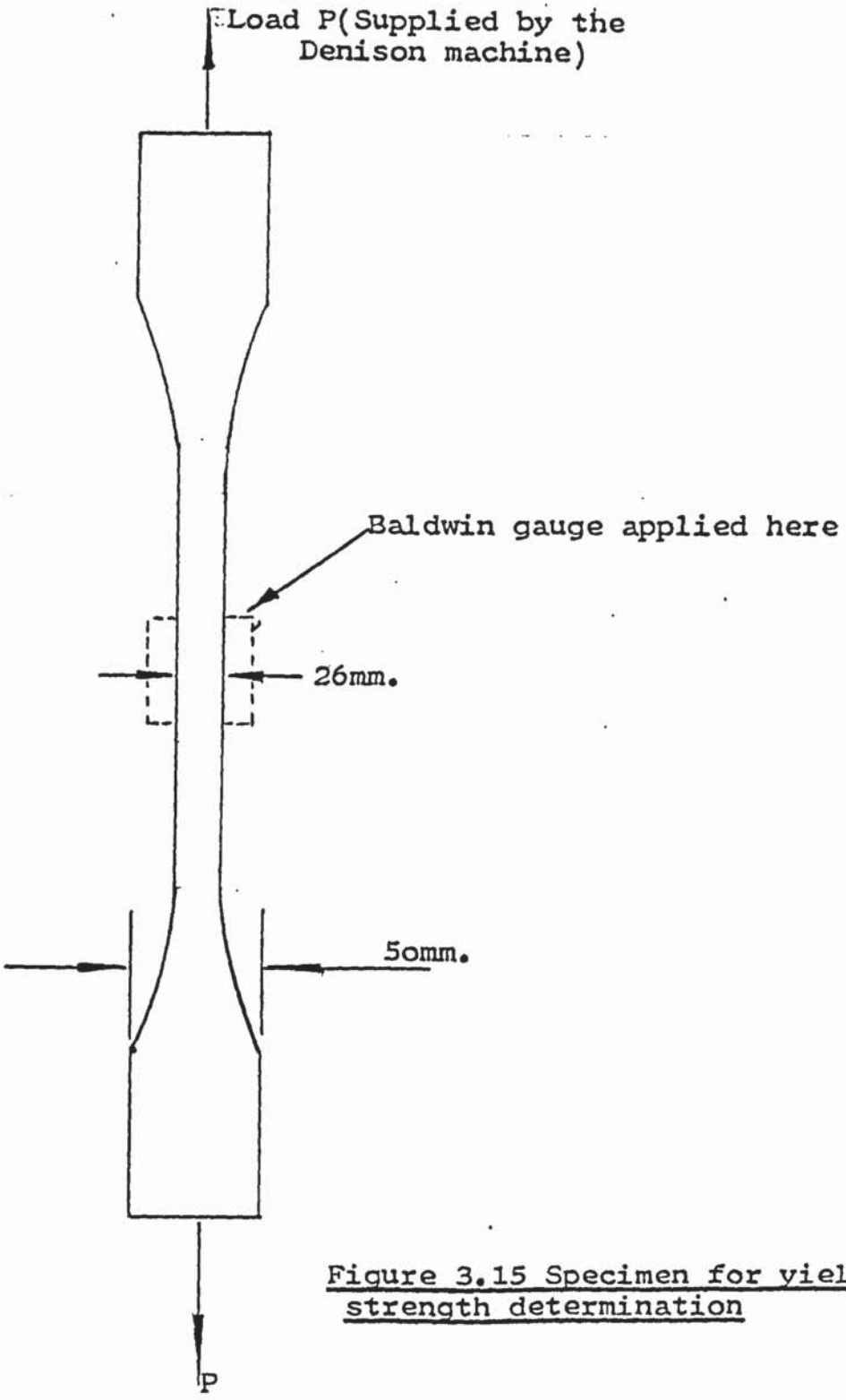

Figure 3.15 Specimen for yield strength determination

locations along the specimen prior to testing. The results given in section 3.3.7 are the mean values for the web and flanges. The tests were carried out on a Denison machine incorporating the Baldwin materials testing equipment (50 mm. gauge length strain recorder and automatic plotter). To give a measure of the dispersion associated with each mean, the standard deviations have been included. The graphs produced by the Baldwin equipment are presented in the Appendix.

The yield strength of the flange of the column was found to be 282.17 N/mm^2 and the yield strength of the web material of the column was found to be 271.13 N/mm^2.

3.3 EXPERIMENTAL RESULTS

In this section, the results of all the tests carried out are presented. Where it has been found more convinient, the results have been tabulated and where tests have been duplicated the means of the results have been presented and the actual test results presented in the Appendix. A description of the behaviour of each test specimen during and after test has also been included in most cases. Results which are thought to be of less importance have been presented in the Appendix.

3.3.1 EXPERIMENTAL RESULTS FOR MAIN BEAM-TO-COLUMN CONNECTIONS

S/D = 0.5

Three specimens were tested at this value of S/D. The first specimen failed at a load of 23.5 tons (234.22 KN), the second at 251.15 KN and the third at 260 KN. Each specimen demonstrated plastic deformation of both the beam and the column flanges at failure, but the beam flange deformation was more excessive than that of the column flange. The maximum permanent plastic deformation of the beam flange was 6.08 mm and that of the column flange 0.79 mm (both measured in the middle of the sections and 50 mm from the weld). Failure was due to the crack in one of the welds in all the three tests. The crack commenced at the midlength of the weld where deformation was greatest. The vertical slip of the beam was sufficient to fracture the weld. The failure plane angle was 80^0 from the beam flange face. There was evidence of slip and rotation about the beam compression flange. There was no beam flange deformation at the supports. All the dial gauge readings are given in Tables 3.1 and 3.2 and table A1, the load-deflection graphs in figure 3.16 and 3.17.

S/D = 1.0

Only one specimen was tested at this value of S/D. The weld failed at a load of 237.21 KN. Inspection of the specimen at failure revealed

Table 3.1 S/D = 0.5 (2) Dial gauge readings

Load Tons	Vertical Slip (mm)		Horizontal Movement (mm)	
	Left	Right	Left	Right
0	0	0	0	0
2.5	0.35	0.48	0.04	0.19
5.0	0.64	0.74	0.02	0.32
7.5	0.73	0.87	0.07	0.45
10.0	0.78	0.94	0.08	0.51
12.5	0.87	1.11	0.09	0.56
15.0	0.95	1.18	0.07	0.60
17.5	1.02	1.24	0.05	0.62
18.0	1.07	1.28	0.03	0.64
19.0	1.11	1.31	0.03	0.65
20.0	1.17	1.36	0.03	0.66
21.0	1.24	1.41	0.01	0.67
21.5	1.27	1.44	0.01	0.69
22.0	1.30	1.47	0.01	0.70
22.5	1.40	1.49	0.01	0.70
24.5	1.81	1.67	0	0.79
25.0	1.77	1.71	0	0.79

Table 3.2 S/D = 0.5 (3) Dial gauge readings

Load Tons	Vertical Slip (mm)		Horizontal Movement (mm)	
	Left	Right	Left	Right
0	0	0	0	0
2.0	0.37	0.41	0.09	0
4.0	0.58	0.64	0.15	0
6.0	0.68	0.73	0.21	0.01
8.0	0.75	0.79	0.26	0.02
10.0	0.80	0.83	0.27	0.03
12.0	0.83	0.87	0.28	0.03
14.0	0.86	0.90	0.28	0.03
16.0	0.88	0.93	0.29	0.03
18.0	0.91	0.97	0.30	0.03
20.0	0.94	1.01	0.31	0.03
21.0	0.96	1.02	0.32	0.02
22.0	0.98	1.04	0.32	0.02
23.0	0.99	1.06	0.33	0.01
24.0	1.02	1.09	0.35	0.01
25.0	1.04	1.11	0.36	0.01

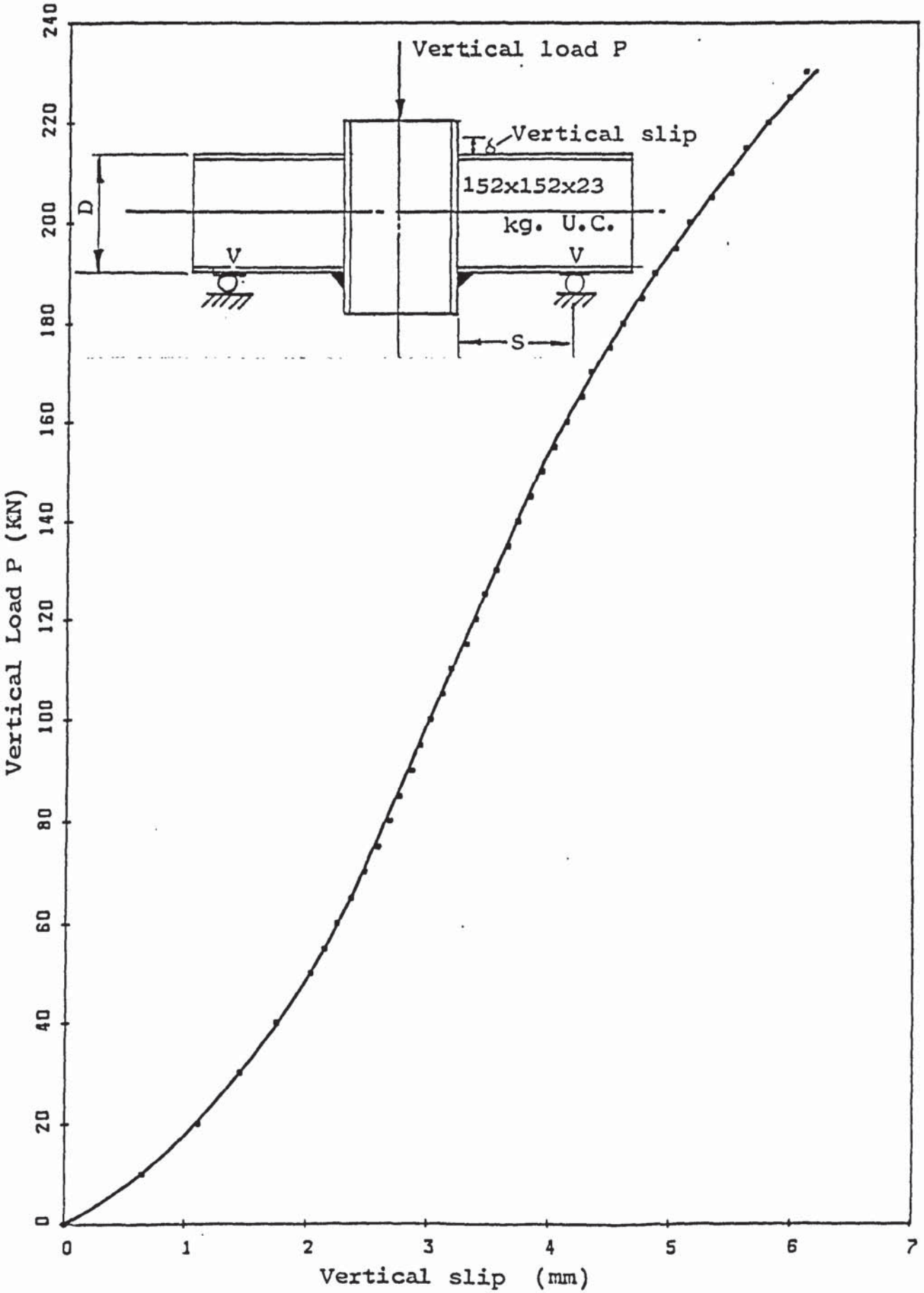

Figure 3.16 Relationship between Load and Vertical slip for S/D=0.5-Beam-to-column connection

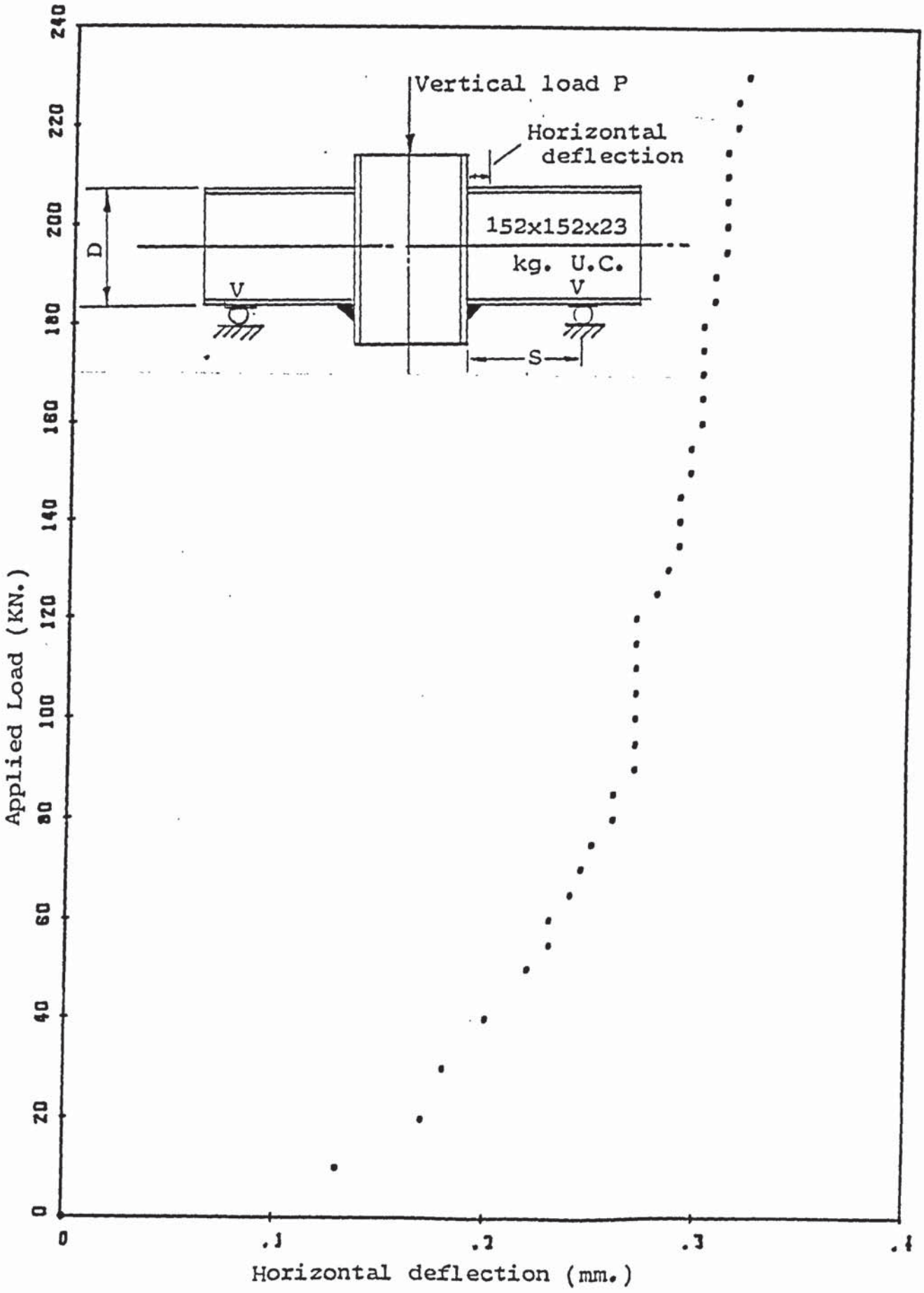

Figure 3.17 Load-Horizontal deflection relationship for beam-to-column connection-S/D=0.5

that there was plastic deformation of both the beam and the column flanges but that of the beam flange was more excessive. There was evidence of slip and rotation about the beam compression flange. Failure of the weld was observed to have started at the midlength of the weld. Fracture of the weld was due to the vertical slip of the beam and the horizontal movement of the beam. The maximum deflection of the beam flange, plastic and elastic was 2.41 mm and that of the column flange 0.25 mm. Both measurements were taken in the middle of the sections and 50 mm from the weld. Failure was due to a crack in the weld and the failure plane angle was 50^0 from the beam flange face. Table A2 gives all the dial gauge readings and Figure 3.18 and 3.19 the load-deflection graph.

S/D = 2

Two specimens were tested at this value of S/D. Both specimens showed plastic deformation of the column flange and slight deformation of the beam flange at failure. In both cases, the weld failed at a load of 128.8 KN. Failure of the weld started at the midpoint of the weld where the deformation of the weld was greatest. Concentrated beam flange force and vertical slip were, in both cases, responsible for the weld crack. There was evidence of vertical slip and rotation about the beam compression flange. The maximum deflection of the beam flange was 1.25 mm and that of the column flange 0.184 mm, each measured in the middle of the section and 50 mm from the weld. The failure plane angle was 30^0 from the beam flange face. All the dial gauge readings are presented in Tables 3.3 and A3 and the load-deflection graphs in Figures 3.20 and 3.21.

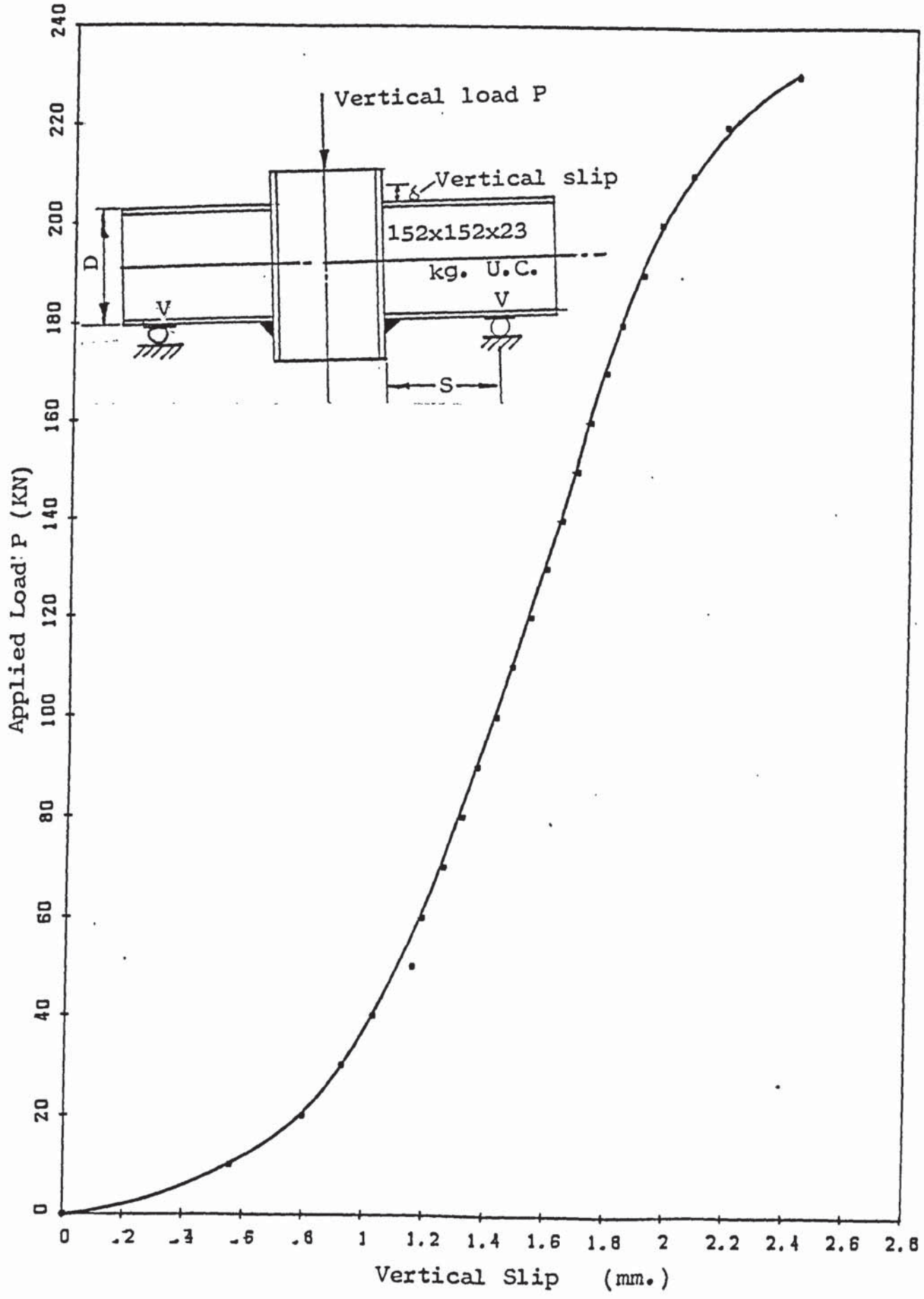

Figure 3.18 Load-Vertical slip relationship for S/D=1.0 Beam-to-column connection

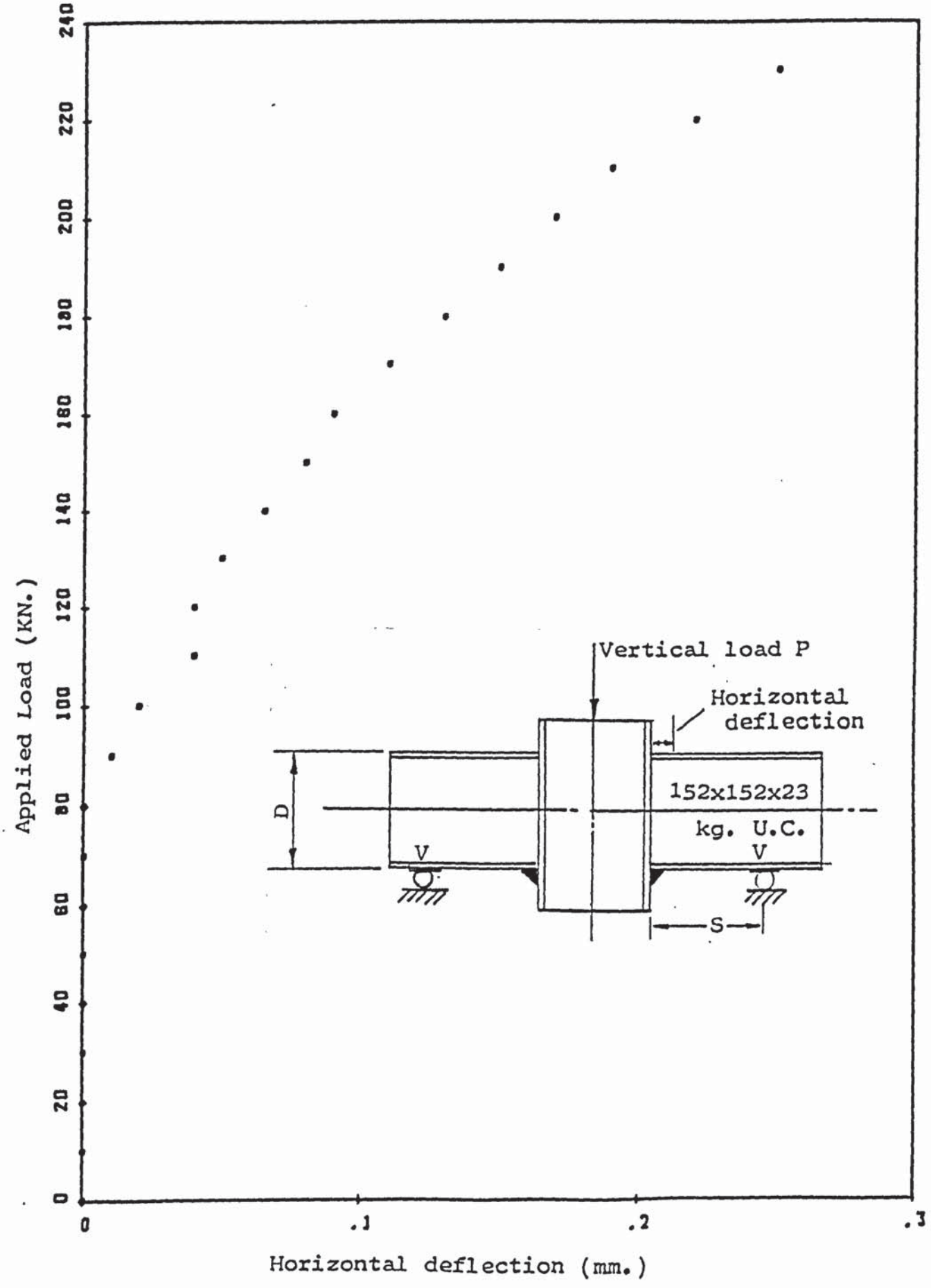

Figure 3.19 Load-Horizontal deflection relationship for beam-to-column connection-S/D=1.0

Table 3.3 Dial gauge readings for Beam-to-column connection test - S/D = 2.0 specimen number 2

Load Tons	Vertical Slip (mm)		Horizontal Movement (mm)	
	Right	Left	Right	Left
1.0	0.14	0.14	0	0
2.0	0.18	0.24	0	0
3.0	0.22	0.29	0	0
4.0	0.24	0.36	0	0
5.0	0.26	0.43	0	0
6.0	0.28	0.50	0	0
7.0	0.31	0.56	0.002	0
8.0	0.33	0.61	0.004	0
9.0	0.36	0.65	0.01	0.002
10.0	0.40	0.70	0.18	0.01
10.5	0.41	0.73	0.02	0.02
11.0	0.44	0.77	0.03	0.02
11.5	0.46	0.80	0.04	0.03
12.0	0.50	0.85	0.06	0.05
12.5	0.54	0.92	0.08	0.07

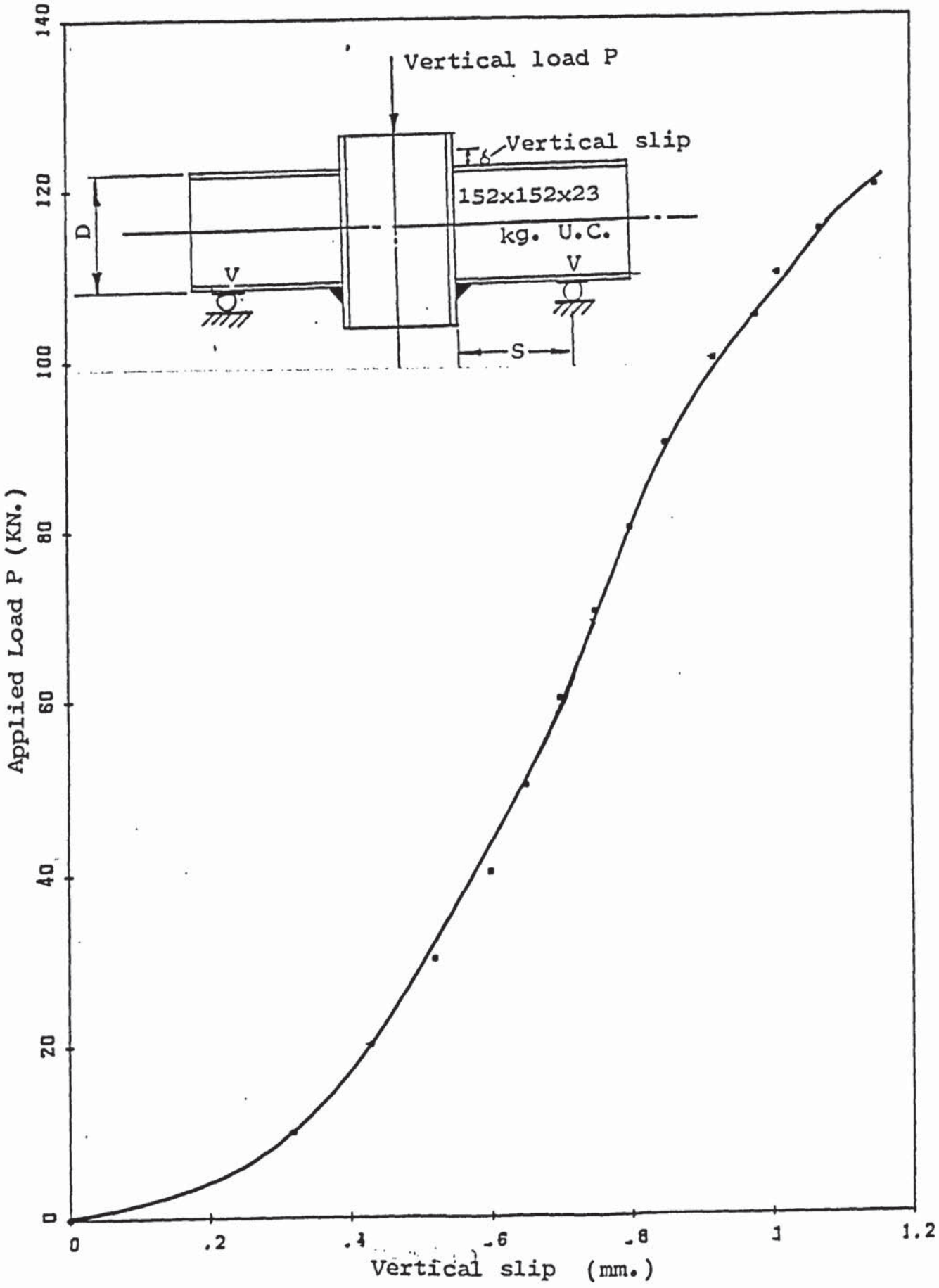

Figure 3.20 Load-Vertical slip relationship for S/D = 2.0 Beam-to-column connection.

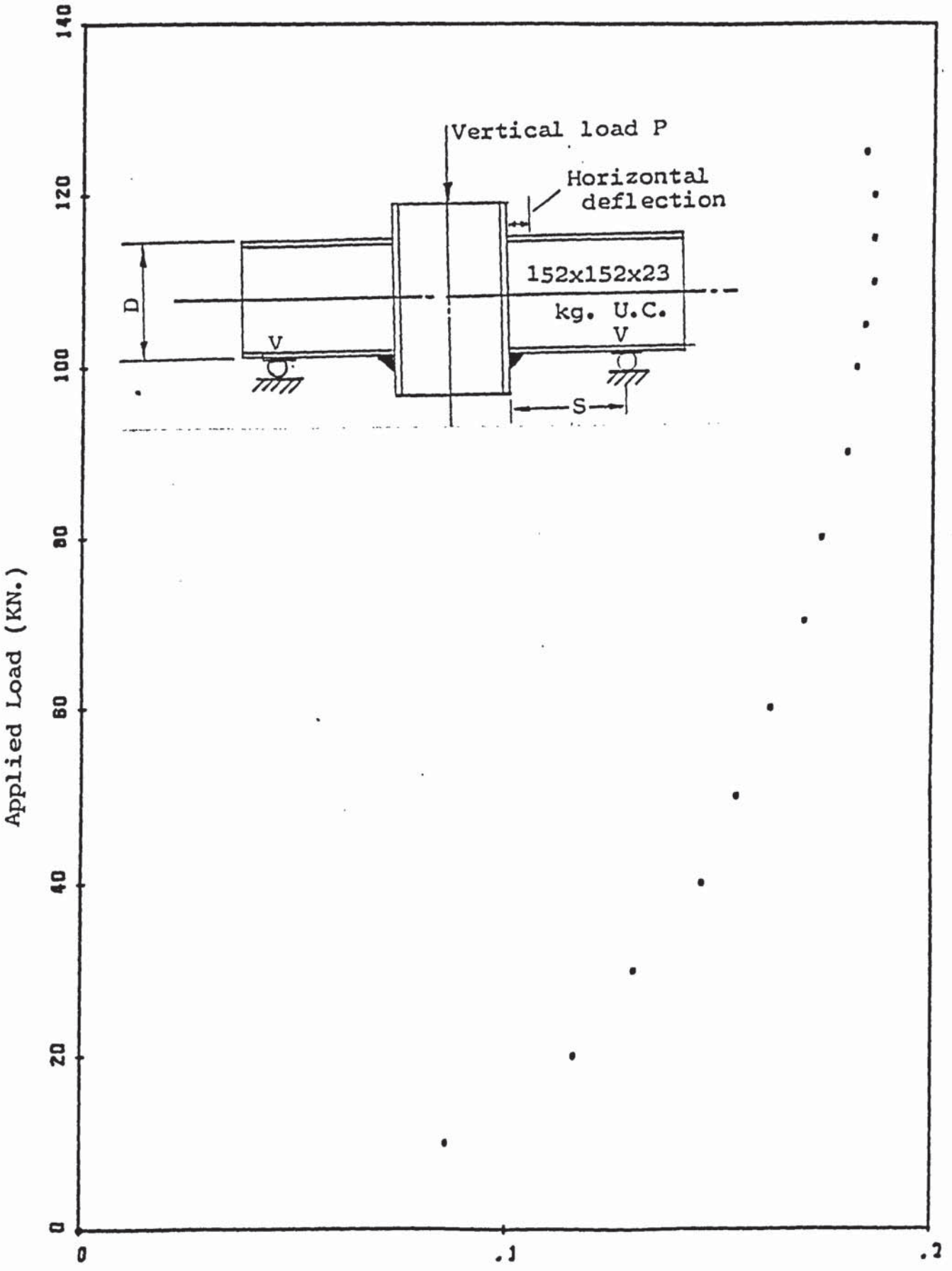

Figure 3.21 Load-horizontal deflection relationship for beam-to-column connection-S/D=2.0

S/D = 3.0

Three specimens were tested at this value of S/D. Observation of the specimens at failure revealed that there was a slight plastic deformation of the column flange and no noticeable plastic deformation of the beam flange. The maximum deflection of the beam was 0.15 mm and that of the column 0.98 mm. The first specimen failed at a load of 74.6 KN, the second at 78.7 KN and the third at 67.8 KN. In all the specimens, failure of the weld started at the middle of the weld. The tensile force in the beam flange pulled the outstanding column flanges as shown in Figure 3.22. Flexibility allowed the beam and column flanges to deform together at the toes of the column flanges. However, deformation was restricted at the middle of the column where it is restrained by the column web and fracture started there.

There was rotation about the compression flange but vertical slip was very small. The failure plane angle was 25^0 from the beam flange face. All the dial gauge readings are given in Tables 3.4, 3.5 and A4 and the load-deflection graphs in Figures 3.23 and 3.24.

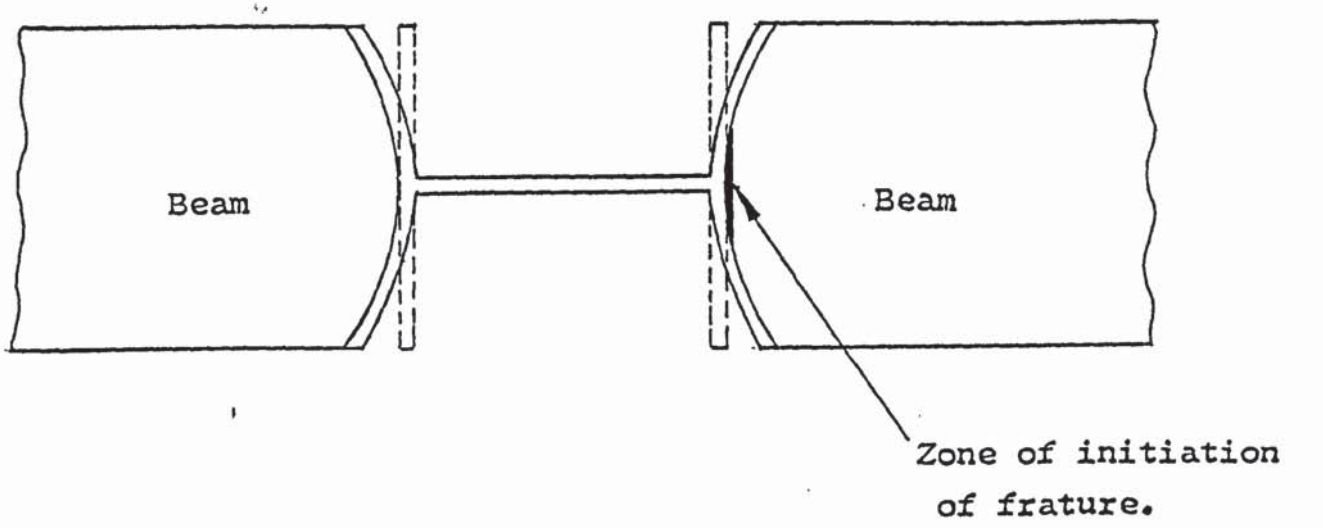

Figure 3.22 Initiation of weld fracture in unstiffened Beam-to-column connection

S/D = 4

Only one specimen was tested at this value of S/D. The weld failed at a load of 58.9 KN. Observation of the connection at failure revealed that there was a slight plastic deformation of the column flange but no noticeable plastic deformation of the beam flange. The maximum beam flange deformation was 0.395 mm and that of the column flange 0.043 mm. Failure of the weld started at the midlength of the weld. This weld fracture mechanism is similar to that when S/D = 3.0. There was rotation about the beam compression flange but vertical slip was very small; i.e. 0.3 mm at failure. The failure plane angle was 20^0, measured from the beam flange face. All the dial gauge readings are presented in Table A5 and the load-deflection graph in Figure 3.25.

Table 3.4 Dial gauge readings for Beam-to-column connection tests - S/D = 3.0 Specimen number two

Load Tons	Vertical Slip (mm)		Horizontal Movement (mm)	
	Left	Right	Left	Right
1.0	0.14	0.49	0.14	0
2.0	0.24	0.65	0.14	0
3.0	0.33	0.73	0.11	0
4.0	0.38	0.79	0.11	0
5.0	0.44	0.84	0.11	0
6.0	0.50	0.88	0.11	0
6.5	0.54	0.91	0.12	0
7.0	0.58	0.94	0.13	0
7.5	0.64	0.98	0.15	0

Table 3.5 Dial gauge readings for S/D = 3.0 Beam-to-column connection test specimen number three

Load Tons	Vertical Slip (mm)		Horizontal Movement (mm)	
	Left	Right	Left	Right
1.0	0.22	0.25	0.06	0.02
2.0	0.30	0.33	0.08	0.04
3.0	0.38	0.40	0.10	0.06
4.0	0.45	0.46	0.11	0.07
5.0	0.55	0.54	0.12	0.08
6.0	0.64	0.63	0.12	0.08
6.5	0.69	0.69	0.12	0.07

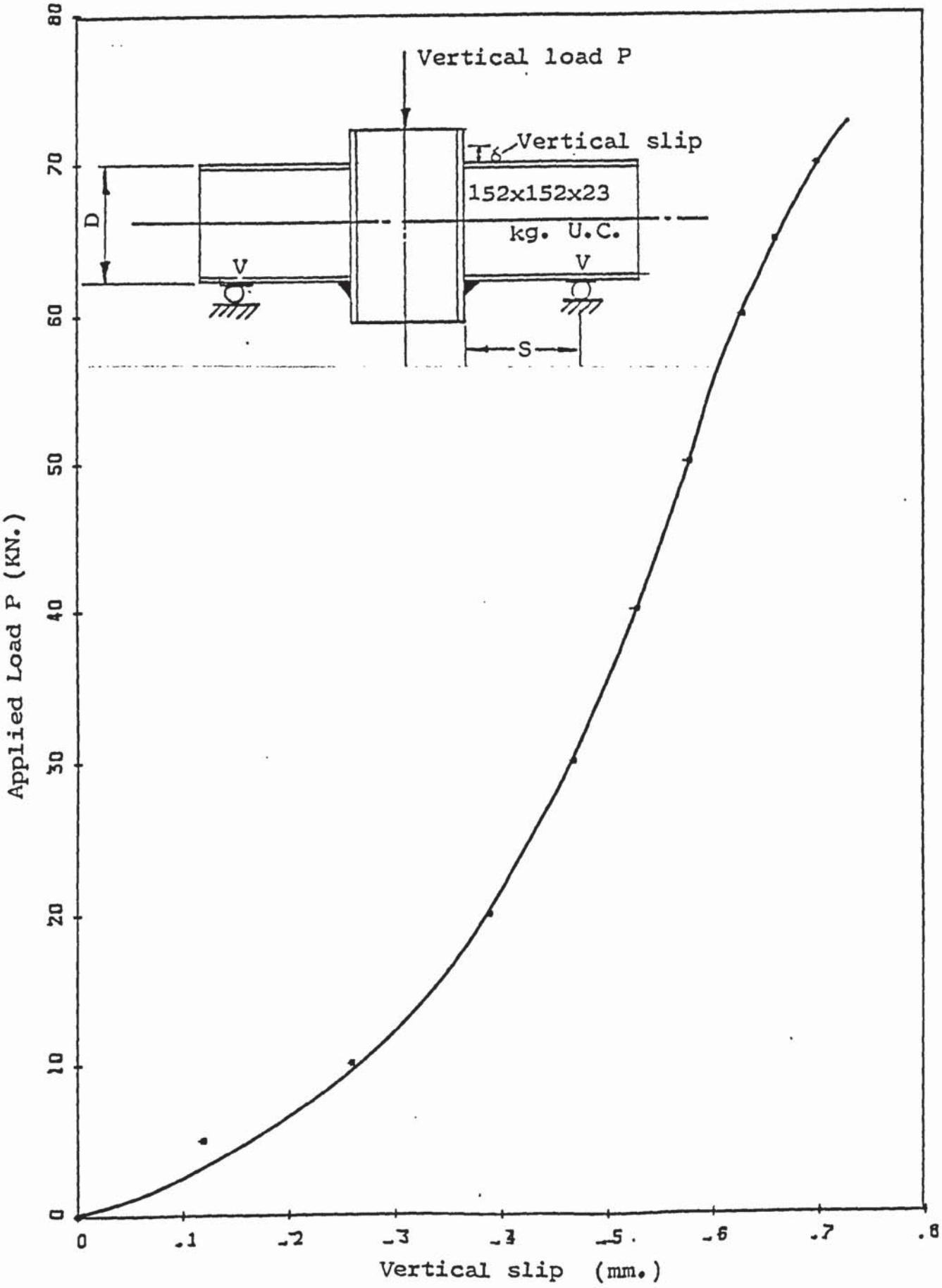

Figure 3.23 Load-Vertical slip relationship for S/D=3.0 Beam-to-column connection

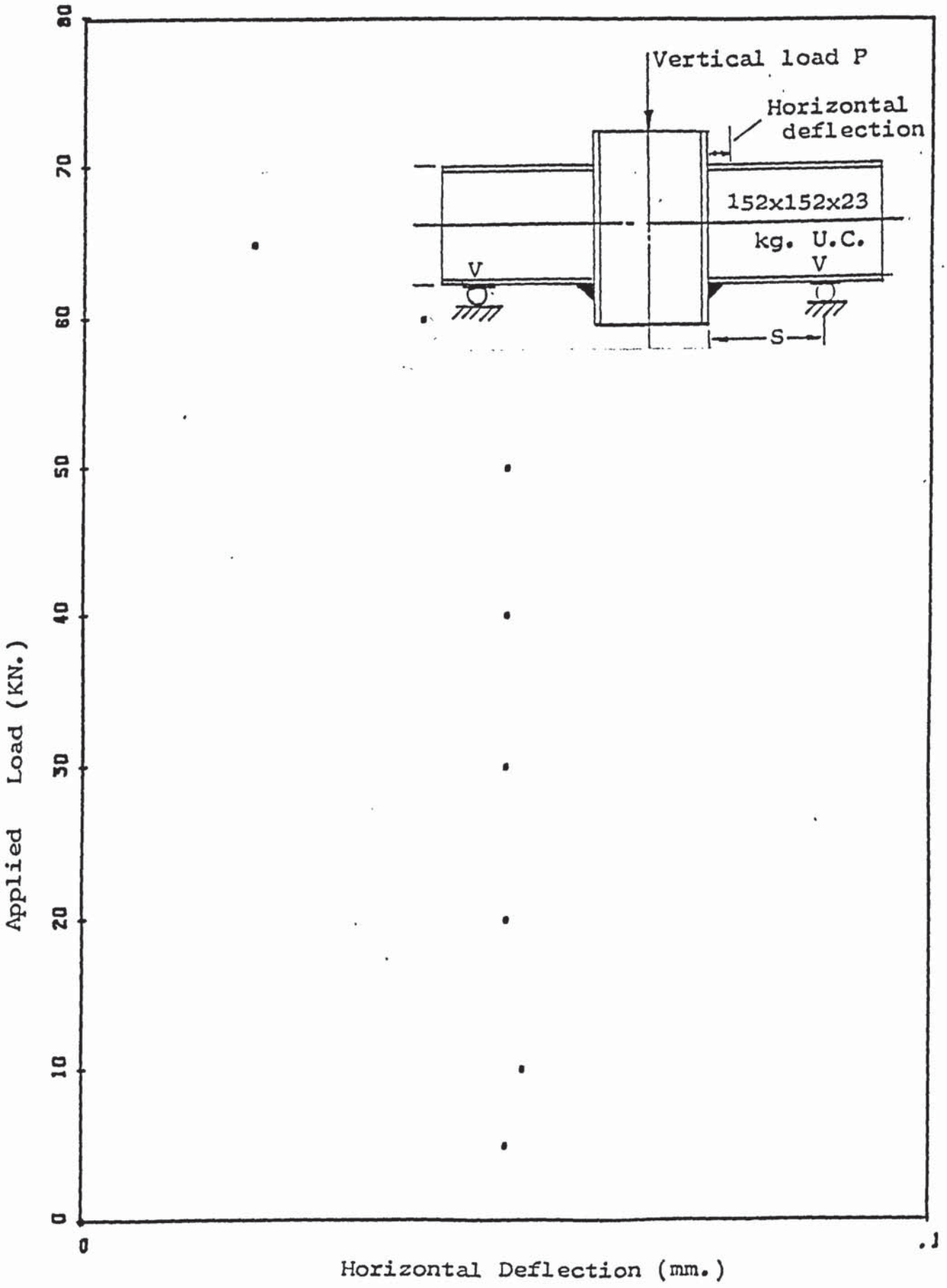

Figure 3.24 Load-Horizontal deflection relation for beam-to-column connection - S/D=3.0

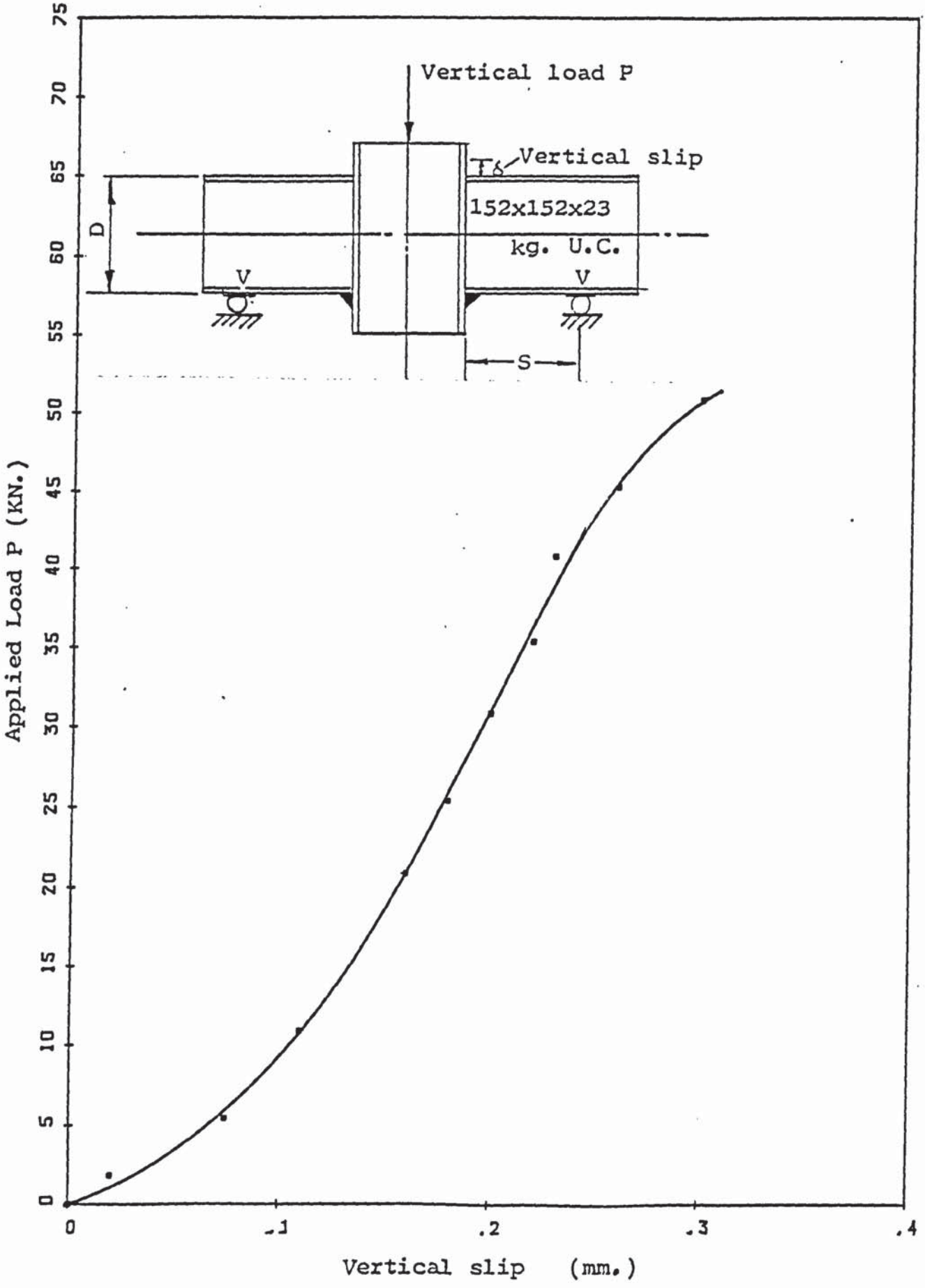

Figure 3.25 Load-Vertical slip relationship for S/D=4.0 Beam-to-column connection.

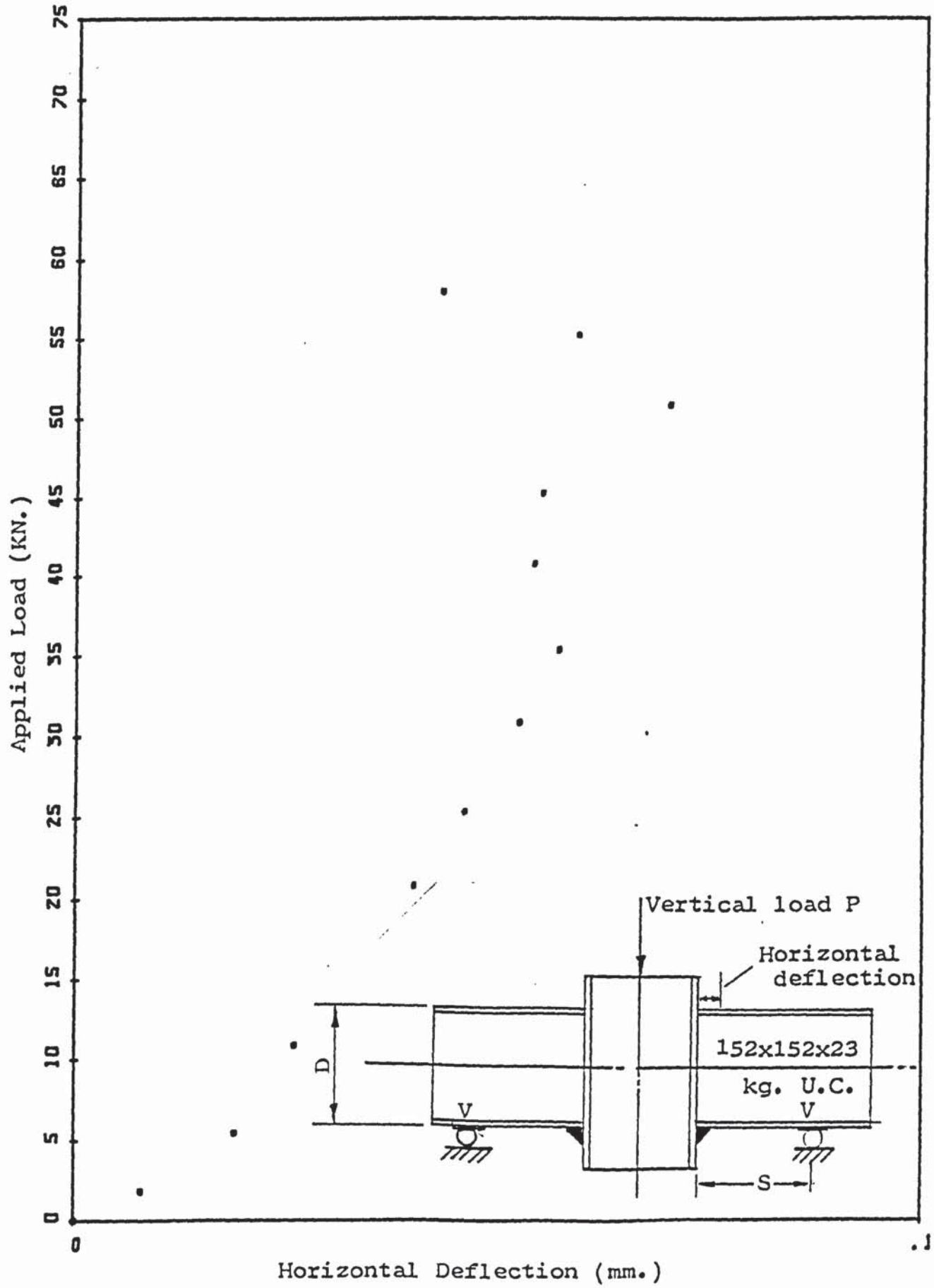

Figure 3.26 Load-horizontal deflection relationship for beam-to-column connection - S/D=4.0

The summary of all the results given above are presented in Table 3.6 below and Figures 3.27, 3.28, 3.29 and 3.30.

$\frac{S}{D}$	Shear load V (mean) KN	Standard deviation σ	Failure plane angle (α)	Maximum beam flange deflection (mm)	Maximum column flange deflection (mm)
0	108.60*	-	90^0	-	-
0.5	124.36	10.7	80^0	6.08	0.32
1.0	117.50	-	50^0	2.41	0.25
2.0	64.40	0	30^0	1.25	0.18
3.0	36.85	4.5	25^0	0.98	0.15
4.0	29.45	-	20^0	0.395	0.043

* Calculated figure

Table 3.6 Summary of experimental results - Beam-to-column connection

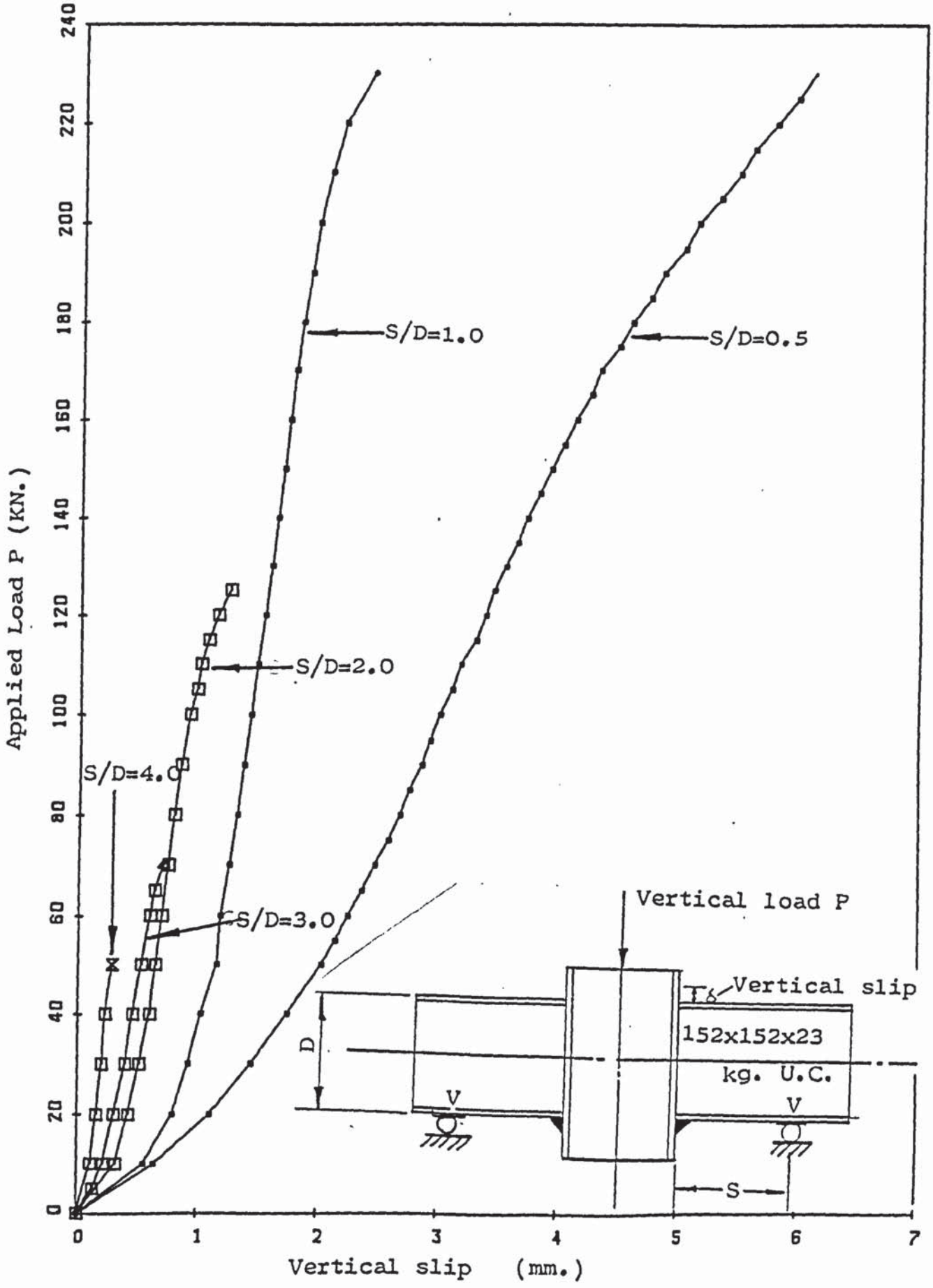

Figure 3.27 Evidence of the reduction of vertical slip as the eccentricity of load increases.

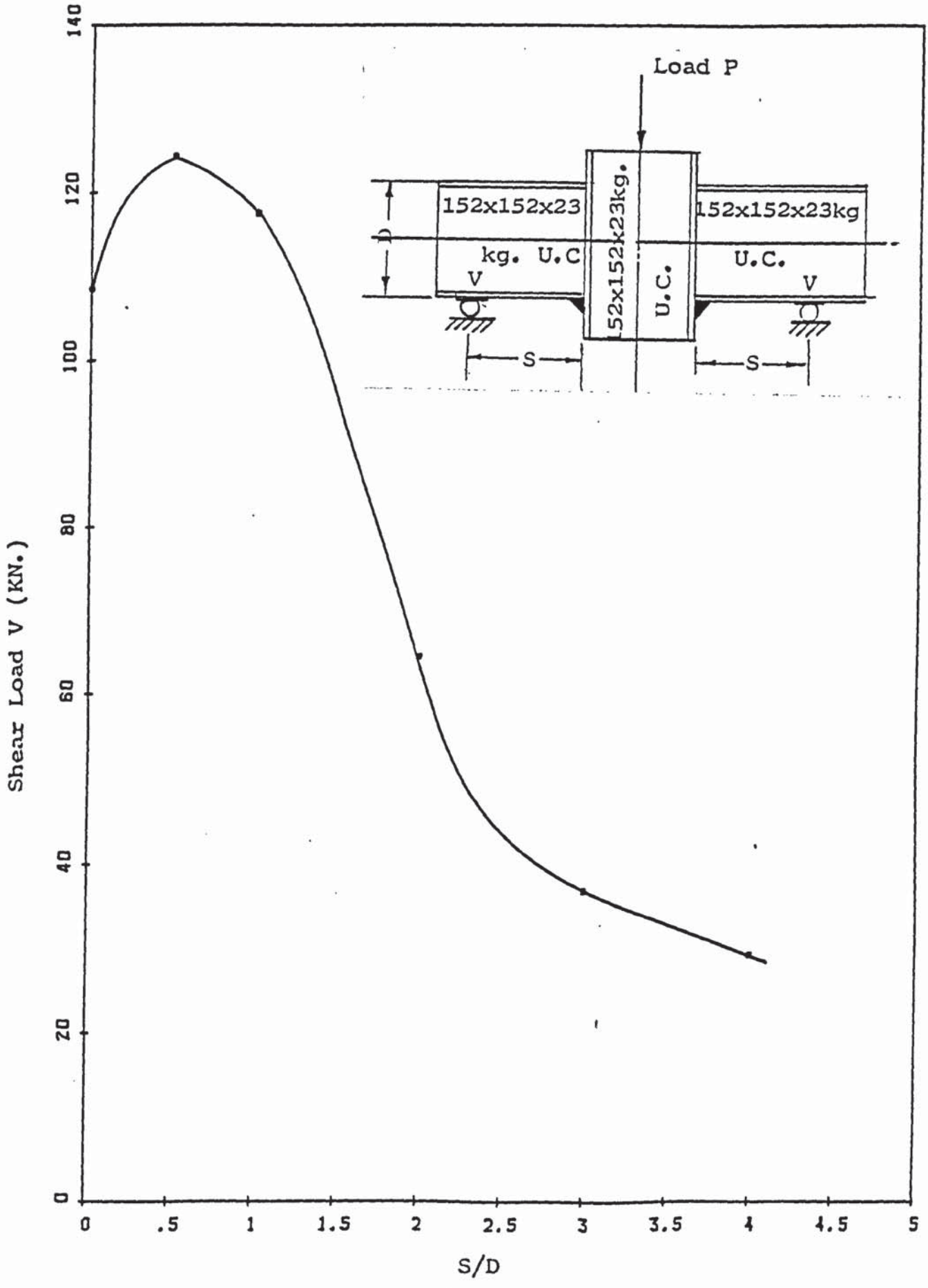

Figure 3.28 Relationship between the shear load V and S/D for Beam-to-column connection.

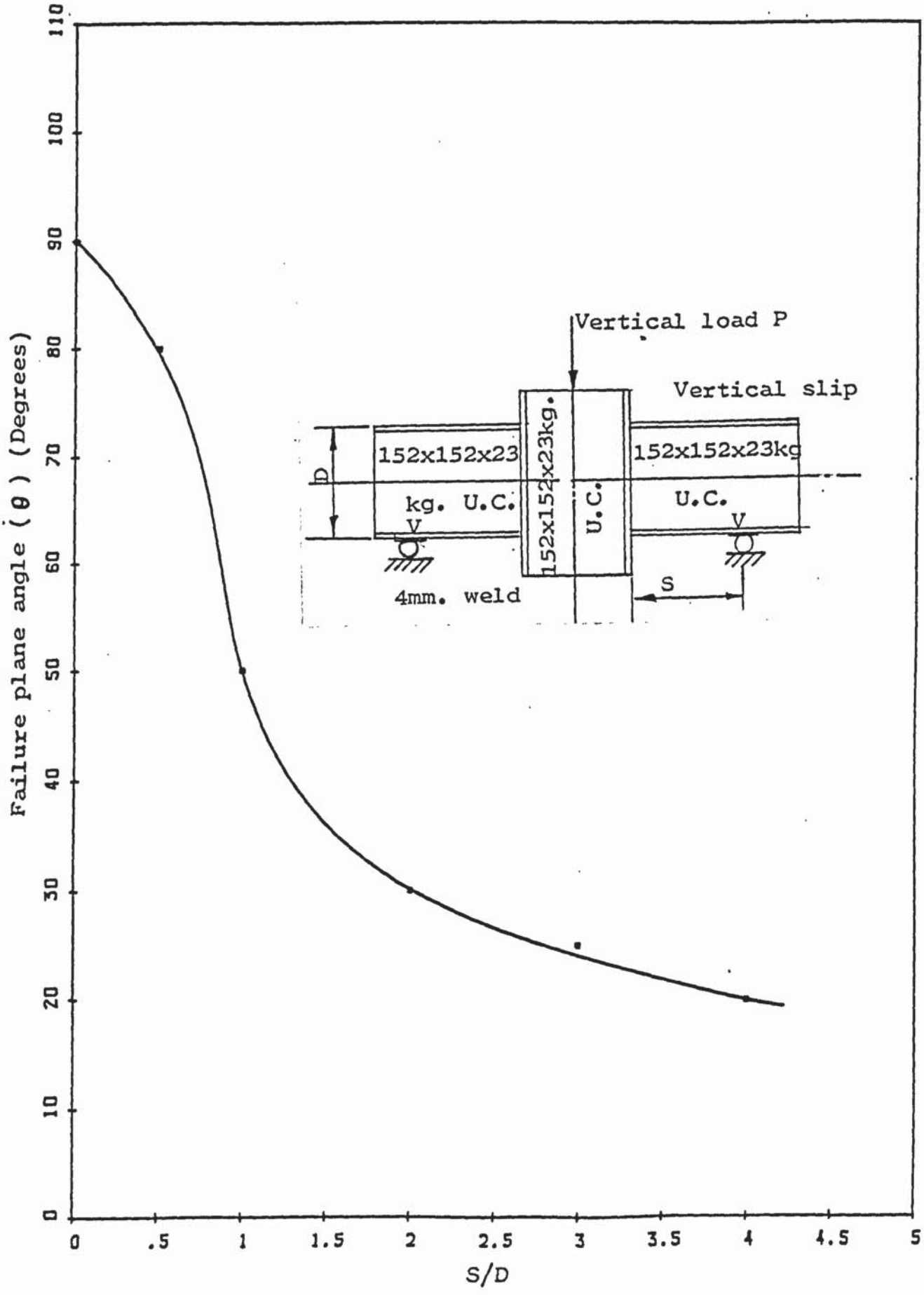

Figure 3.29 Variation of failure plane angle with S/D

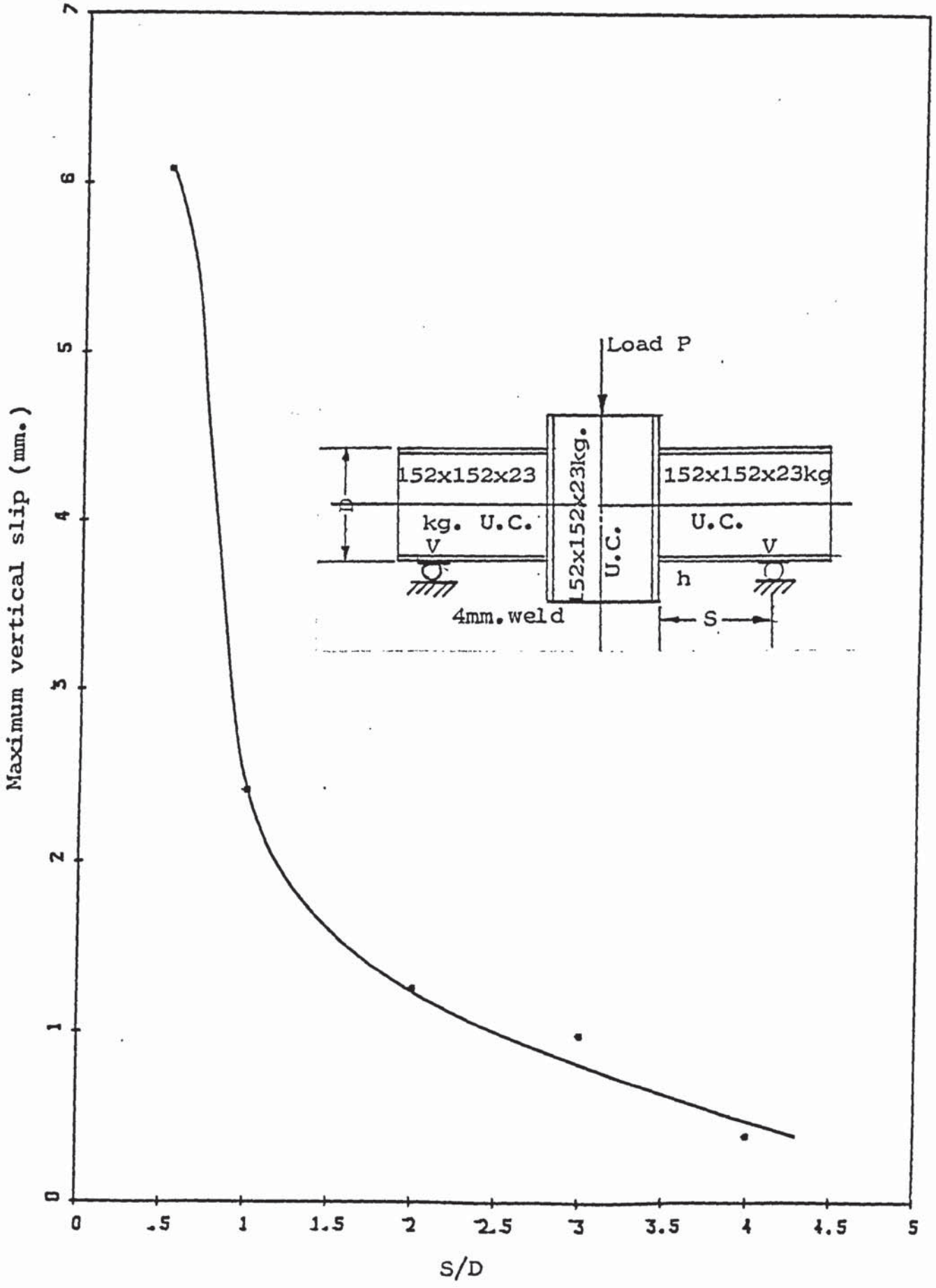

Figure 3.30 Variation of Vertical slip with load eccentricity for Beam-to-column connection.

3.3.2 EXPERIMENTAL RESULTS FOR COLUMN WEB BUCKLING TESTS

NO AXIAL LOAD ON THE COLUMN

Figure 3.5 shows the test arrangement when the column carries an axial load. When no axial load was applied to the column, the column web buckled at a load of 20 tons (199.34 kN). The deformation of the flanges was restricted to the immediate vicinity of the stiff bearings. Yield lines were first noticed at the web and flange junction at a load of about 5 tons (25% of the web buckling load). The strain gauge readings are presented in the Appendix.

AXIAL LOAD = 2.0 TONS

With an axial load of 2 tons (199.34 kN) on the column the column web buckled at a load of 20 tons with plastic deformation of the flanges, the deformation being restricted to the areas around the stiff bearing. Yield lines were first noticed at the web and flange junction at a load of about 5 tons (49.835 kN). The strain gauge readings are presented in the Appendix.

AXIAL LOAD = 20.0 TONS

With an axial load of 20 tons (199.34 kN) on the column, the column web buckled at a load of 20 tons (199.34 kN). Yielding was first noticed

at the web/flange junction at a load of about 4 tons (39.868 kN). The plastic deformation of the flange was restricted to the immediate neighbourhood of the stiff bearing. The strain gauge readings for this test are not presented due to a hardware fault in the data logger.

AXIAL LOAD = 40 TONS

With an axial load of 40 tons (398.68 kN) on the column, the column web buckled at a load of 18.75 tons (186.88 kN) with plastic deformation of the flanges. The plastic deformation was restricted to the immediate neighbourhood of the stiff bearing. Yield lines were first noticed around the flange/web junction at a load of about 3.5 tons (34.885 kN). The strain gauge readings are presented in the Appendix.

AXIAL LOAD = 60 TONS

With an axial load of 60 tons (598.02 kN) on the column, the column web buckled at a load of 14.89 tons (148.41 kN) with plastic deformation of the flanges. The plastic deformation of the flanges was not as great as in the previous cases when values of the axial load were lower. Yield lines were first noticed at the web and flange junction at a load of about 3.5 tons (34.885 kN). The strain gauge readings are given in the Appendix.

AXIAL LOAD = 80 TONS

With an axial load of 80 tons (797.36 kN) on the column, the web buckled at a load of 8 tons (79.736 kN) with marked distortion of the entire section. It appeared as if crushing and web buckling occured simultaneously. Plate (5) shows the specimen at failure. The strain gauge readings are given in the Appendix.

The summary of all the results are given below in Table 3.7 and the interaction curve developed using the test results is given in Figure 3.31.

Axial Load (Tons)	Web Buckling Load (Tons)
0	20.0
2.0	20.0
20.0	20.0
40.0	18.75
60.0	14.89
80.0	8.00

Table 3.7 Summary of test results - column web buckling test

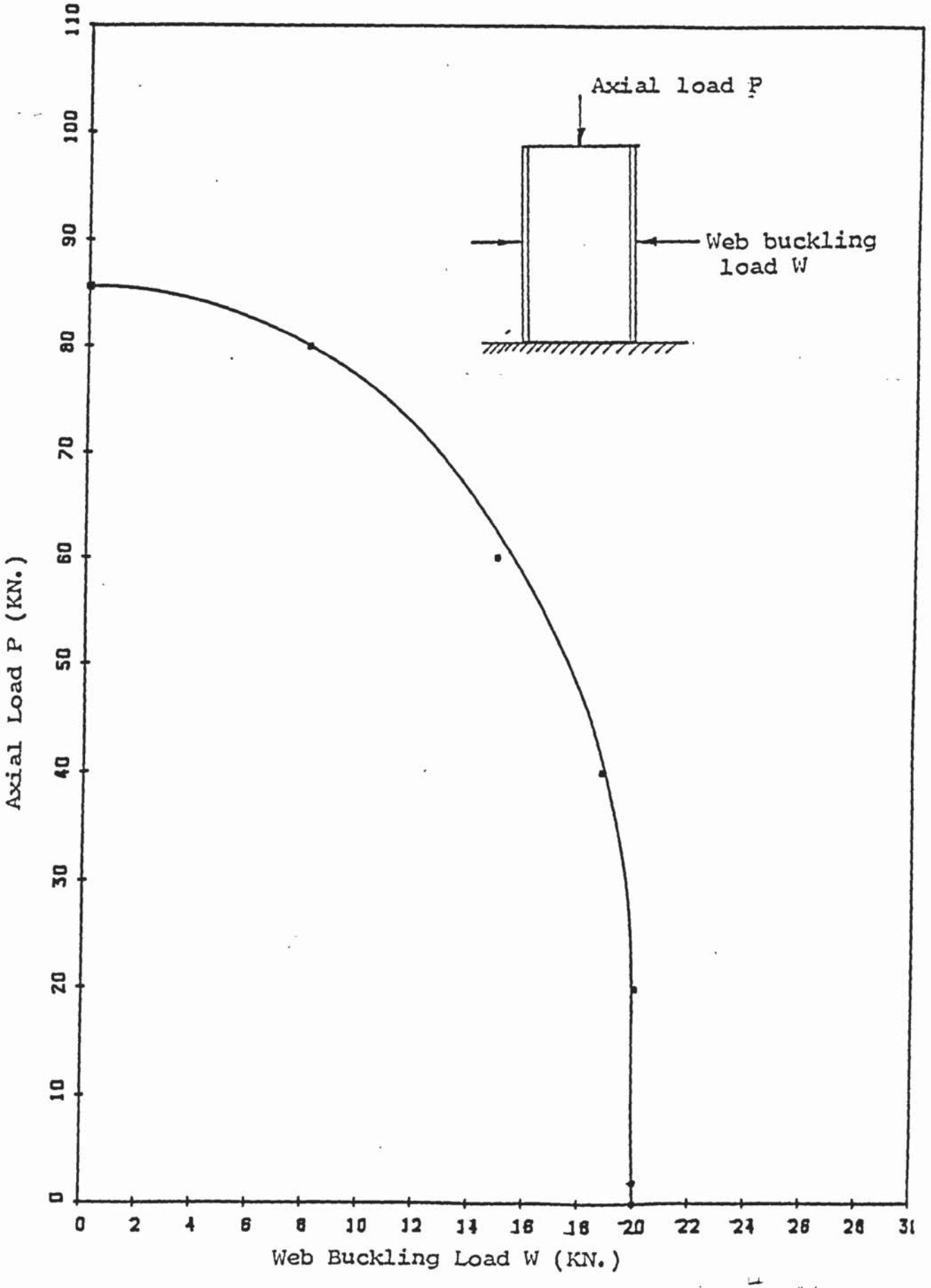

Figure 3.31 Relationship between Axial Load and Web buckling Load for the column.

SUBSIDIARY TESTS TO DETERMINE THE LENGTH OF THE REGION AFFECTED BY THE CONCENTRATED TRANSVERSE LOAD

A test was carried out to determine the length of the region of the column affected by the concentrated transverse load (see theory on column web buckling). Four strain gauges were fixed at 10 millimetre spacing on both sides of the web as shown in Figure 3.24. The column was then subjected to a transverse load with no axial load. The stress distribution at the four positions are given in Figure 3.33.

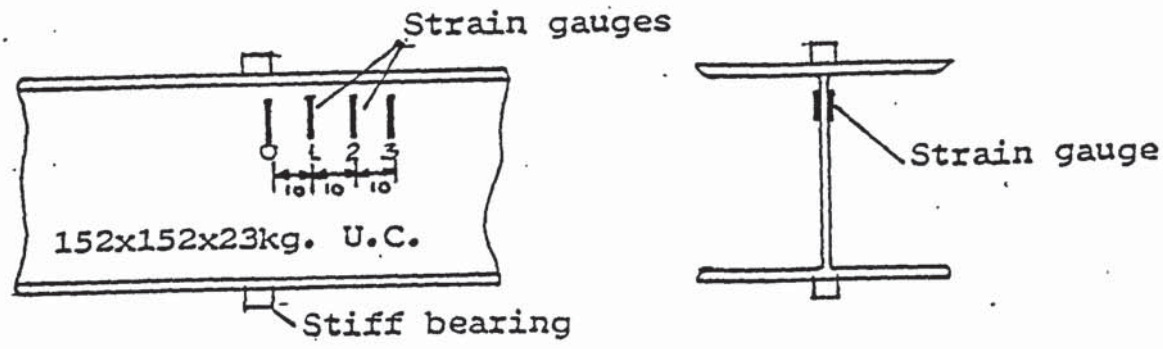

Figure 3.32 Column specimen for the determination of the length of the region affected by the concentrated load on the column.

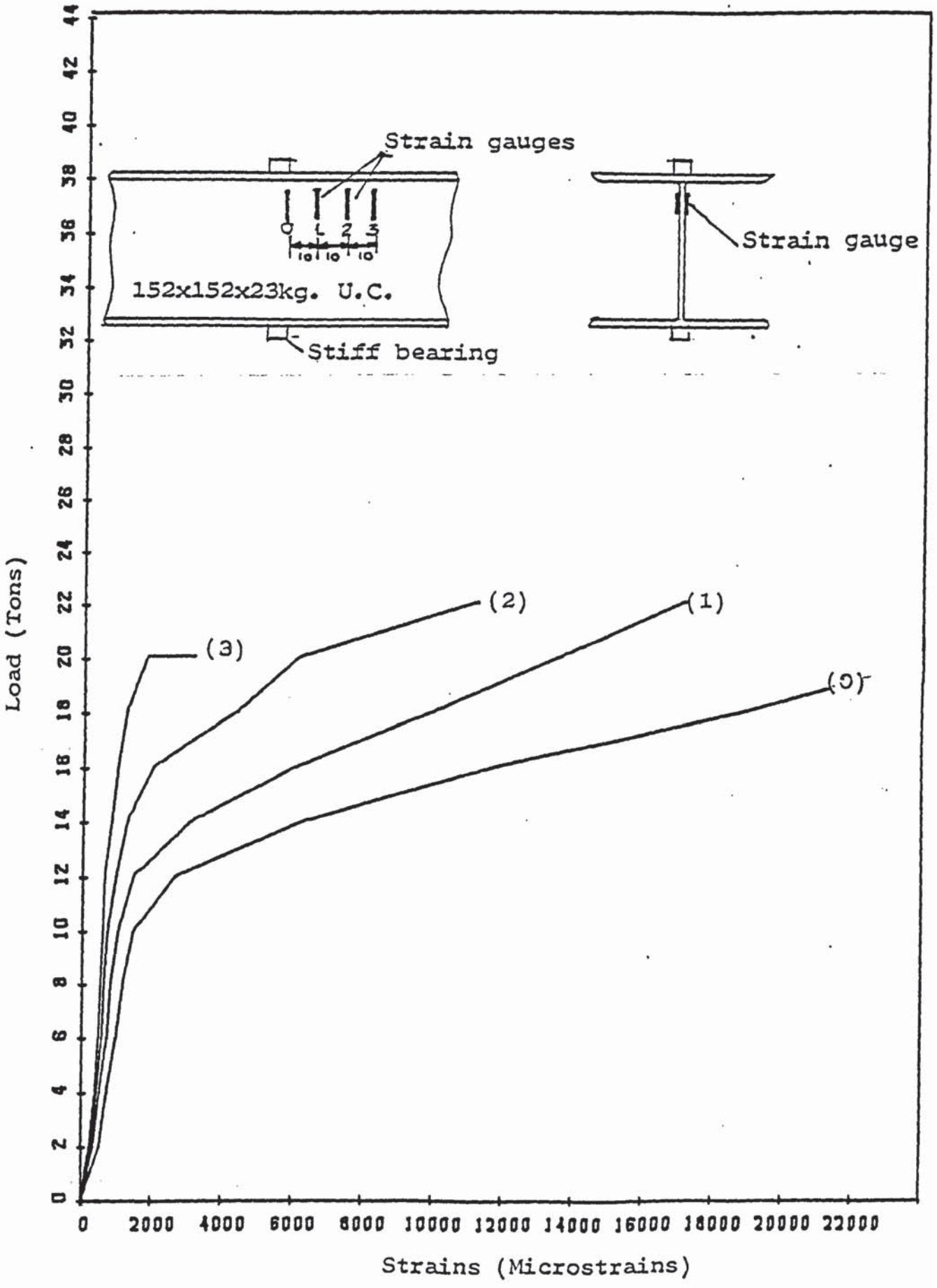

Figure 3.33 Load-Strain relationship for the determination of the length of the section affected by the concentrated load.

3.3.3 EXPERIMENTAL RESULTS FOR SECONDARY BEAM-TO-COLUMN CONNECTION

As mentioned in Section 3.2, four different types of specimens were tested. The behaviour of each type of connection is described in this section. The graphs showing the stress distribution along the tee web and the moment-rotation graph for each type of connection are also presented. The strain gauge and dial gauge readings are presented in the Appendix.

3.3.3.1 CONNECTION A - NO COLUMN STIFFENING

Five specimens were tested in this series. The first specimen with a 4 mm weld between the beam and the tee flange failed at a load of 12.5 tons (124.59 kN). The second and the third with an 8 mm weld between the beam and the tee flange failed at 14.5 tons (144.52 kN), the fourth, with the same size of weld as the latter failed at 13.5 tons (134.55 kN) and the fifth, also with an 8 mm weld between the beam and the tee flange failed at 10.75 tons (107.15 kN). Except for the first specimen where failure was due to the cracking of the weld between the beam and the tee flange in the tension region, failure in the rest of the specimens was due to a crack in the butt weld between the flanges of the column and the tee in the beam tension region (see Plate 7,8). This is due to the fact that the size of the weld between the beam and the tee flange in the latter four specimens was twice that of the first specimen.

Yield lines were observed on the column in the vicinity of the beam compression flange at a load of 6 tons (59.8 kN) in all the tests. Observation of the yield line pattern on the column web at failure gave an indication of rotation about the middle of the beam. Despite the fact that the column was fastened to the rig, it buckled about the beam compression flange. It is possible that plastic hinges could have developed had the column not been fastened to the rig. The yield lines on the column flange were only confined to the compression region. A typical yield line pattern is given in Figure 3.34.

The dial gauge readings and the strain gauge readings are given in the Appendix. Figure 3.35 gives the strain distribution along the tee web at ultimate load, Figure 3.36 the moment-rotation curve, and Figure 3.37 the load-vertical slip relationship.

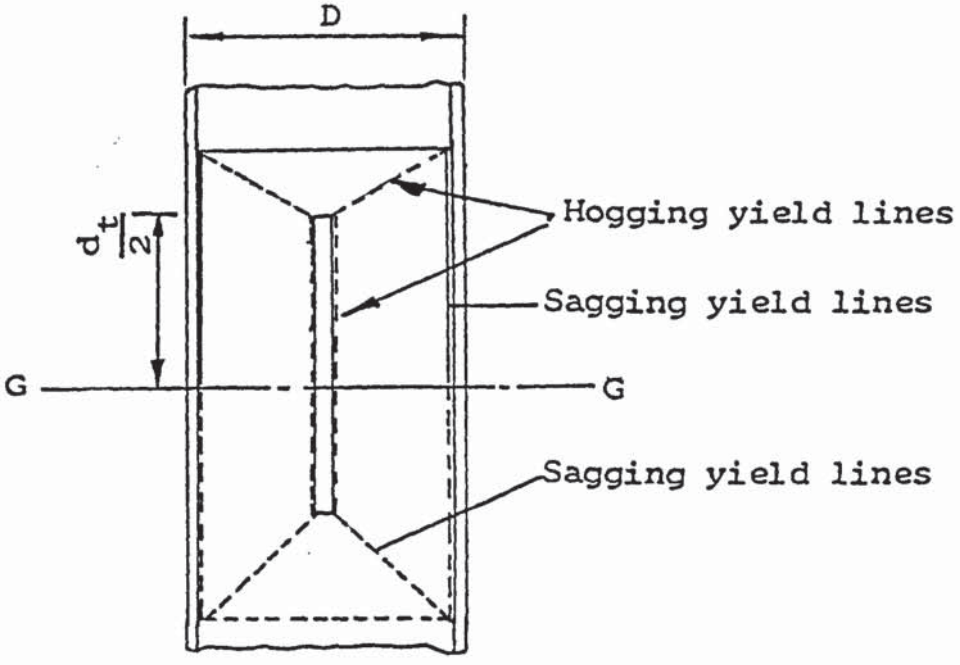

Figure 3.34 Typical yield line pattern on the web of the column of an unstiffened secondary beam-to-column connection.

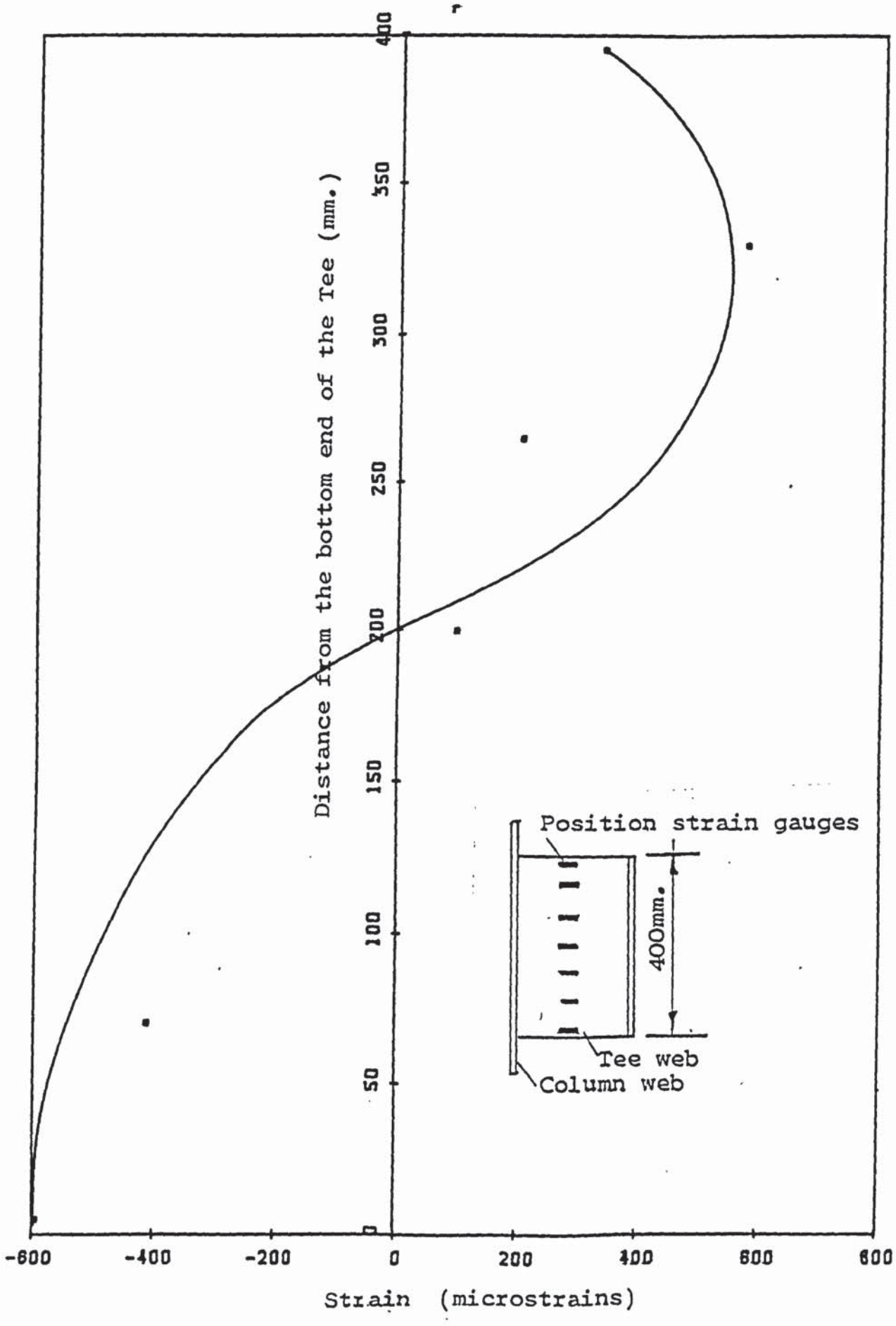

Figure 3.35 Strain distribution in the tee web for unstiffened secondary beam-to-column connection.

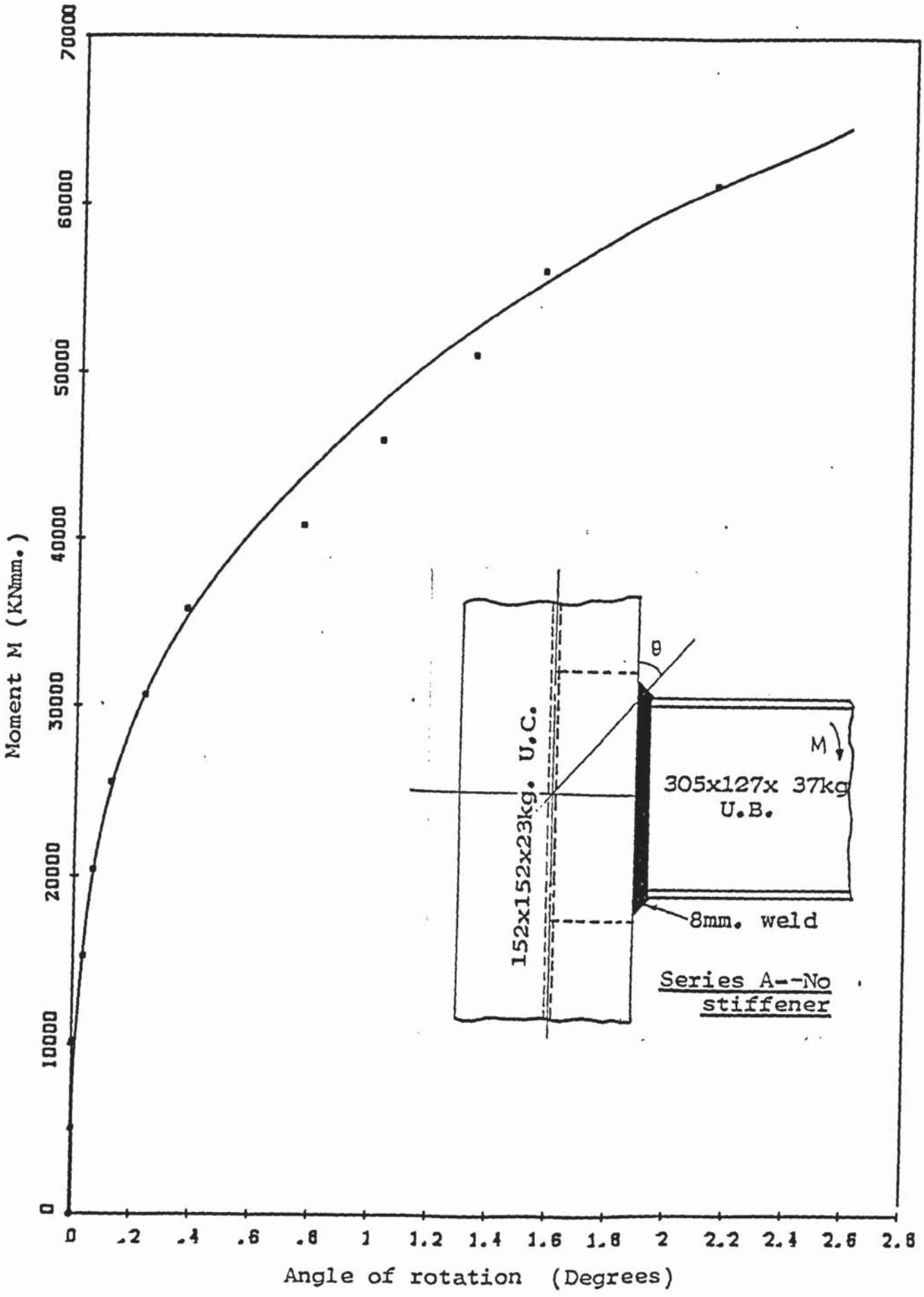

Figure 3.36 Moment-Rotation relationship for unstiffened secondary beam-to-column connection.

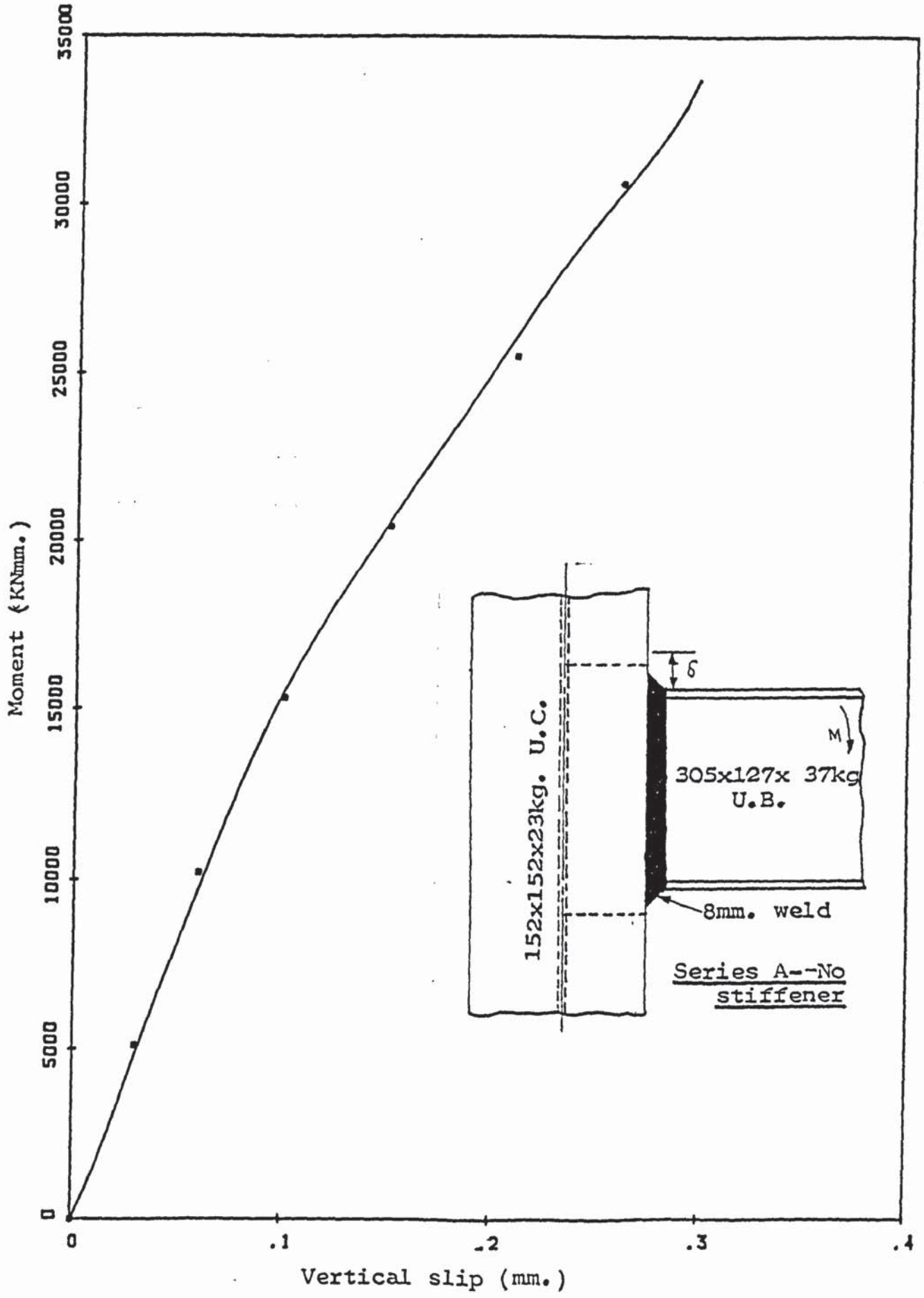

Figure 3.37 Moment-Vertical slip relationship for unstiffened secondary beam-to-column connection.

3.3.3.2 CONNECTION B - STIFFENER IN LINE WITH THE BEAM TENSION FLANGE

Two specimens were tested in this series. The first failed at a load of 13.875 tons (138.29 kN) and the second at 16.25 tons (161.96 kN). Yeild lines first appeared on the column flanges in the vicinity of the compression flange and the Tee/column flange junction. These yield lines extended as the load was increased. Observation of the yield line pattern on the column web at failure gave an indication of rotation taking place about 120 millimetres from the top of the tee. A typical yield line pattern is shown in Figure 3.38.

The dial-gauge and strain gauge readings are given in the Appendix. The strain distribution along the tee web is given in Figure 3.39 and the moment/rotation graph in Figure 3.40. The moment-vertical slip graph is presented in Figure 3.41.

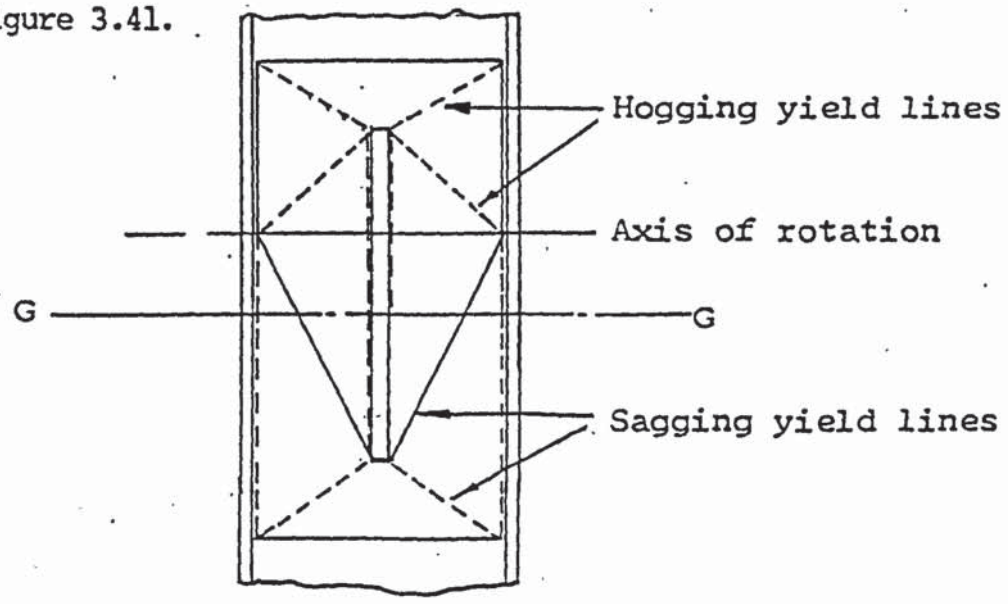

Figure 3.38 Typical yield line pattern on the column web of a secondary beam-to-column connect stiffened in the beam tension region.

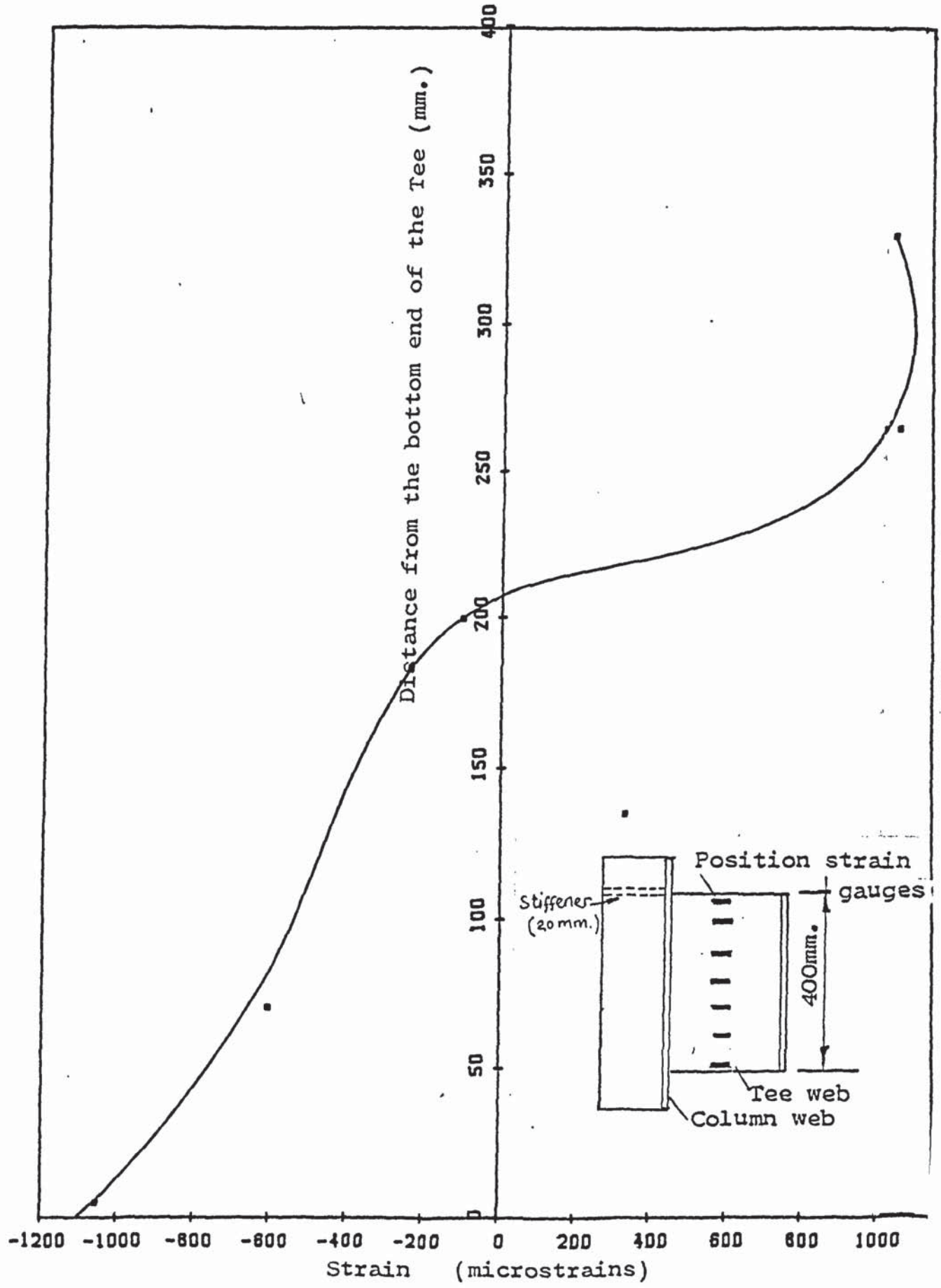

Figure 3.39 Strain values just before failure for secondary beam-to-column connection with column stiffener in the beam tension region.

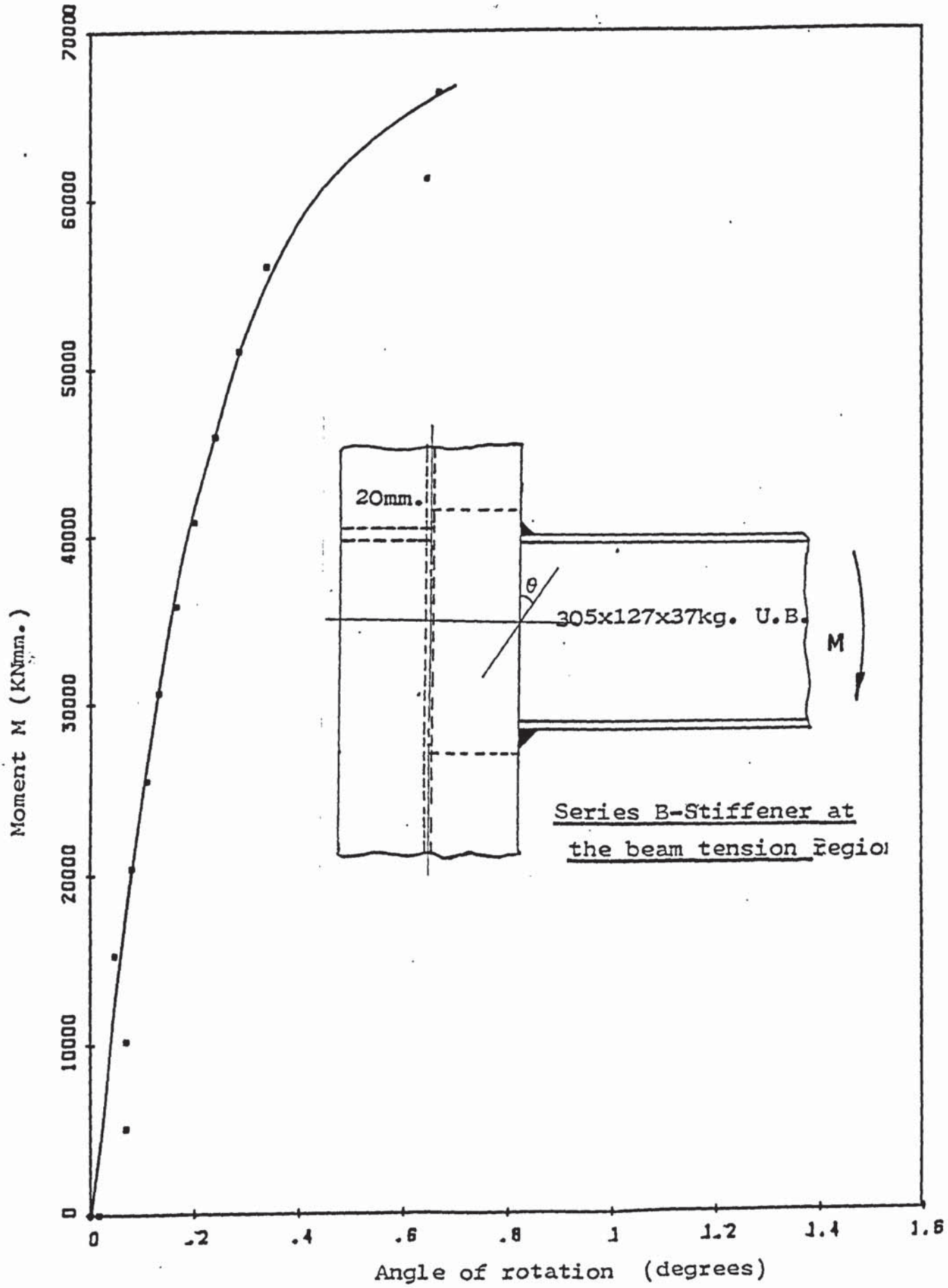

Figure 3.40 Moment-Rotation relationship for secondary beam -to-column connection with column stiffener in the beam tension region.

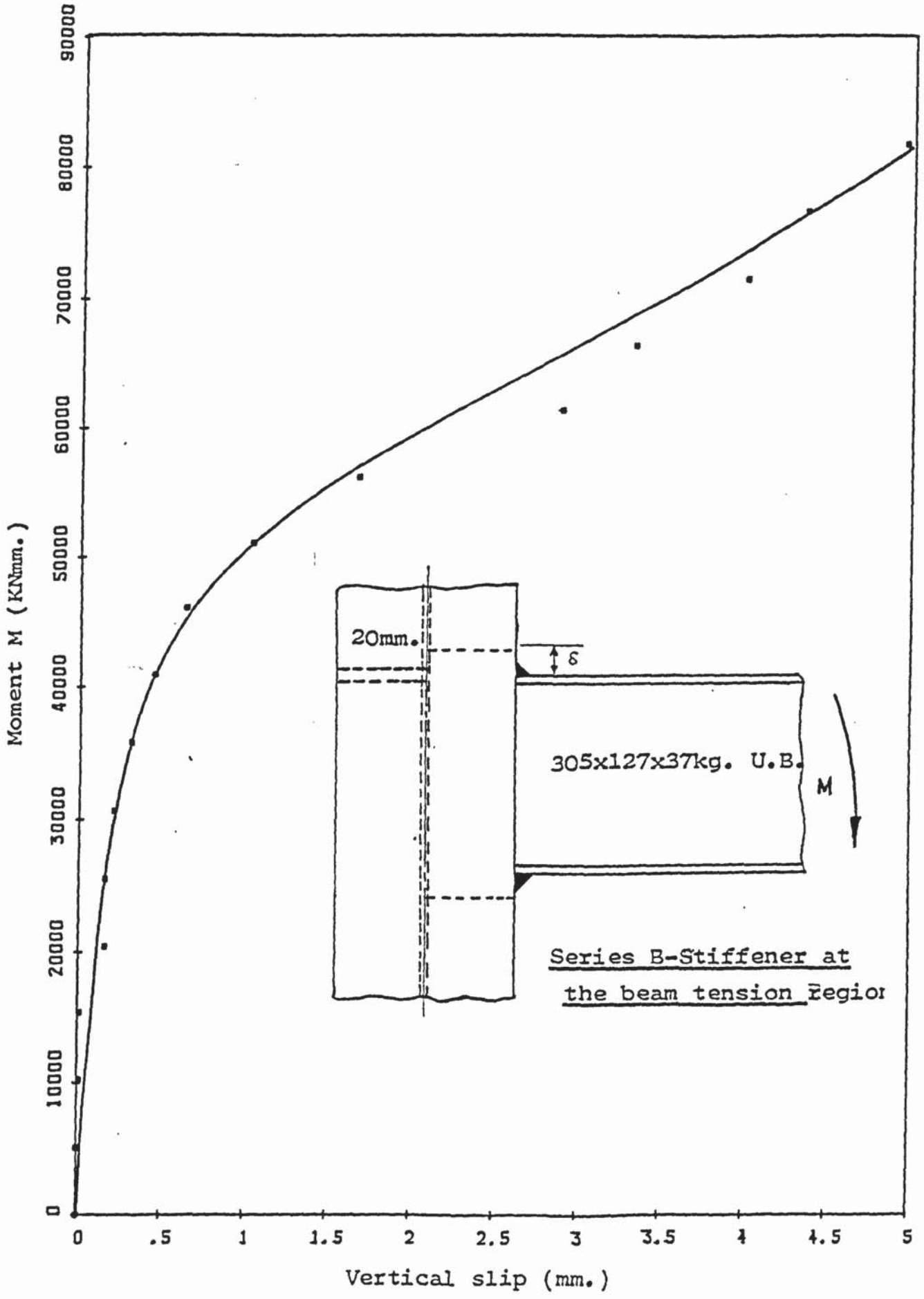

Figure 3.41 Moment-vertical slip relationship for secondary beam-to-column connection with column stiffener in the beam tension region.

3.3.3.3 CONNECTION C - STIFFENER AT THE COMPRESSION REGION IN LINE WITH THE BEAM FLANGE

Three specimens were tested in this series. The first specimen failed at a load of 16 tons (159.47 kN) and the second and the third at 13 tons (129.57 kN). Yield lines appeared in the column in the compression region at a load of about 2.5 tons (24.92 kN). The yield lines extended downwards as the load was increased. Observation of the yield line pattern on the column web at failure, showed that rotation might have occured at the beam compression flange. Figure 3.42 and Plate 10 gives a typical yield pattern line.

All the strain gauge and dial gauge readings are given in the Appendix. The strain distribution along the tee web at ultimate load is given in Figure 3.43, the moment-rotation graph in Figure 3.44 and the moment-vertical slip graph in Figure 3.45.

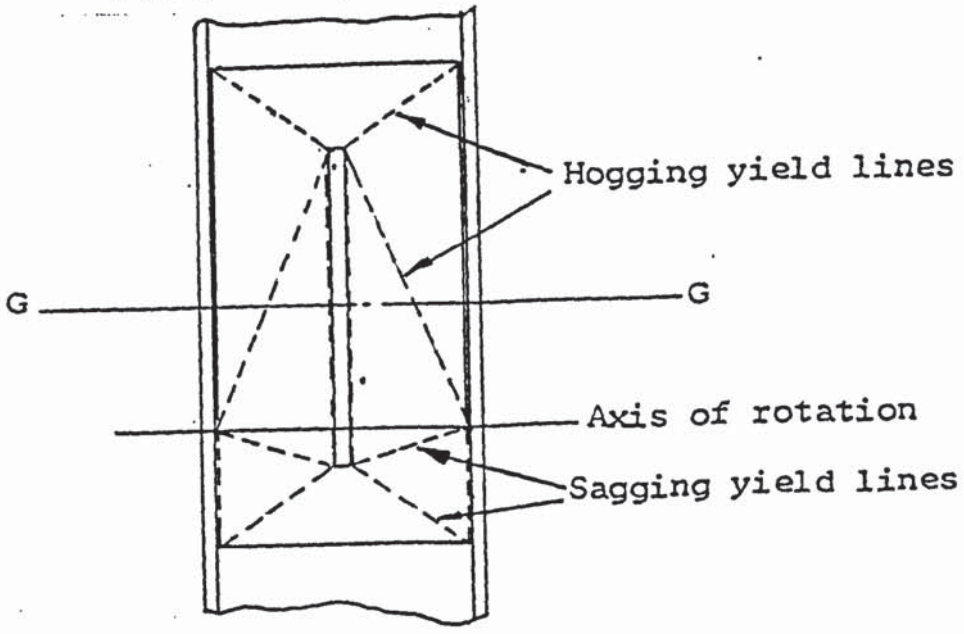

Figure 3.42 Typical yield line pattern on the column web of a secondary beam-to-column connection stiffened in the beam compression region

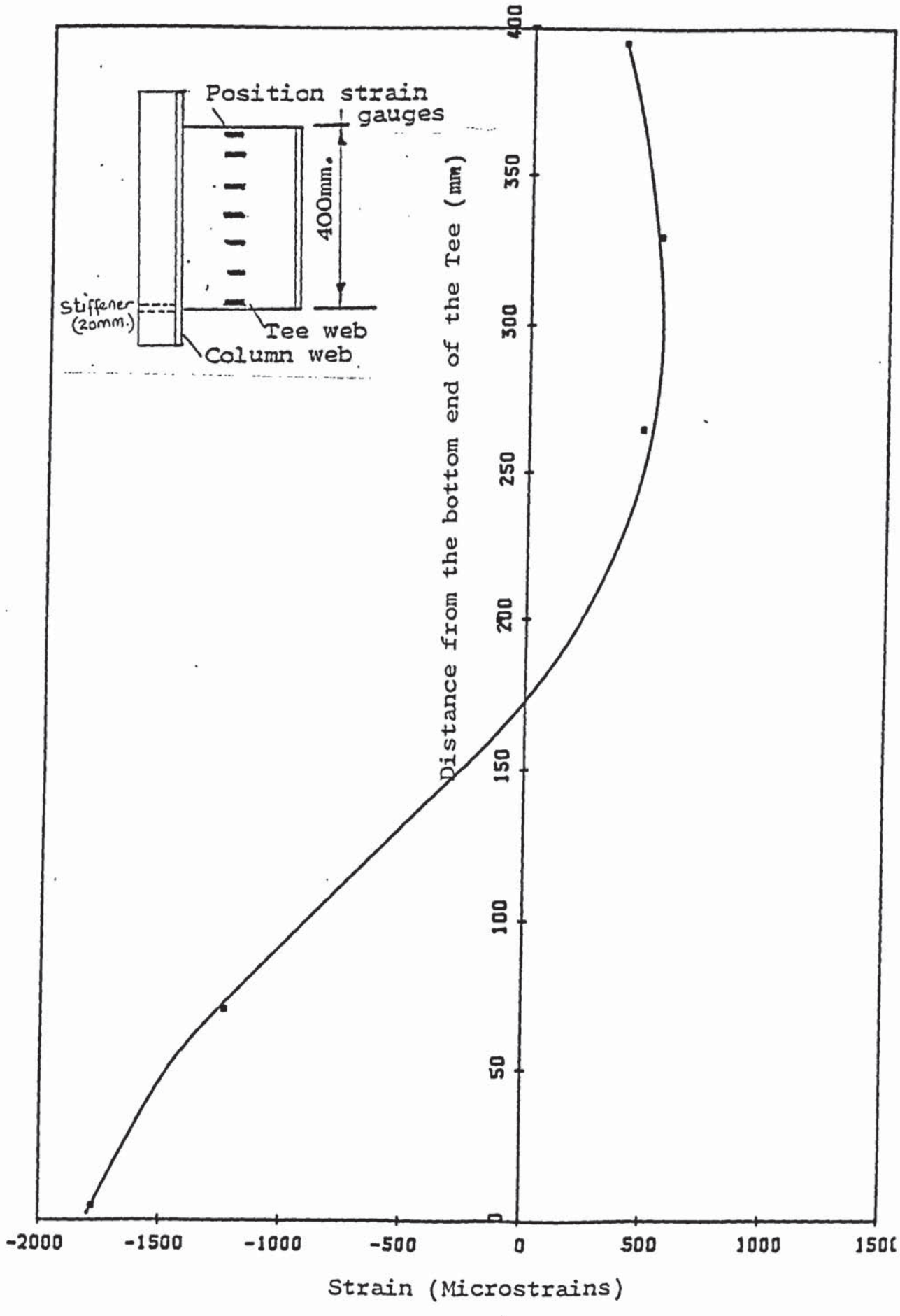

Figure 3.43 Strain values just before failure for secondary beam-to-colmn connection with column stiffener in the beam compression region.

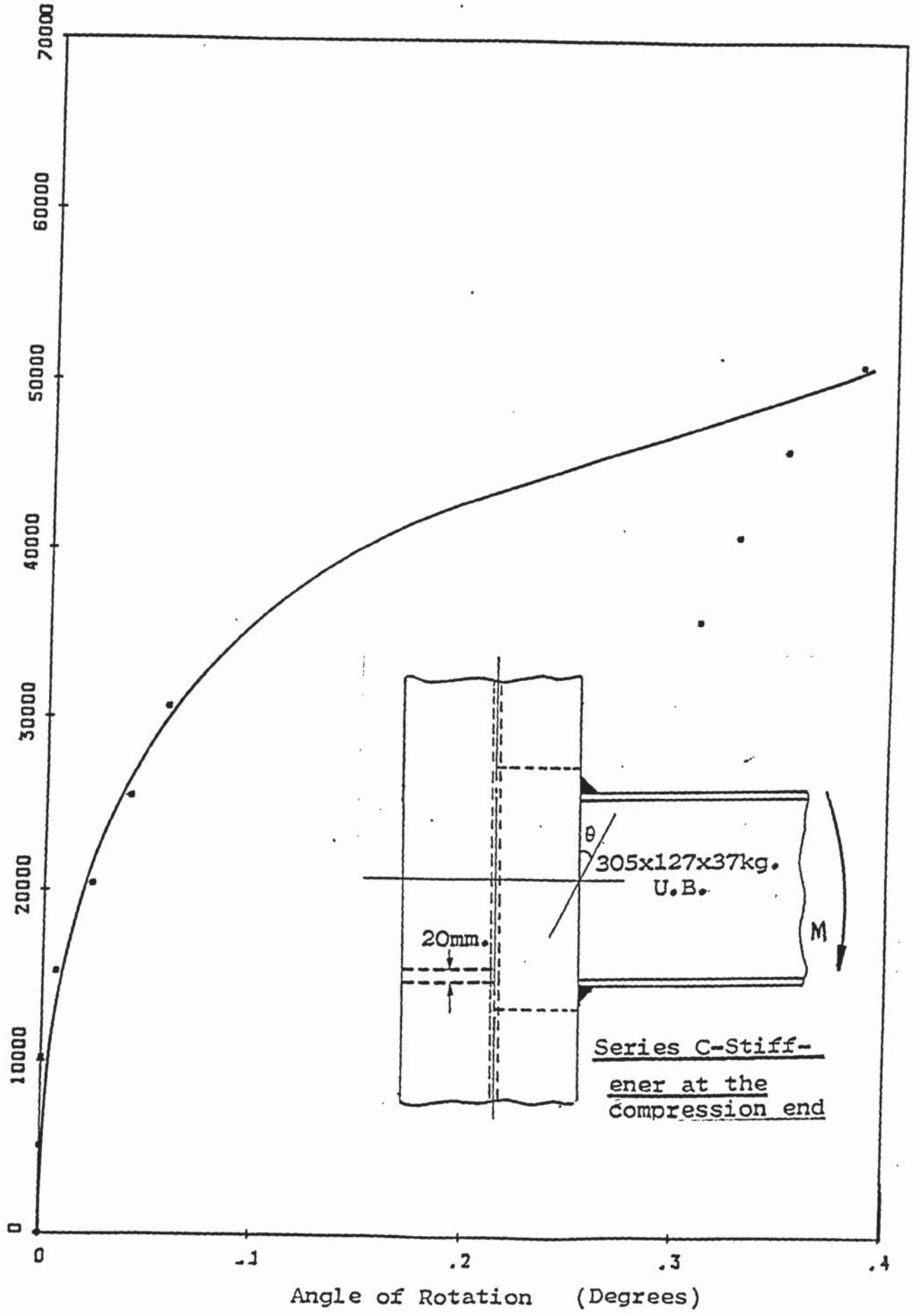

Figure 3.44 Moment-Rotation relationship for secondary beam-to-column connection with column stiffener in the beam compression region.

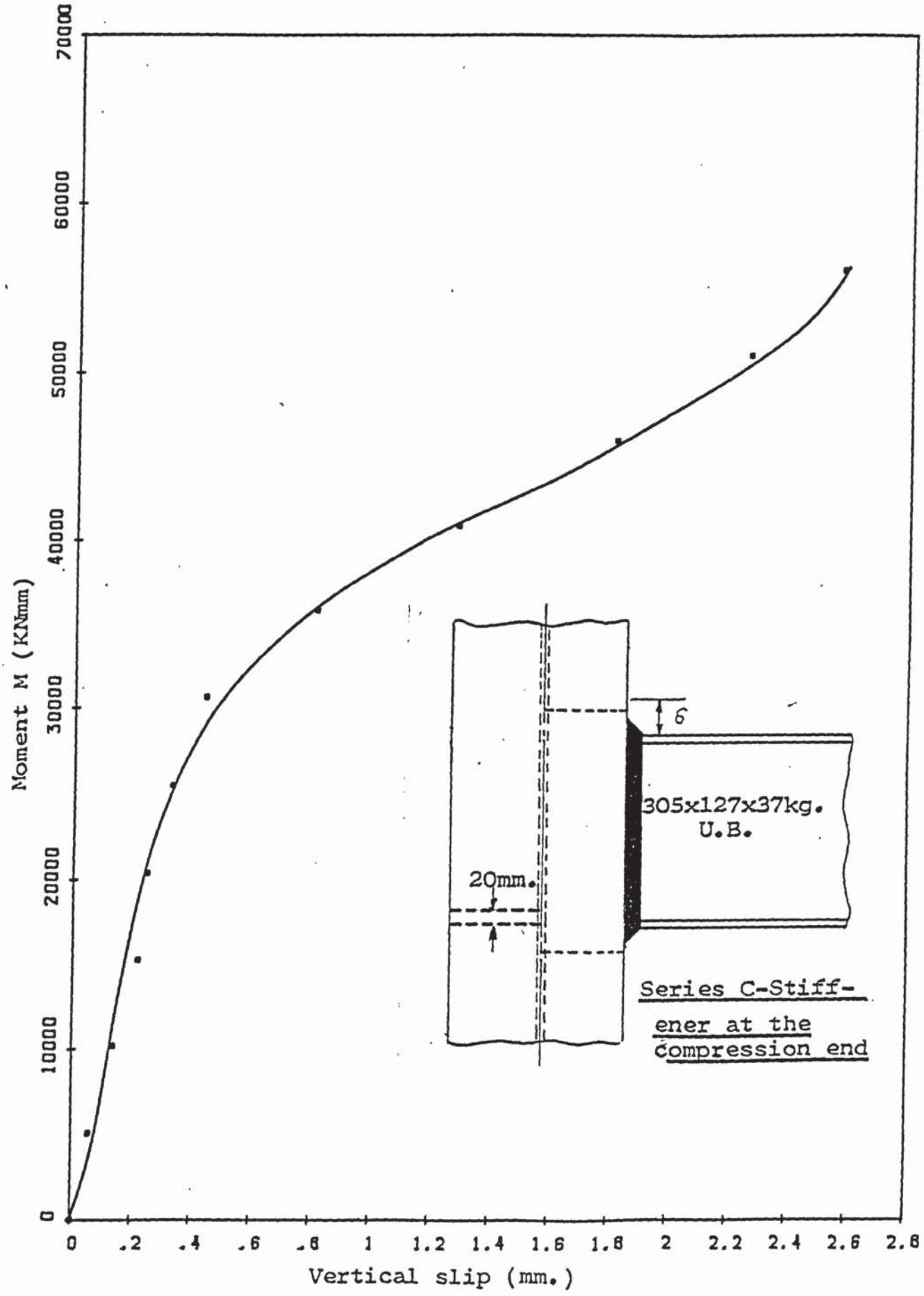

Figure 3.45 Moment-Vertical slip relationship for secondary beam-to-column connection with column stiffener in the beam compression region.

3.3.3.4 CONNECTION D - STIFFENER AT BOTH ENDS

Only one specimen was tested in this series. The welds between the column flanges and the tee failed at a load of 14 tons (139.54 kN). Yield lines appeared on the column flange in the compression region at a load of about 3 tons (29.9 kN). The yield lines extended as the load was increased. Observation of the yield line pattern at ultimate load revealed that rotation may have taken place in the middle of the connection. A typical yield line pattern is shown in Figure 3.46.

All the strain gauge and dial guage readings are given in the Appendix. Figure 3.47 gives the strain distribution along the tee web, Figure 3.48 the moment rotation graph and Figure 3.49 the moment-vertical slip graph.

A comparison of the moment/rotation and the moment/vertical slip relationships of the four connections are presented in Figures 3.50 and 3.51 respectively.

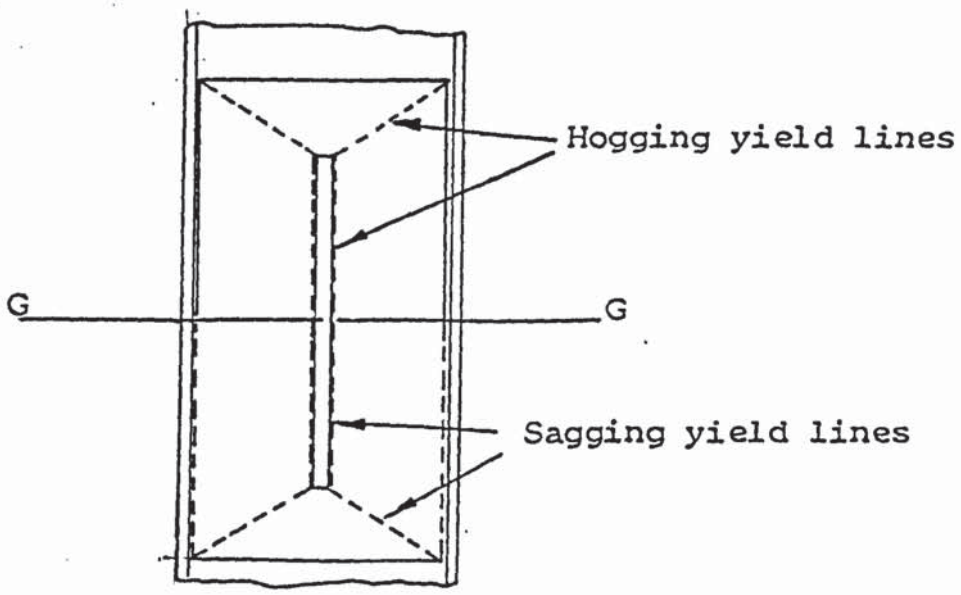

Figure 3.46 Typical yield line pattern on the column web of a secondary beam-to-column stiffened in both the beam tension and the compression region

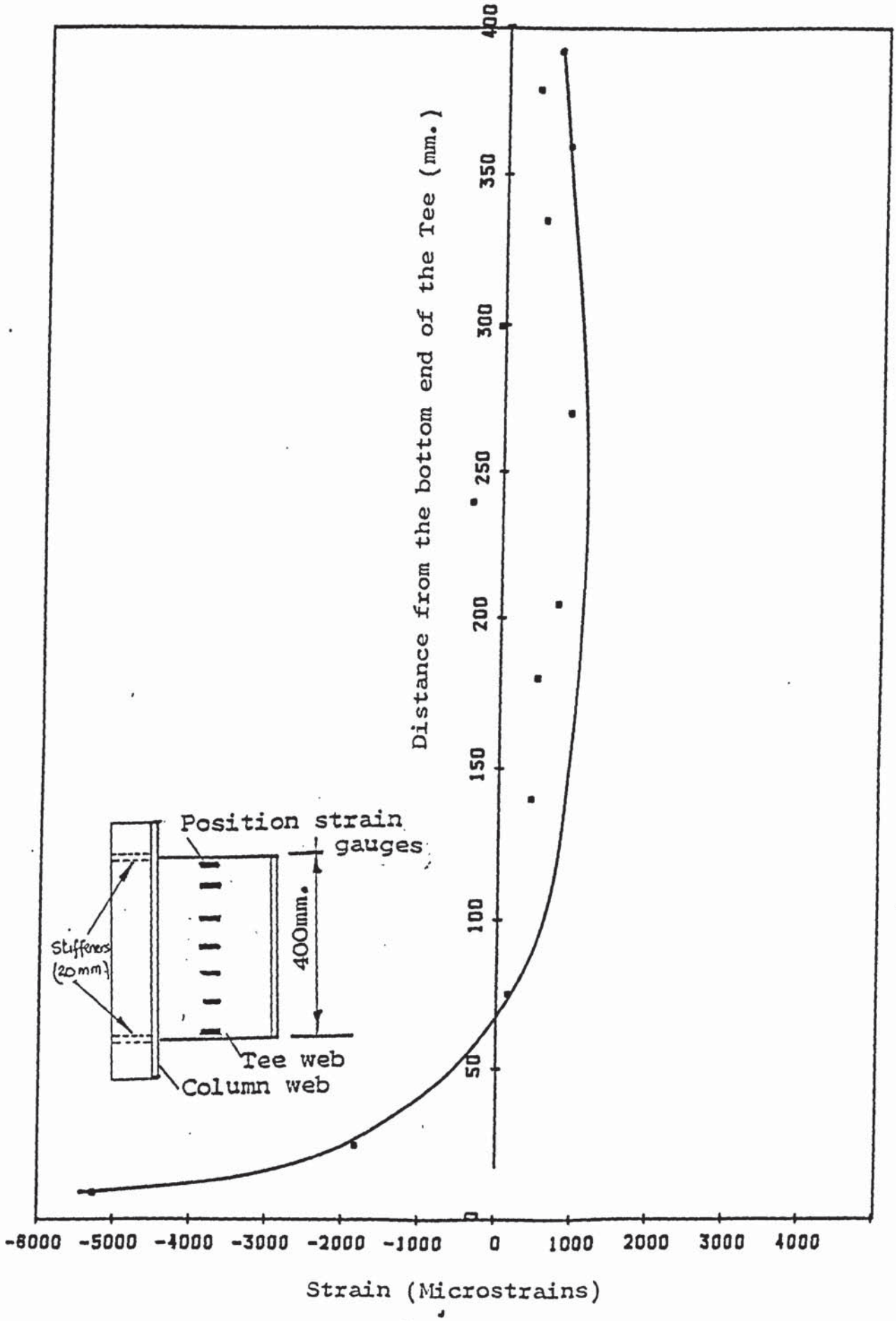

Figure 3.47 Strain values just before failure for secondary beam-to-column connection with column stiffener in the beam tension region and the beam compression region.

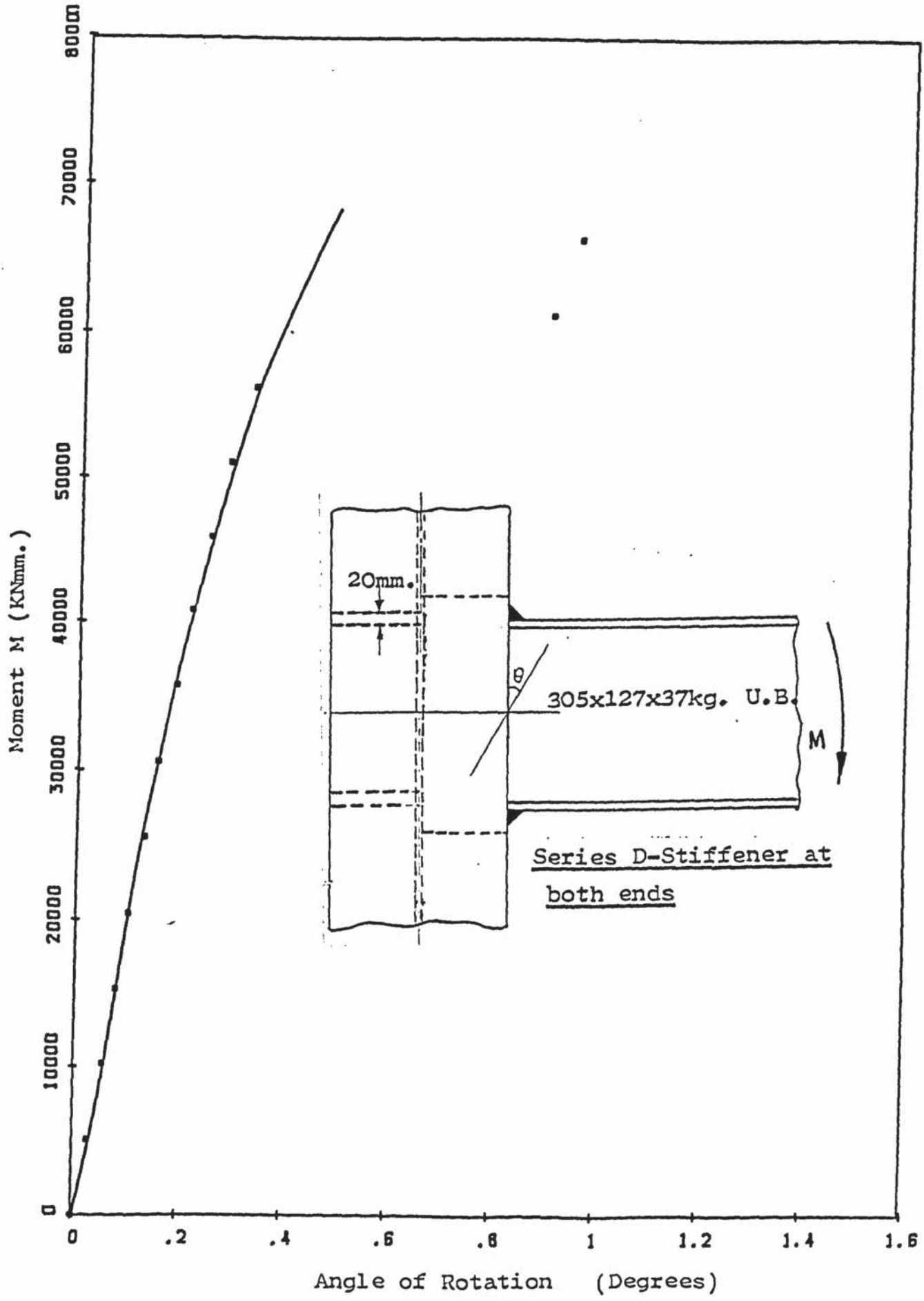

Figure 3.48 Moment-Rotation relationship for secondary beam-to-column connection with column stiffener in both the beam tension and compression regions.

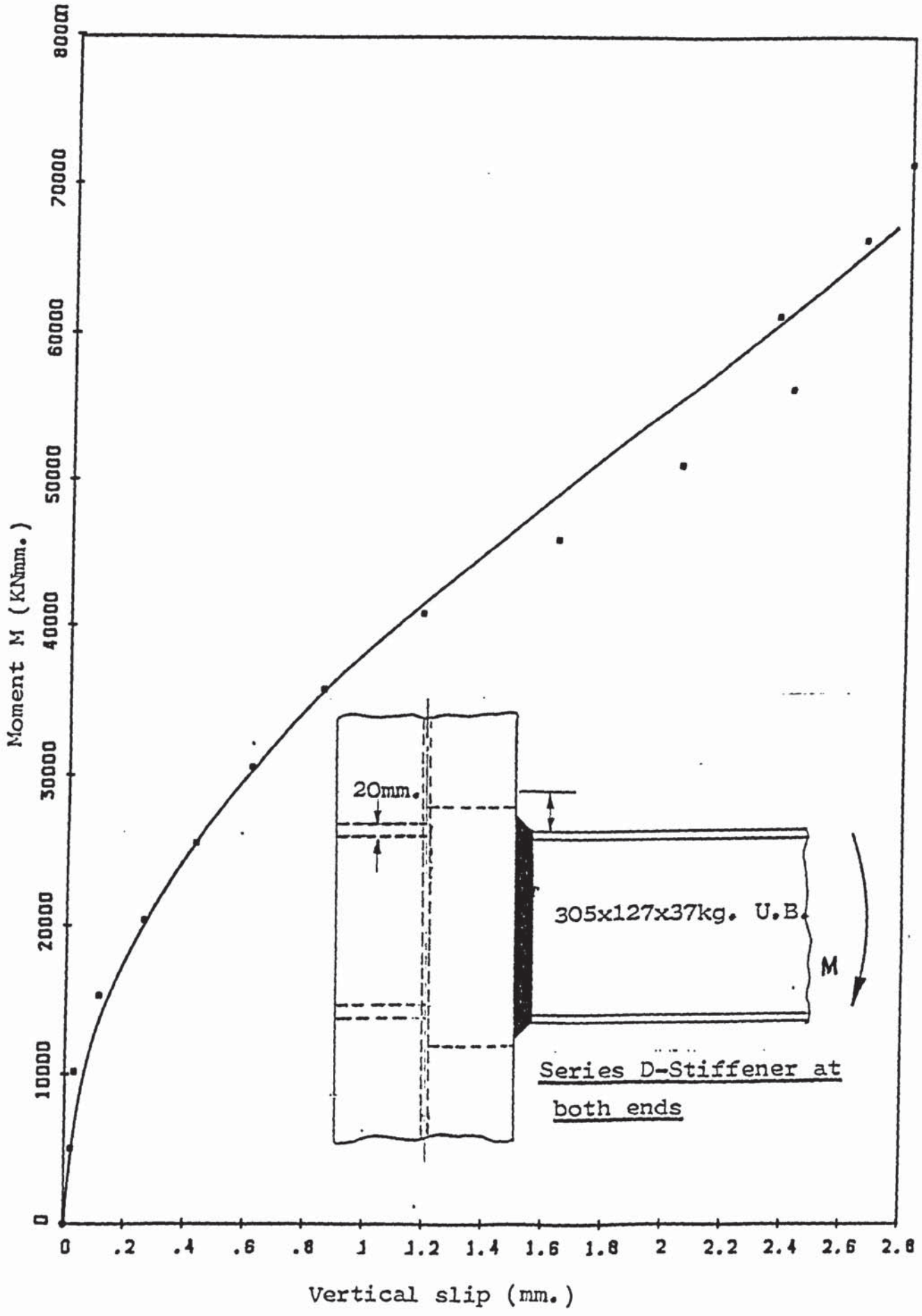

Figure 3.49 Moment-Vertical slip relationship for secondary beam-to-column connection with column stiffener in both the beam tension and compression regions.

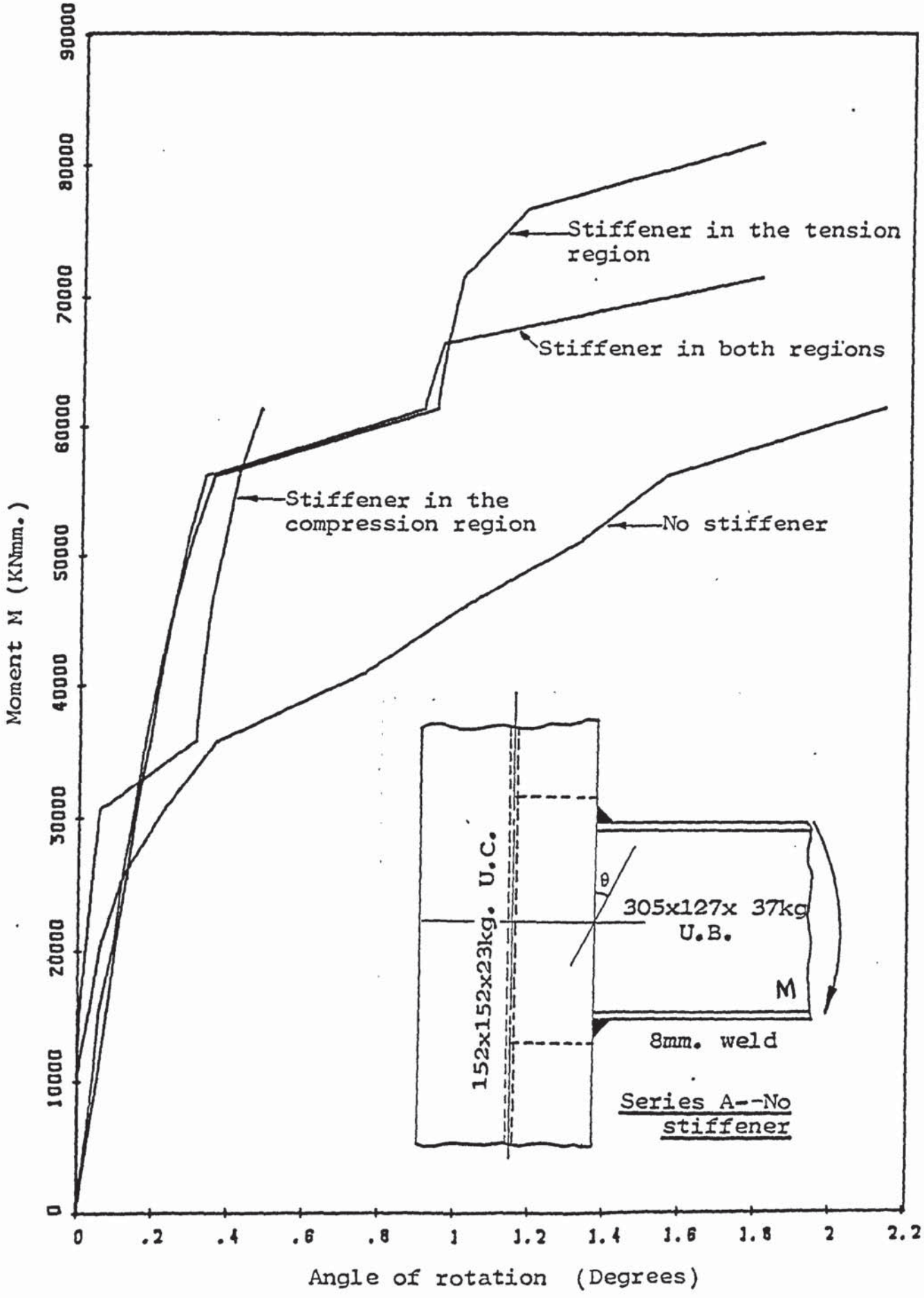

Figure 3.50 Comparison of the Moment-Rotation relationships of the four connections-Secondary beam-to-column connection.

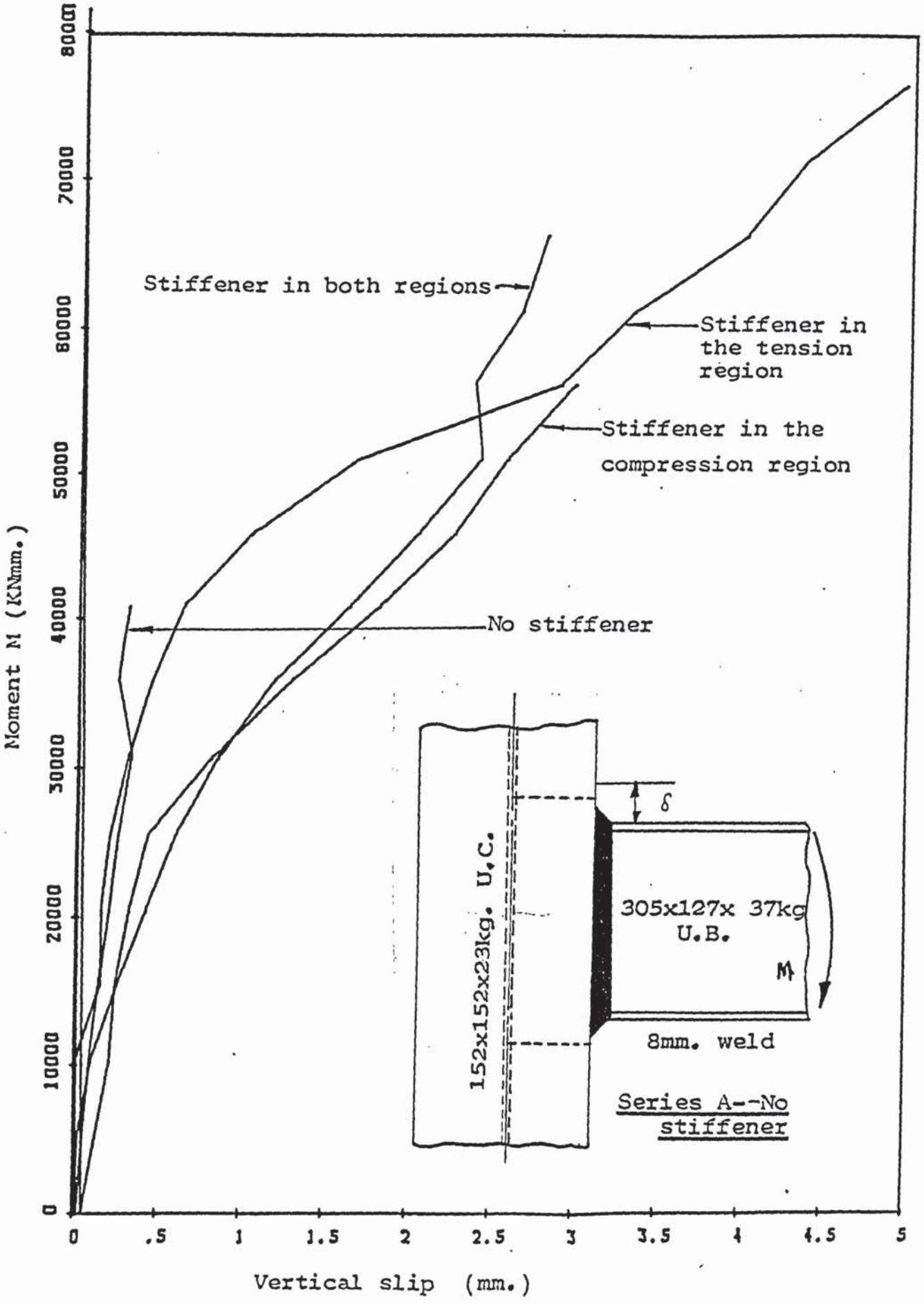

Figure 3.51 Comparison of the Moment-Vertical slip relationshi for the four Secondary beam-to-column connections.

3.3.4 SUBSIDIARY TESTS ON TRANSVERSE STRENGTH OF FILLET WELD

The first specimen subjected to tensile loads failed at a load of 129.6 kN and the second at 135.8 kN. This gives a mean strength of 1.659 Kn/mm run.

Both of the specimens subjected to compressive leads failed at 16.25 tons (161.964 kN). This gives a mean compressive strength of 1.62 kN/mm run.

3.3.5 SUBSIDIARY FAILURE CRITRION TESTS

In all the tests in this series, the failure pattern was similar. Only two out of the four welds failed in most of the specimens. As one of the welds failed, the load was transfered to the weld diagonally adjacent to it which then failed. The first series of tests did not produce useful results because the welds were too short. Consequently, the results have not been presented.

Table A gives the test results and Figure 3.54 the transverse load F_x/ the longitudinal load F_y^* graph.

Transverse load F_x (kN)	Longitudinal load F_y (kN)
124.59	129.57
40.00	130.57
80.00	131.96
120.00	133.56
20.00	137.146
0	141.32

Table 3.8 Test results failure criterion tests

3.3.6 SUBSIDIARY TESTS ON THE EFFECT OF FLANGE FLEXIBILITY

Both specimens showed marked plastic deformation of the column flange at failure. The first one failed at a load of 199.5 kN and the second at a load of 190.37 kN. This gives a mean effective length to the actual length ratio $\frac{B_e}{B}$ of 0.38. The permanent widthwise plastic deformation of the column flange measured from the middle of the column was 6 mm and the lengthwise deformation measured at the tip of the flange was also 6 mm.

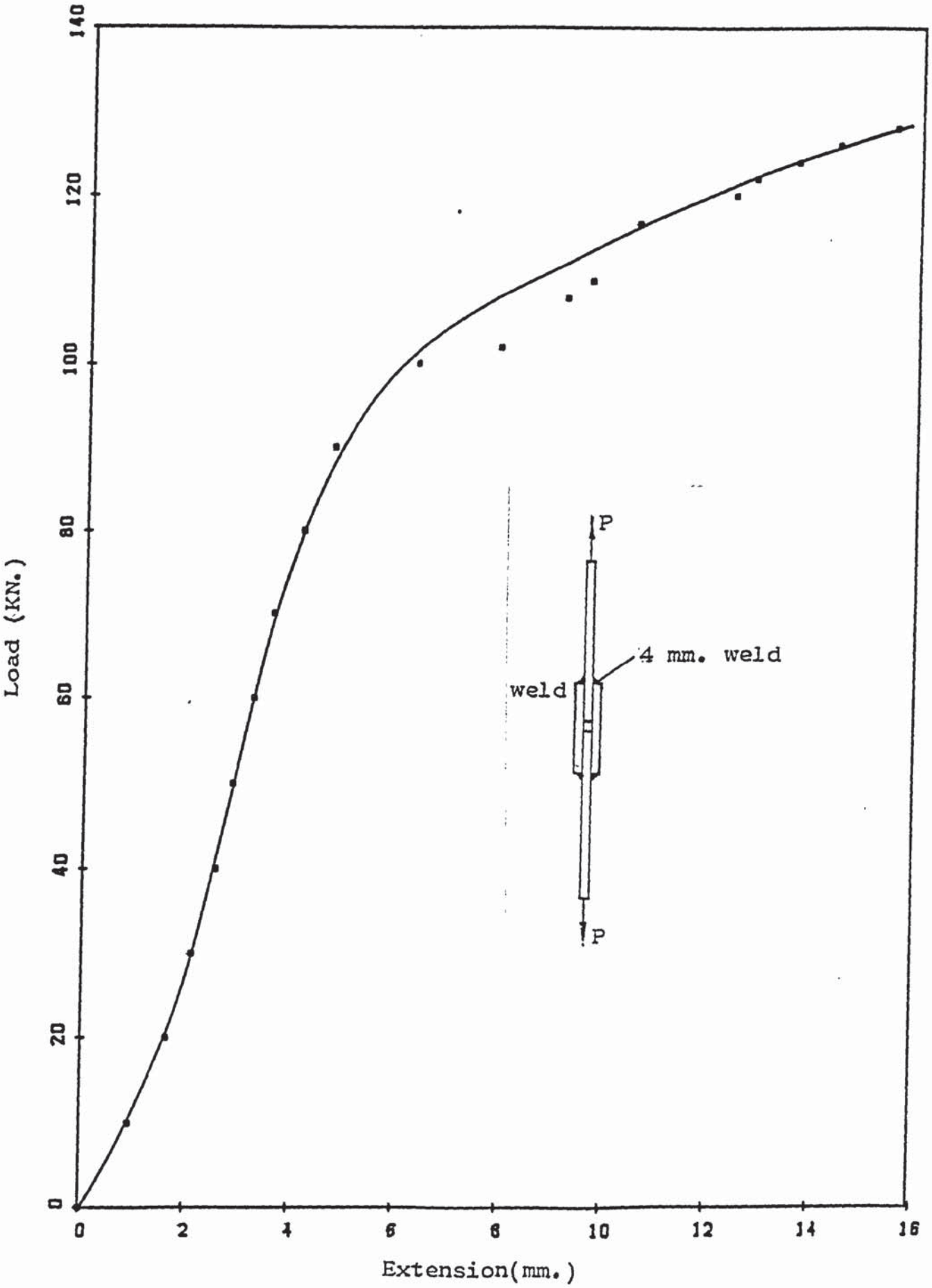

Figure 3.52 Load-Extension relationship for the determination of the transverse strength of fillet weld.

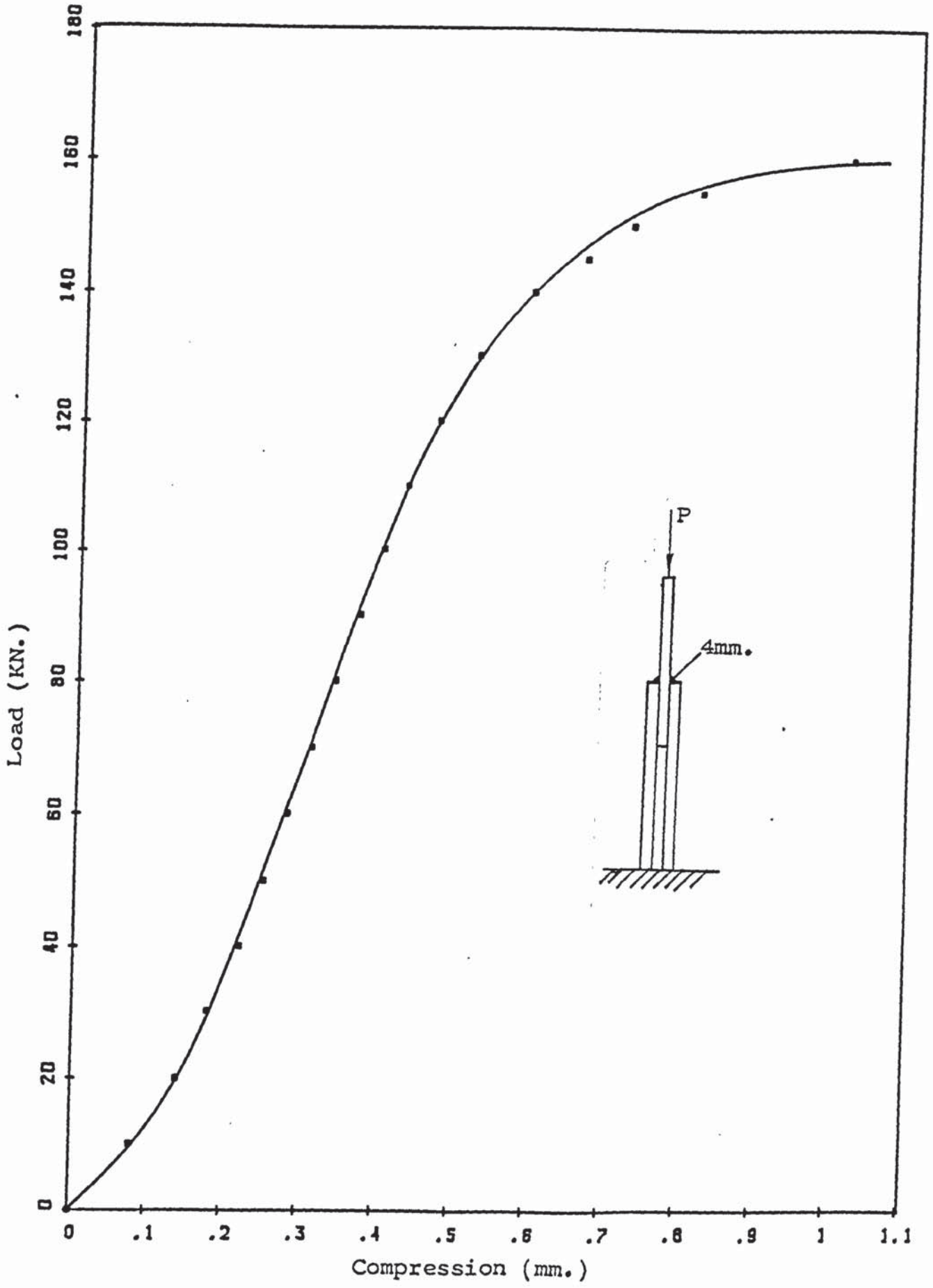

Figure 3.53 Load-deflection relationship for the determination of the transverse strength of fillet weld - compression test.

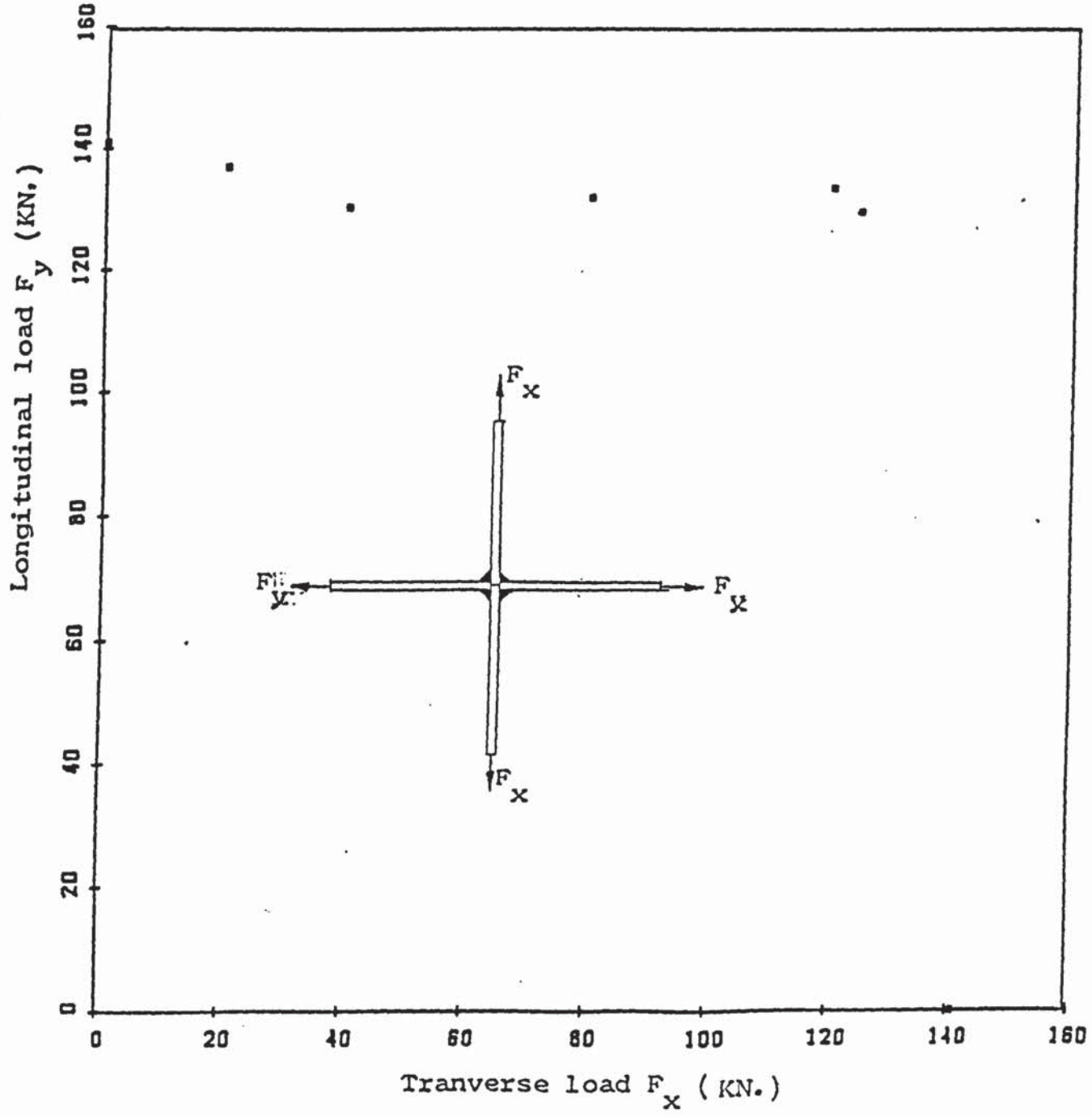

Figure 3.54 Failure criterion for fillet weld.

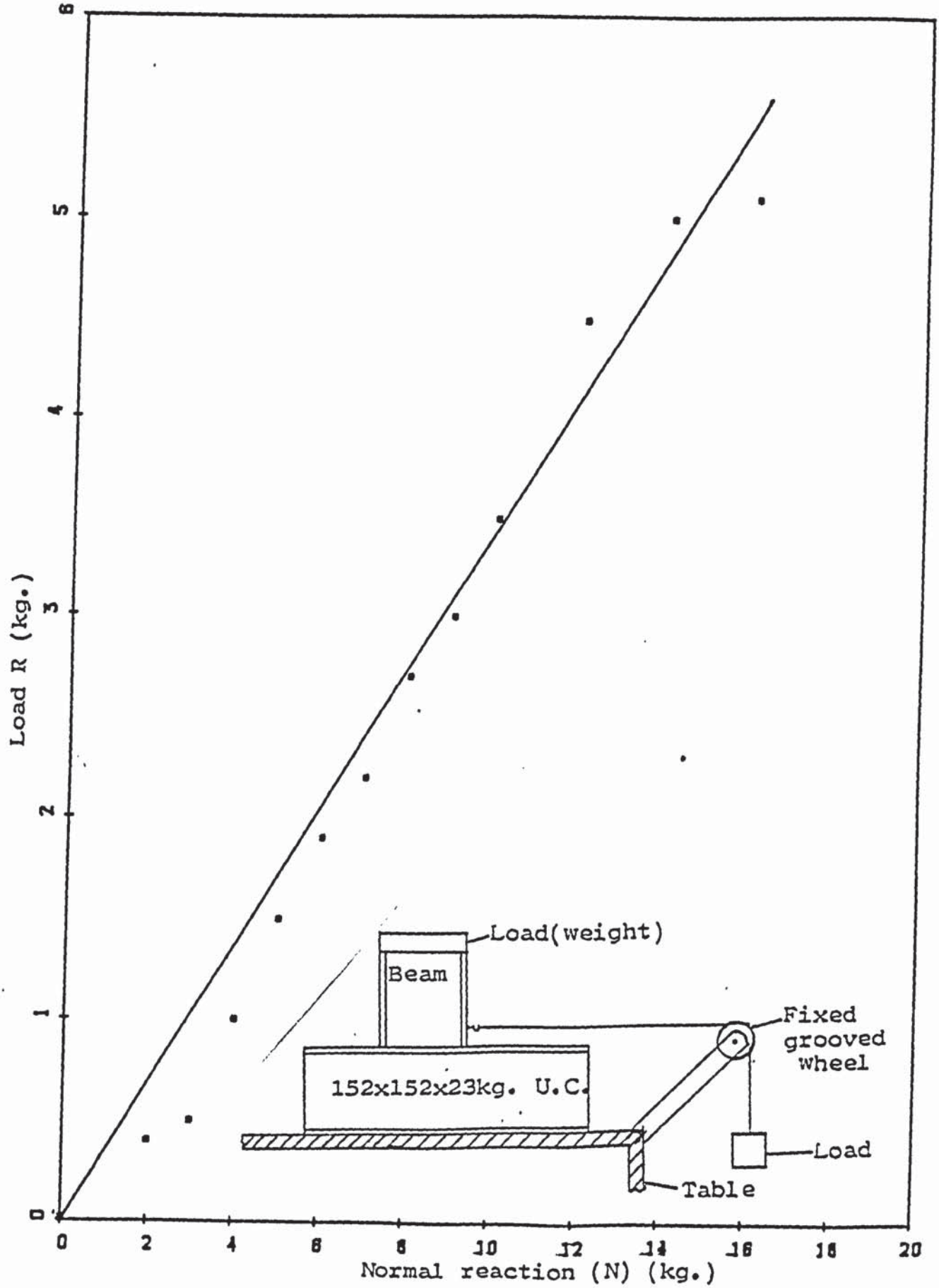

Figure 3.55 Load versus normal reaction for the determination of the coefficient of friction

3.3.7 DIMENSIONS

152 x 152 x 23 kg. Unerversal Column

Flange thickness = 7.095 milimetres with standard deviation of 0.023 or 0.32%

Flange width = 152 milimetres with zero standard deviation

Web thickness = 6.343 milimetres with standard diviation of 0.04 or 0.63%

MECHANICAL PROPERTIES

Flange yield strength = 282.17 N/mm^2

Web yield strength = 271.13 N/mm^2

305 x 127 x 37 kg Universal Beam

Flange thickness = 10.96 mm standard deviation = 0.134 or 1.22%

Flange width = 127 mm standard deviation = 0

Web thickness = 7.54 mm standard deviation = 0.049 or 0.65%

Section depth = 305.0 mm standard deviation = 0

Stiff bearing for column tests

Length = 152 mm

Width = 10.63 mm

Thickness = 10.63 mm

STRAIN GAUGES

Type = Electrical Resistance type PL-5-11

Gauge length = 5 mm

Gauge resistance = 120 ± 0.3 Ω

Gauge factor = 2.00

Lot number A258211

WELDING PARAMETERS

Process - Manual metal arc

Power - A.C.

Current - 120 Amperes

Electrode class - E4333R13 AWS EQUIVALENT E6013

Previous classification E307

Type - Rutile cellulose

Make - Zodian Universal

Diameter - 3.25 mm for 4 mm welds

6.0 mm for 8 mm welds

Voltage - 440 volts

Weld size attained in a single pass; both ends tack welded prior to laying the welds

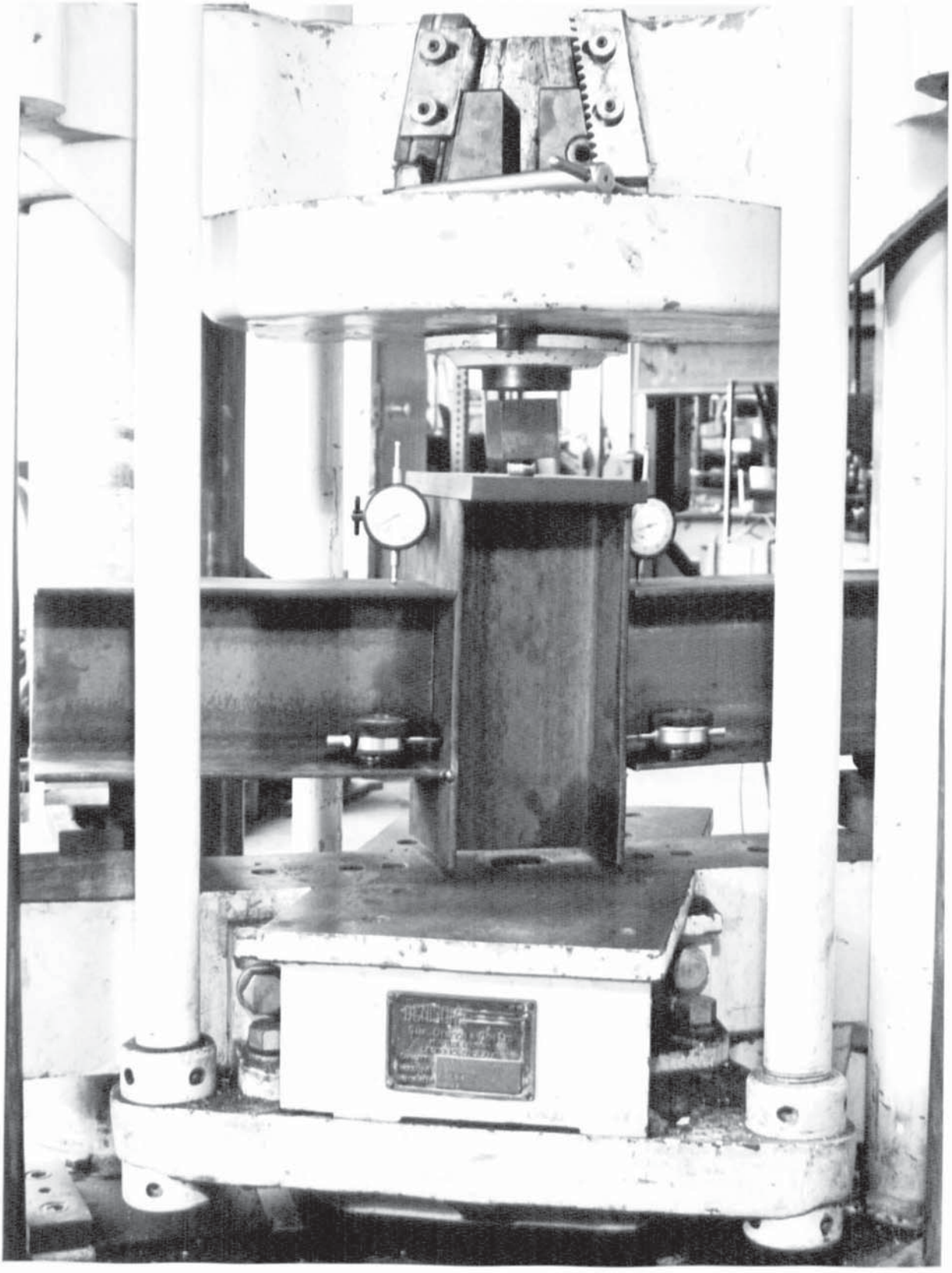

Plate 1 Beam-to-column connection at the end of the test.

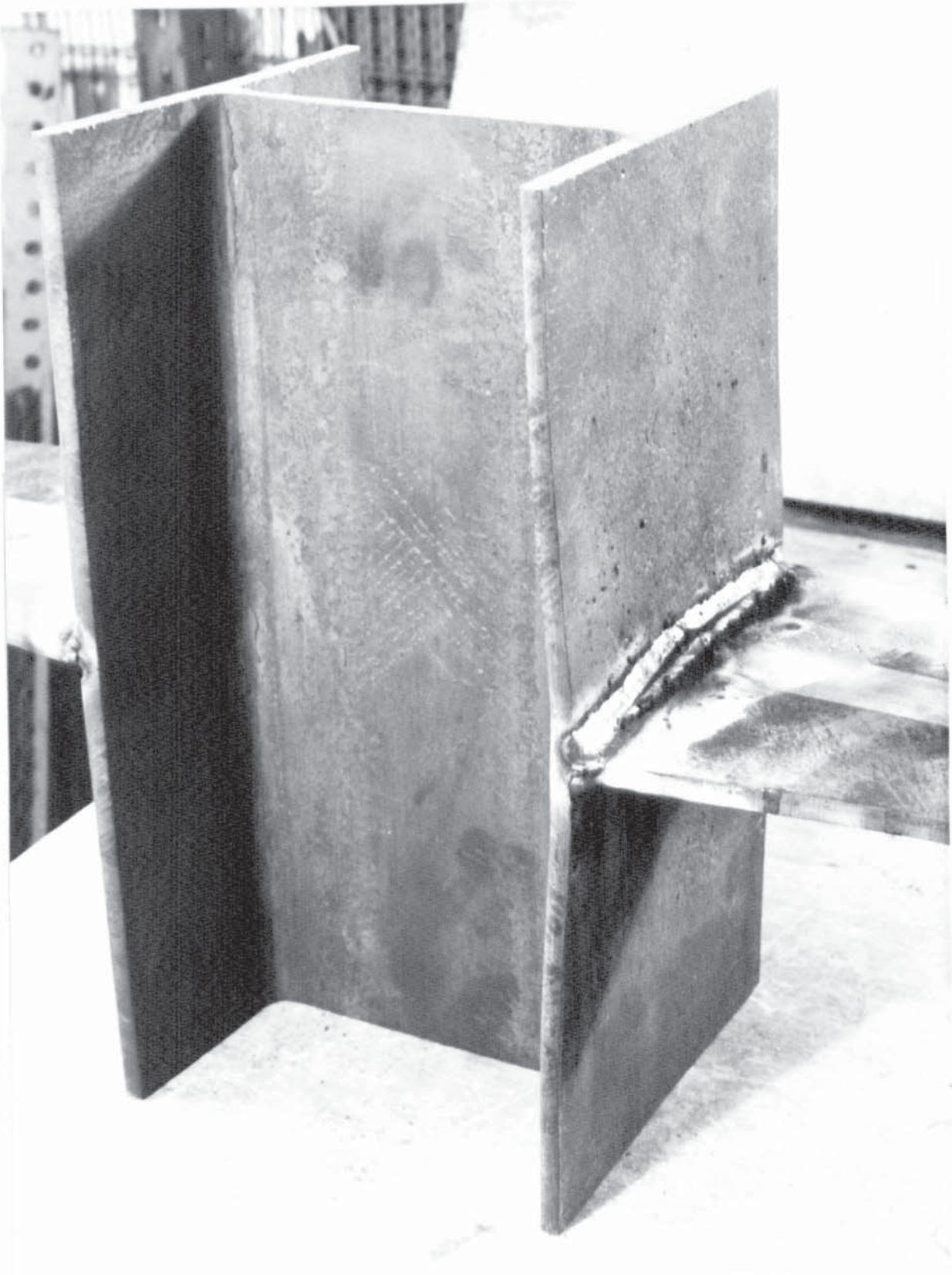

Plate 2 Test specimen for the determination of the effect of flange flexibility showing flange deformation at failure.

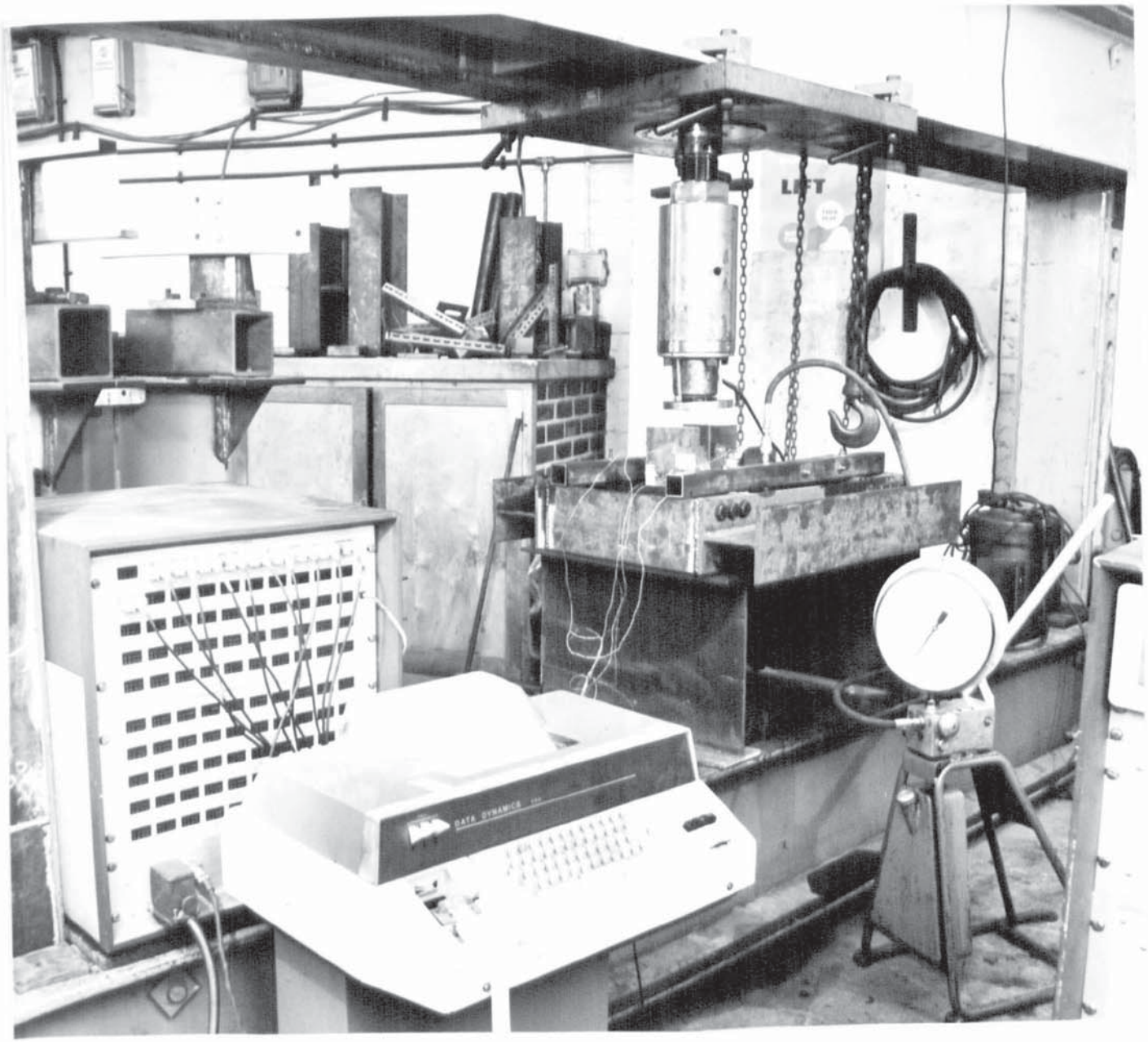

Plate 3 Cplumn specimen in test rig ready for testing.

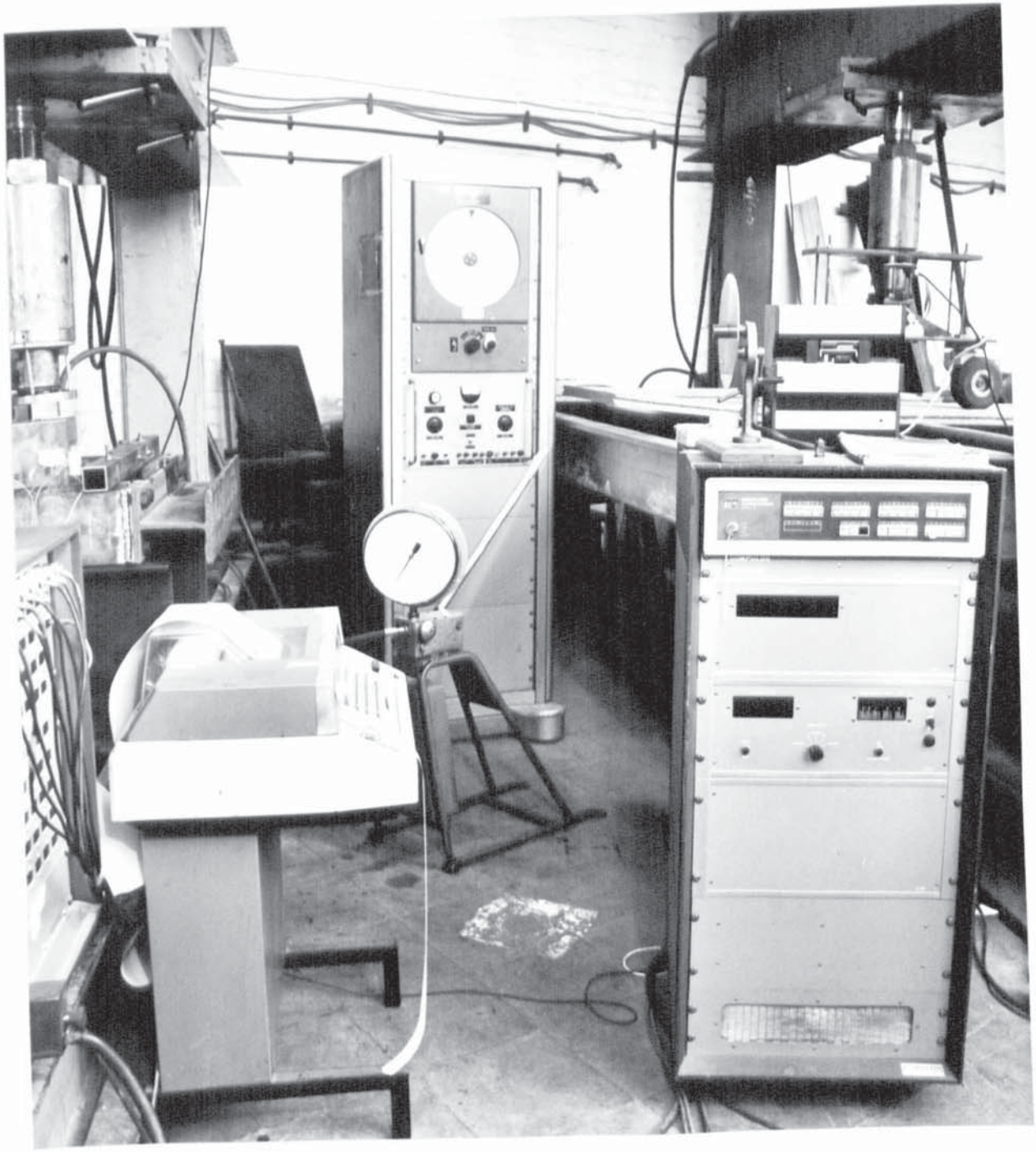

Plate 4 The data logger used for the column tests.

Plate 5 Column with an axial load of 80 tons at the end of the test.

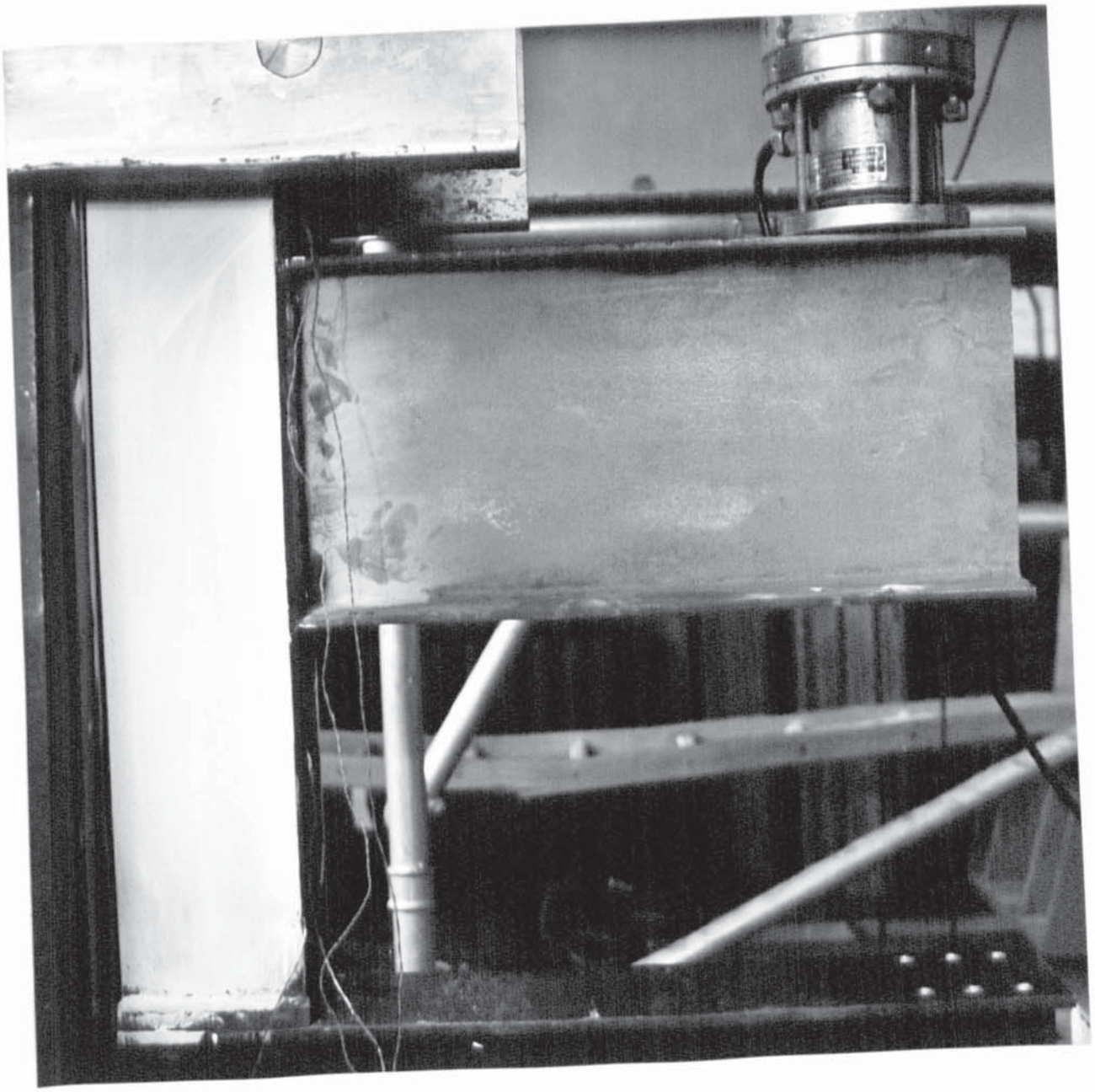

Plate 6 Secondary beam-to-column connection fixed in the rig ready for testing.

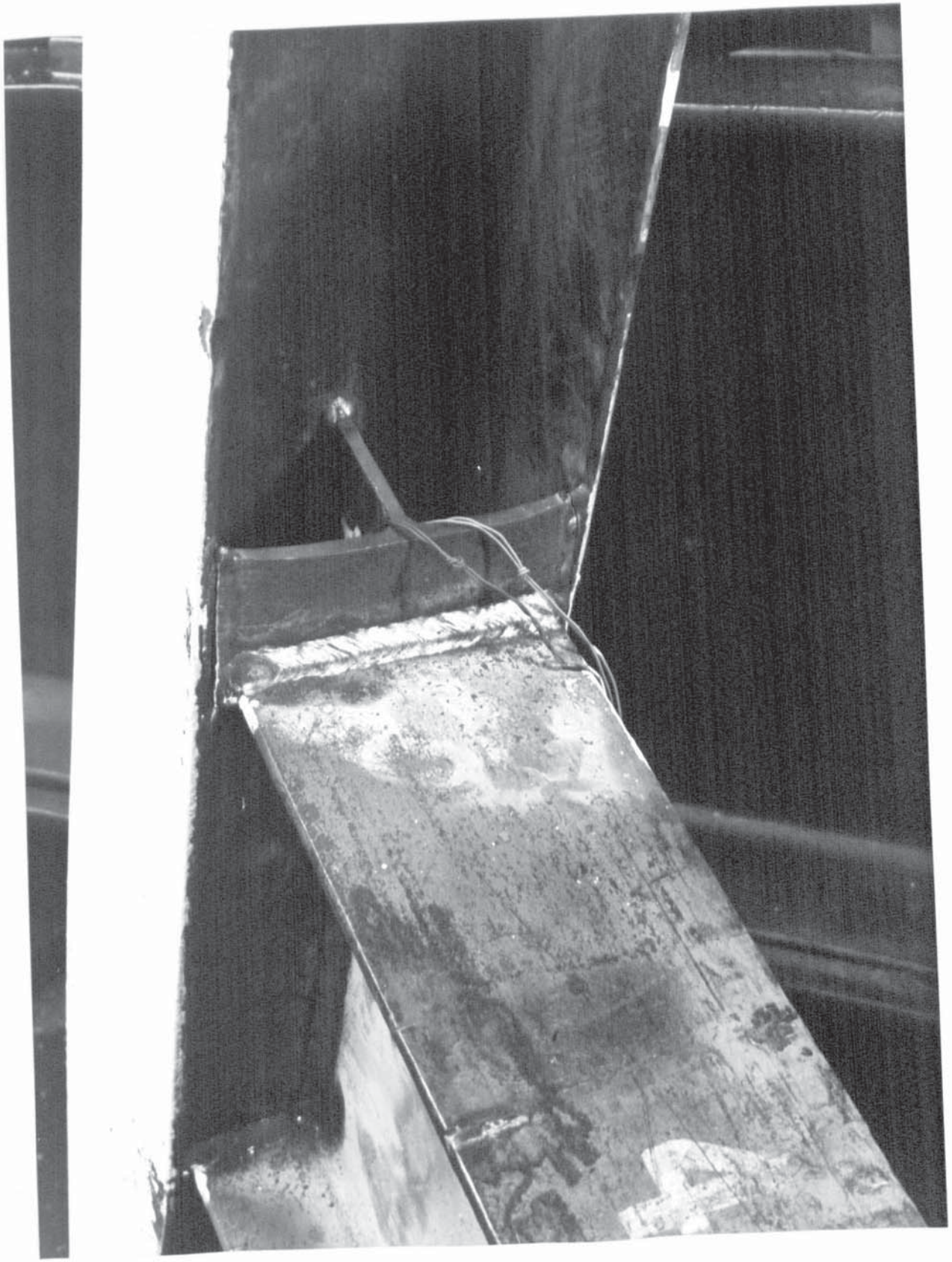

Plate 7 Secondary beam-to-column connection at failure showing the weld cracks in the beam tension region.

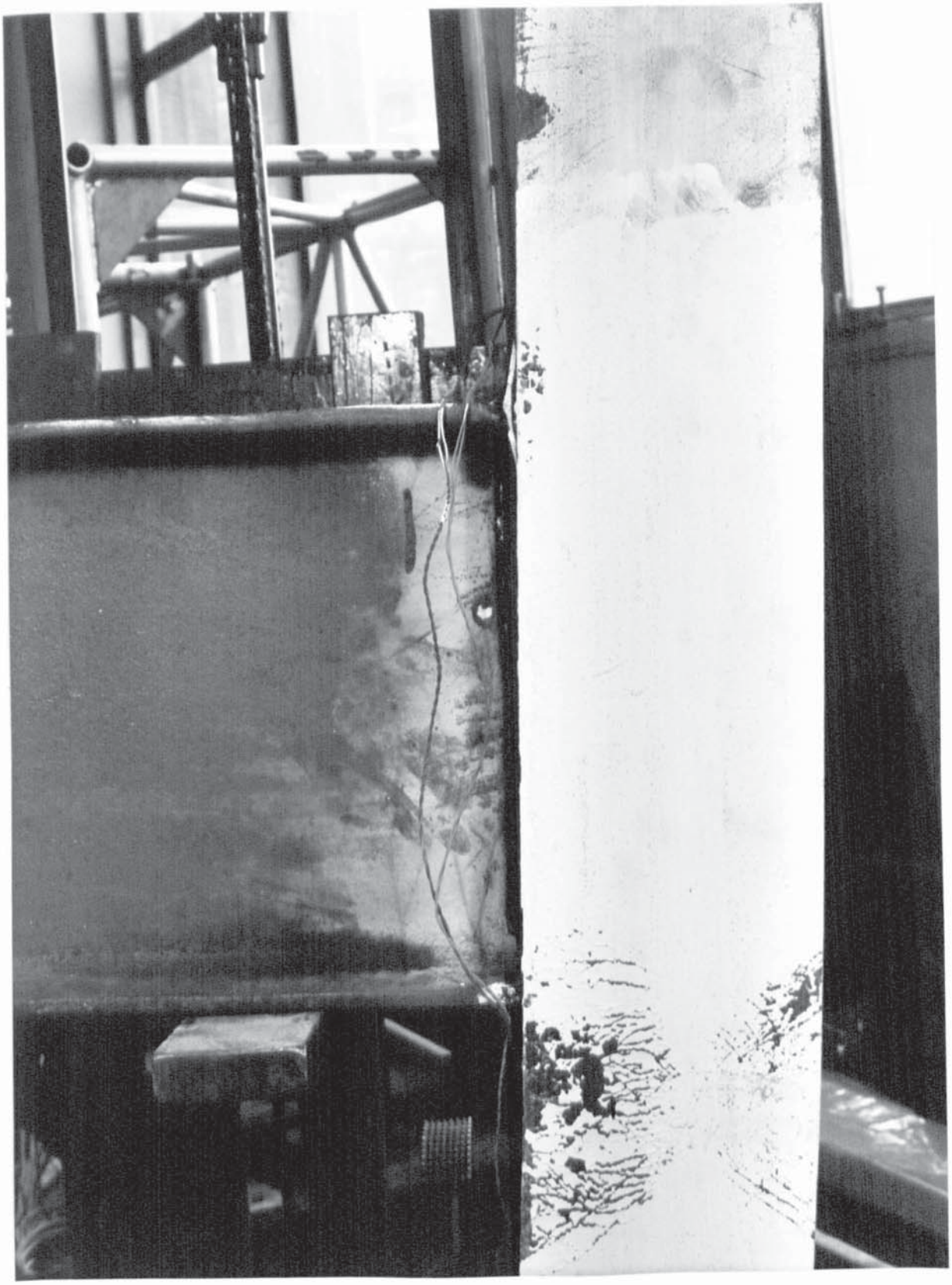

Plate 8 Secondary beam-to-column connection showing yield lines on the column flange in the beam compression region at ultimate load.

Plate 9 Unstiffened secondary beam-to-column connection showing the yield lines on the column web at ultimate load.

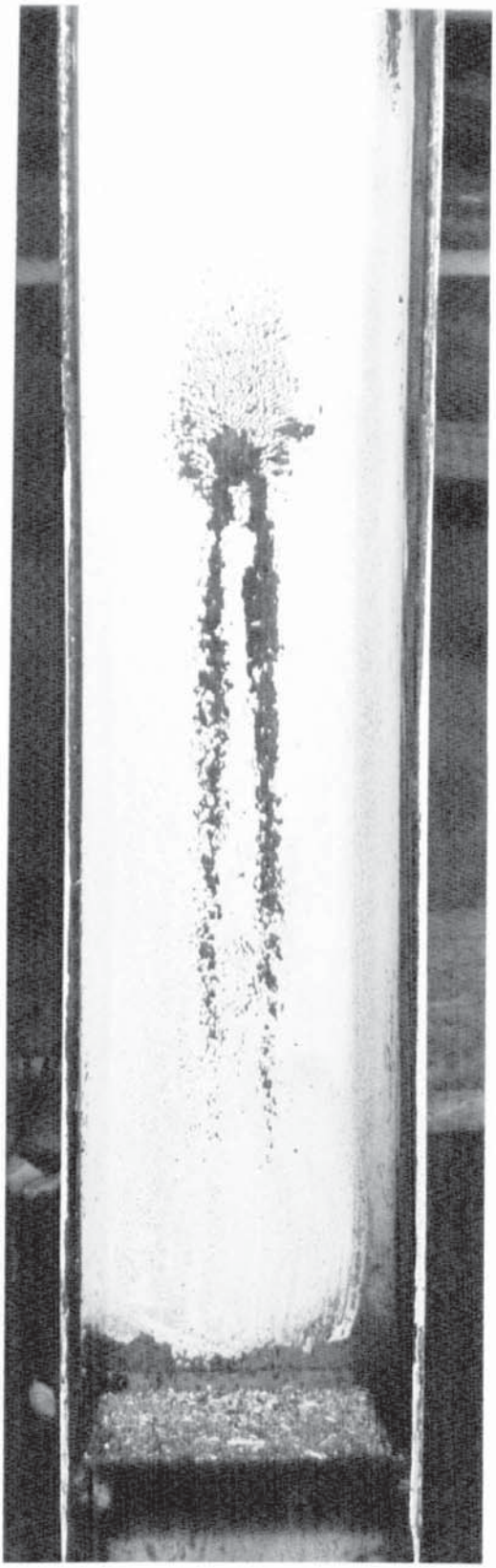

Plate 10 Secondary beam-to-column connection with stiffener in the beam compression region showing yield lines on the column web at ultimate load.

CHAPTER 4

THEORETICAL ANALYSES

4.1 INTRODUCTION

The behaviour of beam-to-column connections is complex. Most beam-to-column connections are statically indeterminate and the distribution of forces and stresses depends on the relative deformation of the component parts and welds or fasteners. It is practically impossible to analyse most beam-to-column connections by a rigorous and exact mathematical procedure. The analyses used in design are approximate and based on simplifying assumptions. In the case of the connections investigated in this thesis, the problems which can be isolated are as follows:

(a) Weld failure

(b) Effective lengths of welds

(c) Crushing of webs of steel I-section

(d) Deformation of the webs of steel I-section

(e) Distribution of load in secondary beam-to-column connection

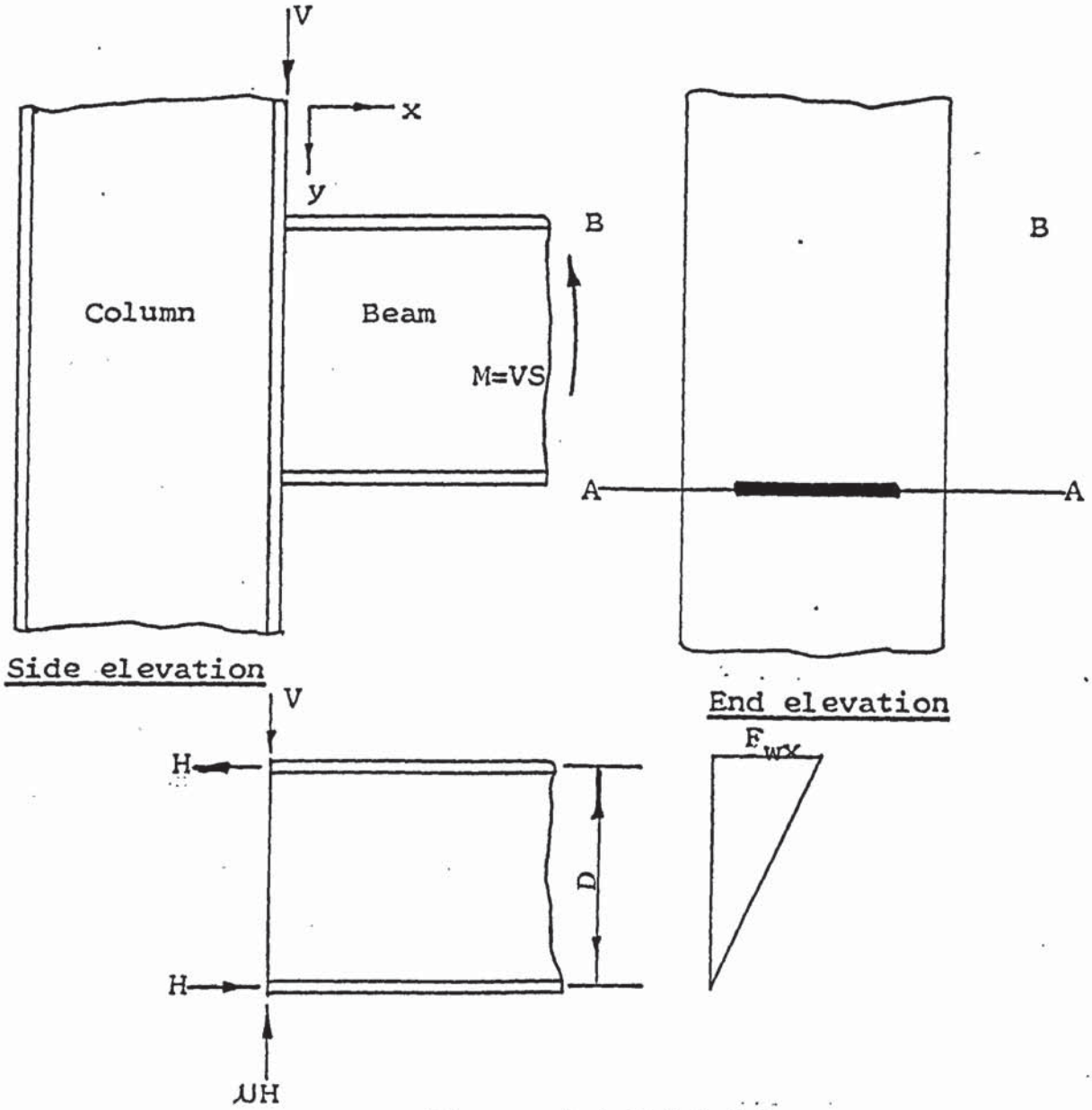

Figure 4.1 Welded beam-to column connection subject to shear and bending.

4.2 WELD FAILURE

Figure 4.1 shows a beam-to-column connection in which the beam is welded directly to the column and Figure 4.1b shows the external forces acting on the weld. For the beam, the axis of bending is at half beam depth, but the rotational axis for the welded joint depends on the stiffness at the support. For a rigid connection, the rotational axis is approximately at the compression beam flange (line AA). This introduces a reactive force H at line AA which is balanced by a horizontal resultant force H_r in the weld in the position shown in Figure 4.1b. The vertical shear force V produces a vertical movement and this introduces a frictional force μH at the axis AA.

The mechanism by which a fillet weld ruptures when subjected to combined streses is complex (51,52). The existing failure criteria are based on approximations and simplifying assumptions. Criteria based on the principal stress, maximum shear stress, strain energy of distortion and the vector addition method which have been used to explain fillet weld behaviour are in this authors opinion more suited to the prediction of the base metal yield mechanism. Moreover, apart from the criteria proposed by Archer et al[26] and Butler[54] the rest have been based on the throat section. In reality the failure plane has been shown to vary[51].

Consider the equilibrium of the forces acting on the beam: (Figure 4.1).

For no vertical slip $V \leqslant \mu H$

Taking moments about axis BB

$HD = VS$

$\therefore \quad H = \frac{VS}{D}$

For no vertical slip $V \leqslant \mu \frac{VS}{D}$

i.e. $V \leqslant \frac{\mu M}{D}$ where $M = VS$

i.e. $\frac{\mu M}{VD} \geqslant 1$

For vertical slip to occure $V > \mu H$

i.e. $\frac{\mu M}{VD} < 1$

4.2.1 CASE I NO SLIP OCCURS $\mu m/VD > 1$

Consider the forces acting when a beam-to-column connection is loaded as shown in Figure 4.1.

When $\mu m/VD > 1.0$ vertical slip is small (see load-vertical slip graph for beam-to-column connection $S/D > 1.0$) and the mechanism of failure may be assumed to be rotation about AA. This rotation produces a stress f_{wx} in the flange weld which may be determined by taking moments of forces about the axis AA.

Taking moments about AA

$$VS = B_e a f_{wx} D$$

Where B_e is the effective length of the weld based on the flexibility of the column flange and is less than or equal to B and a is the throat thickness.

Rearranging:

$$f_{wx} = \frac{VS}{B_e a D} \qquad (4.1)$$

4.2.2 CASE II VERTICAL SLIP OCCURS $\mu M/VD < 1.0$

When $\mu m/VD < 1$ vertical slip is more apparent and an additional equation is required.

Resolving forces vertically:

$$V - B_e \, a \, f_{wy} = \mu H$$

Rearranging:

$$f_{wy} = \frac{V - \mu H}{B_e \, a} \qquad (4.2)$$

Where V is the shear force, B_e is the effective length based on the flexibility of the beam flange, a is the throat thickness and f_{wy} is the longitudinal shear stress is the beam flange.

Taking moments about the axis BB Figure 4.1)

$$HD = VS$$

Rearranging:

$$H = \frac{VS}{B} \qquad (4.3)$$

Combining equations 4.2 and 4.3 to eliminate H

$$f_{wy} = \frac{V - \mu \frac{VS}{B}}{B_e \; a}$$

$$f_{wy} = \frac{V\,(1 - \mu\, S/D)}{B_e \; a} \qquad (4.4)$$

The failure criterion for a fillet weld has been investigated in Section 3.2.5 and can be represented as shown in Figure 4.2. F_x is the force in the weld resisting the beam flange force in the tension region, and F_y is the force in the weld resisting the vertical shear force.

When no slip occurs because the major movement is in the x-direction, the predominant force acting on the weld is in the x-direction (F_x). When slip occurs, the predominant force acting on the weld is in the y-direction because the major movement is in the y-direction.

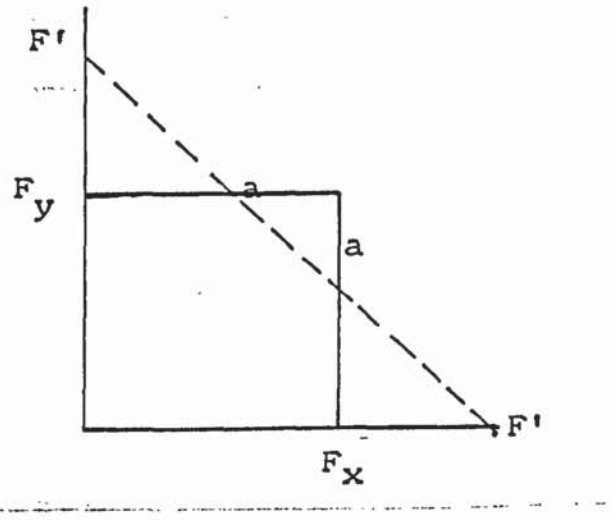

Figure 4.2 Failure criterion for fillet weld

4.2.3 CASE III INTERMEDIATE BETWEEN CASES I AND II

The shape of the weld failure criterion is fortuitous and enables the strength of the connection to be expressed as the lesser value of Equation 4.1 or 4.4. In reality, the weld failure criterion is represented in Figure 4.2 by three lines and the strength of the connection based on line aa is as follows:

$$F_x + F_y = F' \qquad (4.5)$$

Combining equations 4.3, 4.4 and 4.5:

$$\frac{VS}{D} + V(1 - \mu S/D) = F^*$$

This intermediate type of failure occurs when the deformation in the x and y directions are approximately equal, i.e when $\mu m/VD \simeq 1.0$.

4.3 EFFECTIVE LENGTHS OF WELDS

4.3.1 INTRODUCTION

Unless run-on and run-off tags are used, the start and stop sections of a weld cannot be relied upon to provide the full strength. The common practice in design situation is to reduce the actual length by twice the leg length to give the effective length.

If the geometry of the components alters under load as is usually the case in unstiffened beam-to-column connections, the effective length may be further reduced. For such cases empirical formulae for the effective length are available (27, 29, 30, 44) but these do not consider the effect of the flange width on the flexibility of the flange. The reduction in strength of the weld is due to the non-uniform stress distribution in the weld which in turn is due to the flexibility of the flange. It is obvious that the flexibility of the flange is a function of both the flange width and flange thickness.

At ultimate load, both the beam and the column suffer deformations. If the distortion of the flanges is plastic and gives rise to yield lines, the analysis of the connection may be based on the yield line pattern. Consider the connection failure with a yield line pattern on the column flange as shown in Figure 4.3. Due to symmetry, only the right hand half of the column flange is considered.

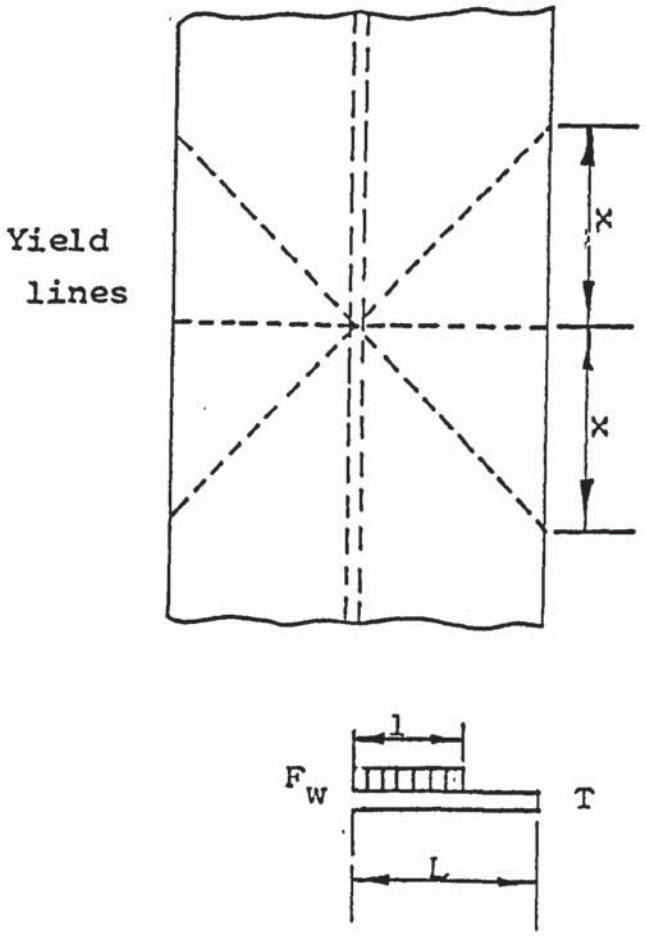

Figure 4.3 Column showing yield lines

Work done by the external load, $W = \Sigma m_p \theta$ (4.6)

Where m_p = the plastic moment of the flange per unit length

θ = angle of rotation of the yield lines

$$\therefore \quad W = \left[4 m_p L \frac{\Delta}{L} + 2 m_p \times \frac{\Delta}{L}\right] \tag{4.7}$$

$$= 2 m_p \left[2 \Delta \frac{L}{x} + \times \frac{\Delta}{L}\right]$$

For minimum work $\frac{dw}{dx} = 0$

$$-\frac{2L}{x^2} + \frac{1}{L} = 0$$

and $\quad \times = \sqrt{2}\, L$ (4.8)

Consider a beam length ℓ simply support carrying a uniformly distributed load which has failed with the mechanism shown in Figure below.

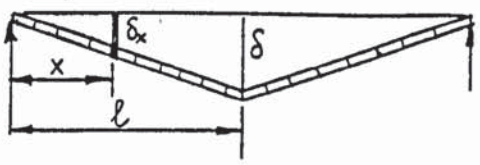

Consider an element distant × from the left hand support and width δ×

Load due to this element = F_w dx

Work done by this element $F_w \, dx \, \delta_x$

But $\delta_x \quad \frac{x}{\ell/2} \quad \delta$

Work done by the element = $F_w \, dx \, \delta \, \frac{x}{\ell/2}$

Total work done by the entire load:

$$= 2\left[\int_0^{\ell/2} F_w dx \, \delta \, \frac{x}{\ell/2} \right]$$

$$= 2\left[\frac{2 F_w}{L} \delta \int_0^{\ell/2} x \, dx \right]$$

$$= 2\left[\frac{2 F_w}{L} \delta \left[\frac{x^2}{2} \right]_0^{\ell/2} \right]$$

$$= \frac{4 F_w}{2L} \delta \left[\frac{\ell^2}{4} \right]$$

$$= F_w \ell \frac{\delta}{2}$$

$$\therefore \quad W = F_w \ell \frac{\delta}{2}$$

If the stress distribution is uniform over the entire width of the flange L and the resulting maximum deflection is Δ then $\delta = \frac{\ell}{L} \Delta$

$$\therefore \quad W = F_w \ell \ \frac{\Delta}{2} \frac{\ell}{L} \tag{4.9}$$

Combining 4.7 and 4.9

$$\therefore \quad \ell \ F_w \ (\ell/L) \ \frac{\Delta}{2} = 2m_p \left[2 \frac{L}{x} \Delta + \frac{x}{} \Delta \right]$$

Rearranging $$\frac{F_w \ell^2}{L} = 4m_p \left[2 \frac{L}{x} + \frac{x}{L} \right] \tag{4.10}$$

Combining 4.8 and 4.10

$$F_w \ell^2 = 4m_p \left[\frac{2L}{\sqrt{2}\ L} + \frac{\sqrt{2}\ L}{L} \right]$$

$$= 4 \ m_p \left[\sqrt{2} + \sqrt{2} \right]$$

$$= 8\sqrt{2} \ m_p$$

$$\frac{F_w \ \ell^2}{L} = 8\sqrt{2} \ m_p$$

Dividing both sides by L and rearranging:

$$\left(\frac{\ell}{L}\right)^2 = \frac{8\sqrt{2}\, m_p}{F_w L}$$

but for the flange $m_p = \frac{T^2 f_{fy}}{4}$

Where T is the flange thickness and f_{fy} is the flange yield stress

$$\therefore \quad \left(\frac{\ell}{L}\right)^2 = \frac{8\sqrt{2}\, T^2 f_{fy}}{4\sqrt{F_w L}}$$

$$= \frac{2\sqrt{2}\, T^2 f_{fy}}{F_w L}$$

effective weld length factor $= \frac{\ell}{L}$

$$= \left[\frac{2\sqrt{2}\, T^2 f_{fy}}{F_w L}\right]^{\frac{1}{2}}$$

$$\text{or} \quad \ell = L\left[\frac{2\sqrt{2}\, T^2 f_{fy}}{F_w L}\right]^{\frac{1}{2}} \qquad (4.11)$$

$$0 < \frac{\ell}{L} < 1.0$$

For a full rigid connection $\frac{\ell}{L} = 1.0$ and for a purely flexible connection $\frac{\ell}{L} \simeq 0$

$\frac{\ell}{L} > 1.0$ if

$2\sqrt{2}\ T^2 f_{fy} > F_w\ L$

i.e. if $f_{fy} > \frac{F_w\ L}{2\sqrt{2}\ T^2}$

In this case if $282.17 > \frac{1659 \times 152}{2\sqrt{2} \times 7.095^2}$

$282.17 \not> 1771.088$

Alternatively consider the distribution of force in the weld over the same length ℓ as shown in Figure 4.4 below:

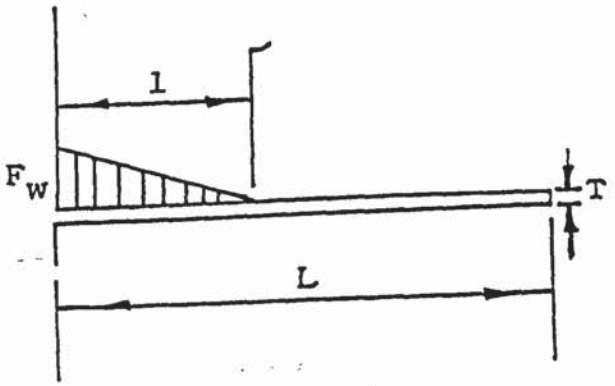

Figure 4.4 Plastic theory for I-section triangular distribution of stress

Again suppose one half of the flange acts as a cantilever fixed in the middle of the column:

Applying the principle of virtual work:

$$\left(F_w \ \frac{\ell}{2}\right) \frac{2}{3}\ell = 8\sqrt{2}\ m_p$$

Rearranging: $$\ell = \left[\frac{24\sqrt{2}\ m_p L}{F_w}\right]^{\frac{1}{2}} \qquad (4.12)$$

The effective width factor in this case is:

$$\frac{\frac{1}{2}\ell F_w}{L F_w} = \frac{\frac{1}{2}\ell}{L}$$

$$= \frac{1}{L}\left[\frac{24\sqrt{2}\ m_p L}{F_w}\right]^{\frac{1}{2}}$$

$$= \left[\frac{6\sqrt{2}\ m_p}{F_w\ L}\right]^{\frac{1}{2}}$$

but $m_p = \frac{T^2 f_{fy}}{4}$

$$\text{Factor} = \left[\frac{3\sqrt{2}\ T^2 f_{fy}}{2\ F_w\ L}\right]^{\frac{1}{2}} \qquad (4.13)$$

4.3.2 ELASTIC THEORY FOR I-SECTION

An alternative theoretical solution to the effective weld length is based on the assumption that the flange behaves elastically.

Consider the weld stress to be uniformly distributed along the column flange over a length ℓ as shown in Figure 4.5.

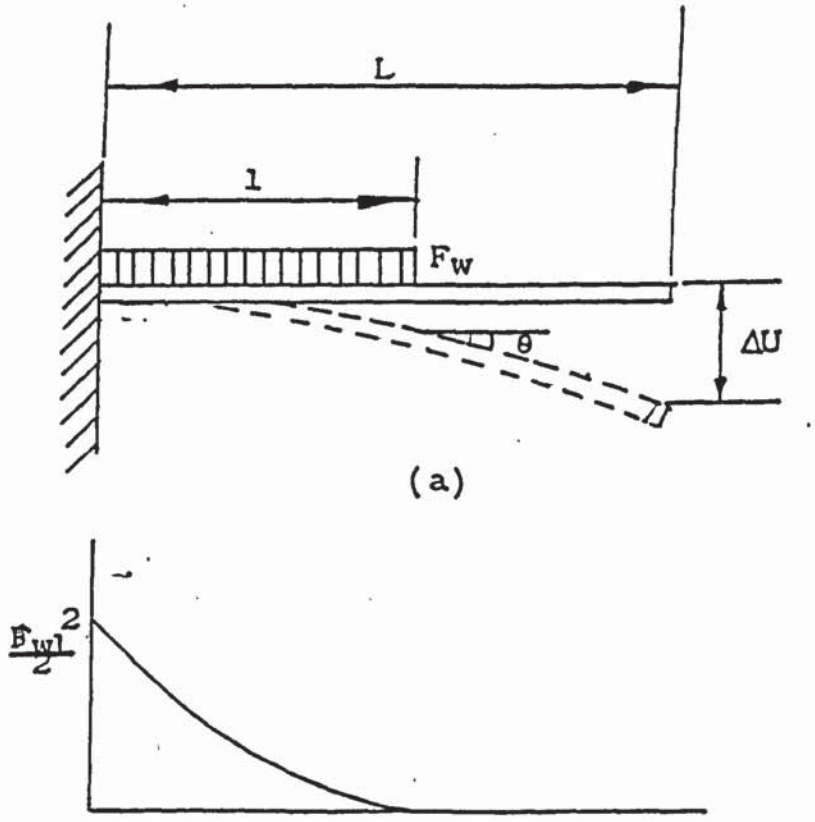

Bending moment diagram

Figure 4.5 Elastic deflection of the flange of the column with a uniformly distributed load over part of the width

Applying the Mohr first moment-area theorem; if the deflection at the end

of the flange is ΔU and the origin is at the support then:

$$\Delta U = \frac{F_w \ell^4}{8EI} + \theta (L - \ell) \qquad (4.14)$$

The total deflection is the deflection at the end of the distributed load plus the deflection due to the unloaded part of the cantilever.

$$\theta_e - \theta_s = \frac{A}{EI} \qquad (4.15)$$

Where θ_e = slope at the end of the cantilever

θ_s = slope at the support (zero in this case)

$$\theta = \frac{1}{EI}\left[1/3 \; \ell \; \frac{F_w \ell^2}{2}\right]$$

$$\theta = \frac{F_w \ell^3}{6EI} \qquad (4.16)$$

The bending moment diagram is as shown in Figure 4.5b $\frac{F_w \ell^2}{2}$ is the bending moment at the fixed end.

Combining 4.15 and 4.13

$$\Delta U = \frac{F_w \ell^4}{8EI} + \frac{F_w \ell^3}{6EI} (L - \ell) \qquad (4.17)$$

Dividing both sides by L^4

$$\frac{\Delta U}{L^4} = \frac{F_w \ell^4}{8EI\ L^4} + \frac{F_w \ell^3 L}{6EI\ L^4} - \frac{F_w \ell^4}{6EI\ L^4}$$

Rearranging:

$$\frac{24\ \Delta U\ EI}{F_w\ L^4} = 4\ \frac{\ell^3}{L^3} - \frac{\ell^4}{L^4}$$

$$\frac{24\ \Delta U\ EI}{F_w\ L^4} = 4\left(\frac{\ell}{L}\right)^3 - \left(\frac{\ell}{L}\right)^4 \qquad (4.18)$$

Alternatively, consider a triangular stress distribution over the same length ℓ as shown in Figure 4.6.

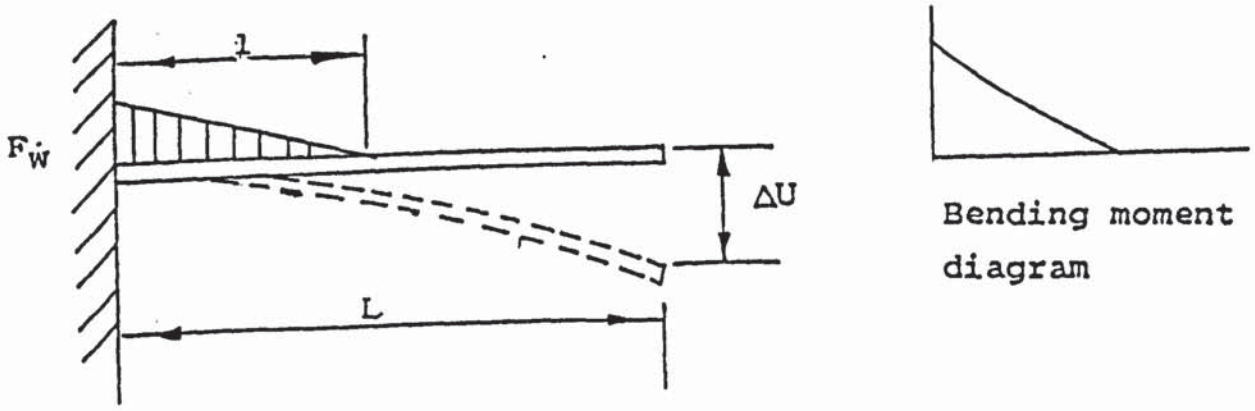

Figure 4.6 Triangular stress distribution - elastic theory for I-section

For this distribution stress:

$$\Delta U = \frac{(\frac{1}{2}\ell F_w)}{15EI} \quad \ell^3 \left[1 + \frac{5(L - \ell)}{4\ell} \right] \tag{4.19}$$

$$= \frac{\ell F_w}{30EI} \quad \ell^3 \left[1 + \frac{5L - 5\ell}{4\ell} \right]$$

$$= \frac{F_w \ell^4}{120\ell EI} \left[4\ell + 5L - 5\ell \right]$$

$$= \frac{F_w \ell^4}{120\ell EI} \left[4\ell + 5L - 5\ell \right]$$

$$= \frac{F_w \ell^3}{120EI} \left[5L - \ell \right]$$

$$= \frac{F_w \ell^4}{30EI} \left[\frac{5}{4}\frac{L}{\ell} - \frac{1}{4} \right]$$

$$= \frac{F_w}{30EI} \left[\frac{5}{4} L\ell^3 - \frac{1}{4}\ell^4 \right]$$

Dividing both sides by L^4

$$\frac{\Delta U}{L^4} = \frac{F_w}{30EI} \left[\frac{5}{4} \frac{\ell^3}{L^3} - \frac{1}{4} \frac{\ell^4}{L^4} \right]$$

Rearranging

$$\frac{30EI\Delta U}{F_w L^4} = \frac{1}{4} \left[5 \left(\frac{\ell}{L}\right)^3 - \left(\frac{\ell}{L}\right)^4 \right]$$

$$\frac{120EI\Delta U}{F_w L^4} = 5 \left(\frac{\ell}{L}\right)^3 - \left(\frac{\ell}{L}\right)^4 \qquad (4.20)$$

Effective width factor $= \frac{\frac{1}{2} (\ell/L)\ LF_w}{L\ F_w} = \frac{1}{2}\frac{\ell}{L}$

Consider also the stress distribution shown in Figure 4.7.

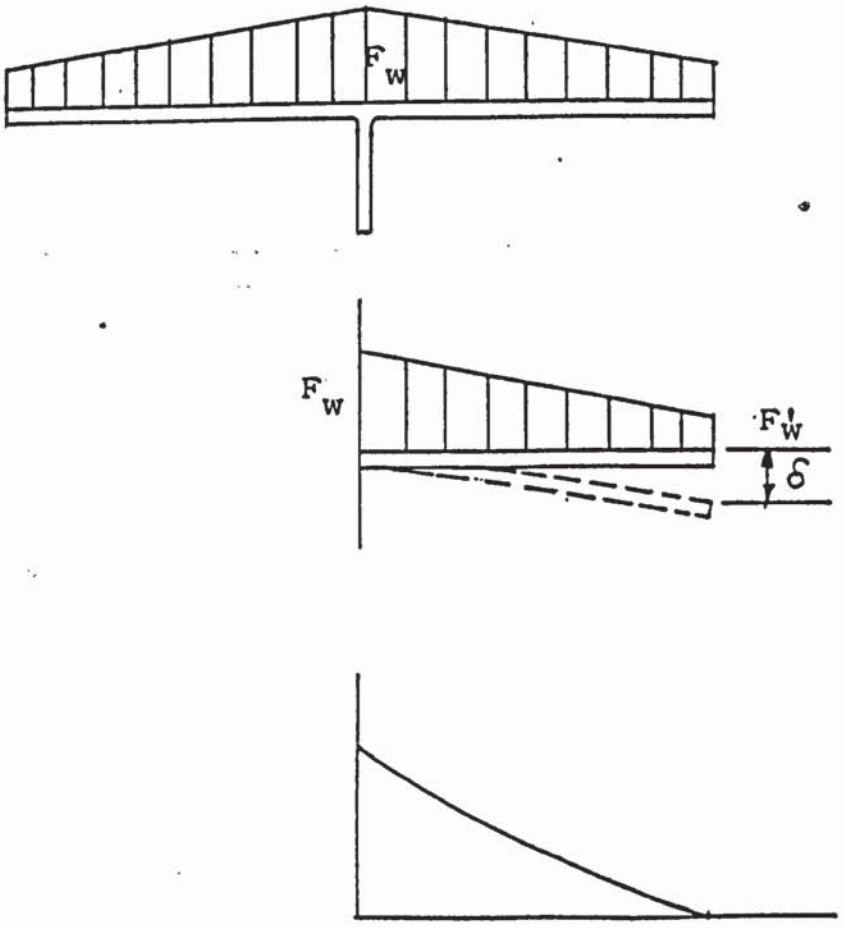

Figure 4.7 Elastic theory, non-uniform stress distribution

$$\Delta U = \frac{F_w L^4}{8EI} \qquad (4.21)$$

$$\delta = \frac{F_w' L^4}{8EI} + \frac{(F_w - F_w')L^4}{30EI} = \frac{11F_w' L^4}{120EI} + \frac{F_w L^4}{30EI} \qquad (4.22)$$

$$\text{Effective width factor} = \frac{F_w + F_w'}{2F_w} = \frac{1}{2}\left[1 + \frac{F_w'}{F_w}\right] \qquad (4.23)$$

$$\frac{\delta}{\Delta U} \quad \frac{\frac{F_w' L^4}{8EI} + \frac{(F_w - F_w') L^4}{30EI}}{\frac{F_w L^4}{8EI}}$$

$$= \frac{F_w'}{F_w} + \frac{4}{15} - \frac{4}{15}\frac{F_w'}{F_w}$$

$$= \frac{11}{15}\frac{F_w'}{F_w} + \frac{4}{15} = \frac{1}{15}\left[11\frac{F_w'}{F_w} + 4\right]$$

$$\frac{\delta}{\Delta U} = \frac{1}{15}\left[11\frac{F_w'}{F_w} + 4\right] \qquad (4.24)$$

$$\therefore \quad \frac{F_w'}{F_w} = \frac{1}{11}\left[\, 4 - 15\,\frac{\delta}{\Delta U} \,\right] \qquad (4.25)$$

$$= \frac{1}{11}\left[\, 4 - \frac{15}{\Delta U}\left(\frac{11\,F_w'\,L^4}{120EI} + \frac{4\,F_w\,L^4}{120EI}\right) \,\right]$$

$$\doteq \frac{1}{11}\left[\, 4 - \frac{15\,F_w\,L^4}{120EI\Delta U}\left(\frac{F_w'}{F_w} + 4\right) \,\right]$$

$$\therefore \quad 11\,\frac{F_w'}{F_w} = 4 - \frac{15\,F_w\,L^4}{120EI\Delta U}\left(\frac{F_w'}{F_w} + 4\right)$$

Rearranging:

$$\frac{11\,F_w'}{F_w} + \frac{15\,F_w\,L^4}{120EI\Delta U}\left(\frac{F_w'}{F_w}\right) = 4 - \frac{60\,F_w\,L^4}{120EI\Delta U}$$

$$\frac{F_w'}{F_w}\left(11 + \frac{15\,F_w\,L^4}{120EI\Delta U}\right) = 4\left(1 - \frac{15\,F_w\,L^4}{120EI\Delta U}\right)$$

$$\frac{F_w'}{F_w} = \frac{4\left(1 - 15\,F_w\,L^4 / 120EI\Delta U\right.}{11 + \dfrac{15\,F_w\,L^4}{120EI\Delta U}} \qquad (4.26)$$

$$\text{Effective width factor} = \tfrac{1}{2}\left[1 + \frac{F'_w}{F_w}\right]$$

$$= \tfrac{1}{2}\left[\frac{1 + 4\left(1 - \dfrac{15\ F_w\ L^4}{120EI\Delta U}\right)}{\left(11 + \dfrac{15\ F_w\ L^4}{120EI\Delta U}\right)}\right]$$

$$= \tfrac{1}{2}\left[\frac{15(1 - 3\ F_w\ L\ /120EI\Delta U)}{11 + 15\ F_w\ L^4/120EI\Delta U}\right] \qquad (4.27)$$

4.4 WEB CRUSHING THEORY FOR STEEL I-SECTION

In beam-to-column connections, the effect of a beam moment on a column is to subject the column to a couple composed of two flange forces and the web forces. The effects of these beam flange forces can be of significance in two regions of the column. The first region is the column flange where bending may contribute to the fracture of the beam flange/column flange fillet weld. The theory on this has already been presented (see Section 4.2). The second region is the column web where the concentrated compressive beam flange force may cause yielding of the web accompanied by buckling and yielding accompanied by fracture due to the beam flange tension force in the tension region. The effect of an axial load on the column on the web buckling behaviour will be examined in this section.

As an illustration of the influence of the column axial load on the web buckling behaviour of the column, consider the local crushing failure and flange yielding mechanism for a column with an eccentric longitudinal load shown in Figure 4.11.

The load W has moved through a distance Δ causing the web to yield at its junction with the root along a length $S_b + 2x$. As this causes the rotation of the flanges, plastic hinges are formed at the positions shown in the figure.

Due to symmetry, only one half of the column depth will be analysed. The load W by moving through the distance Δ does work of magnitude $W\Delta$. The distribution of the bearing stress in the web beneath the flange is assumed to be as shown in Figure 4.11 (inset).

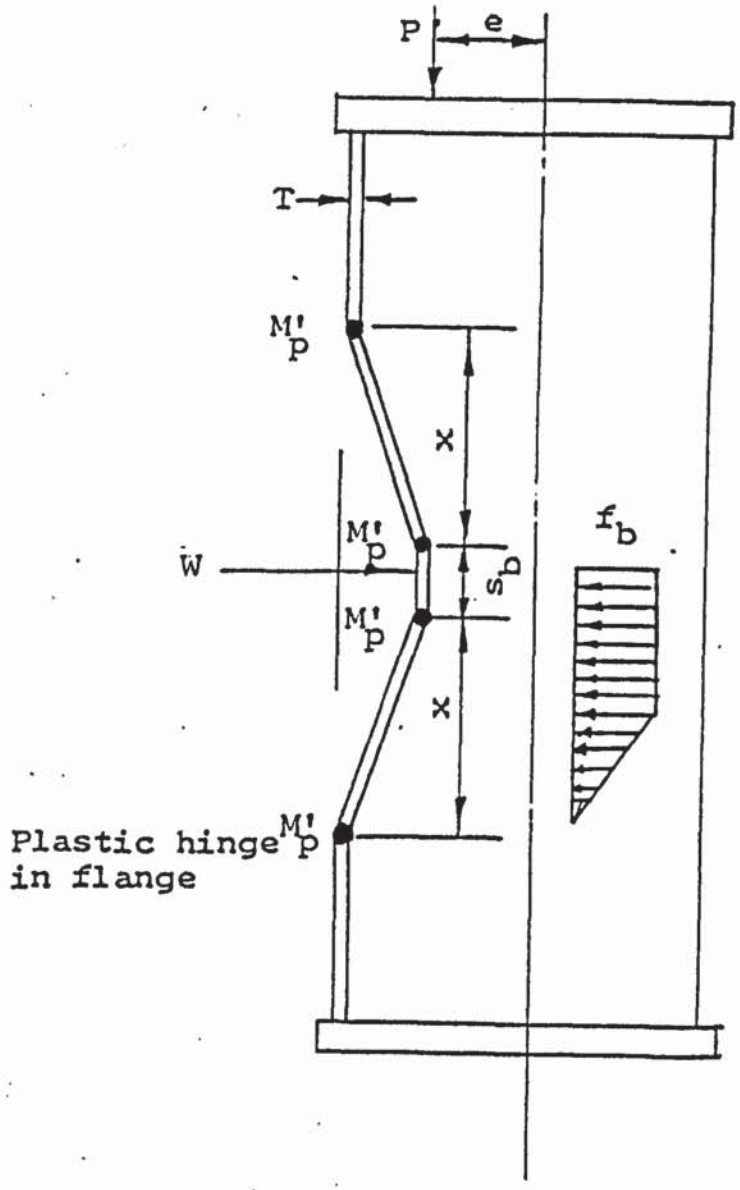

Figure 4.11 Failure mechanism of column subject to longitudinal load and web buckling load

Internal work done by the web and flange =

$$4m_p' \frac{\Delta}{x} + 2x\ t\ f_b \frac{\Delta}{2} + S_b\ t\ f_b\ \Delta$$

Where m_p'' is the reduced plastic moment of resistance due to the

action of the axial load. Applying the principle of virtual work:

$$\Delta W = 4m_p' \frac{\Delta}{x} + 2xtf_b \frac{\Delta}{2} + S_b t f_b \Delta \qquad (4.28)$$

$$W = \frac{4m_p'}{x} + 2xt f_b + S_b t f_b \qquad (4.29)$$

For minimum work $\frac{d_w}{d_x} = 0$

$$- \frac{4m_p'}{x^2} + t f_b = 0$$

$$x = 2 \left[\frac{m_p'}{tf_b} \right]^{\frac{1}{2}} \qquad (4.30)$$

Putting (4.40) in (4.39):

$$W = 4 (m_p' tf_b)^{\frac{1}{2}} + S_b t f_b \qquad (4.31)$$

If the axial stress is assumed not to affect the web bearing capacity, and m_p' is the plastic moment of resistance of the flange when subject to an axial stress then:

$$m_p' = \frac{BT^2}{4} f_{fy} \left[1 - \frac{f_a}{f_{fy}} \right]^2 \qquad (4.32)$$

For a column carrying a longitudinal eccentric load P, the total unit stress is the sum of the stress due to the moment P_e and the stress due to P applied as an axial load, therefore:

$$f_a = \frac{P}{A} + \frac{P_e}{Z}$$

Where A is the cross-sectional area and Z is the elastic section modulus of the column section.

Substituting for f_a in 4.42

$$m_p' = \frac{BT^2 f_{fy}}{4} \left[1 - \frac{\left(\frac{P}{A} + \frac{P_e}{Z} \right)^2}{f_{fy}^2} \right]$$

Rearranging:

$$m_p' = \frac{BT^2}{4 f_{fy}} \left[f_{fy}^2 - \left(\frac{P}{A} + \frac{P_e}{Z} \right)^2 \right] \qquad (4.33)$$

Substituting for M_p' in 4.41

$$W = 4\sqrt{\frac{BT^2}{4 f_{fy}}\left[f_{fy}^2 - \left(\frac{P}{A} + \frac{P_e}{Z}\right)^2 \right]}\, t f_b + S_b\, t\, f_b$$

Rearranging

$$\left[\frac{W - S_b\, t\, f_b}{\frac{2\sqrt{BT^2\, t\, f_b}}{f_{fy}}}\right]^2 + \left[\frac{P}{A} + \frac{P_e}{Z}\right]^2 = f_{fy}^2$$

or

$$\left[\frac{W - S_b\, t\, f_b}{2T\, f_{fy}\sqrt{Bt f_b}}\right]^2 + \frac{1}{f_{fy}^2}\left[\frac{P}{A} + \frac{P_e}{Z}\right]^2 = 1 \qquad (4.34)$$

A comparison of this theory with the experimental results is presented in the next chapter.

4.5 SECONDARY BEAM-TO-COLUMN CONNECTION

Figure 4.12 shows an unsymmetrical secondary beam-to-column connection. The structural tee, in addition to providing a flange for the welded connection, also acts as a stiffener.

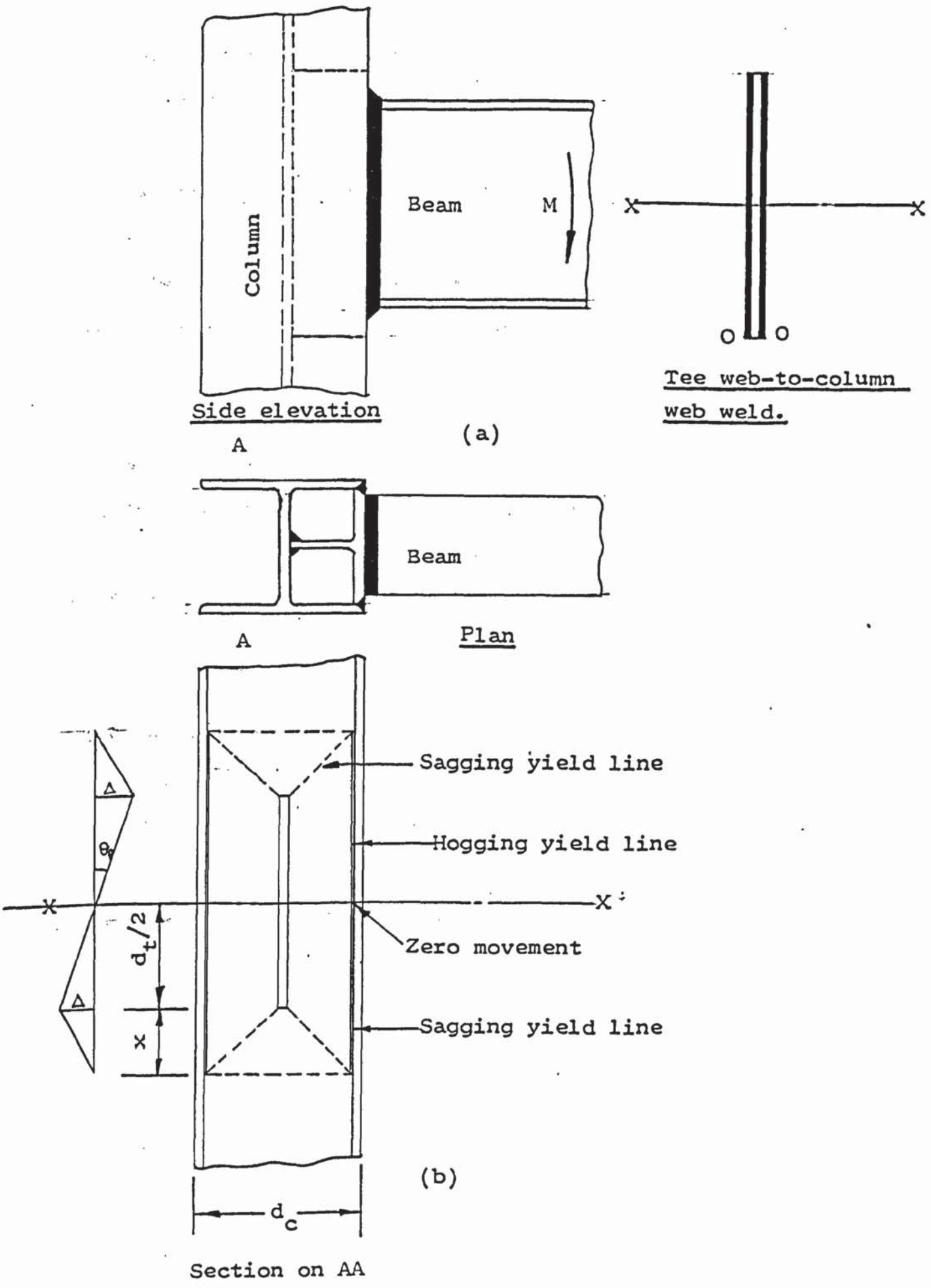

Figure 4.12 Secondary beam-to-column connection.

The plastic moment of the beam is transmitted through the tee to the column web. As the tee flange is connected to the column flanges, a proportion of the plastic moment of the beam is resisted by these butt welds and the remaining proportion by the tee web to the column web fillet weld. Expressions for the moment resisted by the column web and the tee flange will be developed by considering the plastic deformation of the column web. Experimental evidence shows plastic deformation of the column web.

Consider the unstiffened secondary beam-to-column connection shown in Figure 4.12a. The column web may deform with a yield line pattern shown in Figure 4.12b. The resistance of the web to the applied moment can be determined by developing a moment-work equation about the centroidal axis xx.

If the total deflection is Δ and θ_p is the angle of rotation, then the external work done by the applied load is $M_{cwp}\ \theta_p$ where M_{cwp} is the column web plastic moment of resistance.

Assuming small angles of rotation:

$$\theta_p = \tan \theta_p = \frac{\Delta}{dt/2}$$

$$\text{External work} = M_{cwp}\ \frac{\Delta}{dt/2}$$

Internal energy dissipated

$$= m_p \left[4\left(x \frac{\Delta}{dc/2} + dc \frac{\Delta}{x}\right) + 4\left(x \frac{\Delta}{dc/2}\right) + 8\left(\frac{dt}{2} \frac{\Delta}{dc/2}\right) \right]$$

$$= m_p \left[4x \frac{\Delta}{dc/2} + 4dc \frac{\Delta}{x} + 4x \frac{\Delta}{dc/2} + 8\frac{dt}{2} \frac{\Delta}{dc/2} \right]$$

$$= m_p \left[8x \frac{\Delta}{dc/2} + 4dc \frac{\Delta}{x} + 4dt \frac{\Delta}{dc/2} \right]$$

External work = Internal energy dissipated

$$M_{cwp} \frac{\Delta}{dt/2} = m_p \left[8x \frac{\Delta}{dc/2} + 4dc \frac{\Delta}{x} + 4dt \frac{\Delta}{dc/2} \right] \qquad (4.35)$$

For minimum work

$$\frac{d M_{cwp}}{dx} = 0$$

$$\frac{8}{dc/2} - \frac{4dc}{x^2} = 0$$

$$16x^2 = 4dc^2$$

$$x = \frac{dc}{2}$$

Substituting for x in 4.45 and eliminating Δ

$$M_{cwp} = m_p \left[\frac{8dc}{2} \frac{1}{dc/2} + 4dc \frac{1}{dc/2} + 8\frac{dt}{dc} \right]$$

$$= m_p \left[8 + 8 + 8 \frac{dt}{dc} \right]$$

$$= m_p \left[16 + 8 \frac{dt}{dc} \right]$$

$$M_{cwp} = m_p \frac{dt}{2} \left[16 + 8 \frac{dt}{dc} \right]$$

For the column web $m_p = \frac{t_{cw}^2 f_{cwy}}{4}$

$$M_{cwp} = \frac{t_{cw}^2 f_{cwy}}{4} \frac{dt}{2} \left[16 + 8 \frac{dt}{dc} \right]$$

$$M_{cwp} = \frac{t_{cw}^2 f_{cwy}}{4} 4\, dt \left[2 + \frac{dt}{dc} \right]$$

(4.36)

Equation 4.47 expresses the moment resisted by the web of the column section assuming that yield lines form as shown in Figure 4.12b. If this

is the mechanism of failure, then the difference between M and M_{cwp} must be resisted by the weld between the tee flange and the column flanges.

An alternative mode of failure is that the weld between the column web and the stalk could fail without yield lines forming in the column web. In this case, the moment transmitted to these welds could be determined by considering the resistance of the tee flange to the applied moment (the plastic moment of resistance of the tee flange).

Failure could also occur by punching shear on the web of the column. The column web can first be checked for this type of failure.

A further alternative is that the weld between the tee flange and the column flange could fail first. In this case, yield lines may not form on the column web as has been assumed. Failure of the weld may be assumed to be due to rotation about the compression beam flange. The weld between the tee flange and the column flange has to be designed to resist the full plastic moment of the beam.

In the next chapter, the validity of the assumptions in the development of these theories will be tested when these theories are compared with the experimental results and the results of other researchers.

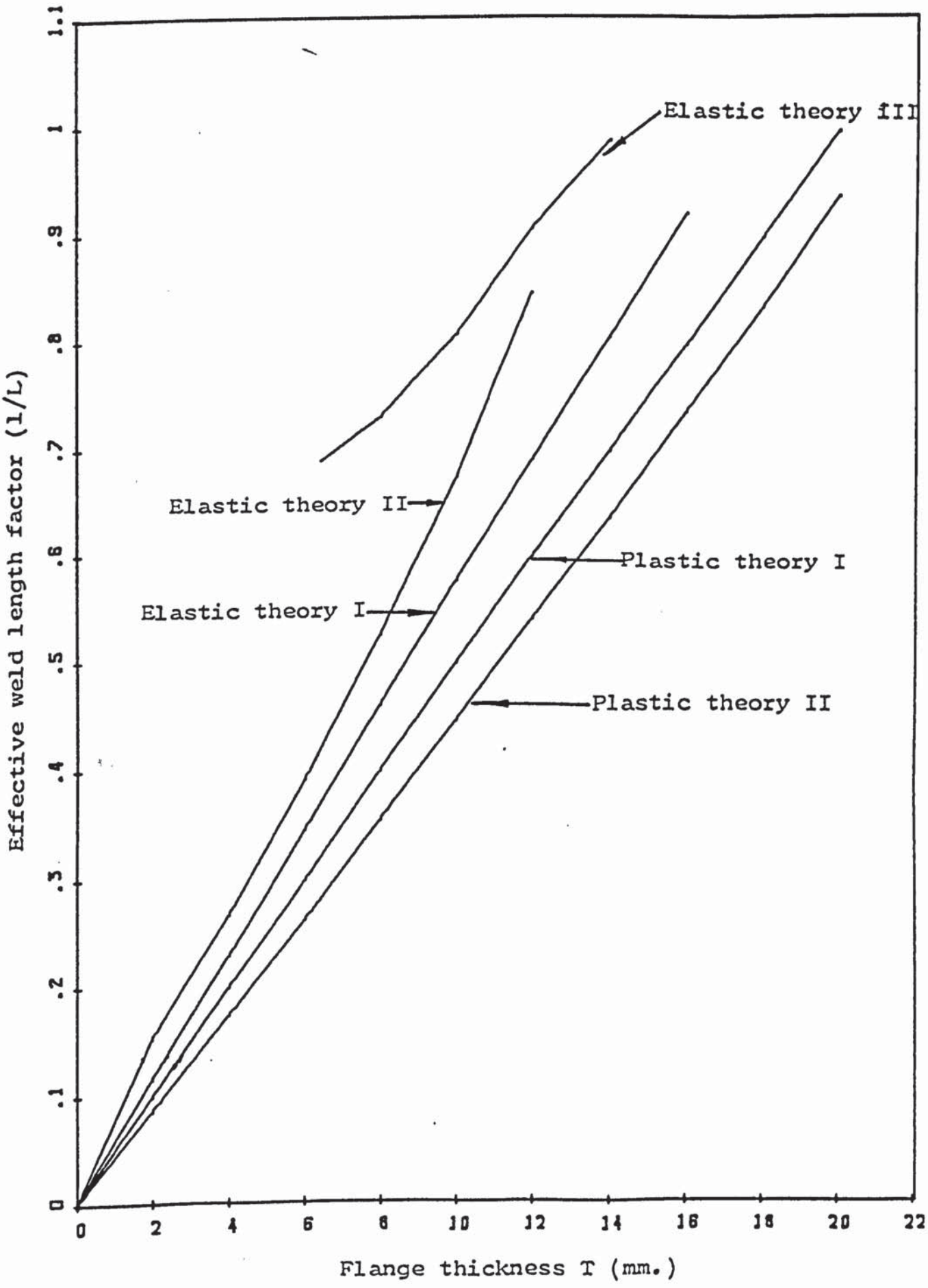

Figure 4.13 The relationship between 1/L and T for all the effective weld length expressions.

CHAPTER 5

COMPARISON OF EXPERIMENTAL RESULTS WITH THEORY

5.1 INTRODUCTION

Several simplifying assumptions were made in the derivation of the theoretical expressions presented in Chapter 4, because of the complexity of the structural behaviour of beam-to-column connections. The purpose of this chapter therefore, is to show whether the actual behaviour of the specimens justifies the theoretical assumptions. This is demonstrated by comparing the predicted results with the author's experimental results, and the results of previous researchers.

The method of comparison adopted for each section is the one that is thought to most lucidly illustrate the differences or similarities i.e. graphs in some cases and tables in others.

5.2 BEAM-TO-COLUMN CONNECTION

5.2.1 FAILURE CRITERION FOR FILLET WELDS

A weld failure criterion is required for the theory for beam-to-column connection and this is considered first to assess its reliability.

Many of the current failure criteria for fillet welds were developed for the prediction of safe working loads and not ultimate loads and are therefore difficult to compare with the author's experimental results. The ultimate load theory of Vreedenburgh[15] was based on the throat as the critical section. Although the limiting stress criterion proposed by Crofts and Martin[55] was based on the actual failure plane, their experimental procedure was different from that of this author.

The F_x - F_y relationship predicted by the theory is compared with the experimental results in Figure 5.1. The experimental results in Figure 5.1 were not expected in view of the results obtained by previous researchers. What was expected was either an elliptical relationship between F_x and F_y given by the expression: $\frac{F_x}{F_w}^2 + \frac{F_x F_y}{F_w^2} + \frac{F_y}{F_w}^2 = 1$ and shown graphically in Figure 5.2, which is the traditional method of ultimate load prediction, or a circular relationship as given by Higgs' results, also shown in Figure 5.2.

The author's results infact agree with Kamtekars' theory which was represented by the expression F_y , $F_x = \frac{L_1 W \sigma\mu}{\sqrt{3}}$ where L_1 is the length of each tension fillet weld, W is the leg length of fillet weld with equal legs and $\sigma\mu$ is the ultimate tensile stress of weld metal. Kamtekars' expression produces an interaction diagram which consists of two straight lines parallel to the x and y axes as shown in Figure 5.1. The authors empirical expression for this relationship between F_x and F_y is $F_y = F_x = f_w \ell$, where f_w is the strength of the weld per unit length

and ℓ is the total length of the weld. The strength of the weld per unit length was found to be 1.659kN/mm run and the total length of weld tested was 80 mm. This then gives $F_y = F_x = 132.72$ kN which gives the two straight lines in the figure.

In addition to the two straight lines given by the above expression, there seems to be a third line which was not considered by Kamtekar. This is the dotted line shown in Figure 5.1. The equation for this line has already been given in Chapter 4 (Equation 4.5).

5.2.2 EFFECTIVE WELD LENGTH

5.2.2.1 INTRODUCTION

The effective weld length is also involved in the failure of the beam-to-column connection because of the flexibility of the beam and column flanges.

None of the current effective weld length expressions viz that of Elzen, Rolloos, Kato et al. Commission XV of the I.I.W. and Witteveen et al., considered the influence of the flange width on the flexibility of the flange. Of the works carried out so far on this subject, only Elzen[27] and Rolloos[29] presented experimental results which can be compared with this author's results. The suitability of this author's theories has however been verified by applying these author's expressions to this author's results and comparing these with the actual

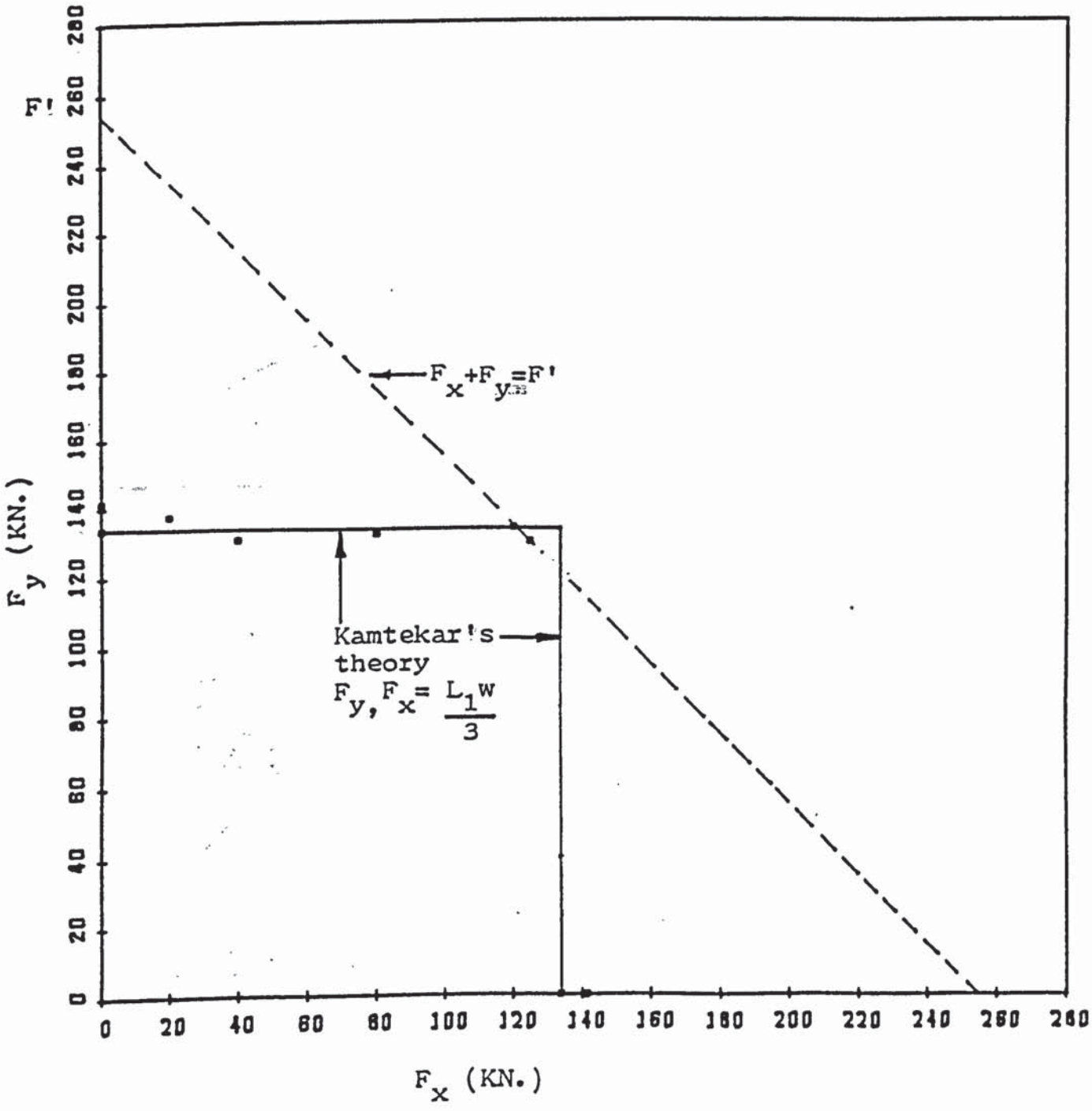

Figure 5.1 Relationship between F_x and F_y for a fillet weld.

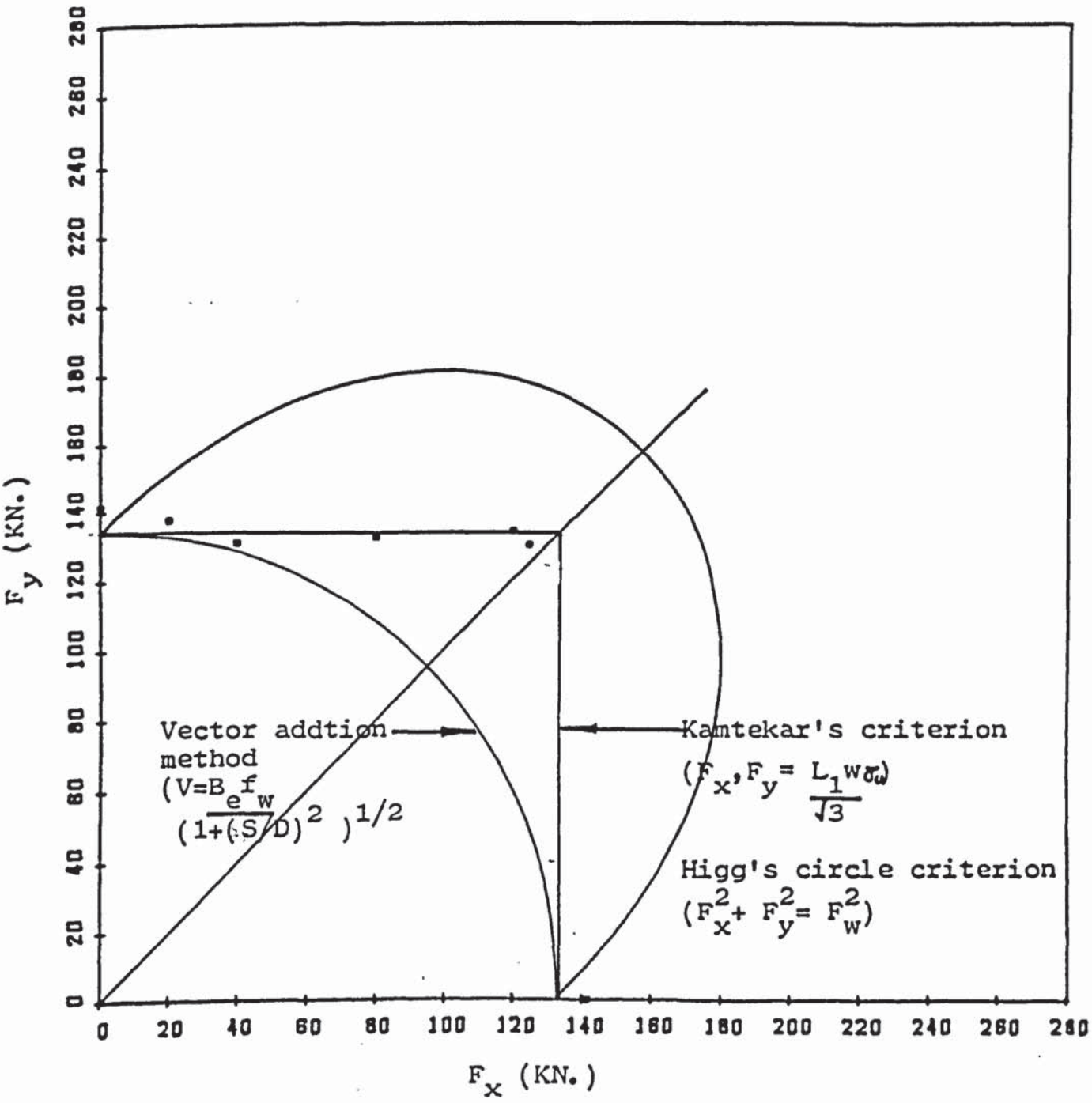

Figure 5.2 Two of the existing failure criteria compared with Kamtekar's criterion.

Theory	Effective Weld Length Factor	Theory / Actual
Finite Element Analysis	0.402	1.047
Plastic Theory (uniform stress distribution)	0.508	1.326
Plastic Theory (triangular stress distribution)	0.440	1.149
Elastic Theory (uniform stress distribution)	0.326	0.851
Elastic Theory (triangular stress distribution)	0.238	0.621
Elastic Theory (trapezoidal stress distribution)	0.374	0.977

Table 5.1 Effective weld length factors predicted by theory compared with the actual effective weld length factor

effective weld length factor as shown in Tables (5.2, 5.3, 5.4, 5.5, 5.6, 5.7), comparing the effective weld length factors predicted by this author's theories with the actual effective weld length factors obtained by both Elzen and Roloos and finally comparing the results predicted by the current theories with the actual results obtained by the author.

5.2.2.2 COMPARISON WITH EXPERIMENTAL RESULTS

The actual effective weld length factor obtained by this author is first compared with the effective weld length factor predicted by the finite element analysis and the theories as shown in Table 5.1. The actual effective weld length factor is taken to be that obtained from the results of the effect of flange flexibility tests which is 0.383. This figure was obtained by dividing the mean of the two failure loads by the product of the weld strength per unit length and the width of the column.

5.2.2.3 COMPARISON OF THIS AUTHOR'S THEORIES WITH ELZEN'S THEORY AND EXPERIMENTAL RESULTS

The empirical effective weld length formula presented by Elzen is as follows:

$$l_e = 2\delta + 7.5\beta$$

where l_e = the effective weld length

Plastic Theory

Flange	Actual Weld	Predicted Weld Length Factor			
Thickness τ (mm)	Length Factor	Theory I*	Theory / Actual	Theory II*	Theory / Actual
6.9	0.400	0.562	1.404	0.481	1.203
7.0	0.350	0.566	1.616	0.488	1.394
10.3	0.575	0.832	1.447	0.720	1.250
10.5	0.580	0.848	1.697	0.734	1.265
13.9	0.690	1.073	1.556	0.972	1.408
13.8	0.670	1.114	1.663	0.962	1.435
			mean 1.564 σ_{n-1} = 0.12 (7.54%)		1.326± 0.098 (7.4%)

Table 5.2 Comparison of the effective weld lenght factors predicted by the two plastic theories with the actual effective weld length factors obtained by Elzen.

* Theory I is the theory that assumed uniform stress distribution and Theory II is the one that assumed triangular stress distribution.

Actual Weld Length Factor	Predicted Weld Length Factor					
	Theory I*	Theory / Actual	Theory II*	Theory / Actual	Theory III*	Theory / Actual
0.400	0.337	0.843	0.195	0.488	0.349	0.873
0.360	0.340	0.944	0.198	0.55	0.350	0.972
0.575	0.500	0.870	0.295	0.513	0.402	0.699
0.580	0.510	0.879	0.300	0.513	0.407	0.702
0.690	0.676	0.980	-	-	-	-
0.670	0.670	1.00	-	-	-	-
		0.91 ± 0.064 (7.07%)		0.517 ± 0.025 (4.9%)		1.83 ± 0.26 (14.2%)

Table 5.3 Comparison of the effective weld length factors predicted by the three elastic theories with the actual effective weld length factors obtained by Elzen.

* Theory I = theory assuming uniform stress distribution.

Theory II = theory assuming triangular stress distribution.

Theory III = theory assuming trapezoidal stress distribution.

N.B. The dashes indicate factors that are greater than one.

δ = column web thickness

β = column flange thickness

The column tested by this author has a web thickness of 6.343 mm and a flange thickness of 7.095 mm. This gives an effective weld length factor of 0.434 with Elzen's expression compared with the actual effective weld length factor of 0.383.

If the difference in the thickness of the web of the section (column) tested by Elzen and that tested by this author is neglected and the effect of the electrode type on the weld strength is also neglected, this author's theoretical prediction of Elzen's effective weld length factor can be compared with the actual values of his effective weld length factor as shown in Table 5.2.

5.2.2.4 COMPARISON WITH ROLLOOS'S THEORY AND EXPERIMENTAL RESULTS

The empirical effective weld length expressions presented by Rolloos are as follows:

$$\text{Fe37} - l_e = 2\delta + 6.6\beta$$

$$\text{Fe52} - l_e = 2\delta + 5.1\beta$$

Actual Effective Weld Length Factor	Predicted Effective Weld Length Factor			
	Theory I	Predicted / Actual	Theory II	Predicted / Actual
0.330	0.598	1.813	0.519	1.573
0.316	0.607	1.920	0.523	1.656
0.468	0.833	1.780	0.720	1.538
0.500	0.822	1.643	0.711	1.423
0.639	-	-	-	-
0.753	-	-	-	-
0.836	-	-	-	-
0.775	-	-	-	-
0.863	-	-	-	-
0.813	-	-	-	-
0.735	-	-	-	-
		1.79 ± 0.114 (6.38%)		1.548 ± 0.097 (6.27%)

Table 5.4 Comparison of the effective weld length factors predicted by the two plastic theories with the actual effective weld length factors obtained by Rolloos (test series III Fe 37).

N.B. Dashes indicate factors which are greater than one.

Actual Effective Weld Length Factor	Predicted Weld Length Factor					
	Theory I	Theory / Actual	Theory II	Theory / Actual	Theory III	Theory / Actual
0.330	0.360	1.091	0.278	0.844	0.300	0.909
0.316	0.365	1.155	0.284	0.897	0.301	0.822
0.468	0.500	1.068	0.402	0.859	0.402	0.859
0.500	0.495	0.99	0.397	0.794	0.400	0.800
0.639	0.716	1.121	-	-	-	-
0.753	0.970	1.288	-	-	-	-
0.836	0.965	1.154	-	-	-	-
0.775	0.970	1.252	-	-	-	-
0.863	0.970	1.124	-	-	-	-
0.813	0.959	1.180	-	-	-	-
0.735	0.970	1.320	-	-	-	-
		1.16 ± 0.098 (8.4%)		0.849± 0.043 (5.01%)		0.85 ± 0.05 (5 .6%)

Table 5.5 , Comparison of the effective weld length factors predicted by the three elastic theories with the actual effective weld length factors obtained by Rolloos (test series III Fe 37).

N.B. Dashes indicate factors greater than one.

Actual Effective Weld Length Factor	Predicted Effective Weld Length Factor			
	Theory I	Theory / Actual	Theory II	Theory / Actual
0.304	0.460	1.512	0.400	1.317
0.319	0.495	1.552	0.431	1.351
0.376	0.693	1.843	0.598	1.591
0.366	0.686	1.874	0.594	1.623
0.361	0.679	1.880	0.587	1.626
0.577	0.962	1.667	0.834	1.446
0.549	0.962	1.752	0.834	1.519
0.531	0.976	1.838	0.846	1.593
0.543	0.969	1.784	0.841	1.55
0.641	-	-	-	-
0.597	-	-	-	-
0.614	-	-	-	-
0.794	-	-	-	-
		1.74 ± 0.14 (8.0%)		1.51 ± 0.11 (7.7%)

Table 5.6 Comparison of the effective weld length factors predicted by the two plastic theories with the effective weld length factors obtained by Rolloos (test series III Fe 52)

NB: Dashes indicate factors greater than one

Actual Effective Weld Length Factor	Predicted Effective Weld Length Factor					
	Theory I	Theory / Actual	Theory II	Theory / Actual	Theory III	Theory / Actual
0.304	0.336	1.105	0.260	0.856	0.345	1.135
0.319	0.366	1.147	0.282	0.885	0.301	0.944
0.376	0.505	1.343	0.406	1.081	0.405	1.077
0.366	0.500	1.366	0.402	1.098	0.402	1.098
0.361	0.497	1.349	0.398	1.102	0.400	1.108
0.577	0.704	1.220	-	-	-	-
0.549	0.704	1.283	-	-	-	-
0.531	0.715	1.347	-	-	-	-
0.543	0.710	1.308	-	-	-	-
0.641	0.964	1.504	-	-	-	-
0.597	0.950	1.591	-	-	-	-
0.614	0.959	1.562	-	-	-	-
0.794	0.973	1.225	-	-	-	-
		1.33 ± 0.15 (11.15%)		0.99 ± 0.1 (11.3%)		1.07 ± 0.07 (6.5%)

Table 5.7 Comparison of the effective weld length factors predicted by the three elastic theories with the actual effective weld length factors obtained by Rolloos (test series III Fe 52).

N.B. Dashes indicate factors greater than one.

where l_e = the effective weld length

δ = the column web thickness

β = the column flange thickness

These expressions give effective weld length factors of 0.392 and 0.322 respectively when applied to this author's results. The actual effective weld length factor obtained by this author is 0.383. These therefore agree reasonably well with this author's result.

Rolloos first series of tests are the same as Elzen's tests. Just like Elzen, Rolloos's experimental sections have thicker webs and flanges than this author's sections. The suitability of this author's expressions is again tested by comparing the effective weld length factor predicted by this author's theories with the actual values of the effective weld length factor obtained by Rolloos. (See Tables 5.4, 5.5, 5.6, and 5.7).

5.2.2.5 COMPARISON WITH THE EXPRESSION PRESENTED BY COMMISSION XV OF THE I.I.W

The effective weld length formula presented by Commission XV of the International Institute of Welding I.I.W is as follows:

$$b_{eff} = C_1 t_1 + 2 t_2$$

where b_{eff} is the effective weld length

C_{11} = 7 for Fe 360 in this case

= 5 for Fe 510 in this case

t_1 = the column flange thickness

t_2 = the column web thickness

Applying the above expression to this author's experimental results give effective weld length factor of 0.410 for Fe 360 and 0.317 for Fe 510 compared to the actual effective weld length factor of 0.383. This suggests that Fe 360 is similar to the steel tested by this author.

5.2.2.6 COMPARISON WITH THE EMPIRICAL EXPRESSION PRESENTED BY KATO ET AL

The work by Kato et al. is a compilation of the work on effective weld length carried out by various researchers in Japan. The expression of significance is that presented by Naka et al. which was referred to as the effective width of the column web. Experimental results were not presented. The empirical effective weld length expression presented by Naka et al is as follows:

$$_{c}b_{e} = {}_{b}t_{f} + \alpha k$$

where $_{c}b_{e}$ = effective width of column web

$_{b}t_{f}$ = beam flange thickness

α = 6.77

k = distance from the outer face of flange to the web toe of fillet of member to be stiffened.

$k = {}_{c}t_{f} + r$

where $_{c}t_{f}$ = column flange thickness

r = root radius

Applying the above expression to this author's experimental results give effective weld length factor of 0.351 compared with the actual effective weld length factor of 0.383.

5.2.2.7 COMPARISON WITH THE THEORY PRESENTED BY WITEVEEN ET AL.

The work by Witteveen et al. was analytical and consequently comparison of the author's results with their results connot be effected. An expression similar that of Naka et al. for the effective width of column flange was also presented. The effective weld length expression

was developed from the experimental results of Bakker and Voorn (reference given in Witteveen et al's paper). The expression for the effective width of column flange is as follows:

$$b_m = 2\,t_{wk} + 7\,t_{fk}$$

where b_m = effective width of column flange

t_{wk} = column web thickness

t_{fk} = column flange thickness

This expression is similar to that presented by Commission XV of the I.I.W.

The expression for the effective weld length is as follows:

$$b_m = t_{wk} + 2rk + 7\,\frac{t^2_{fk}}{t_{fl}}$$

where b_m = effective weld length

r_k = root radius

t_{wk} = Column web thickness

t_{fk} = Column flange thickness

t_{fl} = Beam flange thickness

These expressions when applied to the experimental results of this author give effective weld length factors of 0.39 and 0.466 respectively compared with the experimental effective weld length factor of 0.383.

5.2.2.8 VALUES OF COEFFICIENT OF FRICTION

In the analysis of beam-to-column connections, the value of the coefficient of friction is usually taken to be 0.45 in practice. Table 5.8 gives the values of the coefficient of friction for the different faying surfaces, surface preparation and treatment, but a value for a machined edge on a rusted as delivered section is not given.

The figure of 0.225 determined from the first experiment has not been used because the experimental arrangement was not satisfactory. Accurate angle measuring apparatus was not available and a protractor was used which introduced inaccuracies.

However, a value of 0.32 has been obtained from the second experiment and this is the value used to obtain the respective values of the shear force, V from the expression for V presented in the following section.

The weld failure criterion, the effective weld length and the coefficient of friction for steel are all involved in the theory for the failure of the beam-to-column connections.

Type Of Steel	Treatment	Coefficient Of Friction
A7, A36, A440	Clean milk scale	0.322
A7, A36, A440	Clean milk scale	0.336
Fe37, Fe52	Red lead paint	0.065
A7, A36, Fe37	Grit blasted	0.493
A7, A36, Fe37	Grit blasted exposed (short period)	0.527
A514	Grit blasted	0.331
A7, A36	Semi polished	0.279
A7, A36, Fe37	Hot dip galvanized	0.184
	Vinyl treated	0.275
	Cold zinc painted	0.30
	Metallized	0.48
	Rust preventing paint	0.60
	Galvanized and sand blasted	0.34
	Sand blasted and treated with linseed oil (exposed)	0.26
	Sand blasted	0.47

Table 5.8 Values of coefficient of friction (determined from tension type specimens) from guide to design criteria for bolted and riveted joints by J N Fisher and J H Struik.

The theoretical V- S/D relationship for the beam-to-column connection is compared with the experimental results in Figure 5.3. The two theoretical curves were obtained using the expressions for F_x and F_y in Chapter 4 (Equations 4.1 and 4.4). The vector addition method is based on the elastic properties of the weld metal and the allowable stress in the weld and so is bound to be conservative. The traditional method is to combine the expressions for F_x and F_y (Equations 4.1 and 4.4 respectively) with the failure criterion expression $\left(\frac{F_x}{F_w}\right)^2 + \frac{k\, F_x\, F_y}{F_w} + \left(\frac{F_y}{F_w}\right)^2 = 1$ to obtain a single expression for the shear force V as follows:

$$V = \frac{B_e\, F_w}{\sqrt{(S/D)^2 + (1 - \mu S/D)^2 + k\, S/D\, (1 - \mu S/D)}}$$

This is a version of Higgs method. The vector addition method is $F_x^2 + F_y^2 = F_w^2$.

The traditional method of design which incorporates the vector addition method for full weld strength ignores effective weld lengths and friction is represented on Figure 5.4. This method is unsafe in situations where flanges are flexible but can be modified by incorporating effective weld lengths as shown in Figure 5.4.

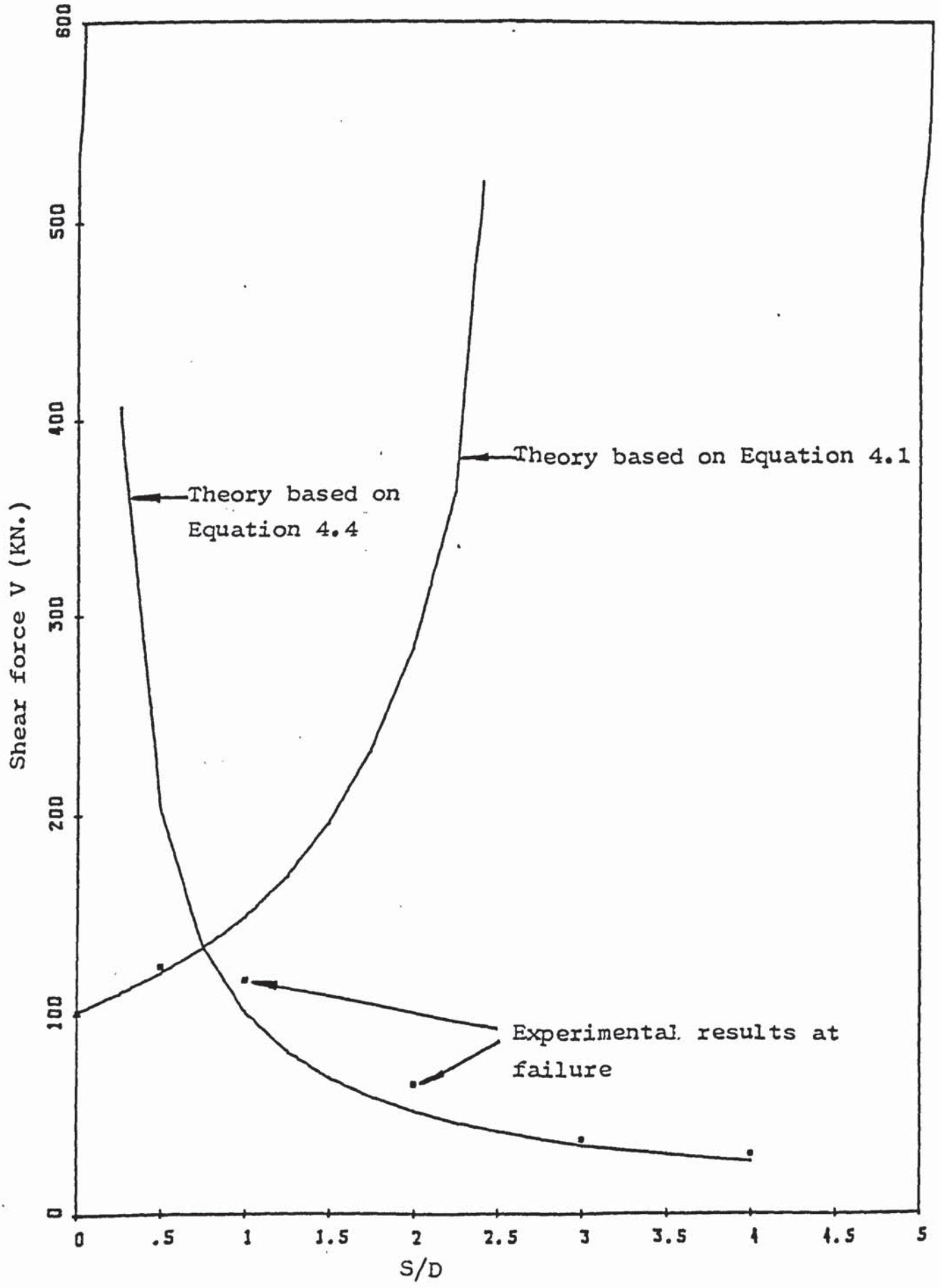

Figure 5.3 Relationship between V and S/D for the beam-to-column connection.

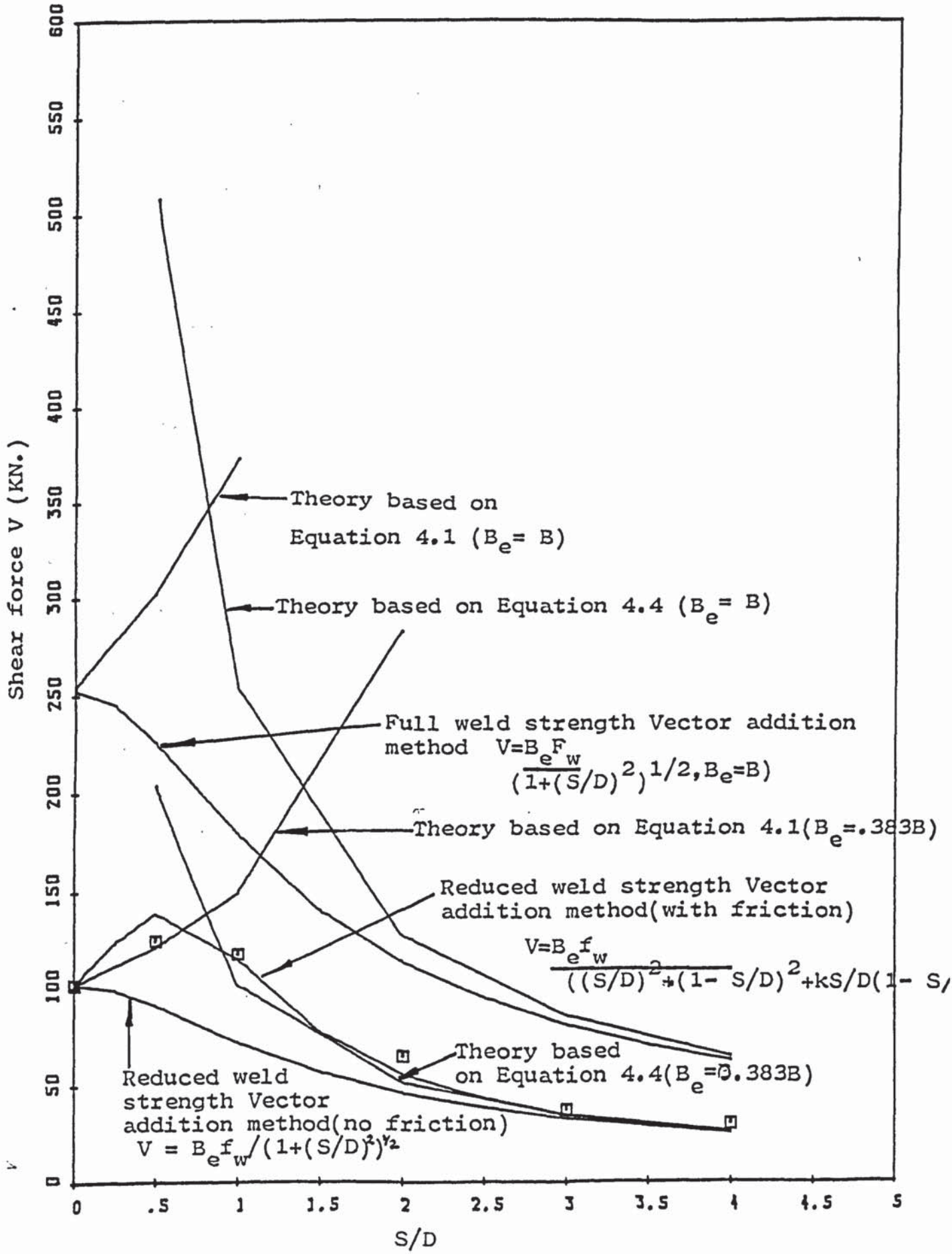

Figure 5.4 Comparison of the relationship between V and S/D of the experimental results with the the theoretical results for the beam-to-column connection.

The vector addition method can be improved further by incorporating frictional forces and weld and parent metal properties.

A further improvement is to use the correct weld failure criterion, i.e. that by Kamtekar, and represented in Equations 4.1 and 4.4. These equations have one disadvantage in that they are discontinuous and inaccurate at $S/D \simeq 0.75$. This situation can be improved by providing a further equation based on the weld failure criterion shown as a dotted line in Figure 5.1.

The V- S/D relationship obtained by using the above equation is compared with the empirical relationship, the theoretical relationship based on the effective weld length, the theoretical relationship based on the full strength of the weld and the vector addition method relationship in Figure 5.4. The results seem to agree with both the author's theory and the vector addition method (with friction). It is clear from this figure that for this beam-to-column connection, the full length of the weld is far from fully effective.

5.3 COLUMN WEB BUCKLING TEST

5.3.1 INTRODUCTION

Web buckling was not present in the author's tests because only one weld was used, but in practice web buckling is a possible mode of failure if stiffeners are not used.

Axial Load P (Tons)	Theoretical Web Buckling Load (Tons)	Actual Web Buckling Load (Tons)	Theoretical / Actual
0	21.250	20.00	1.063
2.0	21.247	20.00	1.062
20.0	20.750	20.00	1.038
40.0	19.150	18.75	1.021
60.0	16.030	14.89	1.077
80.0	9.240	8.00	1.155
84.365	0	0	1
			1.059 ± 0.05 (4.7%)

Table 5.9 Comparison of the theoretical web buckling load with the actual web buckling load.

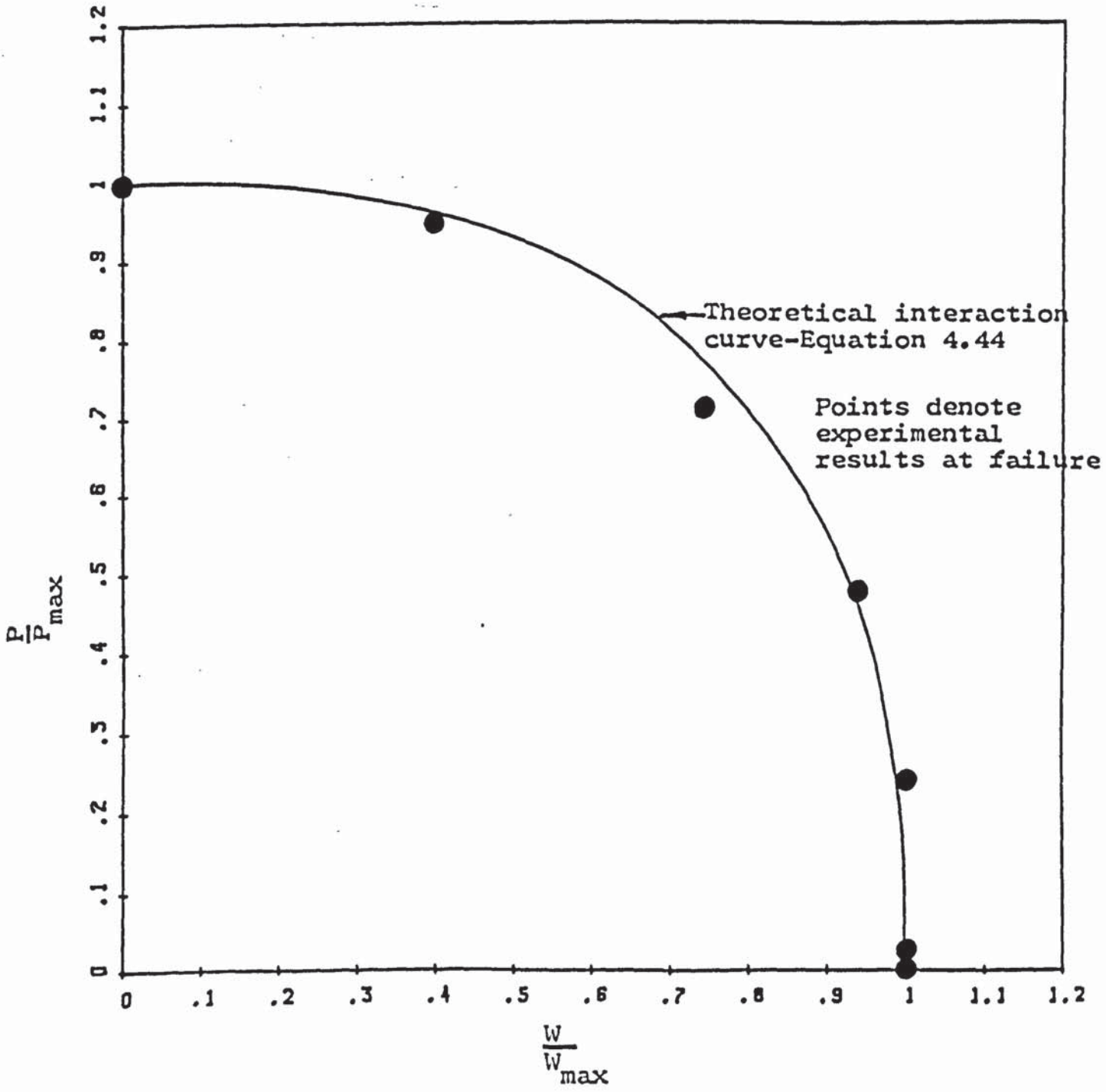

Figure 5.5 The interaction curve for column subject to axial load and web buckling load.

There is no reported work on columns subject to axial load and web buckling load. Consequently, the web buckling load predicted by the theory can be compared with the experimental results only. The web buckling load W, was obtained by putting the various values of the axial load into the web buckling load expression and assuming zero eccentricity of load. The results obtained are compared with the experimental results in Table 5.9. Figure 5.6 shows a comparison of the theoretical interaction curve with the experimental interaction curve.

The theoretical and experimental interaction curves have been obtained by plotting the respective dimensionless axial loads against the dimensionless web buckling loads. These two quantities have been non-dimensionalised by dividing the magnitude of these quantities by their respective predicted plastic limit loads, P'_{max} and W'_{max} (W'_{max} = experimental maximum load).

It has been assumed that when there is no axial load on the column, the column web will buckle at a load equal to W'_{max} which in this case is 20 tons (199.34 kN) and that crushing of the column will take place when $P = P_{max} = A f_y$ where A is the cross-sectional area of the column and f_y is the yield stress of the column material. This then gives

$P_{max} = 2980 \times 282.17 = 84.365$ tons (840.867 kN).

The slenderness ratio of the column has a value below the critical value beyond which elastic buckling of the column could occur.

5.4 SECONDARY BEAM-TO-COLUMN CONNECTION

5.4.1 INTRODUCTION

Although there has been considerable research into the structural behaviour of secondary beam-to-column connections, only Graham et al [23] attempted to investigate the proportion of the beam flange force transmitted through the tee web to the column web. Their analysis was based on the assumption that the flange of the tee acts as a two-span beam on three supports with a uniform load. The proportion of the beam flange force transmitted to the column web through the tee web was found to be dependent on the width of the beam flange in relation to the tee flange width. Their tests showed that when the beam flange extended the full width of the connecting plate as was the case in this authors tests, about 5/8 of the flange force was carried by the web of the tee. This author's theory is based on the yield line pattern depicted on the column web at ultimate load.

Figure (3.35) shows the strain distribution in the tee web for an unstiffened secondary beam-to-column connection. The actual column web moment of resistance was obtained by dividing the whole area under the graph into a number of elements, calculating the moment for each element and summing up all the elemental moments. This procedure can be represented by the following expression:

$$M_{cwp} = \Sigma dAfd$$

where dA = area of element

f = average stress in the element (= average strain X E).

d = distance from the centre of the element to the centre of rotation of the beam.

The area under the graph was divided into ten elements. The actual calculation is presented in the Appendix. This gives $\frac{M_{cwp}}{M}$ ratio of 0.404 compared to the theoretical $\frac{M_{cwp}}{M}$ ratio of 0.419. M is the actual moment applied to the connection i.e. the product of the shear load V and the distance of the load from the face of the tee flange.

The significance of these comparisons are discussed in the next chapter.

CHAPTER 6

GENERAL DISCUSSIONS

6.1 INTRODUCTION

A comparison of the experimental results with the theoretical predictions was presented in the preceeding chapter. In some cases the results predicted by the theory were conservative while in others, the theory overestimated the results. This chapter discusses the results of the tests and the significance of these agreements and discrepancies with the purpose of ascertaining the reliability of the results and providing justifications for the conclusions presented in Chapter 8.

The plastic theories presented in Chapter 4 were based on the yield line theory. It must be pointed out that yield line analysis neglects elastic deformations and assumes all deformations to be concentrated in the yield lines.

6.2 BEAM-TO-COLUMN CONNECTION

6.2.1 WELD FAILURE

The failure criterion tests were designed to simulate the rupture mechanism of the fillet weld in beam-to-column connections. The results

presented in Figure 5.1 were not expected and were expected to follow the pattern of the previous research results, notably Higgs[51] and the Vector addition criteria. The agreement with Kamtekar's theory necessitates a review of the current theories and methods of ultimate load prediction. Kamtekar's theory is based on simplifying assumptions and the replacement of the complex force system with an equivalent force system. The results show that the ultimate strength of a fillet weld in the transverse direction is unaffected by any simultaneous longitudinal force and vice versa, i.e interchanging F_x and F_y does not affect the weld strength. This in contrary to the common belief that the relationship between F_x and F_y is elliptical. The traditional method of ultimate load prediction is based on the failure criterion of Von Mises which in the author's opinion, is more suited for ultimate load prediction of a solid metal.

In all the tests, failure of the flange weld was observed to have commenced from the middle of the connection. This was because of an uneven stress distribution which was related to the flexibility of these flanges, the forces transmitted by the connecting flanges loaded the outstanding portion of the column flanges as a cantilever beam and caused it to deflect. As this deflection took place, the stress in the outer ends of the beam-to-column connecting weld was reduced which caused the centre portion of the weld in line with the column web to be overloaded. At S/D between zero and one ($0 < S/D < 1.0$) both the beam flange and the column flange distorted and at S/D greater than one ($S/D > 1.0$) only the column flange distorted. These distortions caused the stress distribution along the flanges to be non-uniform and this led to premature failure of

the weld. If the flanges are thick enough to preclude distortion of the sections geometry, the length of the weld should be fully effective.

The yield line method of analysis applied to the beam and column flanges gave the best correlation with the experimental results for weld failure associated with deformation of either the beam or the column flange. The yield lines on the test specimens at failure although not fully developed, agreed reasonably with those from theory. There was always a permanent deformation on either the column flange or the beam flange.

Observation of the failure plane angle at ultimate load and the load-vertical slip relationship suggests that there are possibly three distinct modes of failure of the fillet weld viz: failure due to shear only when F_y is dominant, failure due to bending when the beam tensile force F_x is dominant and finally, failure due to the combined action of F_x and F_y when both forces are equally significant. This is evident from the rapid change in failure plane angle from 80^0 at S/D = 0.5 to 20^0 at S/D = 4.0 and the transfer of section deformation from the beam flange to the column flange at the two extreme values of S/D. It is probable that the failure plane angle is only 45^0 when $F_x = F_y$. The vector addition method of ultimate load prediction assumes only one failure mode incorporating a failure plane angle of 45^0. This method is in this author's opinion valid only when both F_x and F_y are of equal magnitude and the assumption of a failure plane angle of 45 is then acceptable.

The F_y dominant failure mode appears to operate within the range of S/D = 0 to S/D = 1.0 ($0 < S/D < 1.0$). The weld fails by shearing in the middle of the connection as a result of overloading resulting from the distortion of the beam flange. Vertical slip occurs with no rotation of the beam.

The F_x dominant failure mode appears to operate at $S/D > 1.0$. The weld fails due to the action of the beam tensile force commencing from the middle of the weld as a result of overloading resulting from the distortion of the column flange. In this case, vertical slip is negligible but the beam rotates about the beam compression region.

Failure due to the combined action of F_x and F_y appears to operate at $0.5 < S/D < 1.47$ possibly mainly at S/D = 1.47. In this case both the beam and the column flange distort. Vertical slip occurs while the beam rotates about the beam compression region.

Higgs[51] identified only two modes of failure from his tests (the failure due to poor fit-up can be prevented). This is probably because he tested a different connection from the one tested by the author. Higgs connection had an end plate welded to the beam. This arrangement precludes beam flange deformation and failure can only be due to either shear at low values of S/D or tension at higher values of S/D, hence his inability to detect the failure mode involving both F_x and F_y.

Figure 3.28 shows the empirical relationship between V and S/D. It is evident from this figure that the failure load decreases as S/D

increases. The initial increase in failure load between S/D = 0 and S/D = 1 could be due to plate bearing and frictional resistance as the beam slips and rotates about the beam compression flange. Between S/D = 1 and S/D = 4, both the beam flange and the column flange distort initially and then only the column flange distorts causing a severe strain on the weld in the middle of the connection. This, combined with a larger leverage at higher S/D values caused the load needed to rupture the weld to decrease. This explains the fall of V as S/D is increased beyond 1.0. It can be seen from Figure 5.3 that the theory is in good agreement with the experimental results. The theory however, underestimated the weld strength. The figure would suggest that the traditional method of ultimate load prediction (Vector addition method with friction) agrees better with the experimental results between S/D = 0.5 and S/D = 4.0 than the author's theory and that the full length of the weld is far from fully effective. It also shows that the vector addition method (without friction) is conservative. It must be pointed out that one experimental result is the mean of three tests.

6.2.2 EFFECTIVE WELD LENGTH

It would have been preferable to obtain experimental results in which the flange thickness and flange width are varied. The difficulties encountered in the attempt to carry out these tests are given in Chapter 3. The agreement between some of the theories, the finite element analysis and the experimental results is reasonable as shown in Chapter 5.

The failure load at S/D = 0 had to be calculated from the theory based on the experimental results of the compression weld strength tests. This was due to the fact that it was difficult to obtain a value from the beam-to-column connection experimental arrangement. The supports of the beam could not be arranged to produce a shear force without bending.

The use of only one weld to make the connection enabled visual examination of slip of the connection at the free end of the beam. In real connections there are at least two flange welds and generally web welds. This investigation is concerned mainly with the determination of the effective weld length and only one length of weld is involved. The use of two or more welds could have made this investigation more difficult. Tests (51) have shown that in beam-to-column connections, the tension weld is the critical weld and always fails first. A knowledge of its failure mode is therefore considered to be the first step to understanding the ultimate load behaviour of beam-to-column connections.

Six theoretical expressions for the effective weld length for beam-to-column connections have been presented in Chapter 4. In general, agreement between theory and experimental results is reasonable. The finite element analysis and the plastic theory I slightly overestimated the effective weld length factor while the others were slightly conservative. The effective weld length factor predicted by the elastic theory assuming trapezoidal stress distribution (elastic theory III) is closer to the actual effective weld length factor than the factor predicted by the other theories (standard deviation of 0.009 compared to 0.15 for finite element analysis, 0.023 for plastic theory I and 0.031 for

plastic theory II). This suggests that the most appropriate effective weld length formula is that given by this theory. The failure of the weld can, however, rarely be regarded as an elastic phenomenon.

Prediction by the empirical expression of Elzen[27] and Rolloos[29], the theoretical expressions of Witteveen et al.[48] and the formula presented by Commission XV of the I.I.W., slightly overestimated the effective weld length. Rolloos's expression overestimated the factor by the same amount as the elastic theory III underestimated the factor. Only the effective weld length expression presented by Naka et al appears to be conservative. Of all these expressions, Rolloos's expression seems to agree better with the author's results.

The relationship between the effective weld length factor and the flange thickness T for all the theories on effective weld length is shown in Figure 4.13. It would appear from this figure that according to plastic theory I, the length of the weld will become fully effective when the flange thickness is about 17.5 mm, 20.2 mm according to plastic theory II, 20.65 according to elastic theory I and about 12.75 according to both elastic theories II and III. To decide on the correct values it is necessary to determine the thickness at which the flange width will become fully effective for a particular flange width by carrying out tests involving beams and columns of varying thicknesses. Such a series of tests should also produce an empirical $\ell/L - T$ relationship.

The plastic theory assumed the yield line pattern in Figure 4.3 on the column flange. Throughout the tests, the yield line pattern observed on either the column flange or the beam flange is not exactly as the one shown in the figure. The yield line pattern observed on the beam flange at ultimate load at S/D = 0.5 is shown in Figure 6.1. The theory assumed straight yield lines but in reality, the lines are not straight. This, perhaps, explains the discrepancy between the actual effective weld length factor and that predicted by the plastic theories. Moreover, the theory assumed different stress distributions from the actual stress distribution along the flange width. The actual stress distribution is taken to be the one given by the finite element analysis. This distribution agrees with the distribution obtained by previous researchers (23, 27 and 29). However, the theory based on the exact stress distribution will be difficult to derive and may be too complicated and therefore unsuitable for use in the design office.

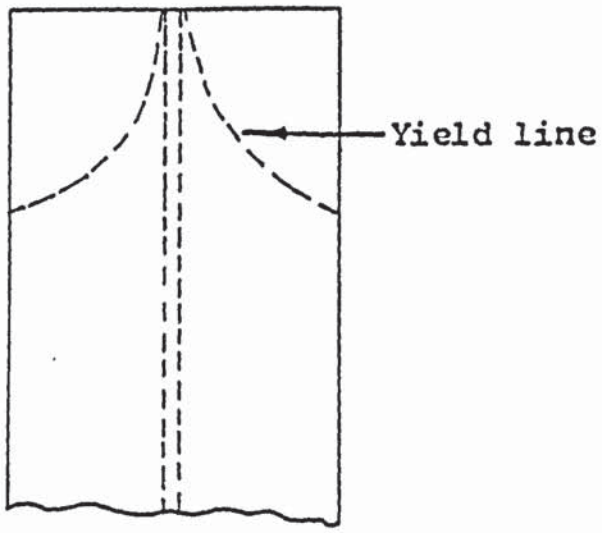

Figure 6.1 Beam flange showing yield lines at ultimate load

The beam-to-column connection is concerned with ultimate load behaviour. The distortion of the geometry of the sections is not elastic and elastic prediction of plastic behaviour is obviously unrealistic. The fact that one of the elastic theories agreed better with the experimental results may be related to the stress distribution assumed. It is likely that the stress distribution assumed for this theory is closer to the actual stress distribution than the stress distribution assumed for the others, or the stress distribution may not be close but an overestimation of the actual stress distribution which therefore compensated for the underestimation by the assumption of elastic behaviour. It is not surprising therefore, that there are discrepancies between the actual effective weld length factor and the factors predicted by the elastic theories.

The fact that none of the previous researchers incorporated the flange width into their effective weld length formula could be taken as a tacit acceptance of the fact that only the flange thickness determines whether a flange is flexible or rigid. One can postulate that irrespective of the width of the flange of a section, if it is thick enough, it will be rigid against distortion and deformation. Alternatively irrespective of the thickness of the flange, if the flange is short, it will be fully rigid. Rolloos stated that he could not see any influence of the flange width on the flexibility of the flange. This conclusion is not surprising since he tested only two flanges of approximately the same width. Similarly Elzen[27] could not have discovered the influence of the flange width from his tests. The Commission XV formula cannot be taken as a standard proven formula since

it was admitted that it was not a detailed specification but a recommendation to be improved upon. The formula by Witteveen et al.[48] was based on the experimental results of Voorn and Bakker[57] which did not include the variation of the flange width, also the formula by Naka et al.[30] is not based on experimental evidence involving the variation of the flange width and the flange thickness. The results presented here are based on both experimental and theoretical analysis of the connection.

The formula to use in any analysis of a beam-to-column connection is dependent on the ratio of S/D. Since the expressions derived are based on the deformation of the column flange, it is recommended that the elastic formula should apply at low values of S/D when the column suffers only elastic deformation and the plastic theory should apply at higher values of S/D when the column suffers plastic deformation.

6.2.3 LOAD-DEFLECTION CURVES

The load-vertical deflection and the load-horizontal deflection curves for beam-to-column connection at the various values of S/D are presented in Figures 3.16, 3.18, 3.20, 3.23, 3.25 and Figures 3.17, 3.19, 3.21, 3.24 and 3.26 respectively. As these connections had only one weld, it was not considered reasonable to compare these curves with previous research results. It can however be seen that the load-vertical slip curves agree with the usual pattern for a fully welded beam-to-column connection. It is possible to determine whether vertical slip occured

from the load-vertical slip graphs in situations where this could not be established from visual inspection of the specimen at failure. The curves can be used in conjunction with the already available information on weld deformation to determine whether the deformations recorded are due to the weld only or due to ralative movement between the beam and column flanges or both.

Figure 3.27 gives a comparison of the load-vertical deflection graphs for the different S/D values. This figure shows that vertical slip decreases as S/D increases. It is possible that the deflections recorded for higher values of S/D are due solely to weld deformation. It was assumed in Chapter 3 that when $\mu M/VD > 1.0$ vertical slip did not occur. This is probably true considereing the fact that the deformations recorded are due to either weld deformation alone or both weld deformation and relative movement between the beam and the column; for example at S/D = 1 the maximum vertical moovement was 2.41 mm, the weld deformation given by Clarke[56] at ultimate load is 2.2 mm. This means that vertical slip is only 0.21 mm.

It is the usual practice in design situations to assume that vertical slip occurs at every value of S/D. The experimental evidence demonstrates that vertical slip probably ceases beyond a certain value of S/D. The exact value of S/D at which vertical slip ceased could not be determined but this graph should serve as a useful guide.

Just as the beam flange deflects due to vertical shear force, the concentrated beam flange force causes the column flange to deflect in the

horizontal direction. The horizontal dial gauges recorded the horizontal deflections of the column flange. The results were presented in the figures listed above. It also provided information on horizontal movement of the entire specimen while the test was in progress. Ideally the two dial gauges should give the same reading at each load.

6.2.4 S/D - θ CURVE

Figure 3.29 shows the relationship between S/D and the angle of rotation θ. Although the connection tested was not fully welded, it is doubtful whether the relationship for a fully welded connection would be different. It is the usual practice in design situations to assume that the weld failure plane angle is always 45^0 irrespective of the value of S/D. Although some researchers (51,55) discovered that the actual failure plane angle varied with S/D, none has shown the exact relationship between S/D and θ. The empirical relationship presented in this thesis should therefore serve as a useful guide. The relationship also seems to validate the assumption that at $0 < S/D < 1.0$ F_y is dominant and at $S/D > 1$ F_x is dominant. The change in failure plane angle from 80^0 at $S/D = 0.5$ to 20^0 at $S/D = 4$ is evident of a change in loading condition from F_y dominant through both F_y and F_x dominant to F_x dominant and hence the transfer of plastic deformation from the beam flange and the column flange to only the column flange.

It is probable that the only time the failure plane angle is 45^0 is when $F_x = F_y$ i.e.

when $\frac{\mu m}{VD} \simeq 1.0$ or

$$\frac{V(1 - \mu S/D)}{B_e a} = \frac{VS}{B_e aD}$$

i.e. when $1 - \mu S/D = \frac{S}{D}$

when $\frac{S}{D} = \frac{I}{1-\mu}$

i.e. when $S/D = 1.47$ ($\mu = 0.32$)

This figure has to be confirmed by experiments.

6.3 COLUMN WEB BUCKLING

The relationship between column axial load and web buckling is shown in Figure 3.31 and this relationship is compared with the theoretical relationship in Figure 5.5. There were no other results or theory with which to compare the author's results, as previous researchers considered other combinations of forces. The agreement between theory and experimental results is reasonable and the theory is simple enough to be used in the design office.

The experiments demonstrated that up to P/P_{max} of 0.24, an axial load on the column has little effect on the ultimate web buckling capacity of the column, but between this value of P/P_{max} and $P/P_{max} = 1$ the web buckling capacity decreases. It is assumed that the crushing of the column occurs when there is no web buckling load, when the axial load reaches Af_y, where A is the cross-sectional area of the column and f_y is the yield stress of the column material. Obviously, this situation cannot be said to be true of a case where the column is long enough to fail by elastic buckling instead of crushing. The tests reported herein were carried out on a column with a slendeness ratio of 60.185. For this area slenderness ratio, the maximum allowable stress on the gross sctional area for axial compression recommended by BS 449 is 126 N/mm^2 for grade 43 steel and 169 N/mm^2 for grade 50 steel. The Perry-Robertson formula from which these allowable stresses have been derived shows that the allowable stress is inversely proportional to the slenderness ratio. It is possible that web buckling could adversely affect the buckling of the column but the author did not carry out tests to verify this.

Although the agreement between the theoretical prediction and experimental results for web buckling is reasonable, the theory overestimated the results throughout. This can only be attributed to the invalidity of some of the assumptions utilized in the derivation of the theoretical expression.

The results obtained are for the 152 x 152 x 23 kg universal column. It is probable that the relationship for the other column sections will be of the same general form but different because of the differences in

flange and web widths and thicknesses. Undergraduate work carried out in this University has shown that the web buckling strength of a column increases with the flange width up to a width of about 200 mm but remains unchanged beyond this width. BS 449 recommends a constant web buckling load for every value of the flange width. The undergraduate work carried out in this University on the effect of flange thickness on the web buckling strength of the column shows that there is an increase in the web buckling strength of the column as the flange thickness is increased up to a web thickness of 14 mm and beyond that further increase in web thickness does not affect the web buckling strength. BS 449 recommends a steady linear increase in the web buckling strength of the column as the flange thickness is increased.

6.4 SECONDARY BEAM-TO-COLUMN CONNECTION

The preparation of the connections for testing proved to be an arduous task. The tee web had to be cleaned thoroughly on both sides prior to fixing the strain gauges. This was made more difficult by the limited access to the two web surfaces. To ease the task, the web surfaces were cleaned before the connections were welded up but despite this, the surfaces had to be thoroughly cleaned again before the gauges could be fixed in their respective positions. This was necessary to remove dirt and weld droplets introduced to these surfaces as a result of weld spatter. It was also not easy to ascertain whether the gauges were fixed in their exact positions. A device was used to ensure this, but it was impossible to cover only the required surfaces with glue.

Consequently the gauges could have been misplaced. The scatter in the experimental results is therefore probably due to this uncertainty. Also, the deviation from the predicted or expected behaviour of the specimen can be ascribed to this uncertainty.

6.4.1 LOAD-DEFLECTION GRAPHS

Figures 3.37, 3.41, 3.45 and 3.49 show the moment-vertical deflection curves for all the four connections tested. It can be seen that all the connections show adequate elastic stiffness at this load. The vertical deflections recorded seem to be purely elastic. There was no evidence of vertical slip from the experiments. Failure was due to the rupture of the butt weld between the tee flange and the column flanges in the beam tension region as a result of the concentrated beam tensile force. It is therefore probable that the vertical deflections recorded are due to the elastic deformation of the connection. The introduction of column stiffeners to any part of the connection did not affect the vertical deflection pattern as was expected (see Figure 3.51).

6.4.2 MOMENT-ROTATION (M-θ) CURVES

The M-θ curves for the four different connections tested are shown in Figures 3.36, 3.40, 3.44 and 3.48, and a comparison of the M-θ curves is shown in figure 3.50. This relationship may be used to assess the rotational capacity of the connection, if the y-axis is taken to represent

perfectly rigid behaviour, the x-axis represents perfectly flexible behaviour and the line x = y represents semi-rigid behaviour. The connection with column stiffeners at both the beam tension and beam compression region was expected to be more rigid than the connection with only one stiffener and the unstiffened connection was expected to be the least rigid of them all. This is expected to have been demonstrated by Figure 3.50 but as can be seen, this is not justified. This deviation from the predicted behaviour would suggest that column stiffening of this type of connection has little effect on the rotational capacity of the connection. It would be interesting to investigate the effect of applying an axial load on a symmetrical connection.

Rotation was small because yielding of the web in both the beam tension region and the beam compression region was restricted by the butt welds between the tee flange and the column flanges; the stiffening action of the structural tee and the impossibility of shear deformation of the column web panel also had the same effect.

6.4.3 STRAIN DISTRIBUTION ALONG THE TEE WEB

The distance-strain graphs for the four connections are shown in Figures 3.35, 3.39, 3.43 and 3.47. In all the cases, the predicted relationship agreed reasonably well with the empirical relationship. For the unstiffened connection, the curve was expected to be symmetrical about the middle of the tee. For this, the strain was expected to increase from its value at 5 mm from the top of the connection to a maximum at 58.8 mm

from the top; it is then expected to decrease steadily to zero at 200 mm from the top of the tee. The remaining half of the graph was expected to be a direct reverse of the first half. This is shown in Figure 3.35. Observation of the connection at failure showed that rotation occured at the beam centre. This rotation was made possible by the combination of yielding of the weld in both the beam tension and compression regions and the concomittant yielding of the column web in these regions. Ideally, the gauges positioned in the middle of the connection should give an average of zero reading but as can be seen from the strain gauge readings in Table (A6), this was not the case. It is however possible that rotation could have occured in the middle with the average strain reading not being zero.

The introduction of a column stiffener to the connection in the beam tension region did not as expected, affect the yielding of the weld initially; but as the weld reached its elastic limit, the force was transmitted to the column web through the connecting tee web. As the column is stiffened in the beam tension region, the column web was unable to deform in this region. Consequently the axis of rotation shifted from the centre to a point just above the middle of the tee web. This situation was reversed when the connection was stiffened in the beam compression region. This phenomenon is demonstrated by Figures 3.39 and 3.43 respectively. Stiffeners in both the beam tension region and the beam compression region only restrict the deformation of the column web in these regions. The axis of rotation of the beam was expected to be the middle of the connection initially. This was the fact discovered from the observation of the yield line pattern on the column web. It is probable

that after the elastic limit of the butt weld in the region of the two flanges had been exceeded, the axis of rotation shifted to the beam compression region and prior to failure, rotation occured at the beam compression region.

The expression for the column web moment of resistance was derived by assuming the yield line pattern shown in Figure 4.12 on the column web at ultimate load. The real yield line pattern was not made up of straight lines as has been assumed. Moreover, the yield line method, an upper bound method, assumes that all deformations are concentrated in the yield lines and neglects elastic deformations. The curve representing the relationship between strain and distance from the top of the tee was developed not by joining all the points on the graph together but by drawing the best curve through the points. It is therefore not surprising that there is a slight discrepancy between the theoretical $\frac{M_{cwp}}{M}$ ratio and the actual $\frac{M_{cwp}}{M}$ ratio. Since the discrepancy is within the acceptable limits under experimental conditions, it is probable that the theoretical expression approximates to the actual behaviour of the connection.

In beam-to-column connection tests, visual examination of the connection at S/D = 0.5 at failure, revealed some evidence of sliding friction. It is therefore important to consider the influence of friction in the analysis of beam-to-column connections. The value of the coefficient of friction normally used for the analysis of beam-to-column connections is 0.45. The coefficient obtained from the author's

experiments was 0.32. The figure of 0.45 was obtained from published results[59] of various tests to determine the coefficient of friction for different steels and different surface preparations and treatment. The establishment of the exact value of this coefficient is important because, as mentioned above, at certain values of S/D ($0 < S/D < 1.0$), vertical slip occurs causing relative movement between the end of the beam and the column flange. In the tests the column flange was not given any special surface treatment prior to assembly and welding of the connection. The coefficient of 0.45 approximates to that for a metallized surface or a grit blast surface which is not the exact description for any of the faying surfaces here. Tests have shown that the coefficient is dependent on the type of steel, surface preparation and treatment. Of the two faying surfaces here, only the beam was given any form of treatment; it was cold sawn and machined to size. The coefficient of 0.32 is therefore the coefficient between the as manufactured surface of the column and the machined end of the beam.

The yield stress of the 152 x 152 x 23 kg universal column section flange was found to be 282.17 N/mm^2 and that of the web 271.13 N/mm^2 as compared with the manufacturers specification of 250 N/mm^2.

The tests to determine the effect of flange flexibility on weld strength was more useful than had been expected. The result of the tests, in conjunction with the results of the weld strength determination tests was used to determine the experimental effective weld length factor of 0.383. Following Elzen and Rolloos, the width of a fully rigid section was taken to be fully effctive. The experimental weld strength of 1.659

KN/mm run cannot be compared with Higgs' figures because the three figures obtained by Higgs were for different sections. The fact that the three figures obtained by Higgs for the three different sections are different would suggest that the weld strength is dependent on the strength of the steel.

Just as the proportion of the applied bending moment resisted by each weld group is important for a proper design of a secondary beam-to-column connection, it is also important to be able to determine the strength of the secondary beam-to-column connection. A calculation of the strength based on the strength of the weld is presented in the Appendix.

CHAPTER 7

DESIGN RECOMMENDATIONS

7.1 INTRODUCTION

In this chapter, recommendations for the design of welded beam-to-column connections are presented. These recommendations are based on the results of the tests carried out by the author, the analysis of the results and the theory.

7.2 BEAM-TO-COLUMN CONNECTION

The fundamental thing in the design of a beam-to-column connection in which the beam is to be welded directly to the column is the establishment of the size of the fillet welds required for the connection. To establish the welds size, it is necessary to first determine the ratio μ M/VD. If the load eccentricity and the maximum shear force the connection is to be subjected to are known, this ratio can easily be obtained.

If the ratio μ M/VD is less than unity, the beam slips relative to the column while rotating about the beam compression flange and the F_y dominant weld failure mode operates. This means that F_y is the dominant force and F_x can be neglected. The next step is to establish whether the

beam flange is flexible or rigid. If the beam flange thickness is less than 12.75 mm and the width is greater than 152 mm it is probably flexible, and consequently the actual lengths of the flange welds have to be reduced to effective lengths. The effective weld length because of the flexibility of the beam flange can be calculated using Equation 4.10. This reduced length may affect the shear properties of the weld group i.e. the length of the weld. If the connection is to be welded all round, the effctive weld length may be calculated using the following formula:

$$L_e = 4B_e + 2d_w$$

where L_e is the effective length of the weld group

B_e is the reduced length of the flange weld

d_w is the depth of the web welds

The ultimate shear strength of the welds is then given by $F_{wy}\ L_e$. If the shear force to which the connection is likely to be subjected to in practice is say F_p then the strength of the weld required for the connection (f_w) will be $\frac{F_p}{L_e}$. The size of the weld for the connection can then be determined using this value of f_w.

If the flange thickness is greater than 12.75 mm and the width is not more than 152 mm the flange is probably rigid and consequently the total length of the flange welds could be taken as fully effective after

subtracting twice the leg length of the weld from each flange weld.

If $1 < \mu M/VD < 1.47$ both F_x and F_y are significant. In this case, the beam slips relative to the column while rotating about the beam compression region. It is necessary in this case, to consider the interaction of both F_x and F_y and the flexibility of both flanges.

If the thickness of any of the flanges is less than 12.75 and the width of any of the flanges is greater then 152 mm., then flexibility has to be taken into consideration. It is necessary therefore to determine the effective length of the flange welds. The worst case is when both the beam and the column flanges are flexible. This case will be treated here.

The effective weld length because of the flexibility of the column flange can be calculated using equation 4.10 i.e. $\ell = L \left(\frac{2\sqrt{2}T^2 f_{fy}}{f_w L} \right)^{\frac{1}{2}}$

This reduced length may affect the bending properties of the weld group i.e. the second moment of area. Consequently, the second moment of area of the effective weld group for unit size of weld about the axis of rotation has to be determined.

The effective weld length because of the flexibility of the beam flange should then be calculated using Equation 4.10 as well. This reduced length affects the shear properties of the weld group i.e. the length of the weld. The total effective length of weld for a unit size of weld has then to be calculated.

The next step is to calculate the value of the distance from the axis of rotation to the resultant force in the weld group by taking moments of forces about the axis of rotation (beam compression region) and equating moment of the whole to the moment of the parts. The Vector addition method should then be used to determine the strength of the weld required. Viz:

$$f_w^2 = f_{wx}^2 + f_{wy}^2$$

$$f_{wx} = \frac{VS}{B_e D}$$

$$f_{wy} = \frac{V(1 - \mu S/D)}{B_e}$$

$$f_w = \frac{V}{B_e} \left[\left(\frac{S}{D} \right)^2 + (1 - \mu S/D)^2 \right]^{\frac{1}{2}}$$

f'_{wx} and f_{wy} could also be obtained using Kamtekar's equation.

If $\mu M/VD > 1.47$ then only F_x is dominant and the F_x dominant weld failure mode operates. In this case the beam rotates about the beam compression region and vertical slip is negligible. This means that F_y can be neglected. The next step is to establish whether the column flange is flexible or rigid. Assuming the column flange is flexible, the actual lengths of the flange welds then have to be reduced to effecttive lengths. The effective length because of the flexibility of the column

flange can be calculated using Equation 4.11. In this case, only the tension welds are the critical welds and the design has to be based more on their total length. If the total effective length of the weld is L_{wt} and the strength of the weld per unit length is f_{wx} then the ultimate strength of the tension welds is $f_{wx}\ L_{wt}$. This must be greater then or equal to the applied bending load i.e.

$$f_{wx}\ L_{wt} = \frac{M}{D}$$

where M is the applied bending moment and D is the depth of the beam

$$f_{wx} > \frac{M}{L_{wt} D}$$

Although it is stated that only the tension welds are the critical welds, the size of the weld obtained from the above expression should be the size of the compression welds as well.

If the connection is such that the column will carry an axial load, then it is necessary to establish the magnitude of the axial load and the slenderness ratio of the column section. If the slenderness ratio is less than sixty and the axial load is less than 24% of the critical crushing load of the column, the column web buckling capacity is unaffected by the axial load and should be ignored. However, if the slenderness ratio is greater than sixty and the axial load is greater than 24% of the critical crushing load of the column, the interaction formula (equation 4.41) should be used to determine the web buckling load for the applied axial load. This should be less than F_x for web buckling not to occur.

7.3 SECONDARY BEAM-TO-COLUMN CONNECTION

The design of the secondary beam-to-column connection should be based on whether it is to resist only shear forces, both shear forces and bending moment or whether it is to act as a moment connection. In addition to this, because the different weld groups forming the connection are not equidistant from the point of application of the applied bending moment, the applied bending moment is not shared equally between these weld groups. The work carried out in this thesis on the secondary beam-to-column connection is however only limited to the determination of the proportion of the applied bending moment transmitted to the weld group connecting the tee web to the column web at a load eccentricity of 512 mm. It was established that at this load eccentricity, just before the attainment of ultimate load, about 40% of the applied moment is resisted by the tee web/column web welds.

The tension welds are the critical welds i.e. failure of the connection will take place if either the fillet weld between the beam and the tee flange in the tension region fails or when the butt weld between the tee flange and the column flanges in the tension region fails.

The tests carried out by the author on the secondary beam-to-column connection did not provide sufficient information for the design of this connection. However, the all welded connections tested by the author proved to be rigid even without stiffeners. Further tests are required to provide information needed for the design of this connection. A design example for this connection is presented in the Appendix.

CHAPTER 8

CONCLUSIONS

The following conclusions are drawn from the experimental results reported in this thesis and the associated theoretical work.

1. The failure criterion for fillet welds of equal leg lengths and subjected to transverse stresses at right angles was of rectangular form as shown in Figure 4.2. The experimental relationship agrees with the theory by Kamtekar [51].

   With regard to the particular beam-to-column connection reported in this thesis.

2. Failure of the weld commenced from the mid point of the length of the connection.

3. The strain distribution in the weld was non uniform and is shown in Figure 4.10.

4. Failure of the weld was accompanied by distortion of either the beam flange or the column flange, or both, depending on the value of S/D.

5. There were three distinct modes of behaviour associated with

failure of the fillet weld:

(a) Failure by shear when F_y is dominant. This occured at $0 = S/D < 0.5$ and was characterized by the distortion of the beam flange.

(b) Failure due to the interaction of F_x and F_y when both forces are equally significant. This occured at $0.5 < S/D < 1.47$ and was characterized by the distortion of both the beam and column flanges.

(c) Failure by tension when F_x was dominant. This occured at $S/D > 1.47$ and was characterised by the distortion of the column flange.

6. The weld failure plane angle varied with S/D.

7. Vertical slip decreased as S/D increased and was difficult to detect at large values of S/D.

8. The longitudinal force in the weld f_x is given by the expression $f_x = \frac{VS}{B_e aD}$ and the transverse force in the weld f_y is given by the expression $f_y = \frac{V(1 - \mu S/D)}{B_e a}$.

9. The effective weld length is a function of the following:

(a) The flange. thickness.

(b) The flange width, but the exact formula to apply in any loading situation depends on:

i. the beam flange width to column flange width ratio,

ii. the ratio S/D.

10. The empirical formulae presented by both Elzen and Rolloos equations are only valid when F_x is dominant.

11. The Vector addition method of ultimate load prediction for welds is conservative.

With regard to the column web buckling tests:

12. When the axial load is less than 24% of the critical crushing load, it has little effect on the web buckling capacity of the column for a universal column with a slenderness ratio of about sixty.

13. An axial load of between 24% and 94% of the critical crushing load lowers the web buckling capacity of the column.

14. The interaction relationship between the column axial load and web buckling load is:

$$\left[\frac{W - S_b\ t\ f_b}{2Tf_{fy}(Btf_b)^{\frac{1}{2}}}\right]^2 + \frac{1}{f_{fy}^2}\left[\frac{P}{A} + \frac{P_e}{Z}\right]^2 = 1$$

With regard to the particular secondary beam-to-column connection reported in this thesis.

15. The connection was rigid even without column stiffeners.

16. Welds in tension were the critical welds and always failed first.

17. The yield line mechanism assumed to form in the web of the column was not fully developed because of the resistance to rotation offered by the butt welds between the tee flange and the column flanges.

18. Just before the attainment of ultimate load, 40% of the applied bending moment was transmitted to the column web/tee web weld through the tee web.

19. Column stiffeners have little effect on the rigidity and ultimate capacity of the connection.

CHAPTER 9

SUGGESTIONS FOR FURTHER WORK

1. As indicated in Chapter 5 and 6, the results for the failure criterion for fillet welds were not expected. Although the experimental results agreed with Kamtekar's theory, further experimental confirmation is required.

2. Further work is required to improve the accuracy of the theoretical expression for the effective weld length. The work should involve tests in which both the flange thickness and the flange width are varied so as to obtain an empirical relationship between the effective weld length and the flange width and thickness.

3. The theory and experimental results presented in this thesis are for beam-to-column connections in which both the beam and the column flanges have equal width. In practical situations, the column flange is often wider than the beam flange and the beam is often much deeper than the column. Tests should be carried out to establish the effective weld length and weld failure mode of such a connection.

4. Tests should be carried out on main beam-to-column connections with weld on both flanges.

5. Tests should be carried out on main beam-to-column connections with web welds only.

6. Tests should be carried out on beam-to-column connections with both flange and web welds.

7. Tests should be carried out to establish the effect of varying the weld sizes.

8. The tests on the secondary beam-to-column connection described in this thesis were carried out at a fixed eccentricity of load. Further work is required with varying eccentricity of load.

9. Further tests should be carried out on secondary beam-to-column connections of varying sizes.

10. As indicated in Chapter 6, there was uncertainty as regards the fixing of the strain gauges in their proper positions due to the limited access to the web surfaces and the lack of an accurate locating device. Confirmation of the results needs to be made by carrying out further tests using more accurate means of locating the strain gauges.

11. Tests should be carried out to determine the strength of the weld connecting the structural tee to the column.

APPENDICES

APPENDIX 1 TEST READINGS

Table A1 S/D = 0.5 (1) Dial gauge readings

Load (Tons)	Vertical Slip (mm)	Horizontal Deflection (mm)	
		Left Weld	Right Weld
0	0	0	0
1.0	0.65	0.04	0.13
2.0	1.11	0.02	0.17
3.0	1.45	0.02	0.18
4.0	1.75	0.06	0.20
5.0	2.03	0.08	0.22
5.5	2.14	0.08	0.23
6.0	2.25	0.09	0.23
6.5	2.36	0.10	0.24
7.0	2.47	0.11	0.25
7.5	2.58	0.11	0.25
8.0	2.68	0.11	0.26
8.5	2.76	0.12	0.26
9.0	2.86	0.12	0.27
9.5	2.93	0.12	0.27
10.0	3.01	0.13	0.27
10.5	3.11	0.13	0.27
11.0	3.18	0.14	0.27
11.5	3.30	0.14	0.27
12.0	3.38	0.15	0.27
12.5	3.45	0.16	0.28
13.0	3.54	0.17	0.29

Table A1 continued

13.5	3.64	0.17	0.29
14.0	3.72	0.18	0.29
14.5	3.82	0.18	0.29
15.0	3.92	0.19	0.30
15.5	4.02	0.19	0.30
16.0	4.12	0.20	0.30
16.5	4.24	0.21	0.30
17.0	4.32	0.21	0.30
17.5	4.47	0.22	0.30
18.0	4.58	0.22	0.30
18.5	4.73	0.22	0.31
19.0	4.84	0.23	0.31
19.5	5.01	0.23	0.31
20.0	5.12	0.23	0.31
20.5	5.30	0.24	0.31
21.0	5.46	0.24	0.31
21.5	5.58	0.24	0.31
22.0	5.77	0.24	0.32
22.5	5.94	0.24	0.32
23.0	6.08	0.25	0.32

Table A3 S/D = 2.0 (1) Dial gauge readings

Load (Tons)	Vertical Slip (mm)		Horizontal Movement (mm)	
	Right	Left	Right	Left
1.0	0.32	0.09	0.09	0.06
2.0	0.43	0.15	0.12	0.07
3.0	0.52	0.21	0.13	0.08
4.0	0.60	0.29	0.15	0.09
5.0	0.65	0.34	0.15	0.10
6.0	0.70	0.38	0.16	0.10
7.0	0.75	0.42	0.17	0.10
8.0	0.80	0.45	0.17	0.11
9.0	0.85	0.48	0.18	0.11
10.0	0.92	0.52	0.18	0.10
10.5	0.98	0.55	0.18	0.10
11.0	1.01	0.57	0.19	0.10
11.5	1.07	0.61	0.19	0.09
12.0	1.15	0.66	0.19	0.08
12.5	1.25	0.71	0.18	0.07

Table A4 S/D = 3.0 1 Dial gauge readings

Load (Tons)	Vertical Slip (mm)		Horizontal Movement (mm)	
	Left	Right	Left	Right
0.5	0.12	0.13	0.01	0.05
1.0	0.26	0.22	0.06	0.05
2.0	0.39	0.31	0.08	0.05
3.0	0.47	0.40	0.09	0.05
4.0	0.53	0.46	0.09	0.05
5.0	0.58	0.53	0.09	0.05
6.0	0.63	0.60	0.08	0.04
6.5	0.66	0.64	0.07	0.02
7.0	0.70	0.71	0.06	0.05

Table A5 S/D = 4.0 Dial gauge readings

Load (Tons)	Vertical Slip (mm)		Horizontal Movement (mm)	
	Right	Left	Right	Left
0.182	0.02	0.06	0.008	0
0.227	0.04	0.09	0.011	0
0.273	0.05	0.12	0.013	0
0.318	0.05	0.15	0.014	0
0.364	0.06	0.18	0.016	0
0.409	0.06	0.21	0.016	0
0.455	0.07	0.23	0.017	0
0.500	0.07	0.26	0.018	0
0.545	0.08	0.28	0.019	0
0.591	0.08	0.30	0.020	0
0.636	0.09	0.31	0.020	0
0.682	0.09	0.32	0.021	0
0.727	0.09	0.33	0.022	0
0.818	0.095	0.35	0.022	0
0.909	0.10	0.36	0.024	0
1.000	0.11	0.37	0.025	0
1.091	0.11	0.38	0.026	0
1.182	0.12	0.39	0.028	0
1.273	0.12	0.39	0.029	0
1.364	0.13	0.40	0.030	0
1.455	0.13	0.40	0.031	0

Table A5 continued

1.545	0.14	0.41	0.032	0
1.727	0.14	0.42	0.035	0
1.818	0.15	0.42	0.036	0
1.909	0.15	0.43	0.038	0
2.000	0.16	0.43	0.040	0
2.091	0.16	0.44	0.040	0
2.182	0.17	0.44	0.042	0
2.273	0.17	0.44	0.043	0
2.364	0.17	0.45	0.044	0
2.455	0.18	0.45	0.045	0
2.545	0.18	0.45	0.046	0
2.636	0.19	0.46	0.048	0
2.727	0.19	0.46	0.049	0
2.818	0.19	0.46	0.050	0
2.909	0.20	0.47	0.050	0
3.000	0.20	0.47	0.054	0
3.091	0.20	0.47	0.052	0
3.182	0.21	0.47	0.054	0
3.273	0.21	0.48	0.048	0
3.364	0.21	0.48	0.050	0
3.455	0.22	0.48	0.056	0
3.545	0.22	0.49	0.057	0
3.636	0.22	0.49	0.054	0
3.727	0.22	0.50	0.054	0
3.818	0.23	0.50	0.054	0

Table A5 continued

3.909	0.23	0.50	0.054	0
4.000	0.23	0.50	0.054	0
4.091	0.24	0.51	0.054	0
4.182	0.24	0.51	0.054	0
4.273	0.25	0.51	0.054	0
4.364	0.25	0.51	0.0530	0
4.455	0.25	0.52	0.053	0
4.545	0.26	0.53	0.055	0
4.636	0.27	0.58	0.073	0
4.727	0.27	0.58	0.074	0
4.818	0.28	0.59	0.074	0
4.909	0.28	0.59	0.073	0
5.00	0.29	0.60	0.072	0
5.091	0.30	0.61	0.070	0
5.182	0.31	0.61	0.069	0
5.273	0.32	0.62	0.065	0
5.364	0.33	0.63	0.062	0
5.455	0.34	0.64	0.059	0
5.545	0.35	0.65	0.059	0
5.636	0.36	0.65	0.057	0
5.727	0.38	0.66	0.051	0
5.818	0.39	0.67	0.043	0

Table A6 Strain gauge readings column test 1

Channel / Load (Tons)	Strains (Microstrain)							
	1	2	3	4	5	6	7	8
2	-67.0	-87.8	-87.8	-114.6	62.8	60.1	42.8	33.7
4	-90.9	-106.9	-116.2	-158.4	59.2	41.3	35.8	-8.2
6	-109.8	-135.3	-158.9	-213.2	41.6	37.2	-5.0	-50.7
8	-106.4	-136.3	-177.4	-244.3	38.9	20.3	-7.7	-87.3
10	-128.9	-155.8	-217.8	-299.6	38.9	13.6	-45.6	-131.3
12	-133.2	-195.8	-306.4	-346.4	41.6	0.6	-115.3	-284.5
14	-175.0	-265.8	-622.1	-1266.0	32.9	-70.6	-260.8	-856.7
16	-200.7	-414.0	-1219.3	-2376.7	13.1	-87.3	-645.8	-1772.4
18	-259.9	-882.8	-2006.8	-3800.0	-23.2	-262.5	-1668.4	-3325.2
20	-370.6	-1240.3	-2740.0	-4966.7	-48.6	-705.0	-2329.0	-4052.3
22	-620.6	-1859.8	-3437.5	-6460.4	-217.3	-1195.9	-2736.2	-4661.9

Table A7 Strain gauge readings for AXIAL = 2 TONS COLUMN TEST

Load (Tons) \ Channel	Strains (Microstrain)									
	1	2	3	4	5	6	7	8	9	10
1	-40.0	-40.0	-13.0	-27.0	-32.9	-36.0	-25.0	-24.0	25.0	-0.9
2	-70.0	-0.9	17.0	-57.9	-56.9	9.0	15.0	-54.9	-37.0	-61.9
3	-97.0	29.0	46.0	-87.0	-69.0	34.0	49.9	-77.0	-160.0	-105.0
4	-124.0	69.0	60.9	-97.0	-99.9	86.0	76.0	-93.0	-331.0	-258.9
5	-145.0	93.0	74.0	-102.0	-119.0	112.0	86.0	-98.9	-479.9	-434.9
6	-164.0	117.0	91.0	-111.0	-130.0	137.0	105.0	-106	-628.9	-730.9
7	-185.0	151.0	119.0	-126.0	-142.0	161.0	123.0	-5857.9	-730.9	-856.9
8	-209.0	187.0	151.0	-145.0	-156.0	189.0	148.0	-134.0	-786.9	-996.9
9	-224.0	252.0	209.0	-177.0	-177.0	238.0	192.0	-156.0	-850.9	-1114.0
10	-279.0	321.0	274.0	-213.0	-195.0	291.0	243.0	-176.0	-972.9	-1177.0
11	-330.0	402.9	358.0	-258.9	-219.0	351.0	301.0	-200.0	-1097.0	-1161.0
12	-408.9	536.9	520.9	-348.0	-262.9	458.9	407.9	-241.0	-1548.0	-1195.0
13	-453.9	714.0	824.9	-496.9	-316.0	640.9	594.9	-288.0	-4681.0	-1670.0
14	-499.9	936.9	1326.0	-818.9	-377.0	843.9	871.9	-392.9	-3021.0	-14548.0

Table A8 Strain gauge readings FOR AXIAL LOAD = 40 TONS COLUMN TEST

Load (Tons) / Channel	Strains (Microstrain)								
	2	4	6	8	10	12	14	16	18
1	134.2	-276.7	-678.3	-1087.5	-1565.8	-1965.8	-2220.0	-2131.7	-2612.5
2	122.5	-261.7	-480.0	-924.2	-1106.7	-1557.5	-1936.7	-2387.5	-2600.0
3	-682.5	-690.8	-690.0	-680.0	-680.8	-686.7	-695.8	-714.2	-645.8
4	-271.7	-253.3	-245.0	-234.2	-229.2	-218.3	-205.8	-298.3	-270.8
5	-1579.2	-1713.3	-1741.7	-1793.3	-1971.7	-1933.3	-2010.8	-2210.8	-2211.7
6	-668.3	-653.3	-644.2	-520.8	-513.3	-490.8	-451.7	-493.3	-251.7
7	-698.3	-694.2	-695.0	-682.5	-679.2	-671.7	-657.5	-517.5	-445.0
8	-515.8	-520.0	-515.0	-500.0	-500.0	-500.8	-510.0	-639.2	-699.2
9	-439.2	-440.0	-438.3	-307.5	-300.0	-283.3	-269.2	-241.7	-309.2
10	-436.7	-440.8	-437.5	-424.2	-422.5	-421.7	-425.8	-435.8	-465.0
11	-482.5	-682.5	-715.0	-728.3	-648.3	-700.0	-870.0	-848.0	-1087.5
12	-445.8	-231.7	-286.7	-235.0	-83.3	50.0	4.2	154.2	395.8
13	-486.7	-456.7	-288.3	-225.8	-273.3	-52.5	-13.3	169.2	391.7
14	-640.8	-864.2	-899.2	-914.2	-943.3	-889.2	-930.0	-947.5	-941.7
15	-675.0	-711.7	-735.8	-850.8	-870.8	-914.2	-857.5	-904.2	-927.5
16	-664.2	-495.8	-446.7	-498.3	-450.8	-250.8	-244.2	-88.3	199.2

Table A9 Test results for Axial Load = 60 tons - Column Test

Load (Tons) / Channel	2	4	6	8	10	12	14
1	-26.1	-52.3	-91.1	-135.9	-178.3	-234.8	-414.2
2	-26.6	-47.6	-89.6	-109.3	-137.8	-180.4	-136.6
3	-1.3	-1.8	-2.3	-3.7	-4.8	-7.5	0.2
4	12.8	14.0	14.8	16.3	18.5	11.7	34.1
5	13.2	12.9	13.3	12.2	0	-6.2	-20.7
6	-1.3	-1.1	-0.4	12.0	14.0	17.6	12.6
7	0.7	12.3	13.3	14.7	17.6	12.5	36.3
8	0	-0.2	-0.4	-0.4	-1.8	-6.2	-4.1
9	12.3	13.8	15.2	16.4	18.8	21.9	17.0
10	-0.6	-0.4	0	0.5	-0.8	0	0
11	-9.7	-2.9	-4.8	-6.4	-7.6	-20.7	-20.8
12	0	0	0	0	0	0	0
13	15.8	33.8	38.4	42.7	36.4	41.4	40.3
14	-0.3	-5.0	-7.4	-9.0	-8.8	-7.8	-7.1
15	-4.7	-6.7	-7.9	-8.8	-20.8	-9.9	-9.3
16	-3.6	0	13.8	18.6	14.1	33.0	37.9

Table A10 Test results for Axial Load = 80 tons Column Tests

Load (Tons) / Channel	2	4	6	8
1	-3.4	-65.9	-131.4	-171.6
2	17.6	-47.0	-94.0	-174.1
3	-240.2	-234.6	-238.1	-255.3
4	-127.9	-113.9	-112.5	-110.1
5	-556.2	-577.0	-620.2	-645.9
6	-472.3	-471.8	-491.9	-494.0
7	-328.3	-327.2	-344.1	-350.8
8	-414.0	-493.3	-537.5	-622.3
9	-192.8	-176.3	-173.3	-179.2
10	-153.9	-154.8	-156.8	-173.1
11	-195.0	-179.7	-178.7	-195.8
12	-222.2	-217.7	-219.3	-212.8
13	2712.8	2712.7	2712.6	2712.4
14	-557.2	-563.1	-580.2	-579.5
15	-345.6	-345.7	-345.9	-355.8
16	-393.8	-407.2	-410.0	-406.6

Table A11 Test results for CONNECTION WITH NO STIFFENER - SECONDARY BEAM-TO-COLUMN CONNECTION

Moment KNmm	Rotation (Degrees)		Vertical Slip (mm)
	θ_1	θ_2	
5103.1	0.0115	0	0.03
10206.2	0.0286	0	0.06
15309.3	0.0401	0.0344	0.10
20412.4	0.0573	0.0630	0.15
25515.5	0.0745	0.120	0.21
30618.6	0.097	0.229	0.26
35721.7	0.120	0.367	0.33
40824.8	0.046*	0.756*	0.24*
45927.9	0.086	1.020	0.31
51031.0	0.132	1.329	0.06
56134.1	0.149	1.558	-0.86
61237.2	0.252	2.130	-0.53

* Specimen slipped from the support

Table A12 Rotation and Vertical slip results for connection B tests - Secondary beam-to-column connection

Moment (KNmm)	Rotation θ (Degrees)	Vertical Slip
5103.1	0.023	0
10206.2	0.046	0.01
15309.3	0.069	0.01
20412.4	0.097	0.16
25515.5	0.120	0.16
30618.6	0.149	0.21
35721.7	0.178	0.31
40824.8	0.212	0.45
45927.9	0.252	0.64
51031.0	0.298	1.04
56134.1	0.355	1.67
61237.2	0.940	2.89
66340.4	0.968	3.33
71443.5	1.008	4.00
76546.6	1.180	4.36
81649.7	1.798	4.95

Table A13 Rotation and Vertical slip results for Connection C tests - Secondary beam-to-column connection

Moment (KNmm)	Rotation θ (Degrees)	Vertical Slip mm
5103.1	0	0.06
10206.2	0	0.14
15309.3	0.006	0.22
20412.4	0.023	0.25
25515.5	0.040	0.33
30618.6	0.057	0.44
35721.7	0.309	0.81
40824.8	0.327	1.28
45927.9	0.349	1.81
51031.0	0.384	2.26
56134.1	0.418	2.57
61237.2	0.476	2.98

Table A14 Rotation and Vertical slip for connection D tests

Moment (KNmm)	Rotation (Degrees)		Vertical Slip (mm)
	θ_1	θ_2	
5103.1	0.029	0.040	0.02
10206.2	0.057	0.086	0.03
15309.3	0.080	0.132	0.11
20412.4	0.103	0.189	0.26
25515.5	0.132	0.246	0.43
30618.6	0.155	0.298	0.61
35721.7	0.189	0.361	0.85
40824.8	0.218	0.435	1.18
45927.9	0.252	0.516	1.63
51031.0	0.286	0.583	2.04
56134.1	0.332	0.716	2.41
61237.2	0.905	1.020	2.36
66340.4	0.957	1.134	2.65
71443.5	1.798	2.702	2.8

DIAL GAUGE READINGS

Table (A15) Secondary Beam-to-Column Connection (2)

Load (Tons)	Deflection (mm) Vertical		Deflection (mm) Horizontal	
	At the Top	At the Bottom	At the Top	At the Bottom
1.0	0.192	0.18	0.022	1.43
2.0	0.214	0.18	0.112	1.87
3.0	0.224	0.18	0.222	2.29
4.0	0.234	0.18	0.358	2.49
5.0	0.244	0.18	0.500	2.75
6.0	0.254	0.18	0.650	2.98
7.0	0.264	0.18	0.774	3.17
8.0	0.276	0.18	0.912	3.30
9.0	0.294	0.18	1.062	3.32
10.0	0.314	0.16	1.184	2.13
11.0	0.340	0.07	1.310	2.47
12.0	0.384	0.29	1.552	1.66
13.0	0.074	0.52	1.984	1.07
14.0	0.400	0.73	3.174	

Table (A16) Strain and dial guage reading for test series A-3 - Secondary beam-to-column connection

Load (Tons)	Strains (μ Strains)				Dial Gauge Readings (mm)		
	Gauge 1	Gauge 2	Gauge 3	Gauge 4	Horizontal Deflection	Vertical Slip (Top)	Vertical Slip (Bottom)
1.0	30.0	75.0	20.0	10.0	0.004	0.02	0
2.0	50.0	95.0	0	55.0	0.014	0.06	0
3.0	85.0	125.0	30.0	95.0	-	0.09	0
4.0	110.0	145.0	70.0	150.0	0.012	0.13	0.13
5.0	130.0	190.0	115.0	210.0	0.026	0.16	0.24
6.0	150.0	235.0	160.0	285.0	0.044	0.23	0.39
7.0	170.0	285.0	185.0	365.0	0.060	0.29	0.58
8.0	200.0	360.0	300.0	495.0	0.078	0.37	1.00
9.0	230.0	430.0	340.0	620.0	0.098	0.48	1.69
10.0	270.0	510.0	405.0	740.0	0.116	0.59	2.31
11.0	300.0	610.0	475.0	835.0	0.140	0.73	3.07
12.0	345.0	735.0	580.0	945.0	0.146	0.86	3.46
13.0	410.0	880.0	670.0	1070.0	0.186	1.06	3.38
14.0	475.0	1025.0	720.0	1205.0	0.238	1.29	2.26

Figure (A17) Strain and dial guage readings for test series C-1 - Secondary beam-to-column connection

Load (Tons)	Strain Gauge Readings (μ Strains)				Dial Gauge Readings (mm)		
	Channel 1	Channel 2	Channel 3	Channel 4	Top Horizontal	Bottom Horizontal	Vertical Slip
1.0	30.0	45.0	-55.0	-45.0	0.03	0.06	0.07
2.0	70.0	75.0	-135.0	-105.0	0.05	0.13	0.16
3.0	90.0	115.0	-215.0	-185.0	0.08	0.25	0.30
4.0	110.0	145.0	-295.0	-255.0	0.10	0.31	0.38
5.0	130.0	195.0	-385.0	-345.0	0.13	0.40	0.55
6.0	150.0	235.0	-485.0	-435.0	0.16	0.50	0.80
7.0	165.0	295.0	-595.0	-495.0	0.20	0.58	1.10
8.0	190.0	360.0	-705.0	-525.0	0.24	0.68	1.63
9.0	215.0	435.0	-535.0	-590.0	0.29	0.80	2.33
10.0	260.0	535.0	-995.0	-605.0	0.33	0.93	2.93
11.0	295.0	675.0	-1245.0	-1175.0	0.40	1.09	3.34
12.0	320.0	825.0	-1555.0	-1505.0	0.51	1.26	3.64
13.0	355.0	1005.0	-1935.0	-2330.0	0.61	1.47	3.88
14.0	410.0	1255.0	-3035.0	-4065.0	0.74	1.76	4.13
15.0	500.0	1475.0	-3965.0	-7360.0	0.94	2.17	4.42

Figure (A18) Strain and dial guage readings for test series C-2 - Secondary beam-to-column connection

Distance from top of Tee (mm) / Load (Tons)	Strain											Dial Gauge Readings (mm)		
	8.0	22.0	7.0	135.0	152.0	200.0	217.0	265.0	330.0	393.0	395.0	Top Horizontal	Bottom Horizontal	Vertical Slip
1.0	20.0	5.0	15.0	10.0	50.0	25.0	50.0	-5.0	-40.0	-20.0	-95.0	0.002	0	0
2.0	85.0	20.0	35.0	20.0	105.0	45.0	105.0	-20.0	-25.0	-110.0	-225.0	0.01	0.012	0.08
3.0	100.0	30.0	65.0	30.0	160.0	55.0	145.0	-35.0	-40.0	-210.0	-360.0	0.016	0.022	0.16
4.0	120.0	50.0	95.0	40.0	225.0	75.0	200.0	-55.0	-85.0	-330.0	-545.0	0.028	0.040	0.23
5.0	150.0	55.0	125.0	55.0	275.0	85.0	235.0	-80.0	-110.0	-450.0	-705.0	0.036	0.060	0.27
6.0	160.0	75.0	155.0	70.0	335.0	105.0	265.0	-90.0	-150.0	-575.0	-865.0	0.042	0.078	0.35
7.0	160.0	95.0	185.0	90.0	390.0	115.0	260.0	-70.0	-185.0	-695.0	-1035.0	0.048	0.10	0.47
8.0	155.0	130.0	210.0	105.0	465.0	125.0	255.0	-60.0	-240.0	-830.0	-1240.0	0.058	0.124	0.61
9.0	150.0	155.0	245.0	130.0	535.0	135.0	240.0	-20.0	-290.0	-960.0	-1450.0	0.068	0.146	0.77
10.0	150.0	210.0	290.0	160.0	645.0	145.0	235.0	5.0	-330.0	-1120.0	-1705.0	0.078	0.178	0.99
11.0	40.0	370.0	345.0	175.0	900.0	-15.0	835.0	260.0	-585.0	-1230.0	-1985.0	0.102	0.194	1.22
12.0	-50.0	560.0	425.0	175.0	1215.0	100.0	2335.0	595.0	-1270.0	-1260.0	-2280.0	0.140	0.200	1.54

Table (A19) Strain and dial guage readings for test series D - Secondary beam-to-column connection

Load (Tons) \ Distance from top of Tee (mm)	Strain (μ strains)														Dial gauge readings		
	9.0	25.0	75.0	120.0	140.0	180.0	205.0	240.0	270.0	300.0	335.0	360.0	379.0	392.0	Top Horizontal	Bottom Horizontal	Vertical Slip
1.0	75.0	65.0	65.0	-10.0	10.0	290.0	15.0	-20.0	-10.0	-10.0	-75.0	0	-70.0	-100.0	0.01	0.014	0.02
2.0	155.0	150.0	140.0	-20.0	30.0	320.0	25.0	-25.0	-10.0	0	-160.0	30.0	-130.0	-235.0	0.02	0.030	0.06
3.0	220.0	230.0	200.0	-10.0	40.0	360.0	45.0	-15.0	15.0	50.0	-230.0	45.0	-210.0	-400.0	0.028	0.046	0.11
4.0	285.0	295.0	250.0	-10.0	50.0	270.0	45.0	-30.0	10.0	75.0	-290.0	60.0	-265.0	-520.0	0.036	0.066	0.26
5.0	340.0	375.0	320.0	-20.0	70.0	315.0	50.0	-25.0	110.0	105.0	-390.0	80.0	-310.0	-650.0	0.046	0.086	0.43
6.0	380.0	480.0	375.0	-20.0	80.0	395.0	50.0	0	190.0	140.0	-490.0	95.0	-365.0	-790.0	0.054	0.104	0.61
7.0	355.0	570.0	410.0	0	80.0	300.0	45.0	0	310.0	170.0	-560.0	80.0	-470.0	-1000.0	0.066	0.126	0.85
8.0	345.0	675.0	440.0	20.0	80.0	370.0	15.0	-30.0	350.0	210.0	-630.0	70.0	-520.0	-1360.0	0.076	0.152	1.18
9.0	305.0	760.0	470.0	35.0	80.0	370.0	-25.0	-60.0	400.0	230.0	-740.0	40.0	-535.0	-1770.0	0.088	0.180	1.63
10.0	295.0	820.0	510.0	60.0	80.0	275.0	-75.0	-60.0	490.0	250.0	-840.0	20.0	-460.0	-2190.0	0.10	0.204	2.04
11.0	265.0	915.0	580.0	80.0	80.0	210.0	-145.0	-20.0	560.0	265.0	-1040.0	5.0	-450.0	-2645.0	0.116	0.250	2.41
12.0	175.0	1030.0	560.0	150.0	70.0	615.0	-220.0	0	600.0	260.0	-1510.0	-60.0	-590.0	-2910.0	0.316	0.356	2.36
13.0	105.0	1260.0	620.0	230.0	40.0	680.0	-465.0	165.0	630.0	275.0	-2490.0	-25.0	-995.0	-3405.0	0.334	0.396	2.65
14.0	690.0	4080.0	820.0	515.0	-60.0	880.0	-405.0	750.0	485.0	420.0	-3990.0	145.0	-1845.0	-5270.0	0.628	0.944	2.80

Figure (A20) Strain and dial guage readings for test series A-4 - Secondary beam-to-column connection

Distance from Top of Tee (mm) / Load (Tons)	Strain (μ Strains)							Dial Gauge Readings (mm)		
	5.0	70.0	135.0	200.0	265.0	330.0	395.0	Top Horizontal	Bottom Horizontal	Vertical Slip
1.0	-80.0	-30.0	-75.0	-75.0	-67.5	-120.0	-102.5	0.004	0	0.03
2.0	-100.0	10.0	-82.5	-82.5	-82.5	-165.0	-170.0	0.010	0	0.06
3.0	-105.0	65.0	-80.0	-80.0	-87.5	-195.0	-185.0	0.014	0.012	0.10
4.0	-95.0	105.0	-62.5	-80.0	-90.0	-220.0	-142.5	0.020	0.022	0.15
5.0	-85.0	135.0	-55.0	-77.5	-102.5	-240.0	-172.5	0.026	0.042	0.21
6.0	-65.0	175.0	-37.5	-10.0	-125.0	-240.0	-222.5	0.026	0.080	0.26
7.0	-45.0	210.0	-22.5	-12.5	-135.0	-252.5	-295.0	0.034	0.128	0.33
8.0	-15.0	245.0	-5.0	-95.0	-30.0	-307.5	-272.5	0.016	0.264	0.24
9.0	10.0	315.0	7.5	82.5	-7.5	-380.0	-360.0	0.030	0.356	0.31
10.0	40.0	395.0	17.5	95.0	-75.0	-482.5	-395.0	0.046	0.464	0.06
11.0	160.0	460.0	27.5	0	-172.5	-577.5	-557.5	0.052	0.544	0.86
12.0	230.0	550.0	15.0	85.0	-232.5	-637.5	-642.5	0.088	0.744	0.53
13.0	255.0	675.0	-155.0	147.5	-420.0	-762.5	-717.5	0.526	0.748	0.36

Figure (A21) Strain and dial guage readings for test series B-1 - Secondary beam-to-column connection

Load (Tons) \ Channel	Strain (μ Strains)														Dial gauge Readings		
	1	2	3	4	5	6	7	8	9	10	11	12	13	14	Top Horizontal	Bottom Horizontal	Vertical Slip
1.0	-35.0	-45.0	5.0	10.0	-15.0	5.0	-5.0	-30.0	-5.0	-60.0	-30.0	-50.0	-5.0	-160.0	0.008	0.006	0.01
2.0	-75.0	-95.0	10.0	10.0	-5.0	20.0	55.0	-30.0	55.0	-45.0	-25.0	-55.0	-155.0	-280.0	0.018	0.014	0.11
3.0	-120.0	-145.0	5.0	10.0	55.0	70.0	190.0	-5.0	220.0	80.0	25.0	185.0	-115.0	-385.0	0.028	0.024	0.20
4.0	-125.0	-150.0	50.0	60.0	40.0	75.0	225.0	-30.0	290.0	85.0	30.0	-30.0	-175.0	-555.0	0.038	0.034	0.29
5.0	-180.0	-220.0	120.0	50.0	35.0	90.0	275.0	-50.0	385.0	105.0	15.0	-50.0	-245.0	-770.0	0.050	0.048	0.39
6.0	-305.0	-320.0	130.0	-5.0	-30.0	85.0	230.0	-25.0	355.0	15.0	-35.0	-75.0	-345.0	-845.0	0.132	0.048	1.23
7.0	-365.0	-340.0	170.0	-15.0	-35.0	125.0	270.0	0	465.0	25.0	-45.0	-10.0	-420.0	-1045.0	0.146	0.064	1.45
8.0	-470.0	-355.0	210.0	10.0	-40.0	165.0	275.0	55.0	565.0	25.0	-30.0	5.0	-440.0	-1140.0	0.162	0.082	1.77
9.0	-570.0	-335.0	265.0	15.0	-45.0	210.0	310.0	85.0	685.0	20.0	-30.0	-5.0	-480.0	-1240.0	0.182	0.098	2.21
10.0	-735.0	-385.0	310.0	-25.0	-55.0	265.0	345.0	255.0	795.0	10.0	-60.0	35.0	-415.0	-1080.0	0.282	0.212	0.03
11.0	-875.0	-450.0	355.0	-50.0	-70.0	325.0	515.0	325.0	950.0	10.0	-105.0	100.0	-400.0	-1010.0	0.306	0.236	0.32
12.0	-1075.0	-490.0	585.0	-110.0	-100.0	395.0	840.0	340.0	1170.0	-5.0	-230.0	145.0	-380.0	-915.0	0.338	0.270	0.75
13.0	-1240.0	-635.0	430.0	-125.0	-140.0	515.0	1635.0	410.0	1560.0	-70.0	-190.0	220.0	-580.0	-870.0	0.372	0.318	1.26

Figure (A22) Strain and dial guage reasings for test series C-3 - Secondary beam-to-column connection

Load (Tons) \ Channel	Strain (μ Strains)														Dial Gauge Readings		
	1	2	3	4	5	6	7	8	9	10	11	12	13	14	Top Horizontal	Bottom Horizontal	Vertical Slip
1.0	15.0	45.0	15.0	0	-10.0	85.0	-225.0	-135.0	-45.0	25.0	5.0	-10.0	0	0	0	0	0.06
2.0	40.0	40.0	25.0	5.0	-10.0	+155.0	-485.0	-310.0	-180.0	-45.0	-55.0	-105.0	-100.0	-105.0	0	0.032	0.14
3.0	-10.0	105.0	-5.0	-85.0	-120.0	-255.0	-695.0	-445.0	-225.0	-20.0	-50.0	-110.0	-105.0	-100.0	0.002	0.050	0.22
4.0	20.0	135.0	10.0	-115.0	-100.0	-330.0	-840.0	-555.0	-275.0	5.0	-45.0	-95.0	-70.0	-70.0	0.008	0.066	0.25
5.0	35.0	165.0	15.0	-70.0	305.0	-400.0	-950.0	-675.0	-340.0	170.0	-50.0	-90.0	-35.0	-40.0	0.014	0.084	0.33
6.0	65.0	195.0	25.0	-65.0	485.0	-485.0	-1060.0	-815.0	-415.0	275.0	-50.0	-80.0	5.0	-5.0	0.020	0.102	0.44
7.0	100.0	235.0	35.0	-60.0	880.0	-640.0	-1215.0	-1030.0	-555.0	430.0	-35.0	-55.0	60.0	25.0	0.108		0.81
8.0	125.0	285.0	40.0	-65.0	1225.0	-760.0	-1365.0	-1155.0	-660.0	540.0	-20.0	-30.0	135.0	85.0	0.114	0.122	1.28
9.0	180.0	345.0	50.0	-60.0	1555.0	-905.0	-1485.0	-1315.0	-815.0	580.0	-25.0	-15.0	190.0	130.0	0.122	0.144	1.81
10.0	235.0	405.0	60.0	-70.0	1870.0	-1025.0	-1610.0	-1475.0	-980.0	625.0	-40.0	-10.0	260.0	185.0	0.134	0.170	2.26
11.0	305.0	490.0	70.0	-80.0	2185.0	-1170.0	-1760.0	-1585.0	-1140.0	675.0	-45.0	5.0	335.0	255.0	0.146	0.198	2.57
12.0	480.0	680.0	105.0	145.0	2340.0	-1240.0	-1885.0	-1670.0	-1235.0	1360.0	-85.0	-10.0	400.0	290.0	0.166	0.24	2.98

Figure (A23) Strain and dial guage readings for test series B-2 - Secondary beam-to-column connection

Channel / Load (Tons)	Strain (μ Strains)												Dial Gauge Reading		
	1	2	3	4	5	6	7	8	11	12	13	14	Top Horizontal	Bottom Horizontal	Vertical Slip
1.0	60.0	95.0	75.0	90.0	65.0	15.0	55.0	175.0	70.0	5.0	-40.0	30.0	0.008	0.006	0
2.0	60.0	140.0	75.0	90.0	55.0	-35.0	50.0	245.0	60.0	-30.0	-110.0	-35.0	0.016	0.024	0.01
3.0	50.0	190.0	80.0	90.0	50.0	-80.0	45.0	325.0	55.0	-45.0	-160.0	-65.0	0.024	0.016	0.01
4.0	50.0	245.0	85.0	95.0	35.0	-125.0	45.0	420.0	60.0	-90.0	-235.0	-110.0	0.034	0.028	0.16
5.0	50.0	295.0	85.0	90.0	20.0	-180.0	35.0	435.0	65.0	-90.0	-260.0	-120.0	0.042	0.038	0.16
6.0	45.0	355.0	85.0	85.0	10.0	-230.0	35.0	420.0	70.0	-90.0	-280.0	-125.0	0.052	0.046	0.21
7.0	40.0	410.0	85.0	85.0	80.0	-285.0	40.0	405.0	80.0	-65.0	-300.0	-120.0	0.062	0.058	0.31
8.0	45.0	515.0	100.0	85.0	200.0	-340.0	45.0	300.0	95.0	-65.0	-330.0	130.0	0.074	0.070	0.45
9.0	45.0	620.0	105.0	80.0	305.0	-420.0	40.0	350.0	100.0	-85.0	-385.0	-170.0	0.088	0.084	0.64
10.0	45.0	735.0	105.0	65.0	415.0	-515.0	35.0	310.0	95.0	-75.0	-465.0	-240.0	0.104	0.100	1.04
11.0	10.0	1175.0	125.0	-130.0	605.0	-670.0	30.0	290.0	60.0	-100.0	-545.0	-280.0	0.124	0.118	1.67
12.0	0	1645.0	125.0	-565.0	590.0	-2030.0	5.0	-220.0	180.0	-50.0	-670.0	-285.0	0.328	0.226	2.89
13.0	5.0	1700.0	120.0	-565.0	585.0	-2070.0	5.0	-170.0	190.0	-50.0	-690.0	-130.0	0.338	0.234	3.33
14.0	5.0	1775.0	140.0	-575.0	570.0	-2230.0	5.0	-120.0	200.0	-30.0	-685.0	-215.0	0.352	0.280	4.00
15.0	5.0	2270.0	70.0	-785.0	520.0	-3060.0	0	-115.0	270.0	130.0	-685.0	120.0	0.412	0.628	4.36
16.0	15.0	-	595.0	-1260.0	-1825.0	-4885.0	5.0	25.0	365.0	470.0	-1055.0	855.0	0.628		4.95

Table A24 Test results for the coefficient of friction

Load (Kg)	Normal Reaction (Kg)
0.4	2.0
1.0	4.0
1.9	6.0
2.7	8.0
3.5	10.0
4.5	12.0
5.0	14.0
5.1	16.0
0.5	3.0
1.5	5.0
2.2	7.0
3.0	9.0

Table A25 Dial gauge readings for tests on the transverse strength of fillet weld - Tension Test 1

Load (Tons)	Deflection (mm)
0	0
1.0	0.95
2.0	1.65
3.0	2.12
4.0	2.57
5.0	2.87
6.0	3.25
7.0	3.63
8.0	4.17
9.0	4.75
10.0	6.32
10.2	7.90
10.8	9.17
11.0	9.65
11.66	10.55
12.0	12.40
12.20	12.80
12.40	13.60
12.60	14.40
12.80	15.50

NB Total extension includes the extension of the parent material.

Table A26 Dial gauge readings for tests on the transverse strength of fillet welds - Tension Test 2

Load (Tons)	Deflection (mm)
0	0
1.0	1.53
2.0	2.02
3.0	2.42
4.0	2.74
5.0	3.06
6.0	3.32
7.0	3.60
8.0	3.94
9.0	4.85
10.0	6.10
10.40	6.75
10.80	7.30
11.00	7.65
11.40	8.25
11.80	9.05
12.00	9.65
12.20	10.25
12.80	11.95
13.00	12.90
13.20	14.00
13.40	14.87

NB Total extension includes the extension of the parent material

Table A27 Transverse strength of fillet-welds - dial gauge readings - welds in compression

Load (Tons)	Deflection (mm)
0	0
1.0	0.08
2.0	0.14
3.0	0.18
4.0	0.22
5.0	0.25
6.0	0.28
7.0	0.31
8.0	0.34
9.0	0.37
10.0	0.40
11.0	0.43
12.0	0.47
13.0	0.52
14.0	0.59
14.5	0.66
15.0	0.72
15.5	0.81
16.0	1.01

Table A28 Finite element analysis results

Distance from one end of flange (mm)	Deflection (mm)
0	0
7.62	0.00577197
15.24	0.0201106
22.86	0.0416654
30.48	0.0686583
38.10	0.0996624
45.72	0.133450
53.34	0.169021
60.96	0.205594
68.58	0.242615
76.20	0.279749
83.82	0.242615
91.44	0.205594
99.06	0.169021
106.68	0.133450
114.30	0.0996624
121.92	0.0686583
129.54	0.0416654
137.16	0.0201106
144.78	0.00577197
152.40	0

Table A29

Calibration of the 50 Ton Ship Jack No 11848170 6000 Psi

Load (Tons)	1	2	Mean
2	250.0	250.0	250.0
4	500.0	500.0	500.0
6	750.0	750.0	750.0
8	1000.0	1000.0	1000.0
10	1225.0	1225.0	1225.0
12	1475.0	1475.0	1475.0
14	1700.0	1700.0	1700.0
16	1925.0	1925.0	1925.0
18	2175.0	2175.0	2175.0
20	2375.0	2375.0	2375.0
22	2600.0	2625.0	2612.5
24	2850.0	2850.0	2850.0
26	3075.0	3075.0	3075.0
28	3300.0	3300.0	3300.0
30	3525.0	3525.0	3525.0
32	3750.0	3750.0	3750.0
34	4000.0	4000.0	4000.0
36	4200.0	4225.0	4212.5
38	4425.0	4450.0	4437.5
40	4675.0	4675.0	4675.0

APPENDIX 2

CALIBRATION GRAPHS AND BALDWIN TESTING MACHINE PLOTS

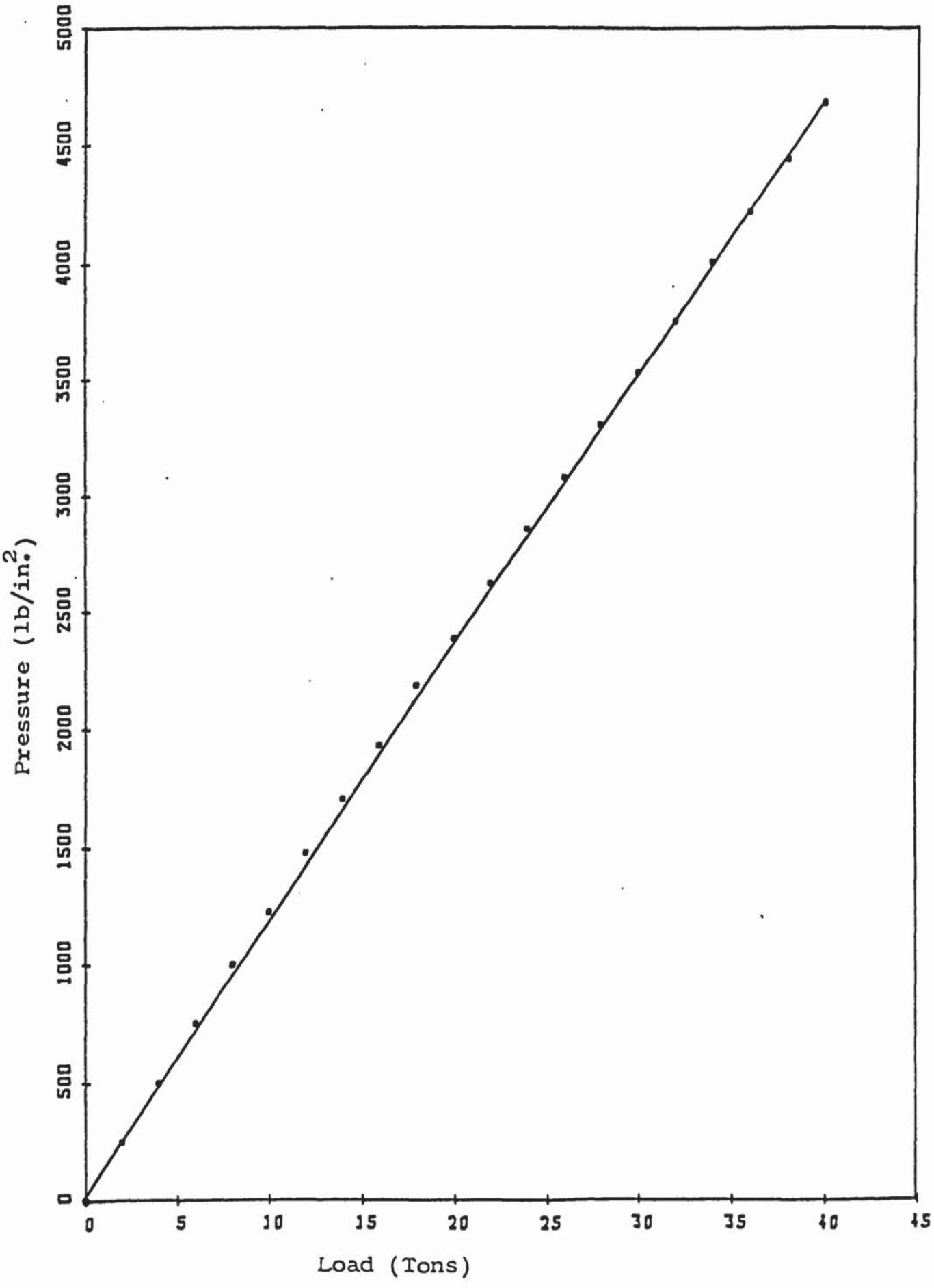

Figure A1 Calibration of the 50Ton ship jack no.11848170 used for the column tests.

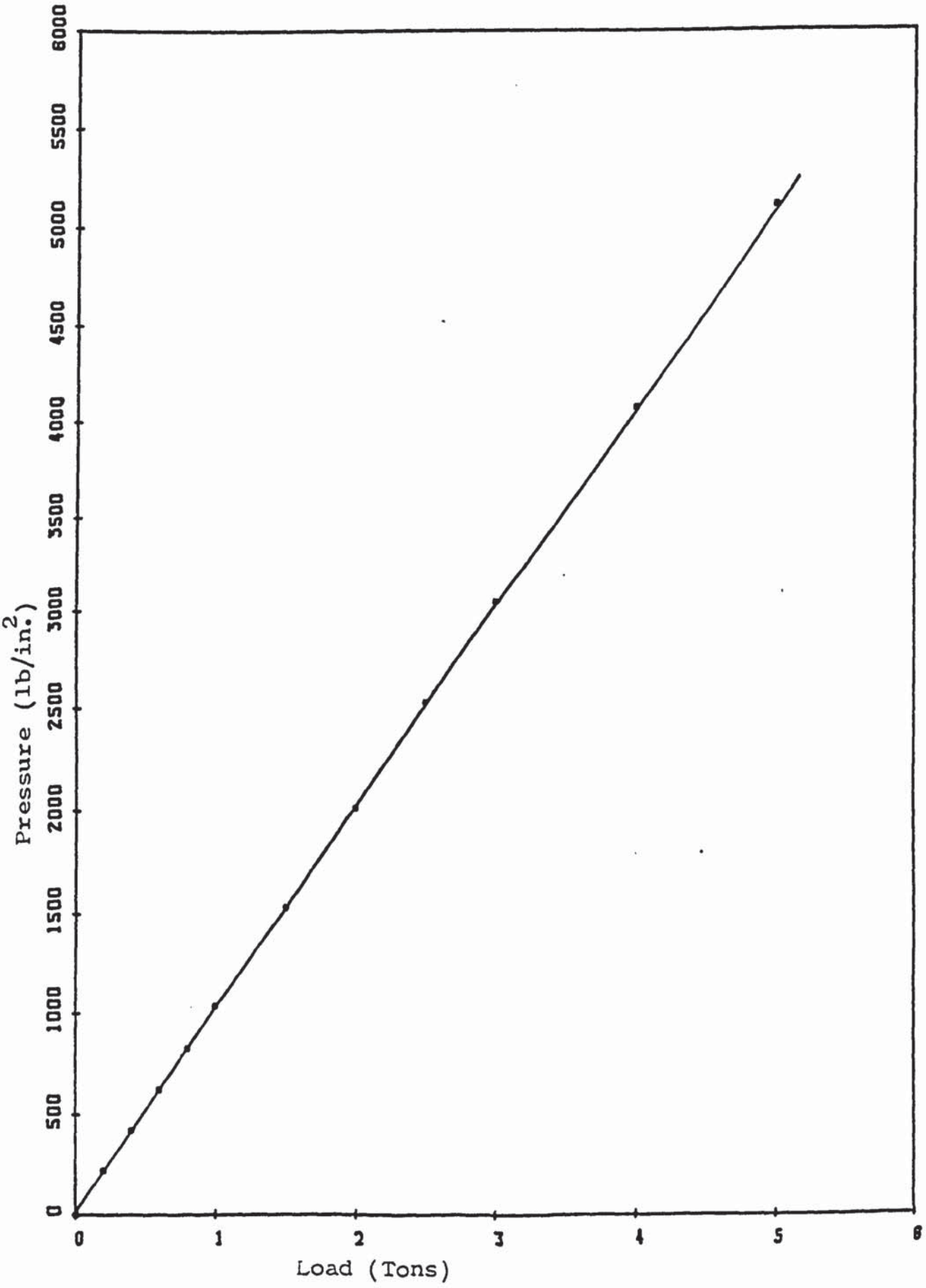

Figure A2 Calibration of Ram and Gauge No.11848170 used for the Failure criterion tests.

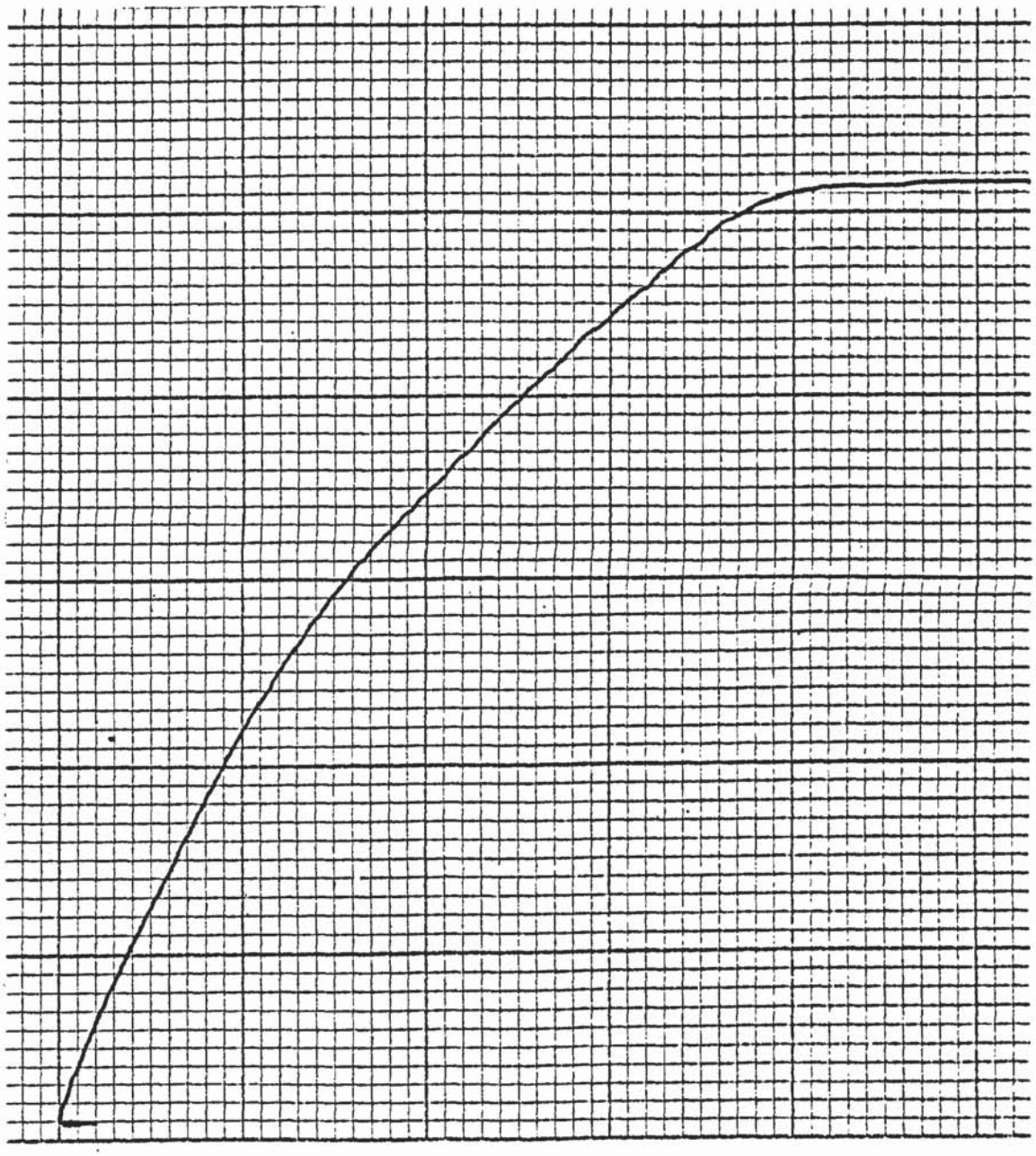

Figure A3 Baldwin testing machine plot-Determination of the yield stress of the I-section flange steel Test 1

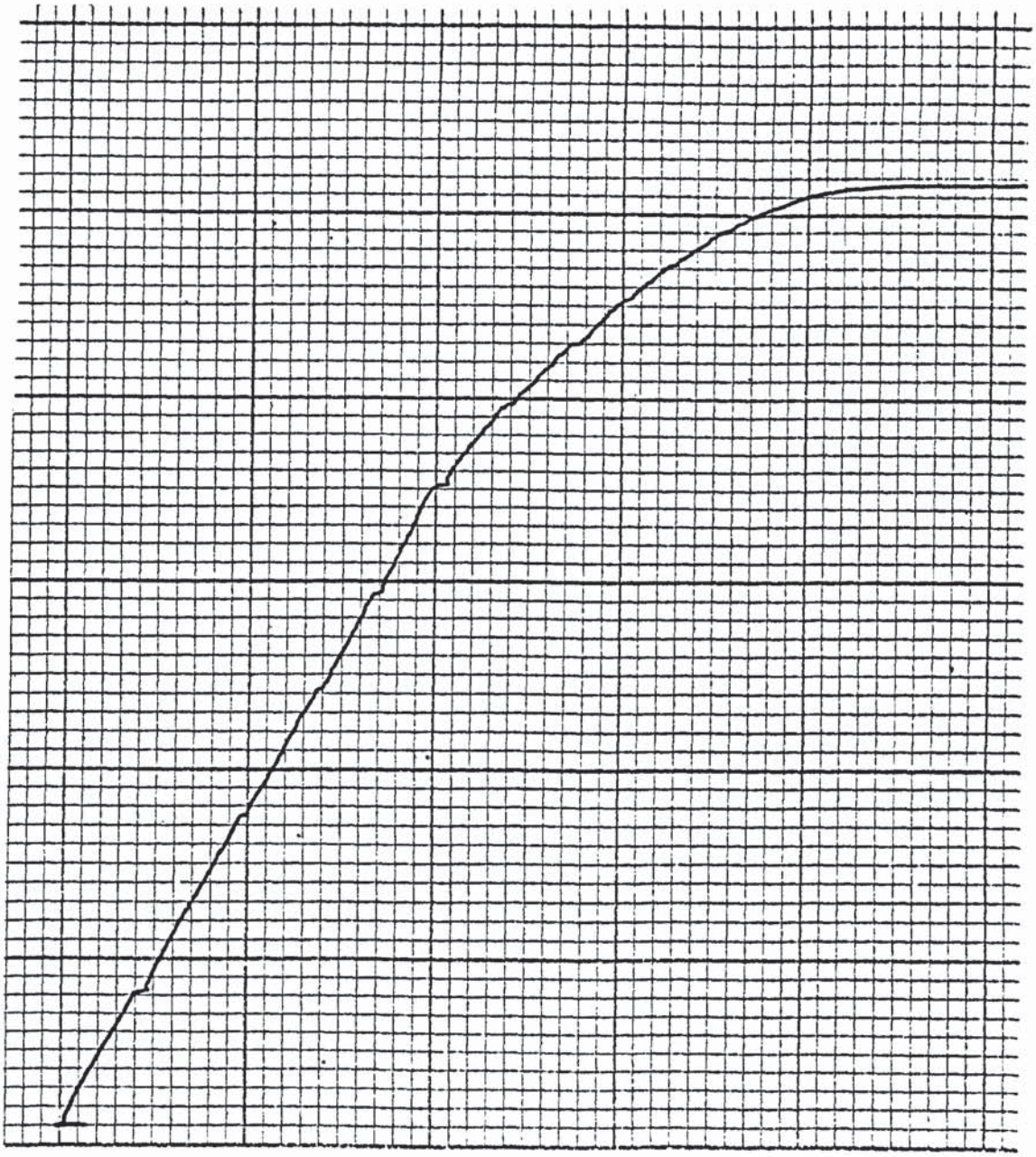

Figure A4 Baldwin testing machine plot-Determination of the yield stress of the I-section flange steel Test 2

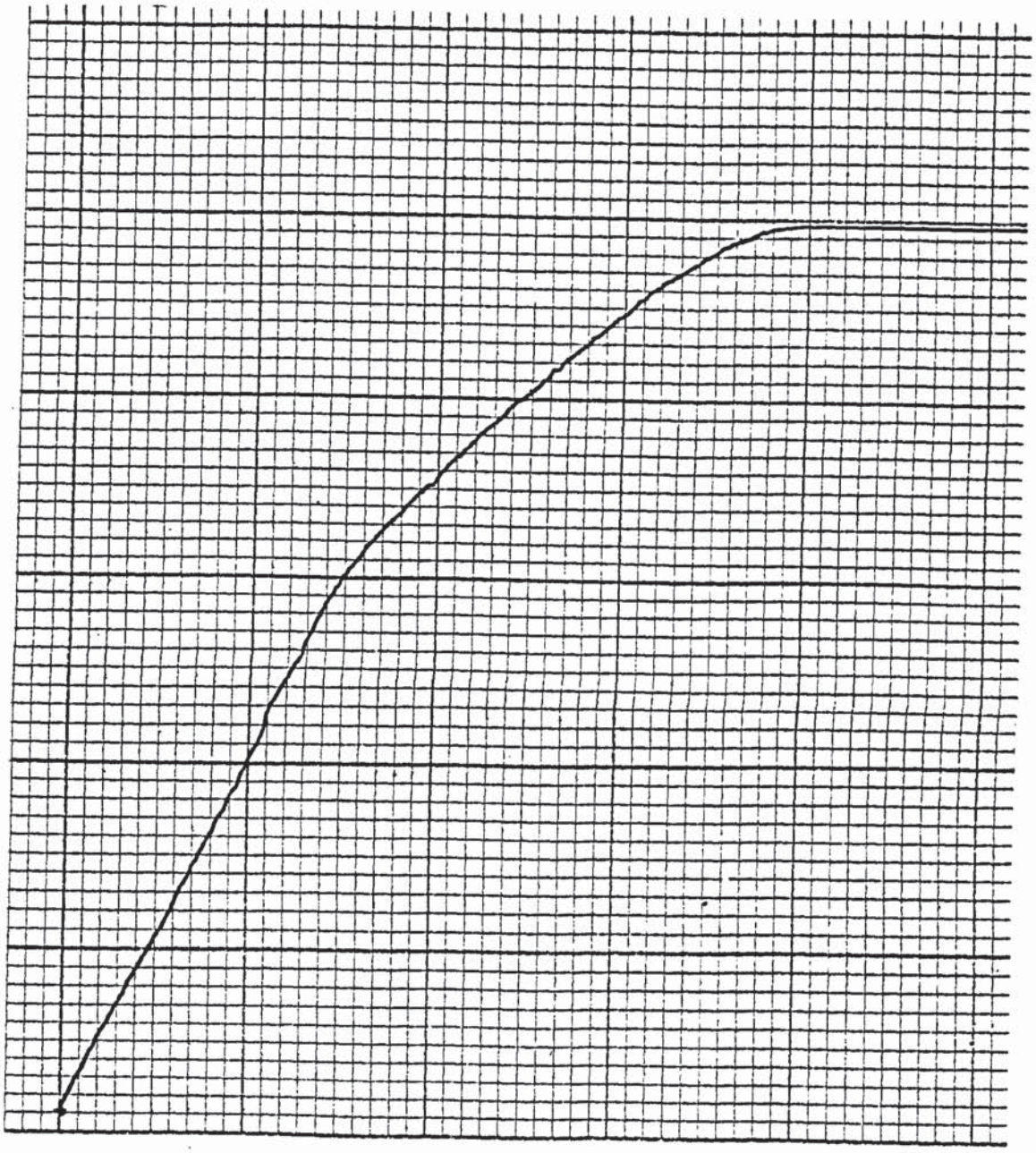

Figure A5 Baldwin testing machine plot-Determination of the yield stress of the I-section flange steel Test 3

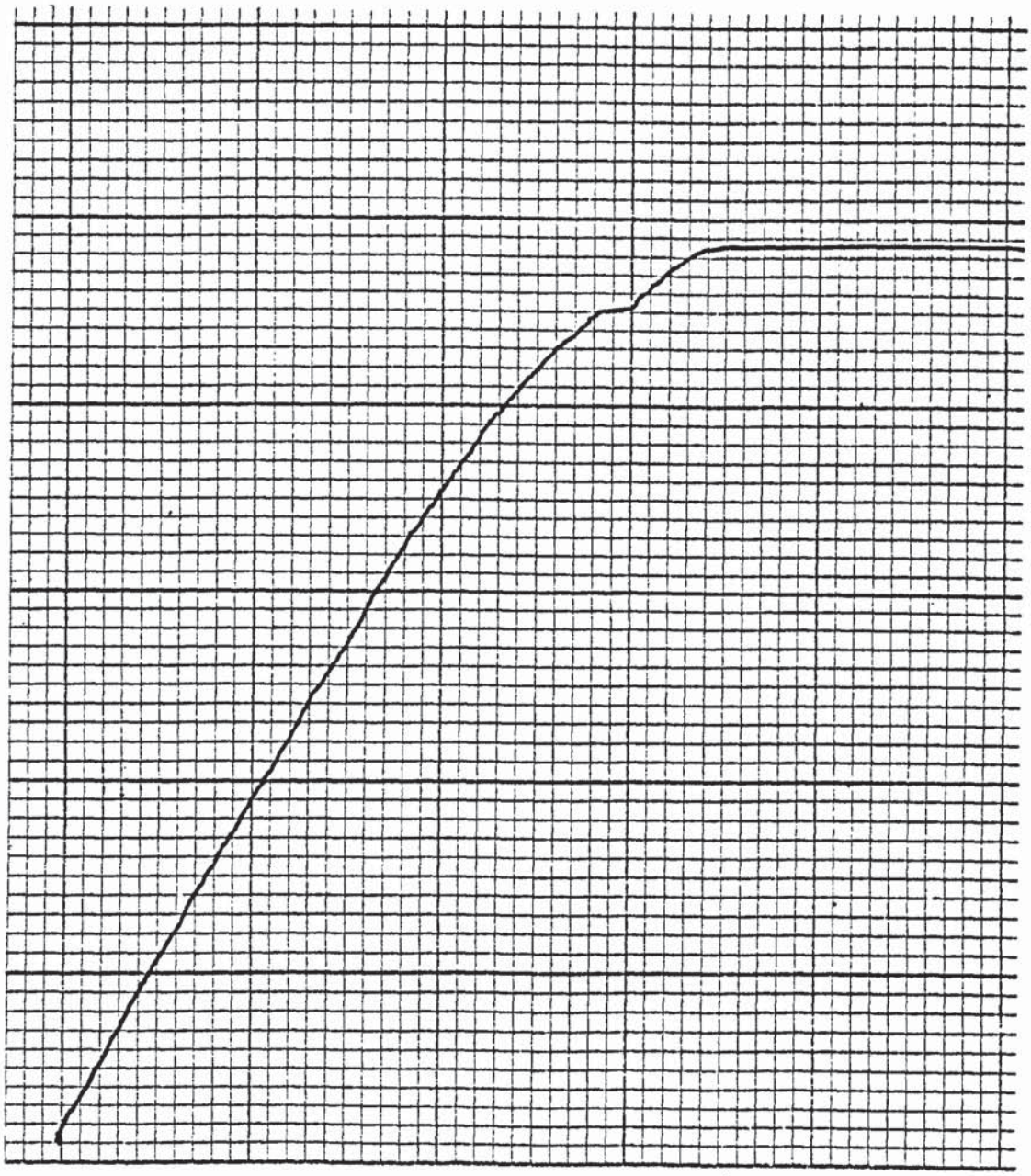

Figure A6 Baldwin testing machine plot-Determination of the yield stress of the I-section web steel Test 1

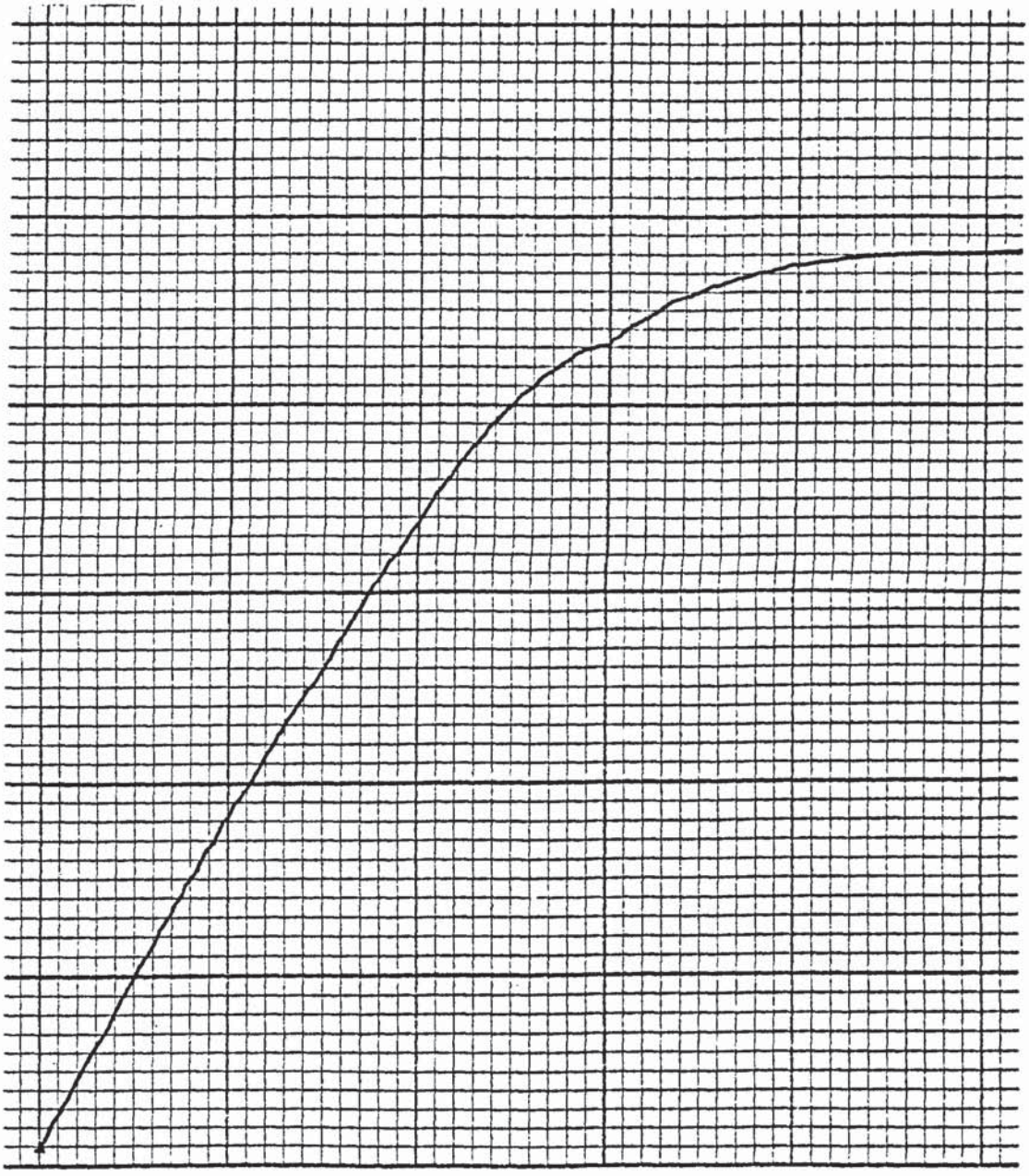

Figure A7 Baldwin testing machine plot-Determination of the yield stress of the I-section web steel Test 2

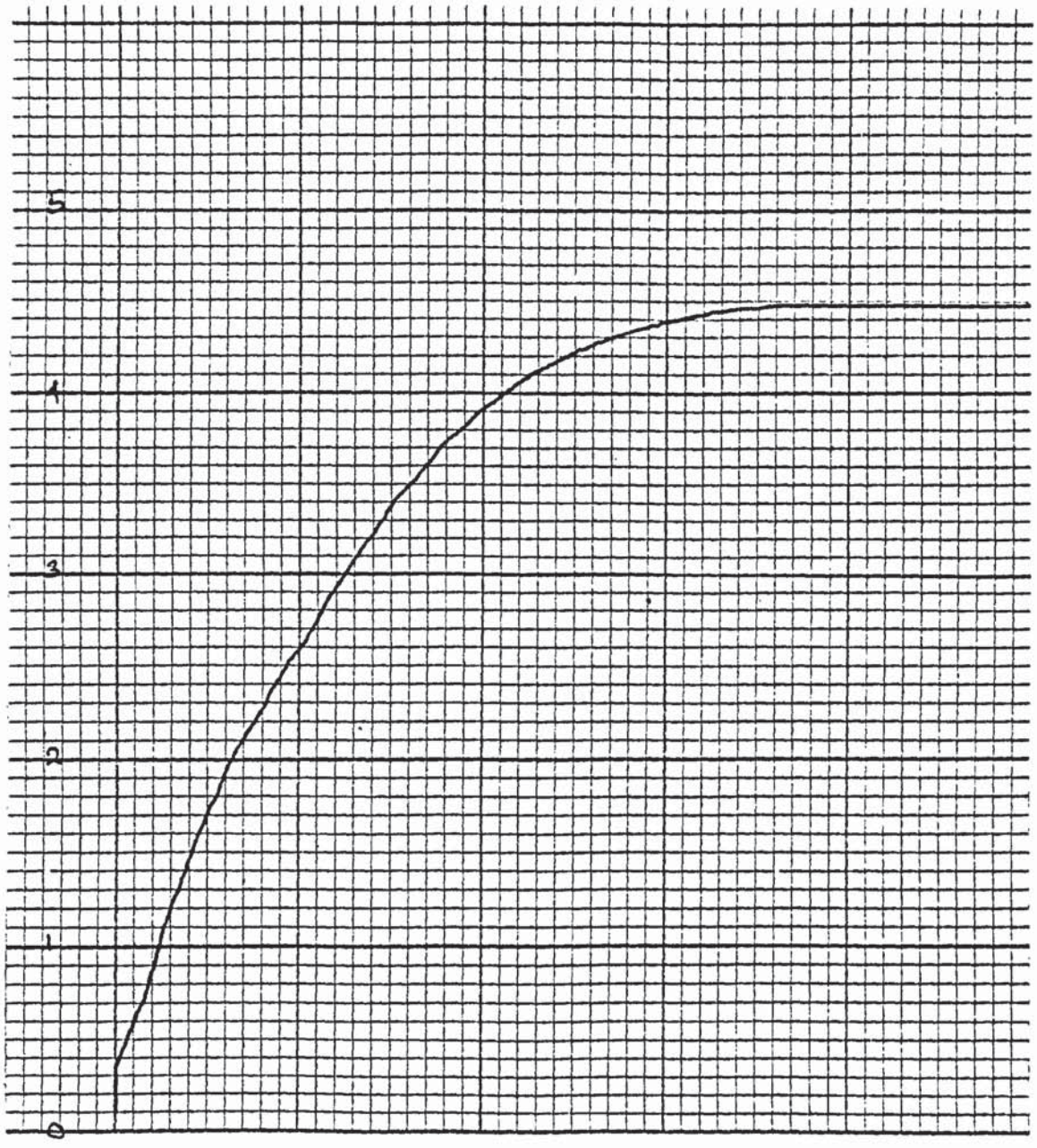

Figure A8 Baldwin testing machine plot-Determination of the yield stress of the I-section web steel Test 3

APPENDIX 3

SPECIMEN DESIGN CALCULATIONS

Presented in this section are the preliminary calculations carried out to determine the most suitable beam and column sections for the beam-to-column connection.

One of the sections considered is the 152 x 152 x 23 kg U.C. Consider a beam-to-column connection involving this section as both the beam and the column and with two flange welds only. The maximum force the weld can resist $P_{max\ weld} = Bf_w$

P_{max} = 2 x 152.4 x 1.659 kN

= 504.6 kN

Reduced strength of the weld due to flange flexibility

$P_{weld\ reduced} = B_e f_w$ = 504.6 x 0.401

= 202.34 kN

(using the effective weld length factor given by the finite element analysis).

WEB CRUSHING

$$V \left[= \left[S_b + 5 (t + \gamma) \right] t_{cw} \sigma_{wy} \right.$$

t = flange thickness

γ = root radius

let S_b = 50 mm

$$V = \left[50 + 5 (6.8 + 7.6) \right] 6.1 \times 250 \times 10^{-3} \text{ kN}$$

$$= 186.05 \text{ kN}$$

This is less than 202.34 kN. Therefore web crushing could occur before weld failure.

WEB SHEAR

$$V = B \times t_{cw} \times 0.6 \sigma_{cwy}$$

$$= 152.4 \times 6.1 \times 0.6 \times 250 \times 10^{-3}$$

$$= 139.45 \text{ kN}$$

One flange weld only is satisfactory.

The other section considered is the 203 x 203 x 45 kg universal bearing pile.

$P_{weld\ max}$ = 2 x 205.4 x 1.659

= 681.52 kN

$P_{weld\ reduced}$ = *(681.52 x 0.401) kN*

= 273.29 kN

WEB SHEAR

$V = d\ t_w\ \sigma y$

= 200.2 x 9.5 (0.6 x 250) x 10^{-3}

= 285.3 kN

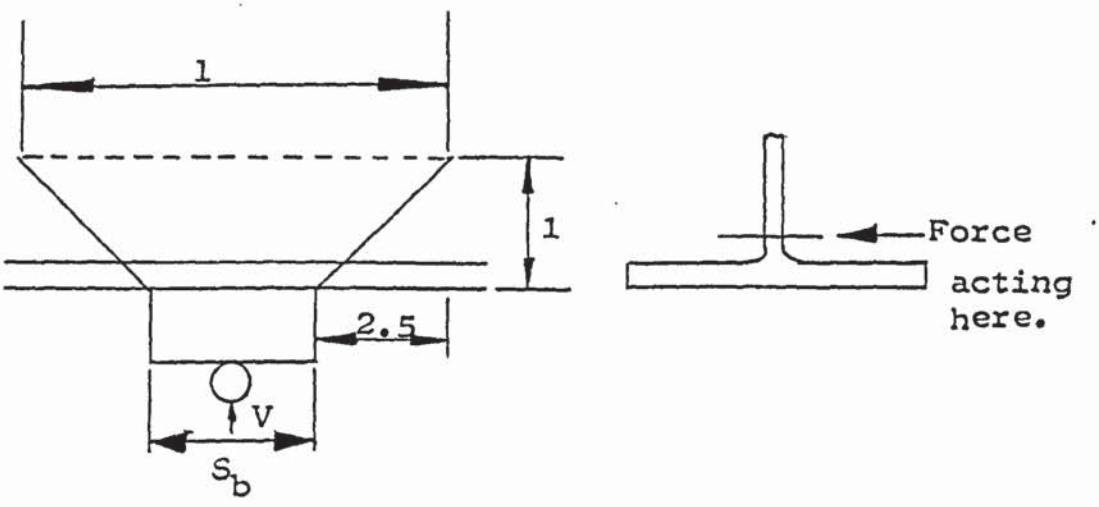

Figure A8

WEB CRUSHING

$$\ell = S_b + 2 \times 2.5 (\tau + \gamma)$$

let $S_b = 50$ mm

$$\ell = 50 + 2 \times 2.5 (\tau + \gamma)$$

$$= 148.5 \text{ mm}$$

$$V = 2(148.5 \times 9.5 \times 250) \times 10^{-3}$$

$$= 705.375 \text{ kN}$$

This is greater than the load to rupture the weld (273.29 kN), therefore web crushing does not occur before weld failure. However, as stated in the text, this section was not used because of the cost and the fact that it is not readily available.

COLUMN WEB BUCKLING TESTS

Some preliminary calculations were carried out to determine the crushing capacity and web buckling capacity of the column for the selection of suitable hydraulic machines for the tests.

Consider a 450 mm length of the 152 x 152 x 23 kg U.C.

Crushing load $P_{max} = A\sigma y$

$= 2980 \times 250 \times 10^{-3}$ kN

$= 745$ kN

A 1000 kN capacity machine will be suitable.

HORIZONTAL LOAD

Using the formula:

$$H \simeq \left[8.84 + 0.34 \frac{T}{t_w} \frac{B}{t_w} + \frac{S_b}{t_w} \right] x\, t_w^2\, \sigma y$$

$$\simeq \left[8.84 + 0.34 \frac{6.8}{6.1} \frac{152.4}{6.1} + \frac{10}{6.1} \right] 6.1^2 \times 250 \times 10^{-3}$$

$\simeq$ 185.57 kN

A 200 kN capacity hydraulic machine will be suitable (A 50 ton hydraulic jack was used for the tests)

SECONDARY BEAM-TO-COLUMN CONNECTION DESIGN EXAMPLE

To determine the size of the welds and components required to connect the secondary 305 x 127 x 37 kg U.B. to the 152 x 152 x 23 kg U.C. of grade 43 steel shown in Figure 3.7

The connection may be subject to some other forces but it is assumed here that the secondary beam is acting as a moment connection. For ultimate limit state design, design the connection to resist 1.1 (plastic moment of resistance of the secondary beam).

Check that the 305 x 127 x 37 kg U.B. behaves as a compact section. If $(b_{bf} - t_{bw} - 2_{rb})$ is less than $7(335/\sigma y)^{\frac{1}{2}}$ then local buckling of the flanges does not occur before full plasticity is achieved.

$$\frac{(123.5 - 7.2 - (2 \times 8.9))}{2 \times 10.7} = 4.6$$

$$7\left(\frac{335}{250}\right)^{\frac{1}{2}} = 8.10$$

$$8.10 > 4.6$$

Therefore satisfactory.

The enhanced plastic moment of resistance of the beam:

$$M_p' = 1.1\, M_{bp}$$

$$= 1.1\, (S_{bx} \times \sigma y)$$

$$= 1.1 \quad 540.5 \times \frac{250}{1.1 \times 1.2} \quad \times 10^{-3} = 112.6 \text{ kNm.}$$

(using a safty factor of 1.2)

This moment may act clockwise or anticlockwise.

If the tee section provides a stiff bearing then rotation occurs about the beam compression flange - axis AA, and the second moment of area of the weld group for a unit size of the weld is:

$$I_{wa} = 2\, \frac{d_b^3}{12} + 2\, d_b \left(\frac{d_b}{2}\right)^2 + 2\, b_{bf}\, d_b^2$$

$$= \frac{2}{3}\, d_b^3 + 2\, b_{bf}\, d_b^2$$

$$I_{wa} = \frac{2}{3}\, (303.8 - 10.7)^3 + 2 \times 123.5 \times (303.8 - 10.7)^2$$

$$= 38.01 \times 10^6 \text{ mm4}$$

Since there is no shear force, no slip occurs. The maximum force per unit length of weld is then:

$$F_{wx} = \frac{M'_p \, d_p}{I_{wa}}$$

$$= \frac{112.6 \times 293.1}{38.01 \times 10^6} \times 10^3$$

$$= 0.891 \text{ kN/mm}$$

The table of design strength per unit length of fillet weld at ultimate limit state in BS 5400 part 3 gives the design strength of a 6 mm end fillet weld as 0.988 kN/mm. This is greater than the applied force per unit strength. European convention for structural steel work (ECSS) (1981) recommends that the throat thickness should be less than half the thickness of the beam flange i.e. 0.5 x 10.7 = 5.35. A 6 mm fillet weld should therefore be used.

As the beam is welded directly to the tee section flange which is in turn welded directly to the column web and flanges both of which may be flexible, it is likely that rotation may occur about the centroidal axis of the weld. In this case:

$$I_{WG} = 2 \, d_b^3 + 4 \, b_{bf} \left(\frac{d_b}{2} \right)^2$$

$$= 2 \times \frac{293.1^3}{12} + 4 \times 123.5 \times \left(\frac{293.1}{2}\right)^2$$

$$= 9.50 \times 10^6 \text{ mm } 4$$

and

$$F_{wx} = \frac{M'_p}{I_{WG}} \quad \frac{d_b}{2}$$

$$= \frac{112.6}{9.5 \times 10^6} \quad \frac{293.1}{2} \times 10^3$$

$$= 1.782 \text{ kN/mm}$$

The table in BS 5400 part 3 refered to above, gives the design strength of a 12 mm weld as 1.978 kN/mm which is greater than the applied shear force.

The arrangement of the fillet welds connecting the web of the tee section to the web of the column is as shown in Figure 4. Because the web of the column does not provide a stiff bearing it is assumed rotation occurs about the centroidal axis GG. The second moment of area of the weld group for a unit size of weld about GG, is:

$$I_{WG} = 2 \frac{d_f^3}{12}$$

$$= 2 \times \frac{400^3}{12}$$

$$= 10.67 \times 10^6 \quad \text{mm}^4$$

Since the weld resists only 40% of the total moment M'_p, the maximum force per unit length of weld at ultimate limit state is:

$$F_{wx} = \frac{0.4 \cdot M'_p}{I_{WG}} \qquad \frac{d_t}{2}$$

$$= \frac{0.4 \times 112.6 \times 10^3 \times 200}{10.67 \times 10^6}$$

$$= 0.844 \text{ kN/mm}$$

From the table referred to above, a 6 mm end fillet weld has a design strength of 0.988 kN/mm for grade 43 steel at ultimate limit state. This is greater than the applied force per unit length.

The column web moment of resistance to web deformation associated with a yield line pattern obtained from equation 4.47 is:

$$M_{cwp} = \frac{t_{cw}^2 \quad f_{cwy}}{} \; d_t \left[2 + \frac{d_t}{d_c} \right]$$

$$M_{cwp} = 6.1^2 \times 271.13 \times 400 \left[2 + \frac{400}{138.8} \right] \times 10^{-6}$$

= 19.7 kNm

Check for failure by punching shear on the web of the column using the following equation (64)

$$M_{cwv} = 2\ P_{cv}\ t_{cw}\ \frac{d_t^2}{6}$$

$$= 2 \times \frac{271.13}{1.05 \times 1.1} \times 6.1 \times \frac{400^2}{6} \times 10^{-6}$$

= 76.37 kNm

This is less than m (112.6 kNm), therefore punching shear is likely to occur (this actually happened in one of the tests).

Check for failure by bearing on the web of the column using the following equation (64) and using a safety factor of 1.05,

$$M_{cwb} = P_{cb}\ t_{tw}\ \frac{d_t^2}{6}$$

$$= \frac{271.13}{1.05 \times 1.1} \times 6.1 \times \frac{400^2}{6} \times 10^{-6}$$

= 38.19 kNm < 112.6 kNm

failure by bearing on the web of the column could occur.

FINITE ELEMENT ANALYSIS

CALCULATION OF AREA UNDER THE STRESS DISTRIBUTION CURVE

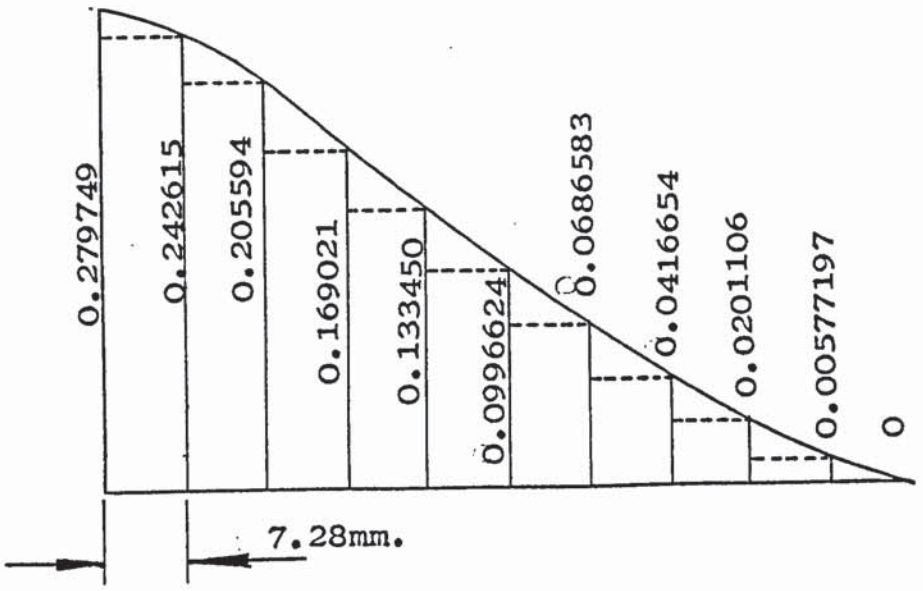

Figure A Stress distribution along one half of the flange as given by the finite element analysis.

The area of the elemental triangles are first calculated assuming the curve tends to a straight line within an element. Because of symmetry only one half of the area under the curve is considered.

TRIANGULAR AREAS

Element	1	Area = 1/2 x 7.28 (0.279749 - 0.242615)	= 0.135
"	2	" = 1/2 x 7.28 (0.242615 - 0205594)	= 0.135
"	3	" = 1/2 x 7.28 (0.205594 - 0.169021)	= 0.133
"	4	" = 1/2 x 7.28 (0.169021 - 0.133450)	= 0.130
"	5	" = 1/2 x 7.28 (0.133450 - 0.0996624)	= 0.123
"	6	" = 1/2 x 7.28 (0.0996624 - 0.0686583)	= 0.113
"	7	" = 1/2 x 7.28 (0.0686583 - 0.0416654)	= 0.098
"	8	" = 1/2 x 7.28 (0.0416654 - 0.0201106)	= 0.078
"	9	" = 1/2 x 7.28 (0.0201106 - 0.00577197)	= 0.052
"	10	" = 1/2 x 7.28 (0.00577197 - 0)	= 0.021

Total rectangular area = 1.018 units

RECTANGULAR AREAS

Element	1	Area = 7.28 x 0.242615	= 1.766
"	2	" = 7.28 x 0.205594	= 1.497
"	3	" = 7.28 x 0.169021	= 1.230
"	4	" = 7.28 x 0.133450	= 0.972
"	5	" = 7.28 x 0.0996624	= 0.726
"	6	" = 7.28 x 0.0686583	= 0.500
"	7	" = 7.28 x 0.0416654	= 0.303
"	8	" = 7.28 x 0.0201106	= 0.146
"	9	" = 7.28 x 0.00577197	= 0.042
"	10	" = 7.28 x 0	= 0

Total rectangular area = 7.182

Area under the curve = (7.182 + 1.018) x 2 = 8.2 units = 16.4 units

The area under the graph for a uniform stress distribution =

0.279749 x (152.4 - 6.8) = 40.731 units

Effective weld lenght factor = $\frac{16.4}{40.731}$ = 0.4026

CALCULATION OF THE EXPERIMENTAL COLUMN WEB MOMENT OF RESISTANCE

Using the expression $M_{cwp} = \varepsilon \, dAfd$

where dA = elemental area

f = stress on the element (= strain x E)

d = distance from the centre of the element to the axis of rotation of the beam

Using the unstiffened connection results:

Ultimate load = 10.75 tons (107.15 KN)

As stated in the text, the area under the graph was divided into ten elements:

$$dA = \frac{400}{10} \times t_w$$

$$= 40 \times 6.343 = 253.72$$

Consider the curve given at a load of 10 tons (99.67 KN) (shown in the figure below).

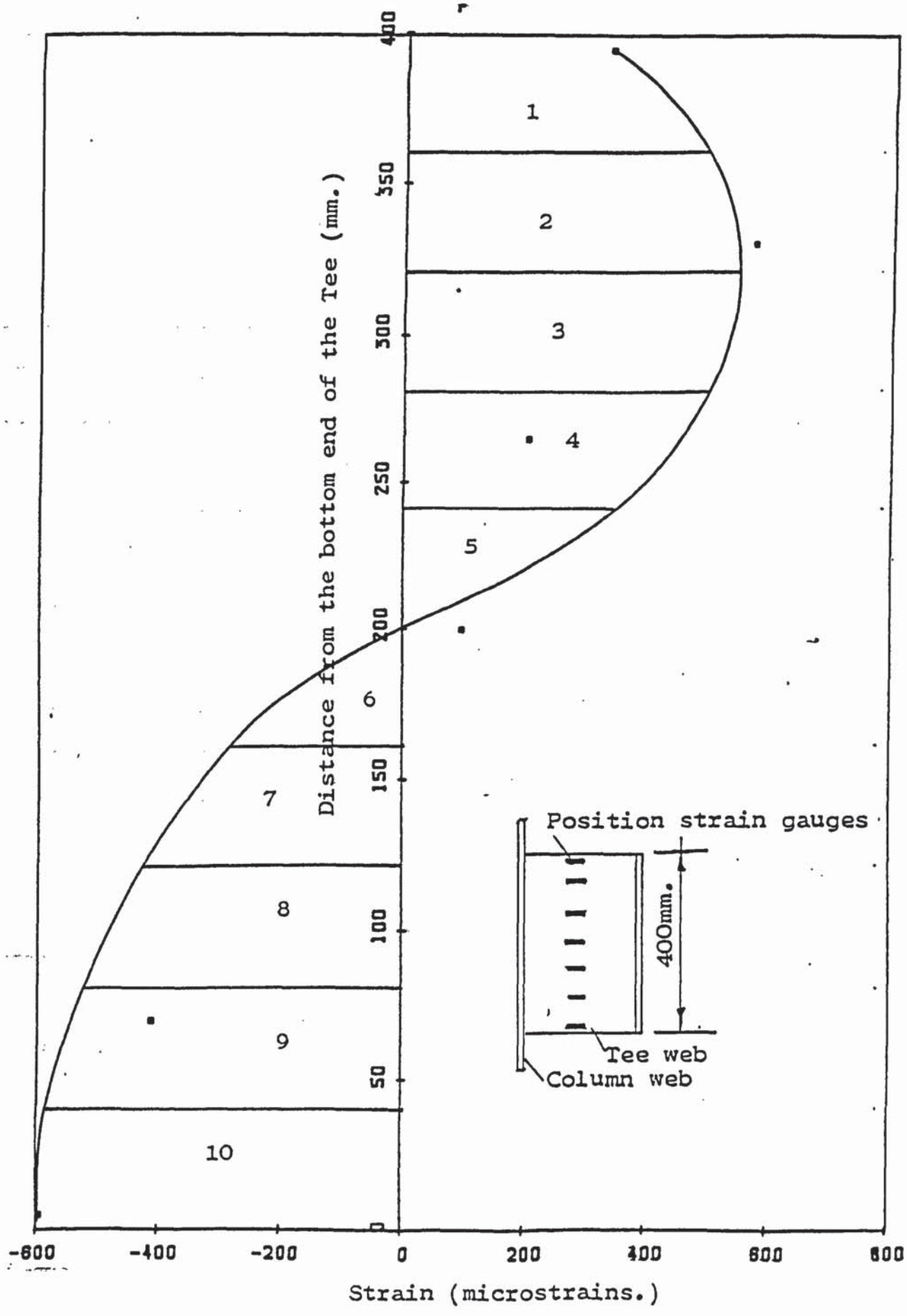
Distance from the bottom end of the Tee (mm.)
400
350
300
250
200
150
100
50
0
1
2
3
4
5
6
7
8
9
10
-600
-400
-200
0
200
400
600
800
Strain (microstrains.)
Position strain gauges
400mm.
Tee web
Column web

Applied moment = 10 x 9.967 x 512 KNmm

= 51031.04 KNmm

$E = 200\ KN/mm^2$

Element	d (mm)	Strain	Strain x d x dA	Elemental M_{cwp}
1	180	375	17.126	3425.2
2	140	550	19.536	3907.2
3	100	510	12.940	2588.0
4	60	190	2.892	578.4
5	20	95	0.482	96.4
6	20	0	.0	.0
7	60	125	1.903	380.6
8	100	265	6.72	1344.0
9	140	440	15.629	3125.8
10	180	565	25.803	5160.6

ε dAfd - 20606.2

$$\text{Experimental } \frac{M_{cwp}}{M} = \frac{20606.2}{51031.04}$$

= 0.404

FINITE ELEMENT ANALYSIS

The finite element analysis was based on the assumption that the flange acts as a cantilever fixed at the centre line and with a uniformly distributed load. The analysis also assumed the following mechanical properties for the steel: Youngs modulus, E = 200 KN/mm^2 and Poisson's ratio, $\nu = 0.3$. The analysis used the value of the column flange width, B, of 152.4 mm and flange thickness T of 6.8 mm and a value of the force on the weld within the elastic range.

The flange was assumed to be symmetrical about the centre line. Consequently, the analysis was applied to only half of the width of the flange which was divided into fifty elements. Figure 4.10 shows the strain distribution given by this analysis. This analysis is purely elastic.

$$\text{Effective width factor} = \frac{a_f}{A_f}$$

Where a_f is the area under the stress distribution graph for a flexible flange see Figure 4.10.

and A_f is the area under the stress distribution graph for a rigid flange.

For a rigid flange the weld stress is assumed to be uniformly distributed throughout the entire width. The stress everywhere along the flange width is therefore equal to the stress in the middle of the

flexible flange.

The area under the stress distribution graph was calculated by dividing the whole area under the graph into ten elements, finding the area of each element and summing all the areas.

Total area under the stress distribution graph of the flexible flange = 8.217 units.

Area under the stress distribution graph of a rigid flange

= 73.13 x 0.279749

= 20.458 units

$$\text{Effective length factor} = \frac{8.217}{20.458}$$

$$= 0.401$$

The data and calculation of areas a_f and A_f are given .

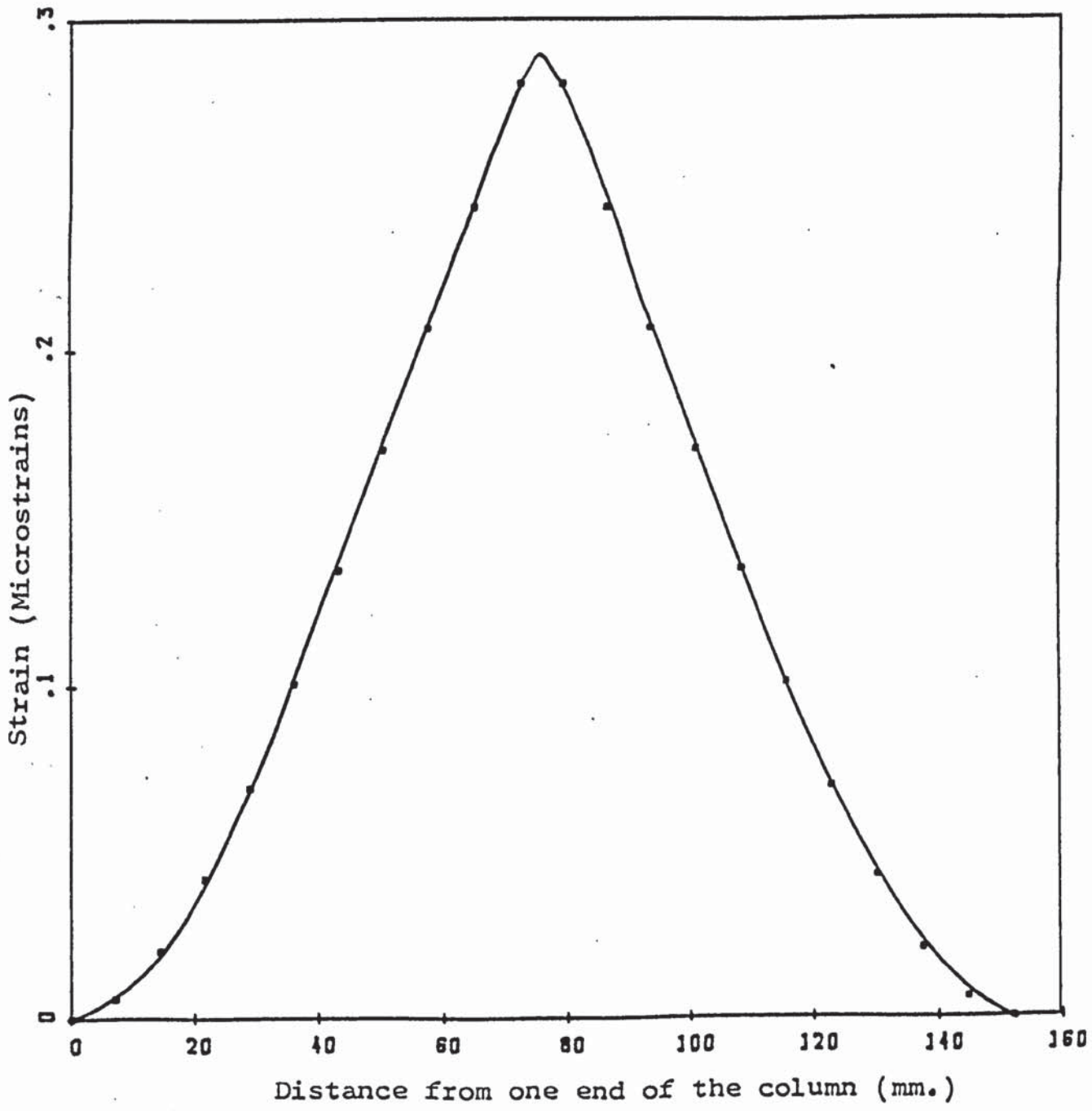

Figure 4.10 Stress distribution along the flange given by the finite element analysis.

REFERENCES

1. Uhler, E H
   Jensen, C D
   "An investigation of welded connections between beams and columns".
   The Welding Journal, April 1930.

2. Biber, L C
   "The theory of stresses in welds".
   The Welding Journal,vol 9,No 4, 1930.

3. Schuster, L W
   "Welded pressure vessels".
   The Welding Journal, vol 9, No 5, May 1930.

4. Freeman, F R
   "The strength of welded joints".
   The Welding Journal, June 1932.

5. Jensen, C D
   "Combined stresses in fillet welds".
   The Welding Journal, No 2, February 1934.

6. Schreiner, N G
   "The behaviour of fillet welds when subjected to bending stresses".
   The Welding Journal, pp 1-16, September 1935.

7. Jennings, C H
   "Welding design".
   The Welding Journal, October 1936.

8. Solakian, A G
   "Stresses in transverse fillet welds by photoelastic methods".
   The Welding Journal, vol 13, 1934.

9. Jensen, C D
   Crispen, R E
   "Stress distribution in welds subject to bending".
   The Welding Journal - reseach supplement, October, 1938.

10. Johnston, B J
    Deits, G R
    "Tests of miscellaneous welded building connections".
    The Welding Journal - research supplement, January, 1942.

11. Norris, C H
    "Photoelastic investigation of stress distribution in transverse fillet welds".
    The Welding Journal, vol 24, p 5575, 1945.

12. Winter, G
    Pian, R H J
    "Crushing strength of thin steel webs".
    Engineering Experiment Station, Cornell University, Ithaca, New York, bulletin No 35, part 1, April 1946.

13. Koenigsberger, F — "Design stresses in fillet weld connections". Proceedings of the Institute of Mechanical Engineers, 165, 1951.

14. Ketler, R L; Beedle, L S; Johnston, B G — "Column strength under combined bending and thrust". Welding Research Supplement - progress report No 6 on welded continuous frames and their components, 1952.

15. Vreedenburgh, C G J — "New principles for the calcualtion of welded joints". The Welding Journal, vol 33, No 8, August 1954.

16. Archer, F E; Fischer, H K; Kitchen, E M — "Fillet welds subjected to bending and shear". Civil Eng. and Public Works Review, vol 54, No 634, April 1959.

17. Lightenberg, F K — "Recent tests on welded beam-to-column connection". Int. Institute of Welding Document, Commission XV, The Netherlands, 1959.

18. Huang, J S; Chen, W F; Beedle, L S — "Behaviour and design of steel beam-to-column connections". Welding Research Council, bulletin 188 October 1973.

19. Regec, J E; Huang, J S; Chen, W F — "Tests of a fully welded beam-to-column connections". Welding Research Council, bulletin 188, October, 1973.

20. Johnson, L G — "Tests on welded connections between I-section beams and stanchions". B W R A report, British Welding Journal, January, 1959.

21. Johnson, L G — "Further tests on welded connections between I-section beams and stanchions" B W R A report No D1/7/58, British Welding Journal 1959, Vol 6, pp 38-46, 1959.

22. Galambos, T V; Ketler, R L — "Columns under combined bending and thrust". Journal of the Engineering Mechanics Division Proceedings of the American Society of Civil Engineers, April, 1959.

23. Graham, J D — "Welded interior beam-to-column

Sherbourne, A N
Khabbaz, A N
connections".
Welding Research Council, bulletin 63, August 1960.

24. Sherbourne, A N
"Bolted beam-to-column connections".
The Structural Engineer, June, 1961.

25. Commission XV of IIW
"Calculation formulae for welded connections subject to static loads".
Welding in the World, vol 2, 4, 1964.

26. Archer, F E
Kitchen, E M
Fischer, H K
"Strength of fillet welds"
UNICIV report r6, University of New South Wales, Australia, November 1964.

27. Elzen, L W A
"Welding seams in beam-to-column connections without the use of stiffening plates".
Report No 6-66-2, IIW, document XV-213-66.

28. Batterman, R H
Johnston, B G
"Behaviour and maximum strength of metal columns".
Jounal of the Structural Division, proceedings of the ASCE vol 93, No ST2, pp 205, April, 1967.

29. Rolloos, A
"The effective weld length of beam-to-column connections without stiffening plates".
Report 6-69-7-HL 12, IIW Doc XV-276-69.

30. Kato, B
Morita, K
Hashimoto, K
"The maximum strength of beam-to-column connections without stiffening plates".
IIW, Doc XV-311-71.

31. Sharma, S S
Gaylord, E H
"Strength of steel columns with biaxially eccentric load".
Journal of the Structural Division, ASCE, vol 95, No ST12 proc paper 6960, pp 2797-2812, December 1969.

32. Brozetti, J
Alpsten, G A
Tall, L
"Residual stresses in a heavy rolled shape 14WF730".
Lehigh University, Fritz Engineering Lab, report No 337.10, January 1970.

33. Fielding, D J
Huang, J S
"Shear in steel beam-to-column connections".
The Welding Journal, vol 50, July 1971.

34. Syal, I C
Sharama, S S
"Biaxially loaded beam-to-column analysis".
Journal of the Structural Division,

ASCE, vol 97, No ST9, proc paper 8384, pp 2245-2259, September 1971.

35. Zoetemeijer, P — "A design method for the tension side of statically loaded bolted beam-to-column connections". Heron vol 20, No 1, 1971.

36. Chen, W F; Atsuta, T — "Interaction equations for biaxially loaded sections". Journal of the Structural Division, ASCE, vol 98, No ST5, proc paper 8902M, pp 1035-1052, 1972.

37. Chen, W F; Atsuta, T — "Ultimate strength of biaxially loaded H-columns". Journal of the Structural Division, ASCE, vol 99, No ST3, proc paper 9613M, pp 469-489, 1973.

38. Chen, W F; Newlin, D E — "Column web strength in beam-to-column connections". Journal of the Structural Division, ASCE, vol 99, No ST9, September, 1973.

39. Chen, W F; Irving J; Oppenheim, A M — "Web buckling strength of beam-to-column connections". Journal of the Structural Division, ASCE, vol 100, No ST1, January, 1974.

40. Dawe, J L; Kulak, G L — "Welded connections under combined shear and moment". Journal of the Structural Division, ASCE, No ST4, April, 1974.

41. Tebedge, N; Chen, W F — "Design criteria for H-columns under biaxial loading". Journal of the Structural Division, ASCE, No ST3, March, 1974.

42. Chen, W F; Rentschler, G P — "Tests and analysis of beam-to-column web connections". Proceedings of speciality conference, Methods of Structural Analysis, vol II, Madison, WI, pp 957-976, August, 1976.

43. Parfitt, Jr, J; Chen, W F — "Tests of welded steel beam-to-column moment connections". Journal of the Structural Division, ASCE, vol 102, No ST1, January, 1976.

44. Commission XV of the IIW — "Design rules for arc-welded connections in steel submitted to static loads".

Welding in the World vol 14, No 576, 1976.

45. Higgs, J D — "Failure of fillet welds and plate bearing effect of structural welded connections under combined bending and shear". MSc Thesis, The University of Aston in Birmingham, October, 1975.

46. Germanou, F — "Web strength of rolled steel beams". PhD Thesis, The University of Aston in Birmingham, April, 1979.

47. Rentschler, G P; Chen, W F; Driscoll, G C — "Tests of beam-to-column web moment connections". Journal of the Structural Division, ASCE, vol 106, No ST5, May, 1980.

48. Witterveen, J; Stark, J W B; Bijlaard, F S K — "Welded and bolted beam-to-column connections". Journal of the Structural Division, ASCE, vol 108, No ST2, February, 1982.

49. Voorn, W J M — "Welded beam-to-column connections in non-sway frames". Report IBBC-TNO, No BI-71-24, Delft, The Netherlands, 1971 (in Dutch).

50. Kato, B — "Beam-to-column connection research in Japan". Journal of the Structural Division, ASCE, vol 108, No ST2, February, 1982.

51. Higgs, J D — "A failure criterion for fillet welds". PhD Thesis, The University of Aston in Birmingham, January, 1981.

52. Kamtekar, A G — "A new analysis of the strength of some simple fillet welded connections". Journal of Constructional Steel Research, vol 2, No 2, June, 1982.

53. Shedd, T C — "Structural design in steel". John Wiley and Sons.

54. Butler, L J; Pal, S; Kulak, G L — "Eccentrically loaded welded connections". Journal of the Structural Division, ASCE, No ST5, May, 1972.

55. Crofts, M R; Martin L H — "A failure criterion for fillet welds". Welding Research International, vol 6, 2, pp 23-30 may, 1976.

56. Clarke, A — "The strength of fillet welded connections". MSc Thesis, Imperial College, University of London, 1970.

57. Bakker, C Th J; Voorn, W J M — "Welded beam-to-column connections in frames". Agon Elsevier, Amsterdam/Brussels, 1974, (in Dutch).

58. Fisher, J N; Struik, J H — "Guide to design criteria for bolted and riveted joints". John Wiley and Sons, 1974.

59. Ghali, A; Neville, A M — "Structural Analysis A unified classical and matrix approach.

60. ASCE — "Plastic design in steel - a guide and commentary". 1971.

61. BS 449 Part 2 — "Use of structural steel in building". 1969.

62. BS 5135 — "Metal-arc welding of carbon and manganese stels". 1974.

63. BS 5400 Part 3 — "Steel concrete and composite bridges". 1982.

64. Holmes, M; Martin, L H — "Analysis and design of structural connections reinforced concrete and steel". Ellis Horwood Series in Engineering Science, 1983.

65 Naka, T. Saito, H. — "Investigation of the strength of welded Beam-column connections Part 9- Distribution of beam force into column web" Transactions of the Architectural Institute of Japan, No.60, Oct. 1958.

66 Miki, S. Oba, H; Susei, S; Nishino, K; Mizuno, K; Atsuta, T — "Some Problems on the strength and rigidity of beam-to-column connection in steel frames" Nov.1964 Kawasaki Dockyard Co. ltd. Steel structure Division.

67 Okumura, T; Hoshino, M; Horikawa, — "Strength of connection due to structural Discontinuities" Doc. X-572-70 I.I.W.